CHAPTER 1.0

INTRODUCTION

1.0 Introduction

Combination chemotherapy with a platinum drug is the cornerstone of cancer therapy for solid tumours such as lung, breast, ovarian, colon and testicular cancer. Many cancer types initially respond well to the platinumdrug cisplatin, but many ultimately relapse with resistant disease. The understanding of the molecular mechanisms of platinum resistance will help the treatment of resistant disease. The development of clinically relevant cellular models of platinum resistance is needed to help elucidate the mechanisms of clinical platinum resistance. This thesis discusses the development of two platinum-resistant small cell lung cancer (SCLC) cell lines. One cell line has been developed to cisplatin, the other to a newer platinum drug oxaliplatin. The development of resistance and mechanisms of resistance will be compared between these platinum drugs. An understanding of the mechanisms of resistance produced in these cell lines will help explain clinical platinum resistance and suggest strategies for circumventing this resistance. This introductory chapter will summarise previous studies into the mechanisms of action and mechanisms of resistance of platinum chemotherapeutics cisplatin and oxaliplatin.

1.1 Cisplatin

Cisplatin has been widely used in the treatment ofcancer patients since 1978 (Figure 1.1A). The anti-proliferative properties of cisplatin were first observed in the 1960s. The first cancer patient received cisplatin in April 1971. Cisplatin quickly progressed through clinical trials and became the first platinum compound approved for cancer therapy (Lebwohl et al., 1998). Cisplatin is used today in combination with other drugs to treat a variety of cancers including smallcell lung cancer. The presence of primary or the emergence of secondary resistance tocisplatin significantly undermines the curative potential of this drug against malignancies (Dempke et al., 2000).

Cisplatin is one of the most successful chemotherapeutics used today, 70-80% of testicular carcinomas are cured by cisplatin-basedcombination chemotherapy. However for those patients who do not respond to first line treatment or those who relapse with resistant disease the prognosis is very poor (Kollmannsberger et al.,

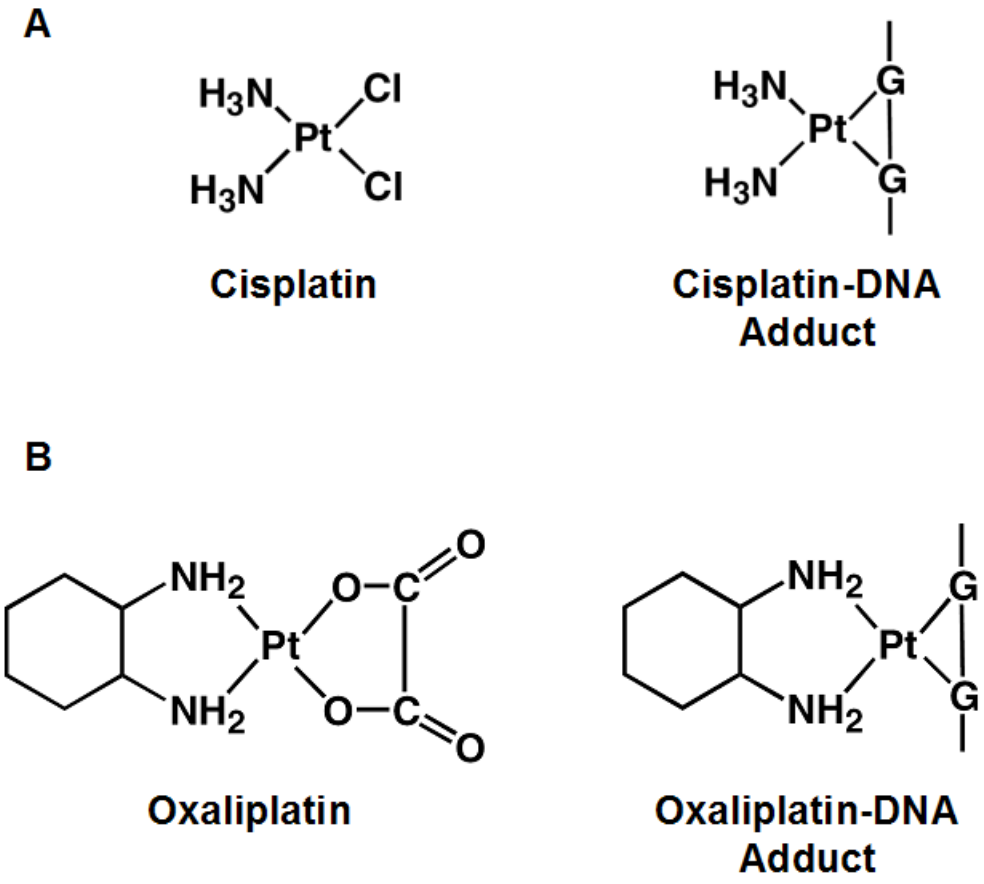

Figure 1.1 Cisplatin and oxaliplatin structure and adduct-DNAstructure. A) Cisplatin and cisplatin-DNA adduct. B) Oxaliplatin and oxaliplatin-DNA adduct. Adapted from Chaney et al., 2004.

2001). The past 30 years have seen extensive research into the mechanism of action of cisplatin, the development of new platinum drugs and research into the mechanisms of platinum drug resistance. The known mechanisms of cisplatin resistance will be outlined in detail later in this chapter.

1.2 Oxaliplatin

Many other platinum drugs have been developed in an attempt to improve on cisplatin. Oxaliplatin is part of the 'dach' family of platinum compounds. This group of platinum compounds were first synthesised in 1972 by substituting the amine radicals of cisplatin with a 'dach' radial (Figure 1.1B) (Chaney et al., 2004). The prototypes of this group showed promising anti-tumour activity but low solubility in water, limiting their potential use in the clinic. Modifications to improve water solubility were made and oxaliplatin was first synthesised in the late 1970s. Oxaliplatin demonstrated both aqueous solubility and anti-tumour activity (Rixe et al., 1996). Oxaliplatin was shown to have activity against colon cancer *in vitro* (Rixe et al., 1996) and is now used as a treatment for colon cancer in combination with 5-fluorouracil (Culy et al., 2000; Ibrahim et al., 2004). Oxaliplatin is also thought to be a better tolerated chemotherapeutic than cisplatin, having fewer side effects, although cases of oxaliplatin toxicity have been reported (Lenz et al., 2003; Tisman et al., 2004).

Oxaliplatin is widely regarded as useful for the treatment of cisplatin-resistant cancer. Evidence for this comes from studies of cisplatin-resistant cell cultures and clinical studies. There is also the notion that because oxaliplatin has a different activity profile to cisplatin in the National Cancer Institute's panel of 60 cell lines (Fojo et al., 2005), oxaliplatin should complement cisplatin treatment and be effective against cisplatin resistance (Rixe et al., 1996). However, the evidence from cellular studies often involve high levels of resistance (20 to 40-fold) to cisplatin (Tashiro et al., 1989). While these highly resistant models are useful to understand the possible mechanisms of resistance, drug resistance in the clinical setting typically occurs at levels of 2 to 3-fold (Kuroda et al., 1991; Kawai et al., 2002) and may therefore involve different mechanisms of resistance.

The evidence that oxaliplatin is active in cisplatin-resistant cancers comes from highly drug-resistant models. Figure 1.2 presents a summary of the data for cisplatin and oxaliplatin resistance in over 20 cell models of acquired drug resistance published in the literature. Cell lines selected for acquired resistance to a drug can be divided into three groups based on their resistance to cisplatin and oxaliplatin. The hypersensitive cell lines (green) have resistance to either cisplatin or oxaliplatin but have become more sensitive to the other drug. Their fold resistance is therefore less than 1. The level of resistance that constitutes cross resistance is a matter of debate in the literature. For the purposes of this study cross resistance is defined as resistance above the level of clinical resistance, that is 2-fold. The non-cross-resistant cell lines (orange) have resistance to one drug and their fold resistance to the second drug is between 1 and 2-fold. The cross-resistant cell lines (red) have greater than 2-fold resistance to both drugs. The literature used in preparation of Figure 1.2 is presented in Tables 1.1, 1.2 and 1.3. The major mechanisms of resistance to platinum for each cell line is also listed if known. The resistance mechanism was not determined for many of the cell lines listed as most of these studies were aimed at showing a differential activity of cisplatin and oxaliplatin rather than determining the mechanisms of platinum resistance.

From this summary of the literature in Figure 1.2 it is clear that the majority of models of acquired platinum resistance are cross-resistant to both cisplatin and oxaliplatin (75%). The evidence for the activity of oxaliplatin in cisplatin-resistant cancers is shown in highly resistant models, where there is above 10-fold to cisplatin and below 10-fold resistance to oxaliplatin (Fukuda et al., 1995; Rixe et al., 1996; Hector et al., 2001). However, as shown in Figure 1.2 the reverse is also true, where there is greater than 10-fold resistance to oxaliplatin there is less than 10-fold resistance to cisplatin (Li et al., 2004; Varma et al., 2005). This suggests that in highly drug-resistant models to one platinum compound there is limited activity to the other compound, as indicated in shaded blue areas of Figure 1.2. Figure 1.2 also shows that there is a limited number of clinically relevant models of cisplatin and oxaliplatin resistance, as most are well in excess of the 2 to 3-fold resistance that occurs in the clinical treatment of cancer.

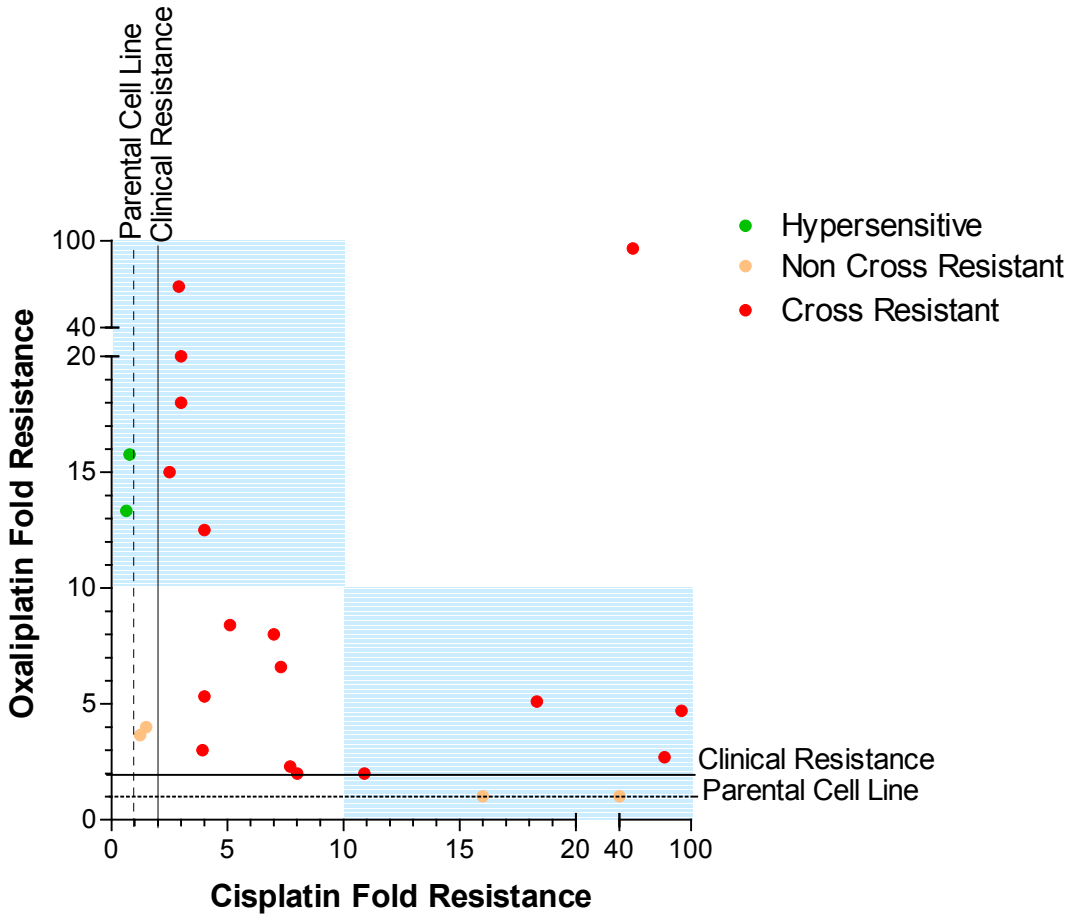

Figure 1.2 Cross resistance between cisplatin and oxaliplatin literature review. Cell lines selected for acquired resistance to a drug can be divided into three groups based on their resistance to cisplatin and oxaliplatin; the hypersensitives (●), non-cross-resistants (●) and cross-resistants (●). In highly drug resistant models to one platinum compound there is limited activity to the other compound as indicated in the shaded blue regions. Literature used in the preparation of this Figure is summarised in Tables 1.1, 1.2 and 1.3.

Table 1.1 Cell lines with cross resistance to cisplatin and oxaliplatin.

Cell Line	Cancer	Selecting Agent (Fold Resistance)	Fold Cisplatin Resistance	Fold Oxaliplatin Resistance	Reference	Mechanism
A2780-E(80)	Ovarian	Cisplatin	92	4.7	(Rixe et al., 1996)	↓Accumulation (Cis and Ox)
KB CP(20)	Ovarian	Cisplatin	78	2.7	(Rixe et al., 1996)	↓Accumulation (Cis and Ox)
H12DDP	Germ Cell	Cisplatin	7.3	6.6	(Dunn et al., 1997)	Not determined
H12DDP	Germ Cell	Cisplatin	8	2	(Dunn et al., 1997)	Not determined
A2780/CP	Ovarian	Cisplatin	10.9	2.0	(Hector et al., 2001)	↓Accumulation (Cis and Ox) ↑DNA Repair Cis-Pt adduct
PC-9/CDDP	NSCLC	Cisplatin	18.33	5.11	(Fukuda et al., 1995)	Not determined
PC-14/CDDP	NSCLC	Cisplatin	7.70	2.3	(Fukuda et al., 1995)	Not determined
P388/DDP	Mouse Leukemia	Cisplatin	7	8	(Tashiro et al., 1989)	Not determined
SKOV3-cis	Ovarian	Cisplatin	4.0	5.33	(Li et al., 2004)	↓Accumulation(Cis), ↓P-gp
A2780-cis	Ovarian	Cisplatin	3.0	20	(Li et al., 2004)	↓Accumulation(Cis), ↑P-gp
KB-3-1/KCP4	Epidermoid	Cisplatin	51.3	94.5	(Mukai et al., 2002)	↑Glutathione ↓Accumulation (Cis) ↑XPF → ↑NER, ↓MSH6
HCT116/R1	Colon	Oxaliplatin	2.1	27.8	(Gourdier et al., 2002)	Not determined
HCT116/R2	Colon	Oxaliplatin	2.9	68.4	(Gourdier et al., 2002)	↓ pro-apoptotic Bax
A2780/C25	Ovarian	Oxaliplatin	5.1	8.4	(El-akawi et al., 1996; Hector et al., 2001)	↓Accumulation (Cis and Ox) ↑Glutathione
CH1oxaliR	Ovarian	Oxaliplatin	3.92	3	(Sharp et al., 2002)	No change GSH or Pt Acc
A2780/C10	Ovarian (clone)	Oxaliplatin	3	18	(El-akawi et al., 1996; Varma et al., 2005)	↑Glutathione
A2780-car	Ovarian	Carboplatin(4.0)	4.0	12.5	(Li et al., 2004)	↓Accumulation(Car), ↑P-gp
A2780-pac	Ovarian	Taxol(3.75)	2.5	15	(Li et al., 2004)	↓Accumulation(Tax), ↑P-gp

Acc – accumulation, Car – carboplatin, Cis – cisplatin, GSH – glutathione, NER – nucleotide excision repair, NSCLC – non-small cell lung cancer, Ox – oxaliplatin, P-gp – P-glycoprotein, Tax - taxol.

Table 1.2 Cell lines with acquired resistance to either cisplatin or oxaliplatin and hypersensitivity to the other compound.

Cell Line	Cancer	Selecting Agent	Fold Cisplatin Resistance	Fold Oxaliplatin Resistance	Reference	Mechanism
HCT116oxaliR	Colon	Oxaliplatin	0.78	15.76	(Sharp et al., 2002)	No change GSH or Pt Acc
HT29oxaliR	Colon	Oxaliplatin	0.64	13.33	(Sharp et al., 2002)	No change GSH or Pt Acc

Acc – accumulation, GSH – glutathione.

Table 1.3 Cell lines with acquired resistance to either cisplatin or oxaliplatin and are non-cross-resistant to the other compound.

Cell Line	Cancer	Selecting Agent (Fold Resistance)	Fold Cisplatin Resistance	Fold Oxaliplatin Resistance	Reference	Mechanism
L1210/DDP	Mouse Leukemia	Cisplatin	40	1.01	(Tashiro et al., 1989; Gibbons et al., 1991)	↑Replicative bypass of adducts (Cis)
(SCLC1)SR-2	SCLC	Cisplatin	16	1.01	(Savaraj et al., 2003)	Increase in mutated MRP4
A2780oxaliR	Ovarian	Oxaliplatin	1.23	3.66	(Sharp et al., 2002)	No change GSH or Pt Acc
SKOV3-car	Ovarian	Carboplatin(3.4)	1.5	4	(Li et al., 2004)	↓Accumulation(Car), ↓P-gp

Acc – accumulation, Car – carboplatin, Cis – cisplatin, GSH – glutathione, MRP4 – multidrug resistance associated protein 4, P-gp – P-glycoprotein.

The clinical evidence that oxaliplatin is active against cisplatin-resistant cancers involves reports of oxaliplatin having greater activity against platinum pre-treated testicular cancer when combined with other chemotherapeutics such as gemcitabine (Kollmannsberger et al., 2004; Pectasides et al., 2004a) or irinotecan (Pectasides et al., 2004b) rather than oxaliplatin as a single agent (Kollmannsberger et al., 2002). In these studies it is difficult to determine whether it is the oxaliplatin or the combination of drugs that produces a response in cisplatin pre-treated patients. This question is unlikely to be resolved by further clinical trails. The development of clinically relevant cellular models of cisplatin and oxaliplatin resistance would therefore help to resolve this issue. The way platinum resistance is defined in the clinic is also a complicating factor. Platinum pre-treated patients and clinical platinum resistance are not necessarily the same and different criteria are used in different clinical trails. When oxaliplatin was studied as a single agent in ovarian carcinoma where patients were divided into platinum resistant or platinum sensitive based on Markman's criteria (Markman et al., 1992), there was a clear drop in response rate to oxaliplatin in the cisplatin-resistant patients (Chollet et al, 1996; Soulie et al., 1997; Dieras et al., 2002). This suggests that oxaliplatin's activity is reduced in cisplatin-resistant cancer as this cohort failed to respond to oxaliplatin as a single agent.

The aim of this study was therefore to develop clinically relevant cellular models of cisplatin and oxaliplatin resistance. These models will then be used to understand the mechanisms of low-level platinum resistance including how it develops. These models will hopefully help to resolve if oxaliplatin is active against cisplatin-resistant cancer. These models will also help find potential methods for preventing the development of resistance or circumventing resistance in the treatment of relapsed platinum-resistant cancer. The carcinoma chosen for this study was small cell lung cancer which is discussed below.

1.3 Small cell lung cancer (SCLC)

Lung cancer is the 5th most common cancer diagnosed in New South Wales, Australia, but is the most common cause of cancer related death. There are five major histological types of lung cancer, namely squamous cell carcinoma (25%), adenocarcinoma (20%), large cell (17%), small cell (14%) and unspecified (22%).

The overall rate of lung cancer incidence has declined in males since the 1980s but continues to increase in females. Rates of SCLC in males in New South Wales, Australia have halved from 13.7 per 100,000 in 1984 to 6.0 per 100,000 in 2003 whereas it has remained constant in females since 1986 at around 4.0 per 100,000. These rates are similar to other industrialised countries (Tracy et al., 2005).

Patients with SCLC typically respond well to first-line combination chemotherapy which includes a platinum drug. However, they inevitably relapse due to the development of drug-resistant disease and the vast majority do not survive more than 1 year (Christodoulou et al., 2005). More than two thirds of SCLC patients are diagnosed as having an extensive disease classified by the tumour not being confined to one hemithorax or with malignant pleural effusion. The remaining one third are diagnosed with limited disease classified by the tumour being confined to one hemithorax comprising hipsolateral, mediastinal or supraclavicular lymph nodes. In both limited and extensive stage disease, combined chemotherapy with a platinum agent is the cornerstone of treatment. This results in an overall response rate of 70–80% for limited disease and 60–70% for extensive disease, indicating that the chemotherapy is improving the survival of patients. In limited disease, median overall survival with combined chemotherapy is about 12–16 months with 4–5% of long-term survivors considered cured. However in extensive disease, median overall survival is 7–11 months with virtually no patients surviving after 5 years (Rossi et al., 2004).

Surgery is not conducted routinely with SCLC patients and is usually only considered in patients presenting with early stage disease. Patients who receive surgery will still receive platinum-based combination chemotherapy and possibly radiotherapy as part of their treatment (Waddell et al., 2004). The survival of SCLC patients is therefore reliant on the success of chemotherapeutic strategies to cure their cancer. SCLC is an ideal model to study the development and mechanisms of platinum drug resistance as it responds quickly to the chemotherapy and then develops a resistant phenotype. Any further insight into this area will help in the treatment of SCLC and all cancers which are treated with platinum-based combination chemotherapy. The aim of this PhD project was therefore to develop clinically relevant platinum-resistant SCLC cell lines to further understand the molecular basis of clinical platinum resistance in SCLC.

1.4 Previous platinum-resistant SCLC sublines

There are a variety of cisplatin-resistant SCLC sublines that have been established with various cisplatin treatment regimens and eleven examples are presented in Table 1.4. There appear to be no reports of SCLC cells selected for oxaliplatin resistance. The majority of these studies focused on mechanisms of resistance and there was little information on how resistance developed or whether their sensitivity to oxaliplatin was altered. Seven of these sublines were produced by continuous cisplatin treatment for periods longer than a week and had cisplatin resistance from 5 to 25-fold. The other four sublines were repeatedly treated with cisplatin for 1 hour to 4 days and gave resistances of 2 to 16-fold.

The time taken to develop some of the cisplatin-resistant SCLC cell lines presented in Table 1.4 was over 1 year in cell culture producing levels of resistance from 3 to 25-fold (Hong et al., 1988; Hospers et al., 1988; Teicher et al., 1991; Moritaka et al., 1998). These time periods are much longer than the life expectancy of a recently diagnosed SCLC patient (Rossi et al., 2004) and levels of resistance produced much higher than that of clinical platinum resistance. Many of the cell lines were also developed with large amounts of dose escalation (Hospers et al., 1988; Teicher et al., 1991; Moritaka et al., 1998). Dose escalation of platinum drugs rarely occurs as part of SCLC treatment (Sandler, 2003). Shorter periods of cell line development, less than 1 year, may therefore produce more useful cell models rather than continuing the development of the cell lines with dose escalation.

Pharmacokinetic studies show that plasma platinum levels after exposure to clinical doses of cisplatin peak at a range of 1-10 μg/ml in 2 hours with a rapid drop to the ng/ml range and then a slow decrease over the next 48 hours (Sockalingam et al., 2002; Liu et al., 2002a). Therefore for this study it was decided to use pulsed rather than continuous drug treatment for the development of the model of resistance as this reflects the pharmacokinetics of cisplatin drug treatment and may result in low-level and possibly more clinically relevant mechanisms of resistance.

As summarised in Table 1.4 there have been many cell models of cisplatin-resistant SCLC showing differing mechanisms of platinum resistance. There have been

Table 1.4 Examples of cisplatin-resistant SCLC sublines developed with cisplatin.

Subline (Fold Resistance)	Treatment	Reference	Mechanism
H69/0.2 (8)	Continuous 50 ng/ml for 1-3 weeks. Escalate dose to 200 ng/ml.	(Hong et al., 1988)	Not determined
H69/0.4 (25)	Same as for H69/0.2 then grown in 400 ng/ml for 1 year.	(Hong et al., 1988; Kumar et al., 2004)	Decreased Bcl-2 No other mechanisms reported
N231/0.2 (8)	Continuous 50 ng/ml for 1-3 weeks. Escalate dose to 200 ng/ml.	(Hong et al., 1988)	Not determined
H69/CPR (5)	Continuous exposure in escalating doses up to 400 ng/ml over 4-6 months.	(Twentyman et al., 1991; Twentyman et al., 1992)	No change cellular glutathione No change Pt accumulation
H69-CP (3)	6 treatments of 100 ng/ml for 4 days with 2-3 weeks recovery between.	(Locke et al., 2003)	Increased glutathione and GSTPl
H82-CP (2)	6 treatments of 100 ng/ml for 4 days with 2-3 weeks recovery between.	(Locke et al., 2003)	Increased glutathione and GSTPl Increased Bcl-2
GLC_4-CDDP (6)	Continuous exposure with more drug added each time the cells grew. 9 such treatments over 1 year. Maintained by 1 hour exposure per month.	(Hospers et al., 1988)	Increased cellular glutathione No change GSTs and GSR Decrease in Pt adducts
SBC-3/CDDP (13)	Continuous starting at 30 ng/ml for 2-3 weeks then escalating up to 1,500 ng/ml over 2 years.	(Moritaka et al., 1998)	Increased cellular glutathione and GSTs Decreased Pt accumulation
H209/CP (11.5)	Continuous 80 ng/ml for several months then maintained by treating every 2 weeks.	(Jain et al., 1996)	Increased cellular glutathione No change GSTs, GSR and GPX Decreased Pt accumulation
SW2/CDDP (3.3)	IC_{90} dose for 1 hour per week with dose escalation of 15-20% per treatment when possible over 14 months.	(Teicher et al., 1991)	Increase in glutathione andGSTs Decreased Pt accumulation
(SCLC1)SR-2 (16)	5 ng/ml for 24 hours per 3 weeks; maintained with 100 ng/ml	(Savaraj et al., 2003)	Increase in mutated MRP4 No other mechanisms reported

GST - glutathione-S-transferase, GSR – glutathione reductase, GPX – glutathione peroxidase, MRP4 – multidrug resistance associated protein 4.

hundreds of platinum-resistant cell lines developed in many other types of carcinoma. However, there is still a need for more clinically relevant models of platinum resistance and in particular models of the newer drug oxaliplatin. There is a large body of research detailing both the mechanism of action and common mechanisms of resistance to platinum drugs. The remainder of this chapter is devoted to summarising this literature.

1.5 Mechanism of action of platinum chemotherapeutics

The mechanism of cellular cisplatin uptake is still not fully understood (Wang et al., 2005a). Early studies suggested that cisplatin enters the cell mainly by passive diffusion, because its uptake proceeded linearly with time (Wang et al., 2005a). However, it has been recently shown that the major copper influx transporter CTR1 can regulate the cellular uptake of cisplatin, carboplatin and oxaliplatin (Safaei et al., 2005).

Upon entering a cell cisplatin generates a positively charged aquated species that can react with nucleophilic sites inside the cell to form protein, RNA and DNA adducts (Kartalou et al., 2001). Figure 1.3 demonstrates how cisplatin interacts with the cell leading to adduct formation, which results in inhibition of DNA replication, RNA transcription, protein translation and/or apoptosis (Kartalou et al., 2001).

Oxaliplatin forms DNA adducts with similar sequence and region specificity to cisplatin (Woynarowski et al., 1998) and therefore also inhibits DNA replication like cisplatin. Oxaliplatin also inhibits RNA and protein function and can trigger an apoptotic response in the cell. The structure of adducts formed by cisplatin and oxaliplatin are similar. However, the bulky oxaliplatin dach group that protrudes into the minor groove of DNA may lead to different biological properties of the two drugs. At equimolar concentrations oxaliplatin induces fewer but more cytotoxic DNA adducts than cisplatin (Woynarowski et al., 1998; Woynarowski et al., 2000).

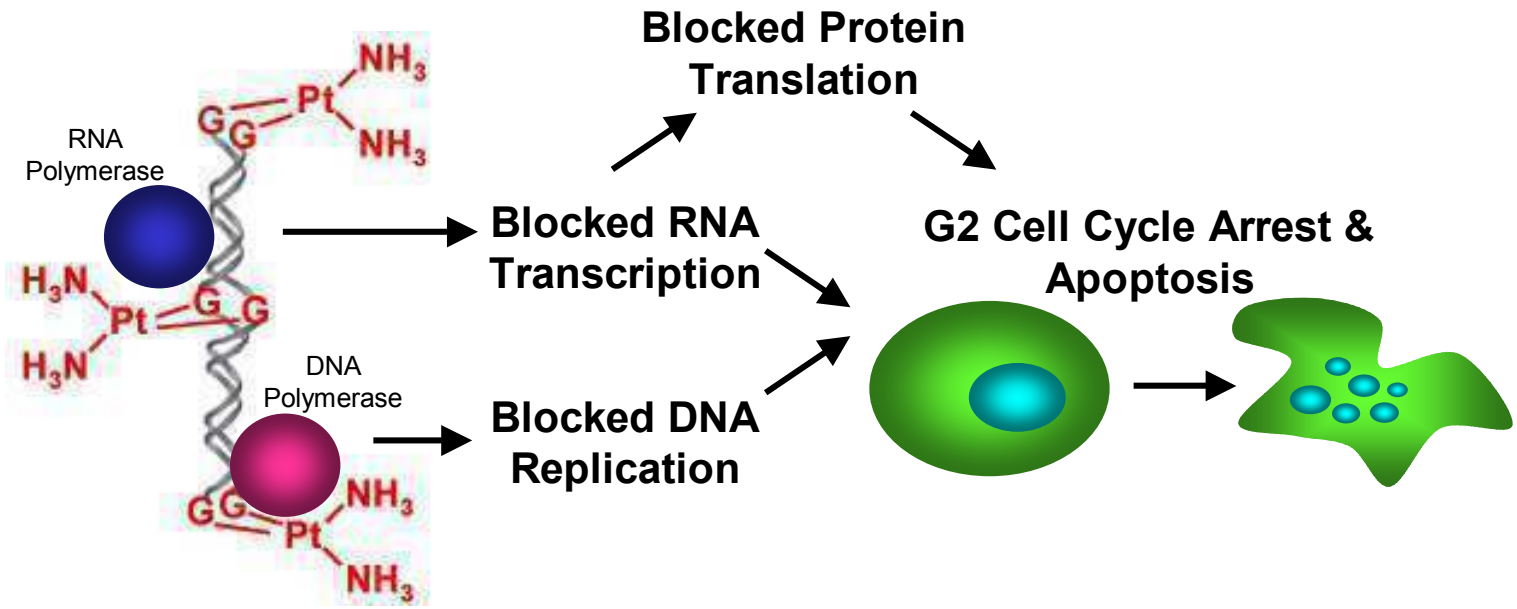

Figure 1.3 Mechanisms of action of platinum chemotherapeutics. Platinum drugs interact with the DNA of a cell leading to platinum adduct formation, which results in inhibition of DNA replication, RNA transcription, protein translation and/or apoptosis.

1.6 Mechanisms of resistance to platinum chemotherapeutics

There are many types of resistance that have been characterised for platinum drugs as summarised in Figure 1.4. Mechanisms include:-

- Reduced intracellular accumulation of platinum thatmay arise because of decreased uptake or increased efflux.
- Increased inactivation by intracellular proteins such as glutathione.
- Increased DNA repair of platinum-DNA adducts.
- Increased ability to replicate by bypassing platinum-DNA adducts.
- Inhibition of the apoptotic response.

Although oxaliplatin has a different spectrum of activity against tumours than cisplatin, oxaliplatin resistance emerges with kinetics that resemble cisplatin. Some features of the cellular pharmacology of cisplatinand oxaliplatin are similar, and oxaliplatin-resistant cells share some of the majorcharacteristics often found in cisplatin-resistant cells (Mishima et al., 2002). However, fewer studies have been performed on oxaliplatin and consequently it has not been definitively linked to all the known mechanisms of cisplatin resistance. More research is needed in order to understand the mechanisms of oxaliplatin resistanceand how they relate to cisplatin resistance in the same models.

Cell lines resistant to platinum often exhibit oneor more mechanisms of resistance, this is also the case in the resistant tumours of relapsed cancer patients. Many studies have examined tumours from patients who have failedto respond to cisplatin. Some studies have found marker genes for resistance while the majority find no correlation between a particular gene and drug resistance. Thisis probably due to the multifactorial nature of resistance to platinum drugs, looking for a global marker may not yield results. There needs to be a shift to individually diagnosing the mechanism of resistance to best choose the next stage of cancer therapy. This approach is years away from the clinic, but characterising individualmechanisms of resistance in platinum-resistant cell lines will eventually enable the proper classification of drug resistance in the clinic.

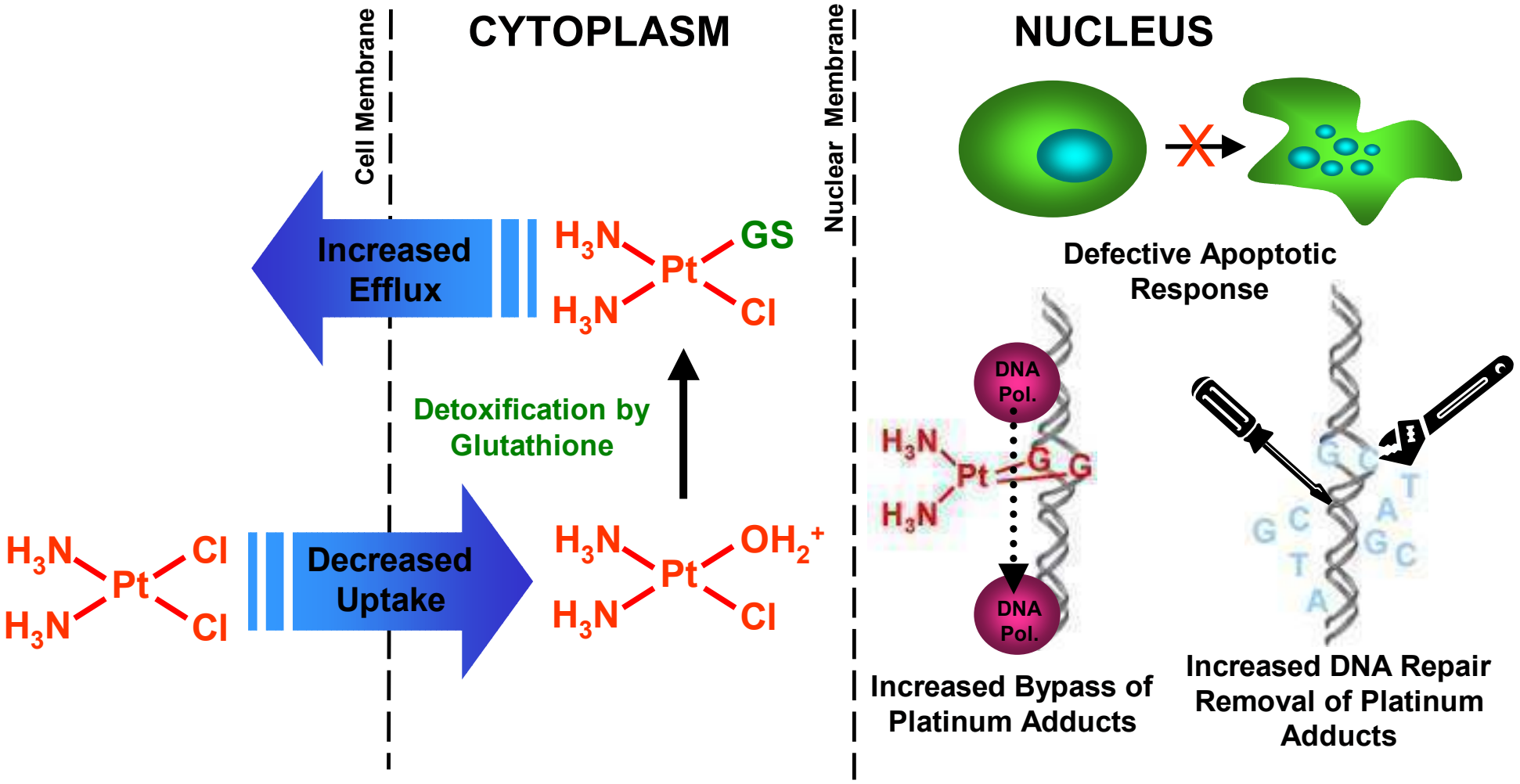

Figure 1.4. Mechanisms of resistance to platinum chemotherapeutics. Adapted from Kartalou and Essigmann 2001.

Pol – Polymerase.

Studies often analyse multiple platinum-resistant cell lines from the same cancer type looking for global markers of resistance. These studies, while useful on one level, experience the same problem as the clinical studies, genes from individual mechanisms of resistance are excluded from the analysis when looking for a global marker. Research groups may have many resistant cell lines but it is unlikely that they will have many independently selected cell lines exhibiting a similar mechanism of resistance. What is needed is larger scale collaboration, cell lines need to be clustered based on both the same type of cancer and the same type of resistance mechanism so markers for that specific type of resistance can be determined.

1.6.1 Redox detoxification of platinum chemotherapeutics

Reactive oxygen species (ROS) can damage nucleic acids and proteins and therefore induce necrotic cell death and/or trigger apoptotic pathways. Many chemotherapeutic drugs, including cisplatin (Miyajima et al., 1997), can produce ROS as a direct or indirect by-product and this is a cause of cytotoxicity (Tew et al., 1999). Therefore, an upregulation of antioxidant defences can be considered a mechanism of drug resistance.

1.6.1.1 Glutathione

The sulfur containing tripeptide glutathione (glutamine-cysteine-glycine) is one of the most abundant molecules in cells. Glutathione was identified as an important determinant in the success of cancer therapy in the 1950s by radiobiologists who found that glutathione depletion sensitised cells to ionising radiation (Calvert et al., 1998). Cisplatin generates a positively charged aquated species in the cell that can form DNA, RNA and protein adducts (Kartalou et al., 2001). Platinum drugs are very reactive towards the cysteine residue of glutathione, which detoxifies these compounds by a rapid binding mechanism (Jansen et al., 2002). The cysteine-Pt bond is more chemically inert than the reactive aquated species formed by cisplatin and therefore conjugation with glutathione detoxifies the drug as it prevents its ability to form adducts (Kartalou et al., 2001; Jansen et al., 2002). Glutathione has the ability to detoxify numerous chemotherapeutics via conjugation and also detoxifies the ROS produced by many chemotherapeutics and radiation.

Resistance to cisplatin has been associated with increased cellular glutathione in many cisplatin-resistant SCLC cell lines (Teicher et al, 1991; Jain et al., 1996; Moritaka et al., 1998; Locke et al., 2003) (Table 1.4). However, some cisplatin-resistant SCLC cell lines show no change in glutathione and its related enzymes (Twentyman et al., 1991; Twentyman et al., 1992). There have been no previous studies of oxaliplatin-resistant SCLC. However, in oxaliplatin-resistant ovarian carcinoma cells, oxaliplatin resistance has been associated with increased glutathione in some models (El-akawi et al., 1996) and not in others (Sharp et al., 2002). The cellular level of glutathione has been shown to increase in the clinical treatment of ovarian carcinoma with platinum-based chemotherapy. Tumours from platinum pre-treated patients had a statistically significant increase in glutathione compared to tumours from chemotherapy naïve patients (Lewandowicz et al., 2002).

The de novo synthesis of glutathione involves peptide bond formation between cysteine and glutamic acid. This is the rate limiting step of synthesis catalysed by γ-glutamylcysteine synthetase. This is followed by peptide bond formation with glycine catalysed by glutathione synthetase (Kartalou et al, 2001) (Figure 1.5). Glutathione can also be synthesised from extracellular glutathione by a salvage pathway mediated by γ-glutamyltranspeptidase in the cell membrane. Cysteine and glycine are recovered from extracellular glutathione and used in de novo synthesis of glutathione (Figure 1.5) (Townsend et al., 2003a).

When cisplatin enters a cell glutathione performs two key roles. Firstly, conjugation to cisplatin which is catalysed by glutathione-S-transferases (Zhang et al., 2003) (Figure 1.5). Secondly, cisplatin causes the formation of reactive oxygen species within the cell, the reactions of oxidising and then recycling glutathione act as a buffer against these agents. These recycling reactions are catalysed by glutathione peroxidase and glutathione reductase respectively (Rahman et al., 1999) (Figure 1.5).

Cellular glutathione levels can be reduced with the use of buthionine sulfoximine (BSO), which is an inhibitor of γ-glutamylcysteine synthetase (Figure 1.5). BSO can reverse cisplatin resistance mediated by an increase in glutathione levels (Jansen et al., 2002). However, this is not the case in all cisplatin-resistant cell lines with

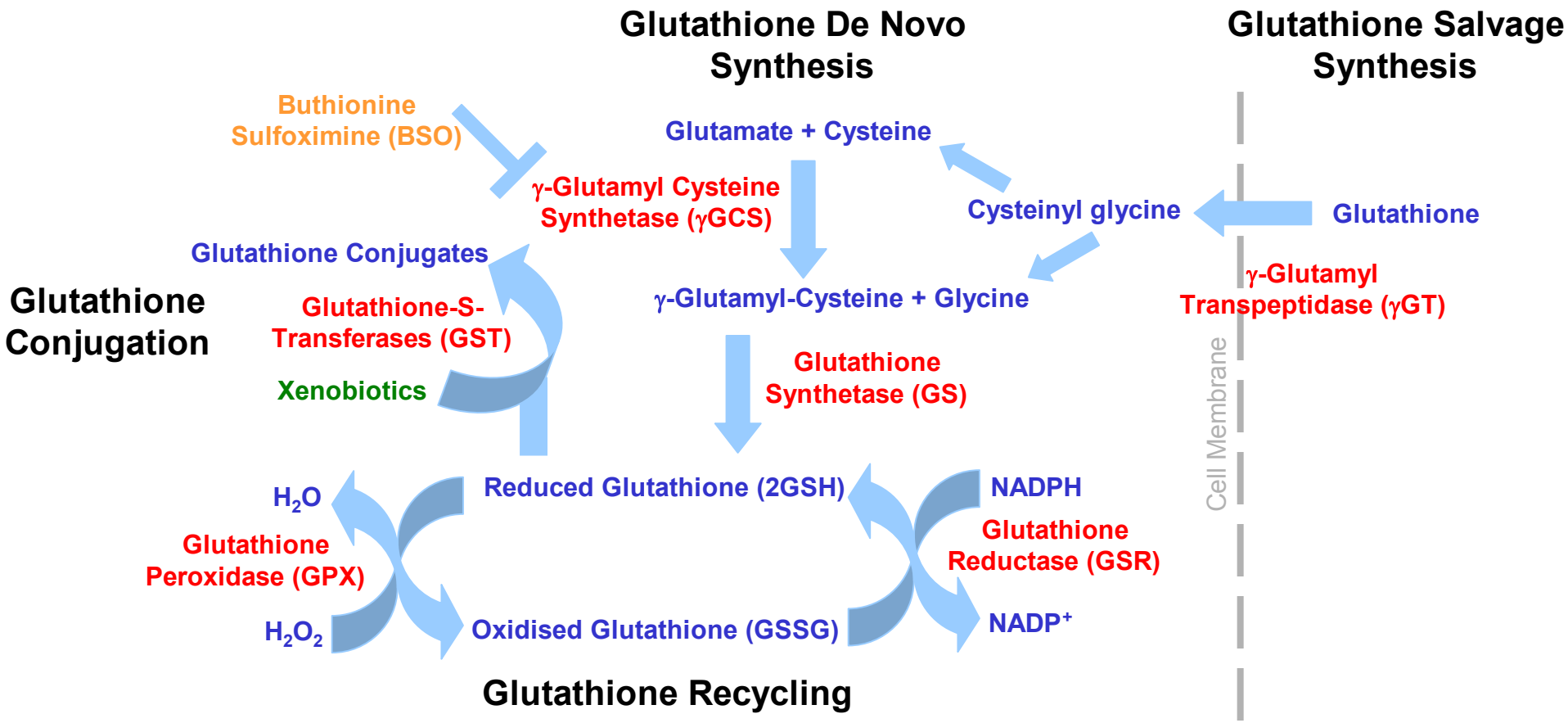

Figure 1.5. Glutathione metabolism. Biochemical pathways for glutathione synthesis, recycling and conjugation to xenobiotics. Adapted from Townsend et al., 2003 and Rahman et al., 1999.

elevated glutathione where treatment with BSO can lead to only minimal reversal (Lai et al., 1995).

1.6.1.2 Thioredoxin

Thioredoxin is another cellular redox protein which contains two redox-active cysteine residues in its catalytic centre, existing in either a reduced form with dithiol or in a oxidised form with the cysteine residues forming a disulfide bridge (Liu et al., 2002b). The cellular concentration of thioredoxin in mammals is normally much lower compared to that of glutathione yet thioredoxin is still an abundant protein. Thioredoxin does not conjugate and detoxify cisplatin like glutathione does. Rather, thioredoxin acts as a redox buffer to limit the damage caused by the formation of ROS in the cell. Thioredoxin has its own system of thioredoxin reductases and peroxidases that oxidise and reduce to recycle thioredoxin in the same way as the glutathione system. Thioredoxin also plays a role in redox mediated apoptotic signalling through apoptosis signal regulating kinase 1 (ASK1). When thioredoxin dissociates from ASK1 in response to increasing ROS apoptotic pathways are activated (Saitoh et al., 1998; Liu et al., 2002b).

The overexpression of thioredoxin can lead to cisplatin resistance (Yokomizo et al., 1995a). However, it seems that the overexpression of thioredoxin in isolation is not sufficient to confer cisplatin resistance in some cell models (Yamada et al., 1997). The Yamada study speculated that differences in the apoptotic pathways between different cell types may account for the lack of cisplatin resistance in response to increased thioredoxin. Differences in ASK1 mediated apoptotic signalling may explain the differences in cisplatin resistance in response to increased thioredoxin in different cell types.

1.6.2 Reduced intracellular accumulation of platinum chemotherapeutics

Reduced intracellular accumulation of cisplatin, which occurs either through reduced uptake or increased efflux, is a mechanism of resistance commonly observed in cisplatin-resistant SCLC cells (Teicher et al., 1991; Jain et al., 1996; Moritaka et al., 1998) (Table 1.4). However, some cisplatin-resistant SCLC cells do not show any

changes in the cellular accumulation of cisplatin (Twentyman et al., 1991; Twentyman et al., 1992). There are no reports of oxaliplatin-resistant SCLC cell lines. However, in oxaliplatin-resistant ovarian carcinoma cells, oxaliplatin resistance has been associated with decreased oxaliplatin accumulation in some models (Mishima et al., 2002) and not in others (Sharp et al., 2002). The study of tumour platinum accumulation is difficult in clinical samples as most surgery occurs before patients receive chemotherapy. The study of platinum accumulation in the clinic and animal models is also complicated by other factors which effect the uptake of drug such as tumour vascularisation. There appear to be no studies examining the levels of platinum accumulation in clinical samples in the context of drug resistance.

Cisplatin is not transported by P-glycoprotein – ABCB1 (P-gp) or multidrug resistance-associated protein 1 – ABCC1 (MRP1) (Hipfner et al., 1999) which are ABC transporters commonly associated with multidrug resistance. The overexpression of MRP2 – ABCC2 induces cisplatin resistance and it is thought that cisplatin is transported by MRP2 as a glutathione conjugate. Cisplatin resistance in cells overexpressing MRP2 has been reversed using an anti-MRP2 hammerhead ribozyme (Materna et al., 2005). However, any association between clinical cisplatin resistance and raised MRP2 levels in tumours remains to be established (Borst et al., 2000).

The major copper influx transporter CTR1 can regulate the cellular uptake of cisplatin, carboplatin and oxaliplatin, and the two copper efflux transporters ATP7A and ATP7B can regulate the efflux of these drugs (Safaei et al., 2005). There is also evidence that platinum drugs are distributed to various subcellular compartments via transporters that have evolved to manage copper homeostasis (Safaei et al., 2005). Increased ATP7B expression has been associated with poor prognoses in ovarian carcinoma patients. The same study found no association with the expression of other transport proteins P-gp, MRP1 and MRP2 (Nakayama et al., 2002). Some cisplatin-resistant cell lines are cross-resistant to copper and have decreased platinum accumulation as their mechanism of resistance (Katano et al., 2002). Cells selected for copper resistance are also cross resistant to cisplatin (Safaei et al., 2004).

1.6.3 Inhibition of the apoptotic response

Apoptosis, or programmed cell death, is a mechanism by which a cell regulates its own death in order to control proliferation or prevent damaged cells from dividing. The apoptotic pathways are complex and interconnected but occur through two main pathways shown in a simplified diagram (Figure 1.6). The intrinsic or mitochondrial pathway releases cytochrome c from the mitochondria when stimulated and consequently activates the death signal. The extrinsic or cytoplasmic pathway is triggered by the activation of the death receptor Fas by Fas ligand (Ghobrial et al., 2005).

Cisplatin and oxaliplatin can induce apoptosis as a consequence of cellular damage. Inhibition of the apoptotic response is therefore another mechanism of platinum resistance. The decreased expression of pro-apoptotic factors or the increased expression of anti-apoptotic factors in response to drug treatment can lead to resistance. The apoptotic pathways are stimulated by a variety of interconnected signalling pathways including p53, NFκB, the ubiquitin proteosome system and the PI3K pathway (Ghobrial et al., 2005). Any change in these pathways that leads to an inhibition of apoptosis will also promote resistance.

Cisplatin resistance has been associated with increased expression of the anti-apoptotic protein Bcl-2 in SCLC cells (Locke et al, 2003). Decreased expression of Bcl-2 has also paradoxically been associated with cisplatin resistance in SCLC cells (Kumar et al., 2004) and ovarian carcinoma cells (Beale et al., 2000). These results suggest two things; that different mechanisms of platinum resistance are at work in these studies and that the apoptotic response of a cell cannot be determined by examining one member of the pathway. The fate of a cell is determined by the balance of all pro- and anti-apoptotic factors.

Changes in apoptotic pathways have been previously associated with two SCLC cell lines selected for acquired resistance to platinum (Table 1.4). This does not mean that changes in apoptotic pathways are not involved with platinum resistance in other models rather that it has not been studied extensively. Once either increased glutathione or decreased platinum accumulation is found as a mechanism of platinum

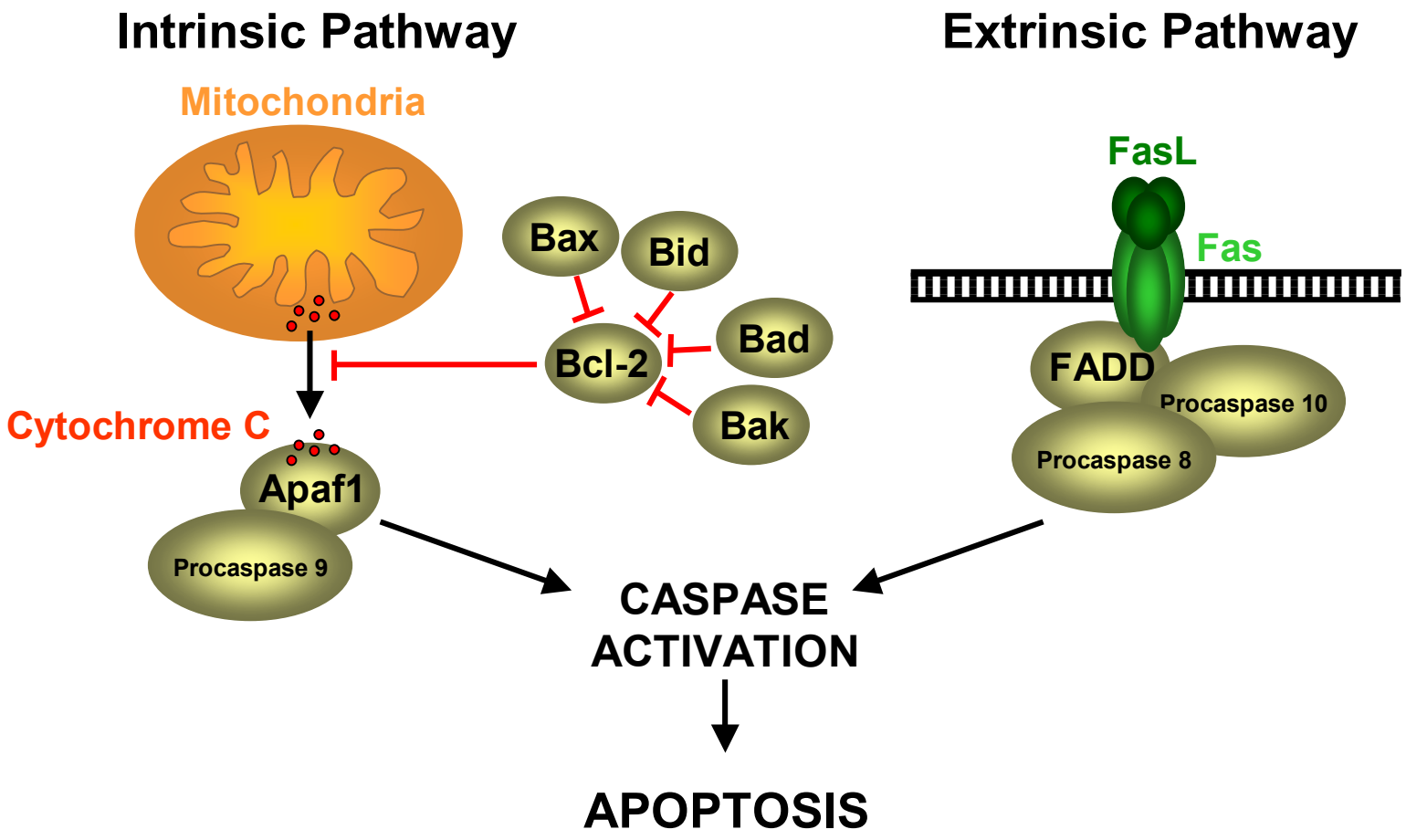

Figure 1.6. Basic apoptotic pathways. The intrinsic or mitochondrial pathway releases cytochrome c from the mitochondria when stimulated and consequently activates the death signal. The extrinsic or cytoplasmic pathway is triggered by the activation of the death receptor Fas by Fas Ligand. Adapted from Ghobrial et al., 2005.

resistance, apoptotic pathways are not always studied (Table 1.4). Apoptotic pathways are also often studied in response to drug treatment rather than in resistant cell lines. With this kind of approach the activation of the PI3K/Akt pathway has been shown to protect against cisplatin induced apoptosis in SCLC cells (Belyanskaya et al., 2005).

Table 1.5 lists some further examples of changes in apoptotic proteins and pathways that have been associated with platinum drug resistance in models of acquired platinum resistance other than SCLC. Platinum resistance when mediated by changes in apoptotic pathways is often associated with increased activity of survival pathways such as the PI3K/Akt pathway, discussed below in section 1.6.3.1, or increased expression of anti-apoptotic proteins such as Bcl-2 and survivin.

1.6.3.1 PI3K/Akt signalling pathway and platinum resistance

Activation of the PI3K/Akt signalling pathway has been associated with cisplatin resistance in ovarian carcinoma cells (Lee et al.,2005) and has been shown to protect against cisplatin induced apoptosis in SCLC cells (Belyanskaya et al., 2005). Inhibition of the PI3K/Akt pathway has also been shown to enhance the sensitivity to cisplatin in SCLC cells (Tsurutani et al., 2005) and squamous cell carcinoma cells (Aoki et al., 2004).

The PI3K/Akt pathway is activated as shown in Figure 1.7. Activation of growth factor receptor protein tyrosine kinases results in autophosphorylation on tyrosine residues. PI3K is recruited to the membrane by directly binding to phosphotyrosine consensus residues of growth factor receptors. PI3K activation results in production of the second messenger phosphatidylinositol-3,4,5-trisphosphate (PIP3). PIP3 recruits a subset of signalling proteins including Akt. Once activated, Akt mediates the inhibition of several pro-apoptotic proteins, resulting in cellular survival, growth and proliferation through various mechanisms (Vara et al., 2004).

PTEN negatively regulates the PI3K/Akt pathway (Vara et al., 2004). The loss or mutation of PTEN has been associated with carcinogenesis and it is considered a tumour suppressor gene. In a comparative study between SCLC and non-SCLC mutations in the PTEN gene were analysed. Loss or mutation of PTEN was not found

Table 1.5 Changes in apoptotic proteins associated with acquired platinum resistance.

Cell Line	Carcinoma	Selecting Agent	Fold Resistance	Changes in Apoptotic Pathways	Reference
OVCAR-3/CDDP	Ovarian	Cisplatin	4.8	Activation of PI3K/Akt with inhibition of pro-apoptotic Bax	(Lee et al., 2005)
2008/C13	Ovarian	Cisplatin	12	Increased expression of apoptosis inhibiting XIAP. Decreased expression of FasL	(Parekh et al., 1996; Mansouri et al., 2003)
LNCaP/C1 LNCaP/C2 LNCaP/C3	Prostate	Cisplatin	6.3 9.1 22.3	Increase in expression of apoptosis inhibiting proteins Bcl-2, XIAP and Survivin	(Nomura et al., 2005)
UM-SCC-23/resSCC-23	Squamous Cell	Cisplatin	5.2	Increased survival signalling pathways PI3K/Akt and Raf/MEK/ERK	(Aoki et al., 2004)
HCT116/R2	Colon	Oxaliplatin	68.4	Loss of pro-apoptotic Bax	(Gourdier et al., 2002)

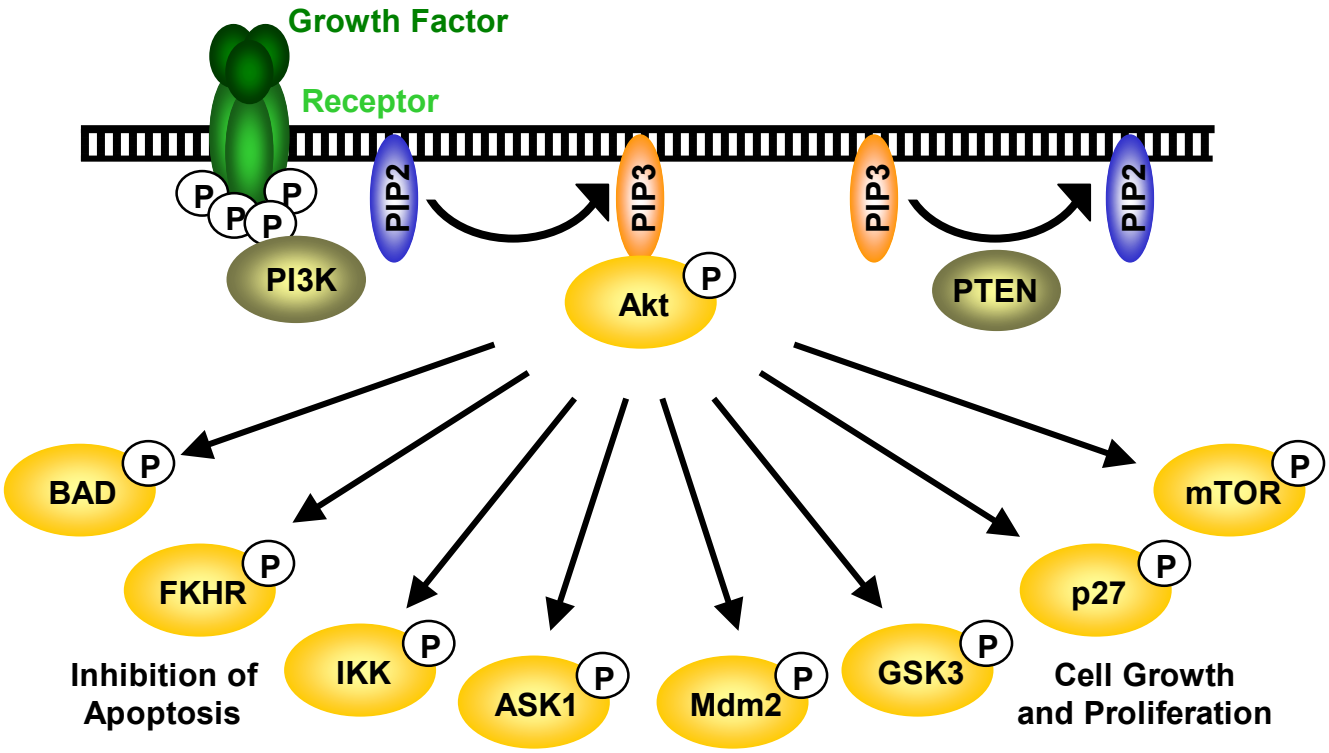

Bad - Suppression of Bad pro-apoptotic activity

FKHR – Forkhead family - inhibition of transcription of pro-apoptotic genes

IKK - Induction of NF-κB transcriptional activity; activation of transcription of survival genes

ASK1 - Inhibition of stress activated kinases

Mdm2 - Inhibition of p53 regulated processes

GSK3 - Inhibition of GSK3 catalytic activity

p27 - Nuclear exclusion; prevention of its antiproliferative activity

mTOR - Modulation of mRNA translation

Figure 1.7 PI3K/Akt signalling. Activation of tyrosine kinase receptors leads to the recruitment of PI3K to the cell membrane. PI3K activation results in the production of a second messenger PIP3 which activated Akt kinase. The downstream effects of Akt kinase include inhibition of apoptotic pathways and promotion of cell growth and proliferation. Adapted from Vara et al., 2004.

ASK1 – apoptosis signal-regulating kinase 1, GSK3 – Glycogen synthase kinase 3, IKK - IκB kinase, PI3K - Phosphatidylinositol 3-kinase, PIP3 - Phosphatidylinositol-3,4,5-trisphosphate, mTOR – molecular target of rapamycin.

in non-SCLC whereas mutations occurred in 18% of SCLC cell lines and 10% of SCLC tumour biopsies (Yokomizo et al., 1998). The PI3K/Akt pathway is often activated in the oncogenesis of SCLC through a loss of PTEN. A loss of PTEN in response to treatment with platinum would also contribute to the platinum resistance phenotype.

1.6.4 Increased bypass of platinum adducts

In DNA replication, the double-stranded DNA is unwound and separated into two complementary strands. DNA polymerases bind to each strand and insert the appropriate complementary bases dATP, dCTP, dGTP and dTTP. The presence of platinum adducts on the strand to be replicated can block the progress of DNA polymerase.

Some DNA polymerases are able to replicate a platinum containing DNA strand relatively well and platinum-resistant cells have either elevated levels of these polymerases or mutant DNA polymerases with enhanced trans-lesion replication activity (Vaisman et al., 2000). This ability is a double edged sword for the cell, while it allows replication it also promotes mutation as some DNA polymerases can insert the incorrect bases while bypassing a platinum adduct (Bassett et al., 2003). The efficiency of bypass of platinum adducts, in human cells as measured by the primer extension assay is pol η (eta) > pol μ (mu) > pol β (beta) >> pol γ (gamma) (Chaney et al., 2005). The properties of the DNA polymerases in respect to bypassing platinum adducts are presented in Table 1.6 (Chaney et al., 2005).

To date no cisplatin-resistant SCLC cell line has been shown to have increased replicative bypass ability. However, the majority of work in this area as summarised in Table 1.6, has been conducted *in vitro* and not in resistant cell lines. Increased replicative bypass by DNA polymerases has been associated with cisplatin resistance in ovarian carcinoma cells (Mamenta et al., 1994). Increased replicative bypass has also been associated with cisplatin and oxaliplatin resistance in platinum-resistant murine leukemia cells (Gibbons et al., 1991). In both of these studies alkaline sucrose gradient sedimentation was used to determine the influence of cisplatin and oxaliplatin adducts on the inhibition of replicon initiation and DNA chain elongation.

Table 1.6 Properties of DNA polymerases in respect to platinum adduct bypass.

DNA Polymerase	Properties
Pol α (alpha)	Pol α stalls replication on meeting a Pt-adduct (Vaisman et al., 2000).
Pol β (beta)	Catalyses synthesis past oxaliplatin adducts with greater efficiency than cisplatin adducts(Chaney et al., 2005). Pol β is able to elongate the arrested replication products of polymerases α and δ, to complete stalled replication but in an error prone manner (Vaisman et al., 2000).
Pol γ (gamma)	Pol γ is localised in the mitochondria and is, therefore, unlikely to contribute to the overall mutagenicity of Pt–DNA adducts (Chaney et al., 2005).
Pol δ (delta)	Pol δ stalls replication on meeting a Pt-adduct (Vaisman et al., 2000).
Pol ε (epsilon)	Pol ε stalls replication on meeting a Pt-adduct (Kartalou et al., 2001).
Pol ζ (zeta)	Bypasses Pt–DNA adducts with very low efficiency and is unlikely to make a significant contribution in vivo. However, several studies have shown that pol ζ has the ability to extend mismatches formed opposite bulky DNA adducts suggesting that it could contribute to error-prone translesion synthesis past Pt–DNA adducts by extending the mismatches formed by other DNA polymerases (Chaney et al., 2005).
Pol η (eta)	Catalyses synthesis past oxaliplatin adducts with greater efficiency than cisplatin adducts(Chaney et al., 2005). Bypasses Pt-adducts in a relatively error free manner (Chaney et al., 2005)
Pol μ (mu)	Bypasses Pt–DNA adducts in a mostly error-prone manner and catalyses a high percentage of frame-shifts in the vicinity of the adduct. Since the other translesion polymerases predominantly catalyse misinsertions opposite Pt–DNA adducts, pol μ may very well be responsible for the 15–20% frameshift mutations seen in the vicinity of cisplatin and carboplatin adducts.(Chaney et al., 2005).

DNA polymerase β is able to elongate the arrested replication products of polymerases α and δ, to complete stalled DNA replication. However, DNA polymerase β completes this stalled replication in an error prone manner (Vaisman et al., 2000). DNA polymerase β also synthesises past oxaliplatin adducts with greater efficiency than cisplatin adducts (Chaney et al., 2005). Increased expression of DNA polymerase β by transfection leads to cisplatin resistance in breast carcinoma cells (Raaphorst et al., 2001). Increased expression of DNA polymerase α and β was associated with cisplatin resistance in colon carcinoma cells (Scanlon et al., 1989). Increased expression of DNA polymerase β has also been associated with the response to cisplatin-based chemotherapy treatment in colon carcinoma patients (Kashani-Sabet et al., 1990).

Stalled RNA polymerases at platinum adducts produce various cellular responses such as nucleotide excision repair (Section 1.6.5.1), polymerase degradation, and apoptosis. The stalled polymerase can be dissociated from the DNA by subsequent polymerases initiated from the same template. A polymerase stalled at a platinum DNA adduct can also resume transcription after the platinum adduct is removed from the template (Jung et al., 2003). There appear to be no studies examining if RNA polymerases bypass platinum adducts like DNA polymerases.

1.6.5 DNA repair

The formation of platinum adducts on DNA is a major mechanism of platinum cytotoxicity. An increase in the efficiency of DNA repair can promote platinum resistance. Cisplatin forms 4 main types of adducts on DNA presented in Figure 1.8. 90% of platinum adducts are the intrastrand variety, the remaining 10% are interstrand cross links which are thought to be more cytotoxic as they can lead to double-strand breaks (Wozniak et al., 2002). There are many kinds of DNA repair which relate to platinum resistance. Nucleotide excision repair is the only mechanism for removing bulky intrastrand adducts which are 90% of platinum adducts. The 10% interstrand cross links are repaired by a combination of nucleotide excision repair and homologous repair which are used to fix double-strand DNA breaks. Other DNA repair mechanisms are often upregulated in response to treatment with platinum, not

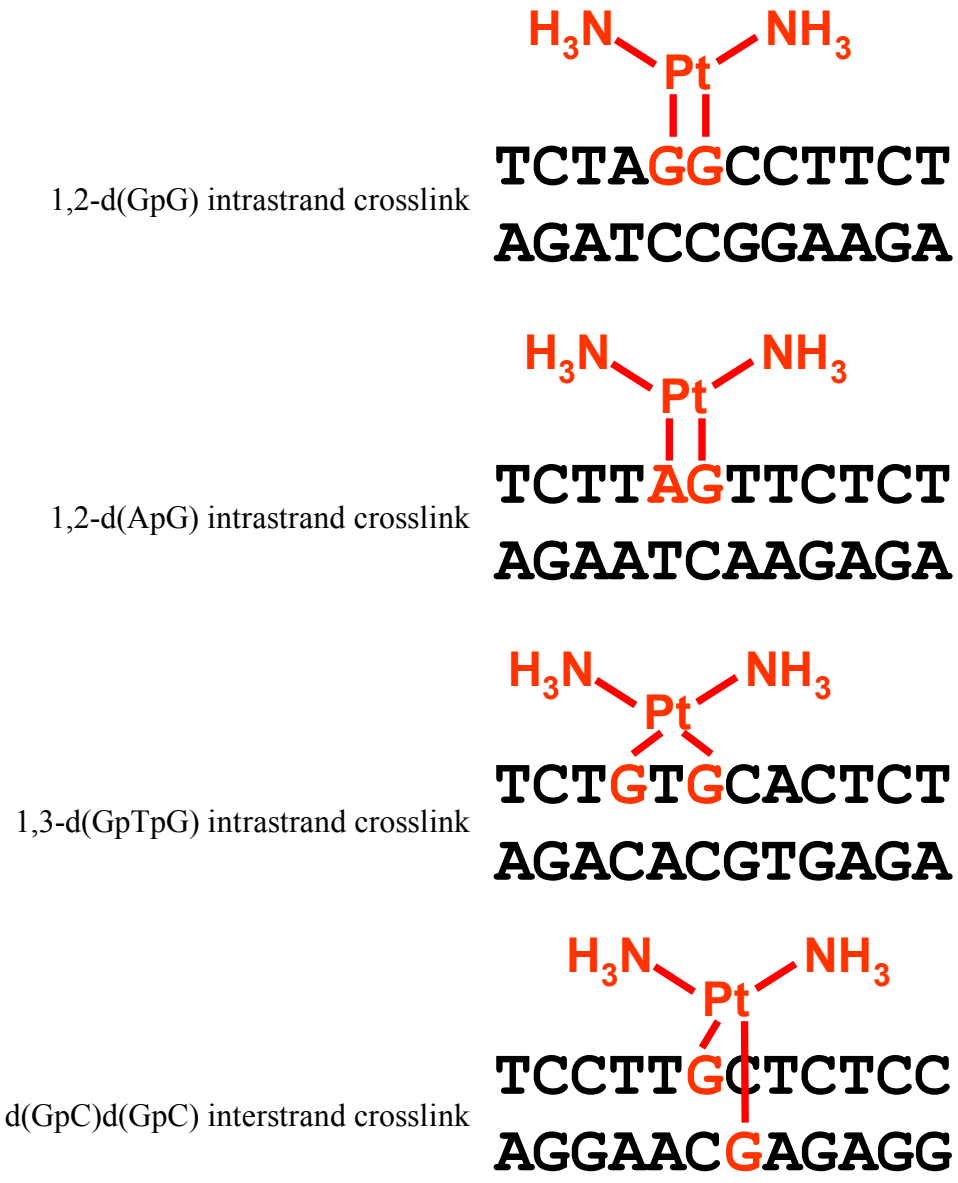

Figure 1.8 Types of platinum adducts. Cisplatin forms three kinds of intrastrand adducts with DNA 1,2-d(GpG), 1,2-d(ApG) and 1,3-d(GpTpG). Cisplatin also forms interstrand crosslinks with DNA d(GpC)d(GpC). Platinated bases are indicated in red. Adapted from Wozniak et al., 2002.

to remove the adducts but to remove other damage such as mispairing of bases made by error-prone DNA polymerases as described in Section 1.6.4.

There is significant cross talk between the major DNA repair pathways and many proteins have dual functions both in DNA repair and apoptosis (Bernstein et al., 2002). These mechanisms normally protect against mutation that leads to carcinogenesis. If there is too much DNA damage and the cell cannot be repaired, apoptosis is initiated.

1.6.5.1 Nucleotide excision repair

Nucleotide excision repair recognises damaged regions of DNA by the abnormal structure of the backbone of the DNA double helix, then excises and replaces them (Sancar et al., 2004). Nucleotide excision repair is the only mechanism by which bulky DNA adducts, including those generated by platinum drugs, are removed from DNA in human cells (Reardon et al., 1999). Cisplatin and oxaliplatin DNA adducts are removed to a similar extent by nucleotide excision repair due to its broad substrate range (Reardon et al., 1999).

There are two pathways in nucleotide excision repair, transcription-coupled and global genome. The transcription-coupled pathway repairs transcription blocking lesions in transcribed DNA strands of active genes whereas the repair of lesions in the non-transcribed strand of active genes and non-transcribing genome is carried out by the global genome pathway (Furuta et al., 2002). Transcription-coupled nucleotide excision repair deficient cells are hypersensitive to cisplatin irrespective of their global genome nucleotide excision repair status. This suggests that the response to cisplatin is governed by the transcription-coupled pathway repairing transcription blocking lesions as a priority over the rest of the genome (Furuta et al., 2002).

Nucleotide excision repair involves the following steps as illustrated in Figure 1.9 (Huberman, 2005):-

a) Damage recognition
b) Binding of a multi-protein complex at the damaged site

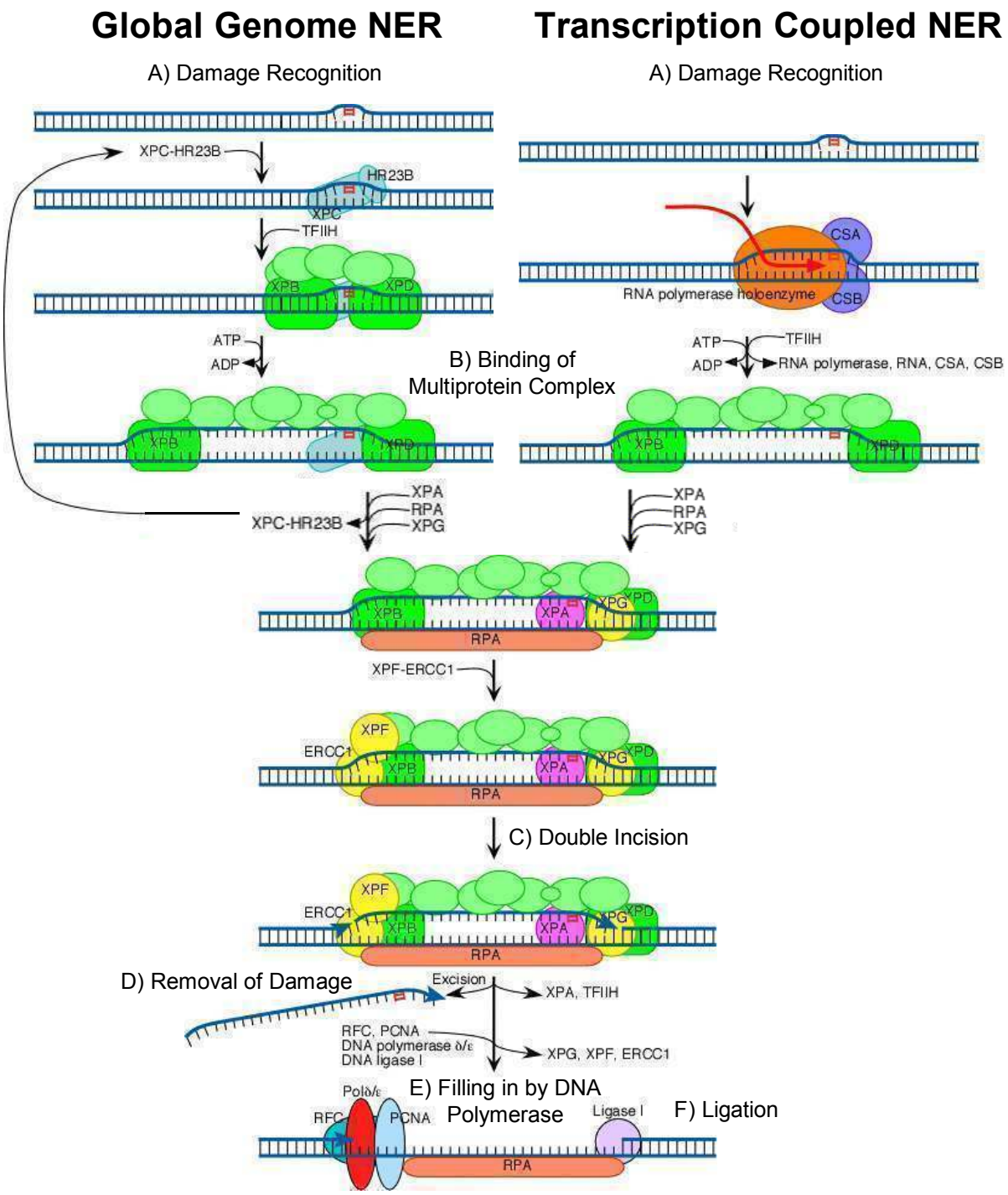

Figure 1.9 Nucleotide excision repair. Nucleotide excision repair (NER) occurs via two pathways. Global genome NER which is detected by the distortion of the double helix. Transcription coupled NER which is detected by the stalling of RNA polymerase. The strand containing the platinum adduct is excised by the ERCC1-XPF complex at the 5' end and XPG at the 3' end. The resulting gap is then filled in by DNA polymerase. Adapted from Sancar et al., 2004.

c) Double incision of the damaged strand several nucleotides away from the damaged site, on both the 5' and 3' sides
d) Removal of the damage-containing oligonucleotide from between the two nicks
e) Filling in of the resulting gap by a DNA polymerase
f) Ligation

Global genome nucleotide excision repair repairs non-actively transcribed genes. DNA damage is recognised by the distortion of the helical structure and bound by a heterodimer consisting of the XPC-HR23B proteins (blue). This permits the binding of the general transcription factor TFIIH, which has 10 subunits (green). Two of these subunits XPB and XPD (bright green) are helicases, which bind to the damaged strand and use ATP to unwind a stretch of 20-30 nucleotides including the damaged site. XPA, RPA and XPG then bind to and stabilise the open complex. XPC-HR23B are then released and are free to be re-used at other damaged sites where the repair process has not yet been initiated (Huberman, 2005).

Transcription-coupled nucleotide excision repair repairs damage in actively transcribing genes. The transcription-coupled pathway is similar to the global genome pathway except for the recognition step. When transcribing RNA polymerase II encounters the DNA lesion and is stalled, two transcription-coupled repair specific factors CSA and CSB bind and activate nucleotide excision repair instead of XPC and HR23B as in global genome repair (Furuta et al., 2002; Huberman, 2005).

The repair process is the same for both types of nucleotide excision repair. XPG cuts on the 3' side of such a junction, while XPF- ERCC1 cuts on the 5' side of the lesion (Rosell et al., 2003). The damage-containing oligonucleotide is displaced with the binding of replicative gap repair proteins (RFC, PCNA, DNA polymerase delta or epsilon), and new DNA synthesis fills the gap. The final nick is sealed by DNA ligase I (Huberman, 2005).

Cisplatin-resistant SCLC cell lines have not had changes in DNA repair genes examined (Table 1.4). Cisplatin-resistant cell lines from other carcinomas have shown increased expression of proteins associated with the nucleotide excision repair pathway. Increases in the ERCC1-XPF complex has been associated with cisplatin

resistance ovarian carcinoma cells (Ferry et al., 2000). Increases in XPF has been associated with cisplatin resistance in epidermoid carcinoma cells (Mukai et al., 2002). Testicular tumour cells also have low levels of the XPA protein and the ERCC1–XPF complex. Therefore the unique sensitivity of testicular cells to cisplatin has been attributed to the inability of these cells to repair cisplatin damage by nucleotide excision repair (Koberle et al., 1999).

Decreased expression of ERCC1 mRNA has been associated with survival of non-SCLC patients receiving platinum-based chemotherapy (Lord et al., 2002). In contrast increased expression of XPA protein suggesting increased DNA repair capacity has been associated with survival in patients with ovarian carcinoma receiving platinum-based therapy (Stevens et al., 2005)

1.6.5.2 Cross links and double-strand breaks

Cross links due to platinum adducts are thought to be repaired by a combination of nucleotide excision repair and homologous recombination repair which is used to fix double-strand breaks. Double-strand breaks are fixed by either homologous recombination (which depends on the RAD51 family of proteins) or by non-homologous end joining mediated by the DNA-PK complex (Figure 1.10). A key intermediate in homologous recombination is the holliday intermediate, in which the two recombining duplexes are joined covalently by single-strand crossovers. Resolvases such as MUS81_MMS4 cleave the holliday junctions to separate the two duplexes. In the single-strand annealing mechanism, the duplex is digested by a 5'to 3' exonuclease to uncover microhomology regions that promote pairing, trimming and ligation. BRCA1 and BRCA2 are also involved in homologous recombination repair, but their precise roles are unclear (Sancar et al., 2004).

A downregulation of RAD51-mediated homologous recombination repair in knockout chicken B lymphocyte DT40 cells resulted in sensitivity to cisplatin treatment (Takata et al., 2000; Takata et al., 2001; Yonetani et al., 2005). Changes in the expression of RAD51 have not been associated with any cisplatin-resistant cell lines. RAD51 has not been previously studied in response to oxaliplatin. The expression of RAD51 was

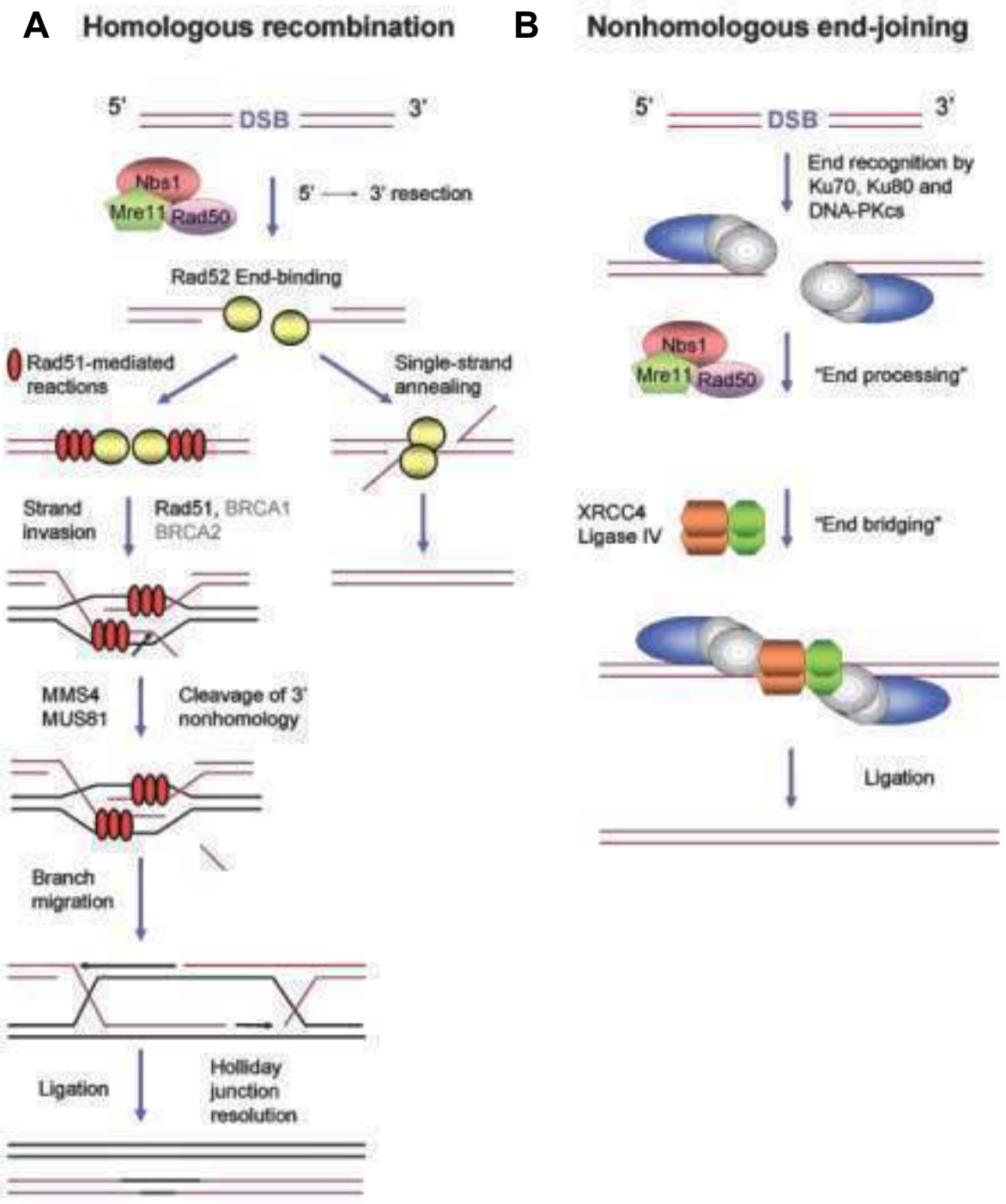

Figure 1.10 Double-strand break repair. Double-strand breaks are fixed by either A) Homologous recombination which depends on the RAD51-family of proteins or by B) Non-homologous end-joining mediated by the DNA-PK complex. Adapted from Sancar et al., 2004.

found to be non-prognostic in the response of non-SCLC to platinum-based combination chemotherapy (Wachters et al., 2005).

1.6.5.3 Base excision repair

Base excision repair removes damaged bases from the DNA strand (Figure 1.11). The damaged base is removed by a DNA glycosylase to generate an abasic site in the DNA strand. Depending on the initial events in base removal, the repair patch may be a single nucleotide (short patch) or 2–10 nucleotides (long patch). When the base damage is removed by glycosylase/AP lyase (3' cleavage) and APE1 endonuclease (5' cleavage), DNA polymerase β fills in the gap and is ligated by the Lig3/XRCC1 complex. When the AP site is generated by hydrolytic glycosylases or by spontaneous hydrolysis, repair usually proceeds through the long-patch pathway. APE1 cleaves the 5' end and the RFC/PCNA-Polδ/ε complex carries out repair synthesis and nick translation, displacing several nucleotides. The flap structure is cleaved off by FEN1 endonuclease and the long-repair patch is ligated by Ligase 1 (Sancar et al., 2004). Base excision repair has not been as strongly associated with platinum resistance as the other DNA repair pathways.

1.6.5.4 Mismatch repair

In normal cells mispaired bases or short insertions/deletions in DNA are recognised by proteins of the mismatch repair system, MutSα (heterodimer of MSH2 and MSH6) or MutSβ (heterodimer of MSH2 and MSH3) (Wozniak et al., 2002). MutSα recognises and corrects base-base mismatches and short insertion-deletion loops, whereas MutSβ recognises and corrects longer insertion-deletion loops (Parker et al., 2003; Meyers et al., 2004). The binding of the mismatch repair complex to damaged DNA can result in either successful mismatch repair or it can trigger an apoptotic response through the inhibition of anti-apoptotic Bcl-2 (Figure 1.12) (Bernstein et al., 2002). Mismatch repair has evolved to correct errors of DNA polymerases that escape their 3' to 5' exonucleolytic proofreading activity. Mismatches can be identified because they fail to form Watson–Crick base pairs. However, because neither nucleotide is damaged or modified it is not obvious

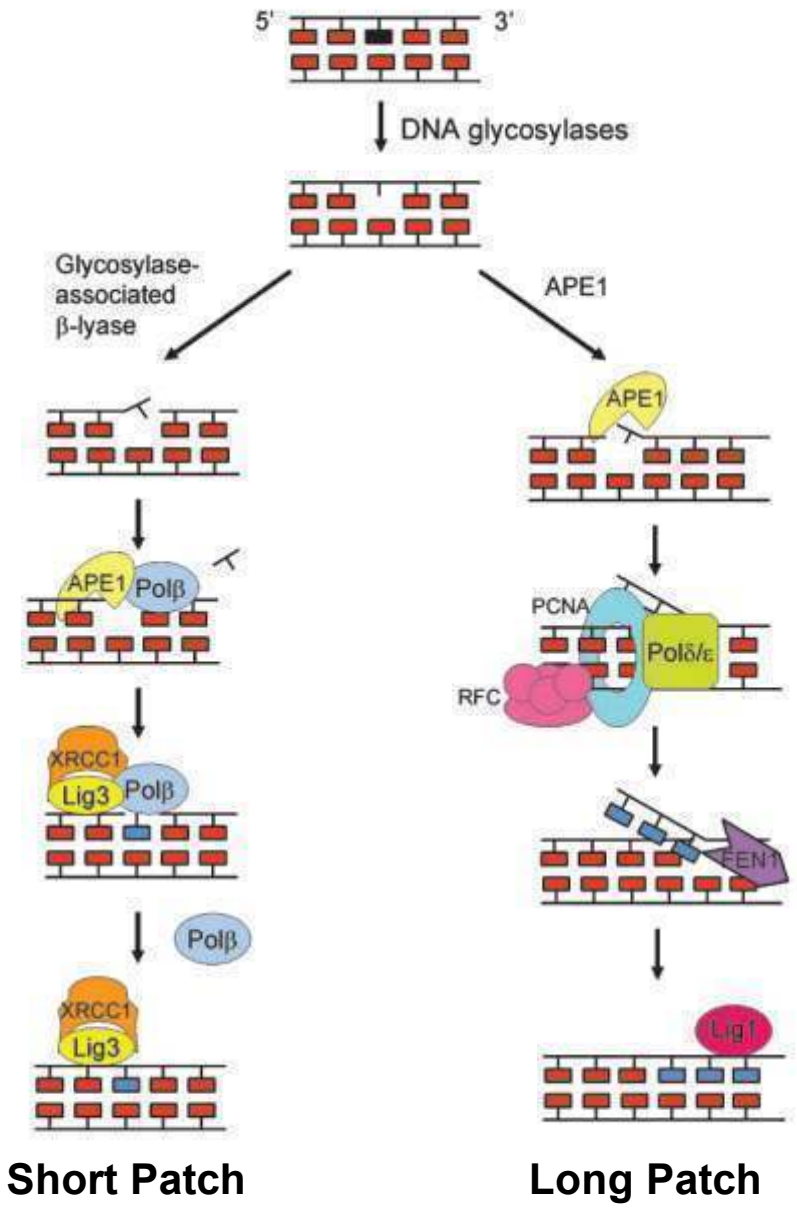

Figure 1.11 Base excision repair. The damaged base is removed by a DNA glycosylase to generate an abasic site. The repair patch may be then be a single nucleotide (short patch) or 2–10 nucleotides (long patch). Adapted from Sancar et al., 2004.

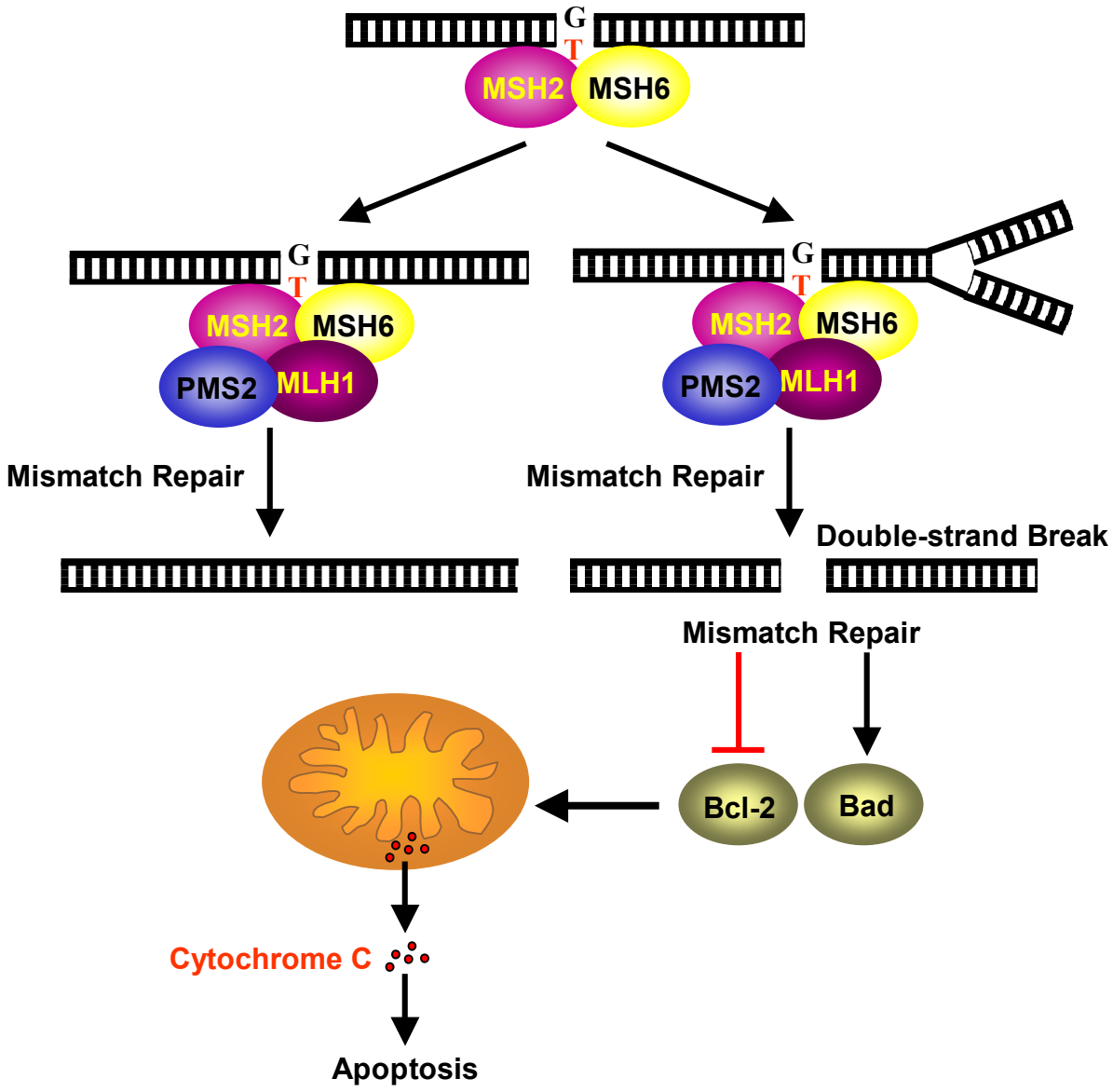

Figure 1.12 Mismatch repair and apoptosis. The binding of the mismatch repair complex to damaged DNA can result in either successful mismatch repair or it can trigger an apoptotic response through the inhibition of anti-apoptotic Bcl-2. Adapted from Bernstein et al., 2002.

which strand carries the correct genetic information and which carries the error. Therefore, mismatch repair cannot be accomplished by a mechanism such as base excision repair or nucleotide excision repair which simply excises the damaged base or a short DNA fragment containing the damage respectively. Unlike base excision repair and nucleotide excision repair, postreplicative mismatch repair has to be targeted exclusively to the newly synthesised strand, which carries, by definition, the erroneous genetic information. The newly synthesised strand can be distinguished in eukaryotes from the template strand by the presence of gaps between Okazaki fragments on the lagging strand, or by the free 3' terminus on the leading strand (Stojic et al., 2004).

Figure 1.13 summarises the steps of mismatch repair of the misincorporation of a thymidine (red) opposite a guanosine during DNA replication. The mismatch repair process commences with the binding of the MSH2/MSH6 heterodimer to the mismatched base and recruitment of the MLHl/PMS2 heterodimer. Both steps are ATP dependent. This complex can translocate in either direction along the DNA strand (green arrows). When it encounters a strand discontinuity (such as a gap between Okazaki fragments) that may be bound by PCNA (blue circle), loading of an exonuclease (EXO1, red) initiates degradation of the nicked strand towards the mismatch. Should the exonuclease dissociate before it reaches the mismatch, the single-stranded gap will be stabilised by RPA (turquoise diamonds). Loading of the second MSH2/MSH6/MLHl/PMS2 complex at the mismatch will stimulate a second round of exonucleolytic degradation. When this process is repeated a third time, the mismatch is removed. The RPA-stabilised single-stranded gap can now be filled in by the replicative polymerase and the remaining nick can be sealed by DNA ligase (Stojic et al., 2004).

The binding of the mismatch repair complex to Pt–DNA adducts appears to increase the cytotoxicity of the adducts, either by activating apoptosis or by causing "futile cycling" during trans-lesion synthesis past Pt–DNA adducts (Chaney et al., 2005). A decrease in mismatch repair protein MSH2 has been associated with cisplatin resistance in cisplatin-resistant cervix squamous carcinoma cells (Lanzi et al., 1998), as this leads to a decrease in adduct cytotoxicity. Similarly a decrease in MSH6 has been associated with cisplatin-resistant epidermoid carcinoma (Mukai et al., 2002).

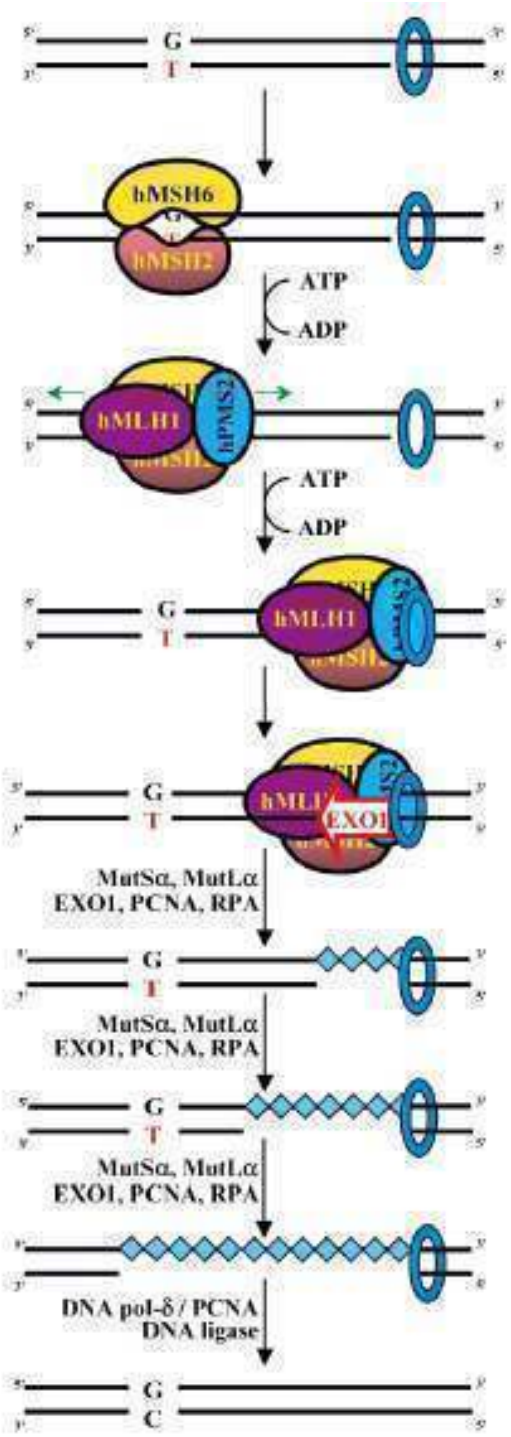

Figure 1.13 Mismatch repair. A G/T mismatch (red) has to be corrected to GC. The binding of MSH2/hMSH6 and then MLHl/PMS2 forms a complex that can translocate in either direction along the DNA strand (green arrows). When the complex encounters a strand discontinuity, loading of an exonuclease (EXO1, red) initiates degradation of the nicked strand towards the mismatch. Should the exonuclease dissociate before it reaches the mismatch, the single-stranded gap will be stabilised by RPA (turquoise diamonds). This process is repeated until the mismatch is removed. The RPA-stabilised single-stranded gap can now be filled in by DNA polymerase and the nick sealed by DNA ligase. Adapted from Stojic et al., 2004.

However, some models of acquired cisplatin resistance do not show changes in the mismatch repair pathways. Cisplatin- and oxaliplatin-resistant teratocarcinoma showed no changes in mismatch repair proteins MLH1 and MSH2 (Rennicke et al., 2005). Similarly, the expression of mismatch repair proteins MLH1 and MSH2 were shown to have no correlation with survival in ovarian carcinoma patients treated with cisplatin based chemotherapy.

The activity of oxaliplatin in cisplatin-resistant cell lines is thought to be due to repair or damage recognition processes that discriminate between cisplatin and oxaliplatin adducts. This has been best established for mismatch repair. Both the MSH2 and MutS components of the mismatch repair complex have been shown to bind with greater affinity to cisplatin adducts than to oxaliplatin adducts. More importantly, defects in mismatch repair increase resistance to cisplatin adducts, but have no effect on oxaliplatin adducts (Chaney et al., 2005).

1.6.5.5 Chromosomal aberrations and genomic instability

Chromosomal abnormality is one of the hallmarks of neoplastic cells, and the persistent presence of chromosomal instability has been demonstrated in human cancers, including lung cancer (Masuda et al., 2002). Chromosome abnormalities can be classified broadly into numerical alterations such as aneuploidy and structural alterations such as deletions, translocations, homogenously staining regions and double minute chromosomes. Missegregation of chromosomes may result from various causes, including defects in the mitotic spindle. Structural alterations of chromosomes may be caused by failure to repair DNA double-strand breaks due to the impairment of DNA damage checkpoints or DNA repair systems (Masuda et al., 2002).

Platinum chemotherapeutics bind to the DNA strand and can consequently cause chromosomal breakage and rearrangement. The chromosome instability phenotype would give lung cancer cells an excellent opportunity to efficiently alter their characteristics so as to be more malignant and suited to their microenvironment, thereby gaining a selective growth advantage (Masuda et al., 2002). Chromosome rearrangement due to treatment with platinum chemotherapeutics may promote the

development of drug resistance if amplifications or deletions of specific loci aid in conferring a platinum-resistant phenotype. Chromosomal rearrangement has been studied extensively in cisplatin-resistant cell lines, but no clear links to mechanisms of platinum resistance have been established by this method. Chromosomal rearrangement has not been studied in oxaliplatin-resistant cell lines.

1.7 Conclusions and Aims of PhD Project

Platinum drug resistance is a complex biological phenomena arising from many possible mechanisms of resistance. Cisplatin and oxaliplatin share many mechanisms of resistance but less is known about the newer drug oxaliplatin. Oxaliplatin is regarded as being active against cisplatin-resistant cancers, yet the mechanism of this activity is not well understood. Many models of platinum-resistant cancer have been developed, but not many at clinically relevant doses. The aims of this PhD project were therefore:-

- To develop clinically relevant cisplatin- and oxaliplatin-resistant small cell lung cancer cell lines by treating with the same doses used to treat cancer patients.
- To investigate if oxaliplatin has activity in cisplatin-resistant small cell lung cancer.
- To study the development of platinum resistance as well as the final stable mechanism of resistance.
- To examine the chromosomes of the platinum-resistant cell lines and attempt to link any changes in copy number to the resistant phenotype.
- To examine the biochemical pathways associated with platinum resistance by studying the mRNA and protein changes between the sensitive and resistant cell lines.

CHAPTER 2.0

MATERIALS AND METHODS

2.1 Materials

All reagents used were analytical grade or molecular biology grade. All solutions were prepared in Milli-Q deionised water. The source of all media, enzymes, antibodies, and commercial kits used is described in detail in the relevant experimental section.

2.1.1 Cytotoxic drugs

The cytotoxic drugs used in this project were obtained from the relevant drug company via Royal North Shore Hospital pharmacy and are summarised in Table 2.1.

Table 2.1 Cytotoxic drugs.

Cytotoxic Drug	MW	Supplier
Carboplatin	371.25	Pharmacia
Cisplatin	300.05	Pharmacia
Daunorubicin hydrochloride	564.0	Pfizer
Epirubicin hydrochloride (Pharmorubicin®)	580.0	Pharmacia
Etoposide	588.6	Pharmacia
Irinotecan hydrochloride (Camptosar®)	677.19	Pharmacia
Vinorelbine tartrate (Navelbine®)	1079.12	Pierre Fabre Medicament
Oxaliplatin (Eloxatin®)	397.3	Sanofi-Synthelabo
Taxol (Paclitaxel®)	853.9	Sigma
Taxotere®	861.9	Aventis
Vinblastine sulfate	909.1	David Bull Laboratories

MW – molecular weight

2.1.2 General solutions

Phosphate buffered saline (PBS)

0.15 M NaCl, 0.03 M NaH_2PO_4, 0.07 M Na_2HPO_4 , pH 7.2 stored at 4°C

10X Dulbecco's PBS (D-PBS)

NaCl (80 g/L), KCl (2 g/L), NaH_2PO_4 (14.4 g/L) and KH_2PO_4 (2.4 g/L), pH 7.2 stored at room temperature and diluted 1:10 before use.

20X SSC

175.3 g NaCl, 88.2 g Na_3Citrate pH 7.0 in 1L H_2O

TE buffer

10 mM Tris, 1 mM EDTA pH 8.0 autoclaved and stored at room temperature

2.2 Cell lines and tissue culture conditions

RPMI 1640 (with L-glutamine) 10% foetal calf serum

1 packet of RPMI (Thermotrace), 4.76 g HEPES (20 mM) and 0.85 g $NaHCO_3$ (1 mM) was added to 900 ml sterile H_2O. The media was adjusted to pH 7.34 with concentrated NaOH, and filtered under positive pressure with a 0.2 µM hollow fiber tip filter. The media was then supplemented with 100 ml sterile heat inactivated foetal calf serum (FCS) (Thermotrace) to a final volume of 1 L.

Cell freezing mixture

50% RPMI 1640, 40% FCS, 10% DMSO.

The human H69 small cell lung cancer cell line was obtained from the American Type Culture Collection. The drug-resistant H69CIS200 and H69OX400 sublines were selected for resistance to the chemotherapeutic drugs cisplatin and oxaliplatin respectively. H69 cells were treated with 200 ng/ml cisplatin or 400 ng/ml oxaliplatin for 4 days and allowed to recover in drug-free RPMI media for 3 weeks. This drug treatment was repeated 8 times. All cells were maintained in a humidified atmosphere with 5% CO_2 at 37°C. All cells were routinely checked and were *Mycoplasma* free. Cells growing in log phase were used for all experiments. Cells were subcultured twice a week to a density of 2.5 – 3.0 x 10^5 cells/ml. Lower densities were avoided as this cell line requires clumping between cells for adequate growth. The drug resistance of the H69CIS200 and H69OX400 cells was confirmed prior to each experiment by MTT cytotoxicity assay as described in Section 2.3.

The sensitive revertant cell lines H69CIS200-S and H69OX400-S were obtained by growing the resistant cell lines in drug-free media for 3 months. The sensitivity of the cells was confirmed by MTT cytotoxicity assay as described in Section 2.3.

2.3 MTT cytotoxicity assay

The resistance of cell lines to drugs was tested using the MTT cytotoxicity assay (Marks et al., 1992). Exponentially growing cells were plated into flat bottomed 96-well microtitre plates (Nunc) at a cell density of 6.0×10^4 cells/well. The cells were treated in triplicate with 2-fold serial dilutions of drug in a final volume of 200 µl. Drug-free controls were included in each assay. The plates were incubated for 5 days at 37°C in a humidified atmosphere with 5% CO_2. 50 µl of MTT (2.5 mg/ml in PBS solution, filtered and stored at 4°C) was then added to each of the wells and the cells incubated for a further 2 hours. The plates were centrifuged at 800g for 5 minutes, the culture medium aspirated and the formazan product dissolved in 100 µl DMSO. The plates were mixed for 15 minutes and the absorbance measured at 570 nm using a Biotek Synergy HT microplate reader. Cell viability was calculated as a percentage of control absorbance values.

$$\% \text{ Cell Viability} = \frac{\text{Average absorbance of triplicate wells}}{\text{Average absorbance of control wells}} \times 100$$

The 50% inhibitory concentration (IC_{50}) was defined as the drug concentration that produced a 50% decrease in cell viability. The relative resistance of the sublines was calculated as follows:-

$$\text{Relative Resistance} = \frac{IC_{50} \text{ of resistant subline}}{IC_{50} \text{ of parental H69 cell line}}$$

2.3.1 Radiation resistance

Exponentially growing cells were plated into flat bottomed 96-well microtitre plates (Nunc) at a cell density of 10^4 cells/well. The lower density was required to see a cytotoxic response to radiation. At the higher density cells entered a growth arrest and survived the radiation. The irradiation was performed by Regina Bromley from the Department of Radiation Oncology at Royal North Shore Hospital. The plate was irradiated with a dose of 8 Gy at the central axis of the plate, with two 60° lead

wedges to produce a gradient of doses across the 96 well plate. The range of doses was 0-22 Gy. The plate was incubated for 5 days at 37°C in a humidified atmosphere and then stained with MTT as described above.

2.4 Flow cytometry cell cycle analysis

Cells (10^6) were centrifuged (800 g for 5 minutes), washed in D-PBS and resuspended in 500 µl of D-PBS containing 50 µg/ml propidium iodide and 0.02% nonodet P-40 on ice. The cells were then incubated on ice for 10-15 minutes and analysed in a Becton Dickinson FACScan flow cytometer. To detect propidium iodide red fluorescence was monitored (FL2) using a 585/42 band pass filter, 10,000 events were collected and the data was analysed using CellQuest software.

2.5 Glutathione assay

Glutathione assay phosphate buffer
250 mM Na_2HPO_4

The glutathione assay was originally described by Suzukake et al 1982. Exponentially growing cells (2.5 x 10^6) were drug treated then were centrifuged at 800 g for 5 minutes, washed in 10 ml PBS, resuspended and transferred to a sterile eppendorf tube. These were then centrifuged the supernatant removed and the pellet resuspended in 150 µl of water at 4°C. Samples were sonnicated using a Sonifer® C Cell Disruptor B-30 (SmithKline) for 40 pulses at 10 V and checked microscopically to confirm disruption of cells. 12.5 µl of 30% sulphosalicyclic acid (SSA) was added and samples were mixed by vortexing. The samples were then incubated on ice for 15 minutes to allow protein precipitation and then centrifuged at 12,000 g for 5 minutes. The protein free supernatant was then collected, and frozen before analysis. Glutathione standards ranging from 0 – 25 µg/ml, prepared in 3% SSA were assayed to ensure the enzymatic reaction was linear over this concentration range (Figure 2.1).

The reaction was carried out in triplicate in flat bottomed 96-well microtitre plates, with each well containing the following:- 20 µl lysate or standard, 20 µl 1 M

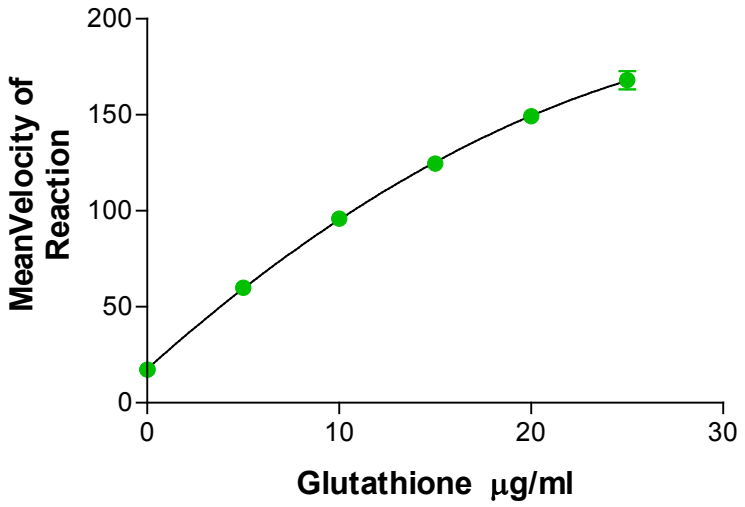

Figure 2.1 Glutathione assay standard curve. Glutathione standards (•) ranging from 0 – 25 μg/ml, prepared in 3% SSA were assayed as described in section 2.5. Means and standard deviations of triplicate wells are shown.

triethanolamine buffer pH 8.0 (Sigma), 120 µl 1 mM NADPH in glutathione assay phosphate buffer and 20 µl 6 mM DTNB in glutathione assay phosphate buffer

The plate was then equilibrated at 30°C for 3 minutes and 0.3 units glutathione reductase (Sigma) added per well. The plate was then read at 412 nm every 34 seconds for 18 readings, mixing for 5 seconds each reading using a Biotek Synergy HT microplate reader. The velocity of the reaction was then calculated for each sample.

2.6 Platinum accumulation

5 x 10^6 cells were treated with platinum chemotherapeutics. Cells were then centrifuged (800 g for 5 minutes), washed in 10 ml PBS, transferred to a sterile eppendorf tube, centrifuged and the supernatant carefully removed. The cell pellets were stored at -20°C prior to analysis. The pellet of platinum treated cells was dried on a heating block for 3 hours, resuspended in 100 µl of nitric acid and incubated at 90°C for 3 hours. Samples were then resuspended in 200 µl of 0.1 M nitric acid and analysed by atomic absorption using a platinum photron hollow cathode lamp in a Varian SpectrAA-400-Zeeman spectrophotometer. Platinum standards (0-300 ppb) were prepared from a commercial platinum standard (Varian) in 0.1 M nitric acid. 20 µl of samples or standards were analysed. The standard curve was linear over this range (Figure 2.2) The furnace operating conditions and instrument parameters were as recommended by Varian and are summarised in Tables 2.2 and 2.3.

Table 2.2 Atomic absorption furnace operating conditions for platinum.

Step	Temperature (°C)	Time (sec)	Gas Flow (L/min)	Read Command
1	85	5	3	No
2	95	40	3	No
3	120	10	3	No
4	1000	5	3	No
5	1000	1	3	No
6	1000	2	0	No
7	2700	1.3	0	Yes
8	2700	2	0	Yes
9	2700	2	3	No

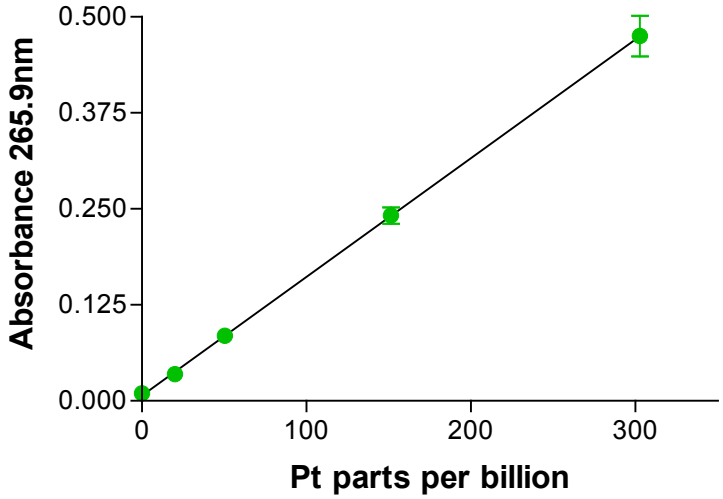

Figure 2.2 Platinum accumulation standard curve. Platinum standards (•) ranging from 0-300 parts per billion were prepared from a commercial platinum standard (Varian) in 0.1 M nitric acid and analysed as described in section 2.6. Means and standard deviations of triplicate samples are shown.

Table 2.3 Atomic absorption instrument parameters for platinum.

Lamp Current	10 mA
Spectral Bandwidth	0.2 nm
Wavelength	265.9 nm
Maximum Absorbance	1.1
MSR%	82%

2.6.1 Analysis of electrolytes which could interfere with the platinum assay

Within the 0.2 nM spectral bandwidth of the atomic absorption wavelength for Pt there are other elements which could add to the Pt signal. There are several trace elements but the element of most abundance and most likely to interfere is sodium at 266.1 nm. The sodium, potassium and chloride concentration of the cells was measured by the PaLMS laboratories at Royal North Shore Hospital. 5 x 10^6 cells were sonnicated in 200 µl of deionised water and analysed by a Roche Modular Autoanalyser & Dimension RxL MAX.

2.7 Genomic DNA extraction

Cell lysis buffer

1.28 M sucrose, 40 mM Tris, 20 mM $MgCl_2$, 4% Triton X-100, pH 7.5

Digestion buffer

800 mM guanidine HCl, 30 mM Tris, 30 mM EDTA, 5% Tween-20,
0.5% Triton X-100, pH 8.0

Equilibration buffer

750 mM NaCl, 50 mM MOPS, 15% isopropanol, 0.15% Triton X-100, pH 7.0

Wash buffer

1.0 M NaCl, 50 mM MOPS, 15% isopropanol, pH 7.0

Elution buffer

1.25 M NaCl, 50 mM Tris, 15% isopropanol, pH 8.5

Genomic DNA was extracted from 5 x 10^6 cells using Genomic tips from Qiagen according to the manufacturers instructions. Briefly, cells were lysed in a 1 in 4 dilution of cell lysis buffer for 10 minutes at 4 ℃, this lyses the cells but stabilises and preserves the nuclei. Lysed cells were then centrifuged at 1300 g for 15 minutes at 4 °C and the supernatant discarded. Pelleted nuclei were washed in cell lysis buffer and recentrifuged as previously. The nuclei were resuspended in digestion buffer and vortexed thoroughly, this lyses the nuclei and denatures proteins such as nucleases and histones. Proteinase K was added to a final concentration of 1 mg/ml and incubated for 1 hour at 50°C to strip the DNA of all bound proteins. The Genomic tip was treated with equilibration buffer and then the genomic DNA sample loaded and allowed to bind to the column. The Genomic tip was washed with wash buffer and then the genomic DNA eluted with the higher salt and pH elution buffer. The genomic DNA was precipitated with room temperature isopropanol and then centrifuged at 3000 g for 30 minutes. The genomic DNA pellet was then washed with ice-cold 70% ethanol and recentrifuged as stated previously. The genomic DNA pellets were then air dried and then resuspended in TE buffer and frozen at –20 °C.

2.7.1 Assessing yield and purity of genomic DNA

10X TBE buffer

54.0 g Tris Base, 27.5 g Boric Acid, 20 ml 0.5M EDTA, pH 8.0 made to 1L

1% Agarose TBE gel with 0.5 µg/ml EtBr

1 g Agarose, 10 ml 10X TBE Buffer, 90 ml H_2O, heated to boiling in a microwave. Solution was cooled and 5 µl EtBr (10 mg/ml) was added prior to pouring.

The yield of DNA in each sample was determined by diluting 1 µl of DNA in 200 µl of TE. Purity was monitored by a A260 nm:A280 nm which was normally 1.8-2.0. The concentration of DNA was determined by the A260 nm using the following equation.

DNA (µg/ml) = Absorbance 260 nm x 40 µg/ml x Dilution Factor

1 µl of purified DNA was combined with 5 µl of 6X DNA loading buffer (Promega) and run on a 1% agarose gel TBE gel in 1X TBE running buffer. The gel was run at 100 V for approximately 60 minutes until the loading dye front had reached the bottom of the gel. The gel was visualised under UV light to ensure there was whole genomic DNA present with no degradation.

2.8 Affymetrix genechip mapping 10K array

The Genechip Mapping 10K Array Xba 131 (Affymetrix) was performed by the CSIRO Division of Molecular and Health Technologies, North Ryde, NSW, Australia. The array provides good genome-wide coverage indicated in red in Figure 2.3, apart from some centromeres and telomeres as indicated in black (Matsuzaki et al., 2004). The array required 250 ng of total genomic DNA at a concentration of 50 ng/µl in TE buffer. The genomic DNA was digested with the restriction enzyme Xba1 and then ligated to adaptors recognising the cohesive four base overhangs. All fragments resulting from restriction enzyme digestion, regardless of size, are substrates for adaptor ligation. A generic primer, which recognises the adaptor sequence, is used to amplify ligated DNA fragments and PCR conditions are optimised to preferentially amplify fragments in the 250-1000 bp size range. The amplified DNA is labelled and hybridised to the Genechip array. The array is washed and stained on a Genechip fluidics station and scanned on a Genechip scanner (Figure 2.4).

The results of the array were then analysed with the Affymetrix chromosomal copy number tool. The Affymetrix system compares the chromosomal copy number tool data to a pool of normal samples in order to determine SNPs that have changed. The data from this study had to be analysed differently to compare cytogenetically abnormal samples to each other. The resistant and revertant samples were compared to the drug-sensitive parent by the following method. The chromosomal copy number data for each chromosome was smoothed by averaging a window of 20 SNPs. Significant differences, indicating amplifications or deletions were defined as any smoothed region which had at least 3 SNPs in a row in which the resistant cell line differed from that of the parental by a gene copy number of at least 0.5.

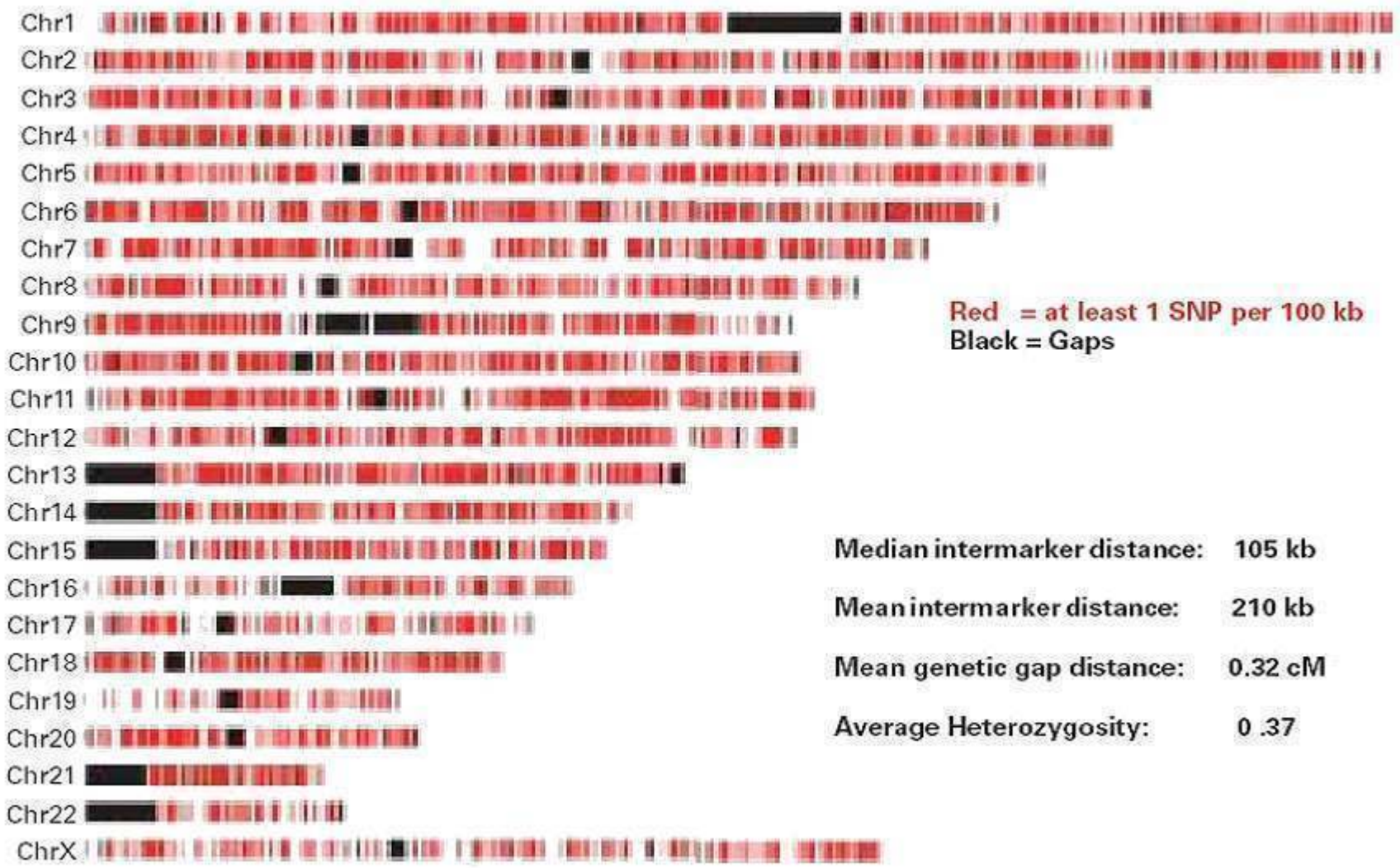

Figure 2.3 Genome coverage of the Affymetrix 10K SNP array. The 10K SNP array provides good genome-wide coverage, indicated in red, apart from some centromeres and telomeres as indicated in black. Adapted from Matsuzaki et al., 2004.

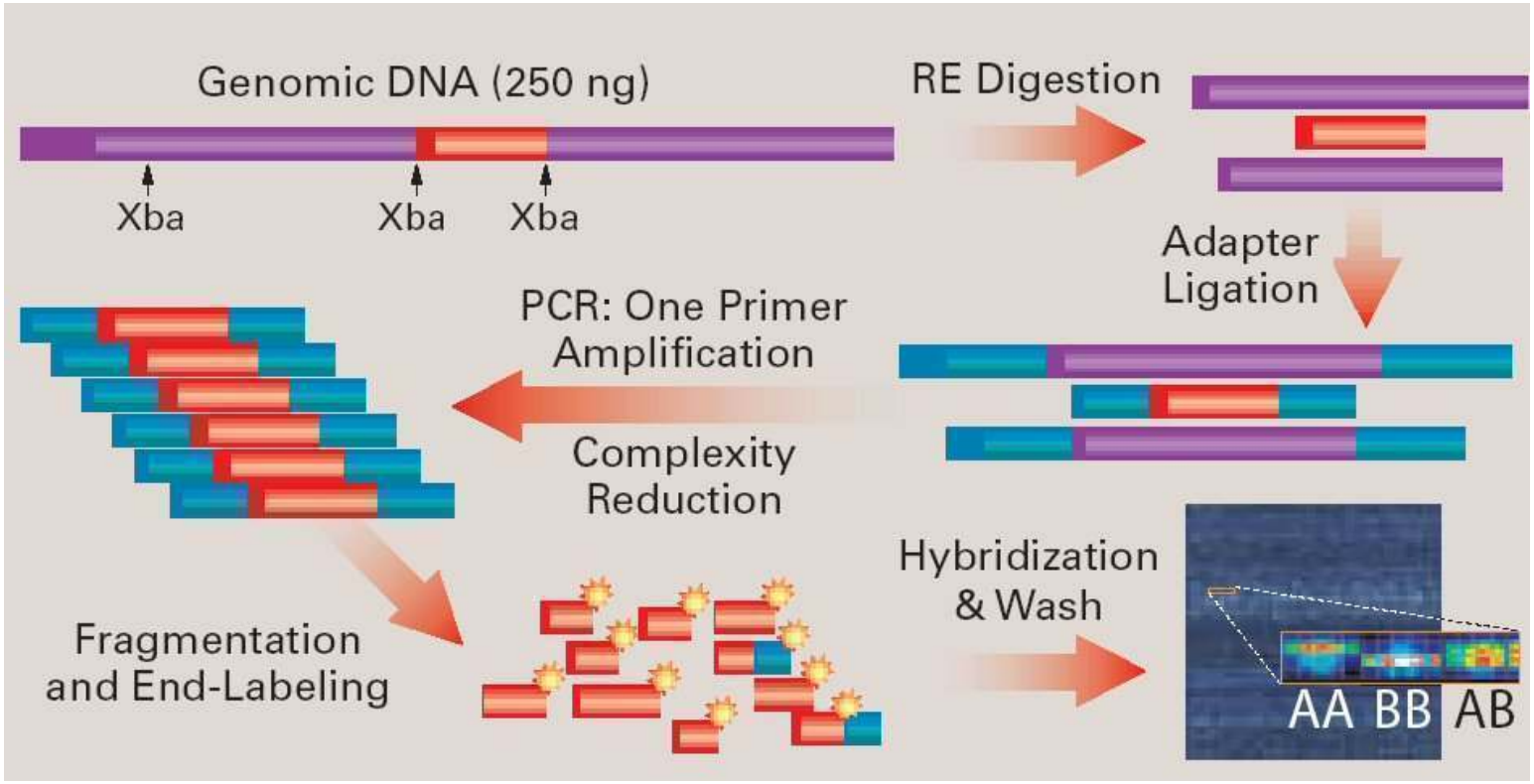

Figure 2.4 Methodology of the Affymetrix 10K SNP array. Summary of the experimental steps of the Affymetrix 10K SNP analysis as described in section 2.8.

2.9 Cytogenetics

2.9.1 Preparation of metaphase chromosome spreads

Fixative

75% methanol, 25% glacial acetic acid (prepared fresh, stored at –20°C immediately before use)

10 ml of confluent cells were incubated with 300 µl of 10 mg/ml colcemid for 12 minutes at 37°C. The cells were divided into two tubes and centrifuged for 6 minutes at 1200 rpm, all further centrifugations were under these conditions. The supernatant was removed leaving 1 ml in the bottom above the cell pellet. The pellet was resuspended by flicking the tube and 10 ml prewarmed (37°C) 0.03 M KCl was added to hypotonically shock the cells. The cells were then incubated for 40 minutes at 37°C, centrifuged, the supernatant removed and the pellet resuspended. 5 ml 5% acetic acid was added in a fast steady stream to form a frothy head; the samples were then centrifuged, the supernatant removed and the pellet resuspended. The cells were fixed with 10 ml freshly prepared fixative and incubated for 30 minutes at room temperature. The cells were centrifuged and the fixative changed twice without further incubation. After the 3rd fixative step the nuclear pellet was resuspended in a small amount of fixative to make a slightly translucent suspension. The cell suspension was then dropped onto a freshly cleaned slide and held under a lamp to aid drying. The slides were then examined under phase contrast to assess the number and quality of metaphase spreads. Slides were stored with desiccant prior to FISH analysis or baked overnight at 60°C prior to G-Banding.

2.9.2 Fluorescent in-situ hybridisation (FISH)

2.9.2.1 Slide preparation

Formamide solution

70% Formamide in 2X SSC

Metaphase slides were incubated with 200 µl RNase A (0.1 mg/ml in 2X SSC) under a coverslip in a humidified chamber at 37°C for 30 minutes. The slides were then washed for 2 x 5 minutes in D-PBS at room temperature. The slides were treated with Pepsin, then rewashed in D-PBS. The slides were dehydrated sequentially through 70%, 90% and 100% ethanol, 3 minutes per wash at room temperature and then air dried. The slides were then incubated in formamide solution for 5 minutes at 75°C in a fume hood. The slides were then immediately dehydrated sequentially through 70%, 90% and 100% cold ethanol (-20°C), 3 minutes per wash with a final wash in room temperature 100% ethanol. Slides were then air dried.

2.9.2.2 Probes used for FISH

A combination of commercial and home made FISH probes were used in this project and these are summarised in Table 2.4 below. The home made probes were made from plasmid DNA containing an insert corresponding to the chromosomal region of interest. Plasmid DNA was purified from bacteria using a Qiagen Midi Kit according to the manufacturers instructions. Briefly, the cells were pelleted by centrifugation, lysed by alkaline lysis, the lysate filtered through filter paper and then applied to the Qiagen column. The DNA in the lysate bound to a column and the column was washed. The DNA was eluted by sealing the column and incubating with 1ml of elution buffer at 60°C for at least 1 hour. This elution was repeated twice more with the second elution incubated overnight. The plasmid DNA was then precipitated with 0.7 volumes isopropanol, washed in 70% ethanol, air dried and resuspended in TE buffer. 2 µg of purified plasmid DNA was then flourescently labelled using a Vysis nick translation kit according to the manufacturers instructions. Briefly, 2 µg DNA was combined with 2.5 µl of either spectrum green/orange dUTP 0.2 mM, 10 µl dNTPs 0.1 mM, 5 µl nick translation buffer (propriety), 5 µl nick translation enzyme and incubated at 15°C for 16 hours. The reaction was stopped by incubation at 70°C for 10 minutes, then chilled on ice. 1 µg COT1 DNA, 2 µg salmon sperm DNA, 5.7 µl 3 M Na acetate and 160 µl 100% ethanol were added and the labelled DNA allowed to precipitate at –80°C for several hours. The DNA was pelleted by centrifugation for 15 minutes, 13000 rpm at 4°C, dried and resuspended in a formamide mastermix and heated at 37°C until dissolved.

Table 2.4 Probes used for FISH.

Probe	Preparation	Source
6p21.2	Made from plasmid RP11-262E12	Cell & Gene Therapy Resource Unit, Murdoch Children's Research Institute, Parkville, Vic, Australia
6p12.3	Made from plasmid RP11-876F11	
6q15	Made from plasmid RP11-124K9	
6 Whole Chromosome Paint	Commercial	Cambio
6p sub-telomere	Made from plasmid 62I11	Incyte Genomics
C-myc (8q24.12-q24.13)	Commercial	Vysis

2.9.2.3 FISH probe hybridisation and visualisation

DAPI counterstaining solution

1/1500 dilution of DAPI 5 mg/ml stock in 4X SSC 0.2% Tween

2 µl of each probe used (per slide) was combined and denatured at 77°C for 6 minutes and then placed on ice to cool. 4 µl was pipetted onto slide and a 15 mm round coverslip placed on top. Art cement was then used to seal the coverslip to the slide. Slides were hybridised overnight at 37°C in a humidified atmosphere. The coverslip was then removed and the slides washed in 0.4X SSC 0.3% NP40 for 2 minutes at 75°C. The slides were then washed in 2X SSC 0.1% NP40 for 1 minute at room temperature. The slides were counterstained in DAPI solution for 5 minutes at room temperature in the dark, then rinsed 3 times in tap H_2O and then 3 times in distilled H_2O. The slides were air dried and coverslipped using a drop of anti-fade mounting media. Slides were shielded from light photographed using Cytovison software.

2.9.3 G-banding of metaphase slides for karyotyping

Hanks buffered salt solution

0.137 M NaCl, 5.4 mM KCl, 0.25 mM Na_2HPO_4, 0.44 mM KH_2PO_4, 1.3 mM $CaCl_2$, 1.0 mM $MgSO_4$ and 4.2 mM $NaHCO_3$

Leishman stain solution

1 g Leishman stain in 500 ml methanol. Stir for 4 hours and allow stain to age at least one day prior to use. If stain is not dissolved, filter stain through a 0.45 µm filter.

Metaphase slides were trypsinised for 8 seconds and then immersed in Hanks buffered salt solution with 5% foetal calf serum to stop the reaction. The slides were then washed in Hanks buffered salt solution, counterstained with Leishman stain solution, washed again in Hanks buffered salt solution and coverslipped. The karyotyping was performed by Dr. Greg Peters (Department of Cytogenetics, Westmead Children's Hospital, Sydney, Australia).

2.10 Total RNA purification

RNA was extracted and purified for microarray analysis and real-time PCR using the Atlas pure total RNA labelling system (BD Biosciences) according to the manufacturers instructions. Briefly, 10^7 cells were washed once in PBS and then flash frozen in liquid nitrogen and stored at –70°C until the RNA purification was performed.

On the day of the extraction 1 ml of denaturing solution was added to the frozen cell pellets, and vortexed until defrosted and homogenised. The samples were then incubated on ice for 10 minutes, all subsequent incubations were also carried out on ice. The samples were then revortexed and centrifuged at 3000 g for 10 minutes at 4°C to remove any cellular debris. All subsequent spins were at 3000 g and 4°C. The supernatant was then transferred to a new tube and 2 ml saturated phenol was added, vortexed for 1 minute and incubated for 5 minutes. 0.6 ml of chloroform was then added, vortexed for 2 minutes and incubated for 5 minutes. The samples were then centrifuged for 30 minutes to separate the aqueous and organic phases. The upper aqueous phase was then transferred to a new tube and a second round of phenol/chloroform extraction performed. The second extraction used 1.6 ml phenol and 0.6 ml chloroform. 2 ml of isopropanol was then added to all samples mixed well and then incubated for 10 minutes. The samples were then centrifuged at for 40 minutes, the supernatant removed and the translucent pellet washed with 1 ml 80% ethanol. The samples were centrifuged for 15 minutes the supernatant removed and the pellet air dried then dissolved in RNase free H_2O.

2.10.1 DNase treatment of total RNA

10X Termination mix

0.1 M EDTA pH 8.0, 1 mg/ml glycogen

The following were combined in a 1.5 ml microcentrifuge tube and incubated for 30 minutes in a heating block:-

500 µl Total RNA (1 mg/ml)
100 µl 10x DNase I Buffer
50 µl DNase I (1 unit/µl)
350 µl Deionised H_2O
1.0 ml Total Volume

The reaction was terminated with 100 µl 10X termination mix. The RNA was then extracted with 1 ml saturated phenol and 600 µl chloroform. The sample was then vortexed and centrifuged at 14000 rpm for 10 minutes at 4°C to separate phases. All further centrifugations were at 14000 rpm and 4°C. The upper aqueous phase was transferred to a new tube and re-extracted with 550 µl chloroform. The samples were recentrifuged for 10 minutes and the aqueous phase transferred to a new tube. A 1/10 volume (50 µl) of 2 M sodium acetate and 2.5 volumes (1.5 ml) of 95% ethanol were added. The samples were vortexed thoroughly and incubated on ice for 10 minutes. The samples were then centrifuged for 15 minutes and the supernatant removed. The RNA pellet was overlayed with 500 µl of 80% ethanol to wash then centrifuged for 5 minutes. The supernatant was discarded and the RNA pellet air dried then dissolved in 250 µl of RNase free H_2O.

2.10.2 Assessing yield and purity of total RNA

O.D. buffer

10 mM Tris, 0.1 mM EDTA pH 7.5 stored at room temperature

10X MOPS buffer

0.4 M MOPS, 0.1 M Na acetate, 10 mM EDTA pH 7.5 autoclaved to sterilise

1% Denaturing agarose RNA gel

1 g agarose, 82.5 ml H_2O, 10 ml 10X MOPS buffer heated in microwave, allowed to cool and 7.5 ml formaldehyde

RNA sample loading solution

45 µl formaldehyde, 45 µl formamide, 10 µl 10X MOPS buffer, 3.5 µl EtBr (10 mg/ml), 1.5 µl 0.1 M EDTA, 8 µl bromophenol blue dye (in 50% glycerol)

The yield of RNA in each sample was determined by diluting 2 µl of Total RNA in 400 µl of O.D. Buffer. Purity was monitored by a A260 nm:A280 nm which was normally 1.8-2.0. The concentration of RNA was determined by the A260 nm using the following equation.

RNA (µg/ml) = Absorbance 260 nm x 40 µg/ml x Dilution Factor

The RNA was run on a 1% denaturing agarose gel, 10-15 µl of RNA loading solution was added to 1-2 µg of total RNA and mixed well. The samples were heated at 70°C for 10-15 minutes, cooled on ice and loaded on the 1% denaturing gel and run in 1X MOPS buffer for 90 minutes at 100 V. The gel was then visualised under UV light to ensure there was no RNA degradation.

2.11 Atlas nylon array analysis

RNA was analysed using an Atlas Toxicology 1.2 Array (BD Biosciences) which contained hybridisation spots for 1000 genes of interest in drug and stress response. A complete list of genes on the array can be obtained from www.atlas.clontech.com catalogue number PT3573-3.

2.11.1 Poly A^+ RNA enrichment and probe synthesis

Binding buffer and Wash buffer

Propriety buffers supplied with kit

5X Reaction buffer

250 mM Tris-HCl pH 8.3, 375 mM KCl, 15 mM $MgCl_2$

10X Termination mix

0.1 M EDTA pH 8.0, 1 mg/ml glycogen

10X dNTP mix

5 mM each dCTP, dGTP and dTTP

The streptavidin magnetic beads were resuspended by inversion and 15 µl of beads per probe synthesis reaction transferred into a 0.5 ml tube. The beads were separated on a magnetic particle separator, and supernatant discarded. The beads were washed in 150 µl binding buffer 3 times and resuspended in a final volume of 15 µl binding buffer per probe reaction.

50 µg total RNA was diluted to 45 µl in deionised H_2O. 1 µl biotinylated oligo(dT) was added, mixed by pipetting and incubated at 70°C for 2 minutes in a heating block. The RNA was cooled at room temperature for 10 minutes. 45 µl of 2X binding buffer was added and mixed by pipetting. 15 µl of washed resuspended streptavidin magnetic beads were added and the RNA mixed on a vortexer for 30 minutes at room temperature. The magnetic beads were separated and the supernatant carefully pipetted off and discarded. The beads were gently washed in 50 µl wash buffer, separated and the supernatant again discarded. The wash was repeated and the beads resuspended in 50 µl 1X reaction buffer. The beads were separated and the supernatant discarded again and the beads were resuspended in a final volume of 3 µl of deionised H_2O. cDNA probe synthesis mastermix was prepared at room temperature:-

	Per reaction
5X Reaction buffer	4 µl
10X dNTP Mix (for dATP label)	2 µl
[α-^{32}P]dATP (3000 Ci/mmol, 10 µCi/µl)	5 µl
DTT (100 mM)	0.5 µl
Total Volume	11.5 µl

The radioactivity used [α-^{32}P]dATP (Perkin Elmer) contained no added dye as this interferes with the probe synthesis reaction. 1 µl of Atlas toxicology array 1.2 primer mix was added to each poly A^+ RNA sample, mixed well and spun briefly in a microcentrifuge. The RNA was incubated at 70°C for 2 minutes, then 48°C for a further 2 minutes. 1 µl MMLV reverse transcriptase per reaction was added to the master mix and kept at room temperature. After the 2 minute 48°C incubation 8 µl of master mix was added to each reaction tube and incubated for a further 25 minutes at 48°C. The reaction was stopped by adding 1 µl of termination mix.

2.11.2 Column chromatography purification of cDNA probe

Buffer NT2, NT3 and NE

Propriety buffers supplied with kit

To purify the labelled cDNA from unincorporated ^{32}P labelled nucleotides and small (<0.1 kb) cDNA fragments the beads were separated and the supernatant (~20 µl) transferred into 180 µl buffer NT2. The probe was transferred into a nucleospin column and centrifuged at 14,000 rpm for 1 minute. The collection tube and flowthrough was discarded into the radioactive waste container. The nucleospin was washed 3 times with 400 µl of buffer NT3. The column was soaked with 100 µl buffer NE which and incubated at room temperature for 2 minutes. The nucleospin column was then centrifuged at 14,000 rpm for 1 minute to elute the purified probe. The radioactivity of the probe was determined by scintillation counting. 2 µl of each purified probe was diluted in 5 ml scintillation fluid (Perkin Elmer), and counted on the ^{32}P channel. Probes made by this method typically had an activity of 1-10 x 10^6 cpm. Probes were stored at –20°C prior to hybridisation.

2.11.3 Nylon array hybridisation

ExpressHyb solution

Propriety buffer supplied with kit

Wash solution 1

2X SSC 1% SDS

Wash solution 2

0.1X SSC, 0.5% SDS

Before hybridising labelled cDNA probes to the Atlas array the quality of each probe was analysed by hybridising it to a control (blank) nylon membrane. This estimates the level of non-specific background resulting from impurities in the RNA samples. The same protocol was used as for the experimental hybridisation (see below) with 1/5 of the probe and other reaction components. If a high level of background was observed the RNA sample needed to be retreated with DNase I and the probe remade.

The nylon arrays were placed in hybridisation bottles with the aid of deionised water to prevent the creation of air pockets. 0.5 mg sheared salmon testes DNA (per array) was incubated at 95-100°C for 5 minutes then chilled on ice and mixed with 5 ml prewarmed ExpressHyb solution. The arrays were prehybridised for 30 minutes with continuous agitation (5-7 rpm) at 68°C. The cDNA probe was prepared for hybridisation by adding 5 µl Cot1 DNA (1 mg/ml) and incubating at 100°C for 2 minutes. The probe was cooled on ice for 2 minutes and then added to the prehybridisation solution and incubated overnight with continuous agitation at 68°C. The membrane was in contact with the hybridisation solution at all times.

The next day the hybridisation solution was removed and discarded into radioactive waste. The solution was replaced with 200 ml of 68°C wash solution 1 and washed for 30 minutes with continuous agitation at 68°C. This wash step was repeated 3 more times. The solution was then replaced with 200 ml 68°C wash solution 2 and washed for 30 minutes with continuous agitation at 68°C. The final wash was performed in 200ml 2X SSC with agitation for 5 minutes at room temperature. Using forceps the array was removed from the container and placed in deionised H_2O to prevent the membrane drying out. The arrays were then wrapped in plastic wrap sealing the edges of the plastic using a heat sealer. The array was then exposed to X-ray film at –70°C or a phosphoimager at room temperature. The arrays were used twice by removing the

cDNA probes by stripping the hybridised probes in 500 ml of boiling 0.5% SDS for 30 minutes.

2.11.4 Analysis of Atlas arrays

The image obtained from the phosphoimager was saved as a *.tif file in PC format. This file was then analysed with Atlas Image version 2.7 (BD Biosciences). The array was aligned using two highly expressed spots and the intensity of each spot on the array was determined. Figure 2.5A shows an example of an Atlas toxicology array hybridised with P^{32} labelled mRNA and exposed to a phosphoimaging screen and B) the guide to the location of the hybridisation spots as provided by the manufacturer. Spots were defined as any region which reached 1500 units above the background intensity of the array. The most differentially expressed genes were chosen for real-time PCR analysis.

2.12 Real-time PCR

2.12.1 Conversion of RNA to cDNA

RNA was purified using the total RNA purification protocol as described in section 2.10. RNA was converted to cDNA using Bioscript RNase H Minus (Bioline) according to the manufacturers instructions.

Total RNA	2 µg
Oligo$(dT)_{15}$	0.5 µg
H_2O	up to 12 µl

Heated for 5 minutes at 70°C then chilled on ice, then the following was added:-

RNase Inhibitor	10 units
dNTP Mix	0.4 µl (100 mM dNTP mix)
5X Reaction Buffer	4 µl
Deionised H_2O	up to 19.75 µl
Bioscript	0.25µl (200 u/µl)

A

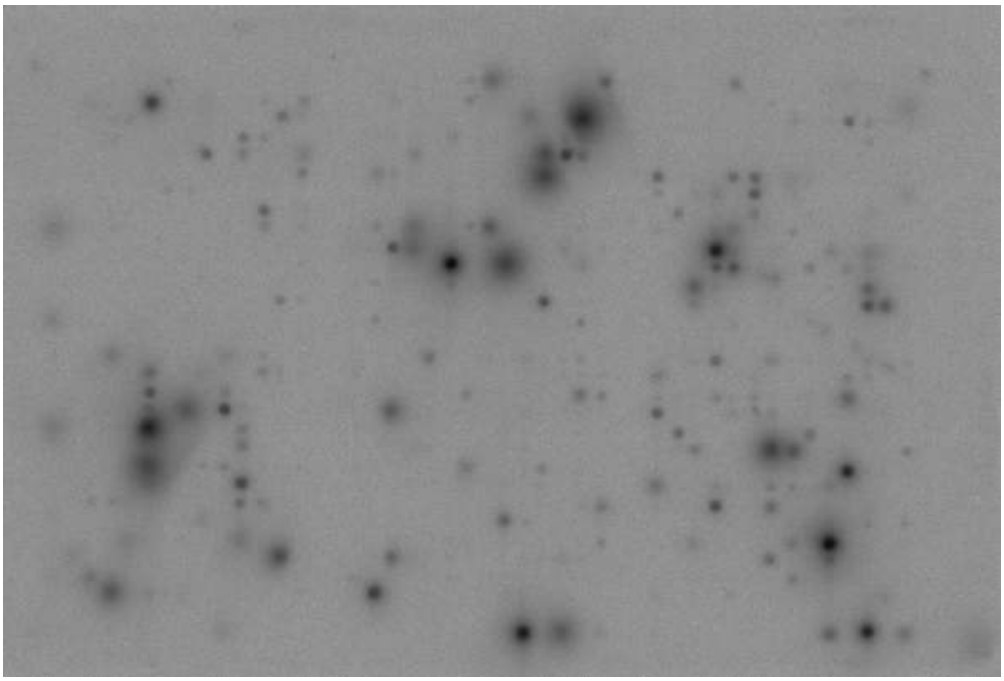

B

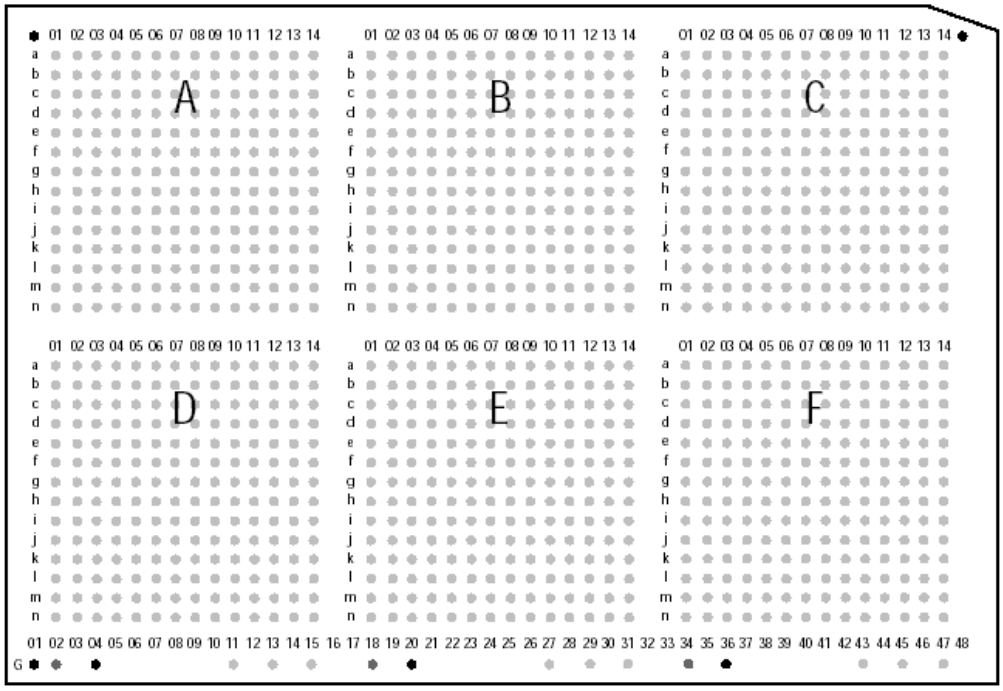

Figure 2.5 Atlas toxicology 1.2 nylon array. A) Atlas nylon array hybridised with P^{32} labelled cDNA and scanned on a phosphoimager as described in section 2.11 B) Atlas nylon array spot orientation guide supplied by the manufacturer.

Incubate at 42°C for 60 minutes, and stop the reaction by heating at 70°C for 10 minutes. The cDNA was stored at –20°C prior to analysis.

2.12.2 Designing of primers for real-time PCR

Table 2.5 presents the primers used for real-time PCR analysis in this project. They were designed as follows. mRNA sequences for the genes of interest were downloaded from Genbank. These sequences were blasted (Altschul et al., 1997) against other homo sapiens mRNA sequences, regions that had homology to other mRNAs were excluded from the primer design process. Where more than one mRNA variant existed for the gene of interest a region that shared homology between the variants was chosen. The mRNA sequences were also analysed with Blat (James, 2002) to determine the intron/exon splice sites. Ideally primers chosen spanned the intron exon boundary, as indicated in Table 2.5, therefore avoiding binding to any contaminating genomic DNA. If this was not possible primers were chosen so that an intron/exon boundary was within the amplicon, as indicated in Table 2.5. This does not prevent primers binding to contaminating DNA but enables the contamination to be detected. In some cases neither of these scenarios were possible due to homology to other genes in intron/exon boundary regions or unsuitability of the sequence for primers. These genes were always analysed on samples which had already been assayed for another gene and shown no genomic DNA contamination. Primers were designed with Primer 3 (Rozen et al., 2000) with the following parameters, optimum Tm of 60°C, and optimum amplicon length of 120 bases. Primers were Guaranteed Oligos^{TM} synthesised by Sigma-Proligo (Lismore, NSW).

2.12.3 PCR reaction and cycling conditions for real-time PCR

2X Immomix (Bioline) was chosen for the real-time PCR as it reduces the amount of pipetting required to set up each reaction and therefore error. Syber Green 10,000X stock was from Invitrogen - Molecular Probes. The general 25 µl reaction mix for real-time PCR was as follows:-

Table 2.5 Primers designed for real-time PCR.

		Forward Primer					Reverse Primer							
Gene Name	Accession	Pos	Len	Tm	GC	Sequence	Pos	Len	Tm	GC	Sequence	Amplicon	Primer I/E	Amplicon I/E
40S RPS3	NM001005	656	20	59.8	45	GCATTGTGGAACCCAAAGAT	779	20	60.25	55	CTGCCAAGGAGACCCTGTTA	123	X	
60S RPL39	NM001000	13	20	59.75	55	TCCCTCCTCTTCCTTTCTCC	135	20	59.94	40	ATGGGACGATTTTGCTTTTG	122		X
Alpha Tubulin	NM006000	346	20	59.87	50	AGAGGATGCTGCCAACAACT	465	20	60.25	55	AGGAAGCCCTGAAGTCCTGT	119		X
Beta Actin	NM001101	1642	20	59.8	45	TTGAATGATGAGCCTTCGTG	1771	23	58.93	52.2	CTGGTCTCAAGTCAGTGTACAGG	129		X
CD81	NM004356	680	20	60.59	55	CTTCCACGAGACGCTTGACT	798	20	59.98	55	CCTCCTTGAAGAGGTTGCTG	118	X	
ERCC1	NM001983	841	20	62.86	55	TCTCCCGGGTGACTGAATGT	970	20	60.93	55	GGGCATAAGGCCAGATCTTC	129	X	X
FAP48 (GLMN)	NM007070	51	20	60.44	50	AGGGTTCTGGCCGATTTTAG	176	20	57.03	40	AGGCCAAAATCCTCTTCTTT	125	X	
GCS-Cat	NM001498	643	20	59.92	50	AAACCCAAACCATCCTACCC	761	20	59.72	50	GCATGTTGGCCTCAACTGTA	118	X	
GCS-Reg	NM002061	411	20	60.5	50	AGCGAGGAGCTTCATGATTG	523	21	58.19	47.6	GCATGAGATACAGTGCATTCC	112	X	
GSR	NM000637	1267	20	60.11	45	ACTTGCCCATCGACTTTTTG	1386	20	60.22	50	ATGGCTTCATCTTCCGTGAG	119	X	
GSTO1	NM004832	267	20	59.55	55	TGCCATCACCTGTGAGTACC	388	20	60.07	50	CCAAGGATGGCACCTTAGAA	121	X	
GSTP1	NM000852	192	20	60.11	55	AAGTTCCAGGACGGAGACCT	314	20	60.23	50	GTCATTCACCATGTCCACCA	122		X
GSTT1	NM000853	505	20	60.25	55	GTAGCCATCACGGAGCTGAT	621	19	60.45	63.2	GAAGAGGTCCTCCCCCACT	116		X
HSP40hom	NM006145	224	19	58.56	58	GAGATCTTCGACCGCTACG	346	20	59.93	50	AAACATGGCATGAGGGTCTC	122		X
HSP90Beta	NM007355	2081	20	60.57	50	CTGGCTTTTCCCTTGAGGAT	2203	20	60.41	50	CATCAGGAACTGCAGCATTG	122		X
IGFBP2	NM000597	706	20	59.29	55	GAGAAGGTCACTGAGCAGCA	830	20	60	55	ACCTGGTCCAGTTCCTGTTG	124		X
MAP4	NM002375	2966	21	60.14	48	AAGCCCACTGCCATTAAGACT	3078	20	60.36	50	TTCATGGAACTGGTGGAGGT	112	X	X
MSH2	NM000251	2271	20	60.66	50	ATCCTCAGGTCTGCAACCAA	2409	20	60.68	40	CAAACATGCAAAAAGCACCA	138	X	
MutY	NM012222	948	20	59.67	50	CCAGGAGATTTCAACCAAGC	1071	20	59.99	60	GTTCCTGCTCCACTCTCTGG	123	X	
NM23-H1	NM198175	714	20	60.12	50	AGATCGGCTTGTGGTTTCAC	833	20	60.13	50	GAAGGAGGGGAAATGGATGT	119		
p107	NM002895	1785	20	60.32	55	GTCACGATTCTGCACTGTGG	1904	20	59.93	50	GATGTCCCTGCACATTTCCT	119		X
POLD1	NM002691	801	20	60.32	45	TTTGAGATCCGGTTCATGGT	904	20	59.64	55	CACTGCGTAGCCTTCTCCTT	103	X	
PTPL1	NM080685	5990	20	59.75	55	CCAGCTCAAAGAGGTCTGCT	6108	20	59.56	45	AGCAACCGTGGAGAATGAAT	118	X	X
RAD51B	NM002875	1021	20	57.84	45	TCGCTGATGAGTTTGGTGTA	1143	20	60.15	40	ATGCATGGGCGATGATATTT	122	X	
RANBP1	NM002882	208	20	59.96	55	AGTCCAACCATGACCCTCAG	330	20	60.25	50	CAGAGGCAAATCGGAACAGT	122		X
RAR-alpha	NM000964	1716	20	59.99	60	GAGGCCAGGAACTGAGTGAG	1827	20	60.69	50	TGCTGGTGATGAAGATGTGG	111		
XPA	NM000380	673	20	60.22	50	CAAAGGAAGTCCGACAGGAA	787	20	59.53	45	ACAATCGTCTCCCTTTTCCA	114		X

Pos – position, Len – length, Tm – melting temperature, GC – GC percentage, Primer I/E – Primer spans intron exon boundary
Amplicon I/E – Amplicon spans intron exon boundary.

12.5 µl	2X Immomix (Bioline)
0.75 µl	Forward primer 10 µM
0.75 µl	Reverse primer 10 µM
1.2 µl	Sybr-Green 10X stock (10,000X stock in DMSO diluted with water)
1 µl	cDNA
8.8 µl	Sterile H_2O

The real-time PCR reaction was carried out on a Rotor Gene real-time PCR machine (Corbett Research). FAM-Sybr Green was detected during the 72°C extension step of each cycle and a melt curve was performed at the end of the run to confirm the amplification of a single product. The cycling conditions were as follows:-

Step 1	95°C	10 minutes (Activates Immomix)	
Step 2	95°C	20 seconds	
	60°C	20 seconds	40 Cycles
	72°C	20 seconds	

2.12.4 Testing of primers for real-time PCR

<u>10X TAE buffer</u>

48.4 g Tris base, 10.9 g Glacial acetic acid, 3.72 g Na EDTA in 1 L H_2O, pH 8.18-8.29

<u>2% Agarose TAE gel with 0.5 µg/ml EtBr</u>

2 g Agarose, 10 ml 10X TAE buffer, 90 ml H_2O, heated to boiling in a microwave. Solution was cooled and 5 µl EtBr (10 mg/ml) was added prior to pouring.

Primers were tested on H69 control cDNA with reaction and cycling conditions as described in section 2.12.3. 1 µl of PCR product was combined with 5 µl of DNA loading buffer (Promega) and was run on a 2% agarose TAE gel with 1X TAE running buffer at 100 V for approximately 60 minutes or until the dye front had reached the bottom of the gel. PCR products were confirmed to be of the correct size by comparing to Promega Benchtop 100bp markers. PCR products were confirmed to

have no additional banding for each primer set, which would indicate the formation of multiple PCR products.

2.12.5 Analysis of real-time PCR data

The real-time PCR reactions were analysed with Rotor Gene 6 software (Corbett Research). A β-actin standard curve using H69 control cDNA was performed in each real-time PCR run. The H69 control cDNA was serially diluted from 1:10 to 1:10000 in deionised water and used as the template in the PCR reaction described in section 2.12.3 (Figure 2.6A). The reaction rate of each primer set was the same as the β-actin primer set. A Ct value is calculated by Rotor Gene 6 for each unknown sample and standard and relative expression of each unknown sample was interpolated from the β-actin standard curve in each run (Figure 2.6B).

2.13 Protein analyses

2.13.1 Preparation and quantitation of total protein extracts

Cell lysis buffer
0.01 M Tris/HCl, pH 7.4, prepared in deionised water, stored at 4°C

5 x 10^6 cells were centrifuged at 800 g for 5 minutes at 4°C, washed in 10 ml cold PBS, resuspended and transferred to a sterile eppendorf tube. These were then centrifuged the supernatant removed and the pellet resuspended in 100 µl of lysis buffer at 4°C. Samples were then frozen at –20°C before sonnication. 10 µl complete protease inhibitor (Roche) was added to samples immediately prior to sonnication. The samples were sonnicated using a Sonifer® C Cell Disruptor B-30 (SmithKline) for 40 pulses at 10 V and checked microscopically to confirm disruption of cells.

To ensure equal protein loading on gels, protein concentrations were determined using a protein assay. A standard curve ranging from 0-0.75 µg/ml of protein was prepared with bovine serum albumin (BSA) diluted with deionised water (Figure 2.7). Total cell extracts were diluted 1: 40 with deionised water. 10 µl of the BSA standards and

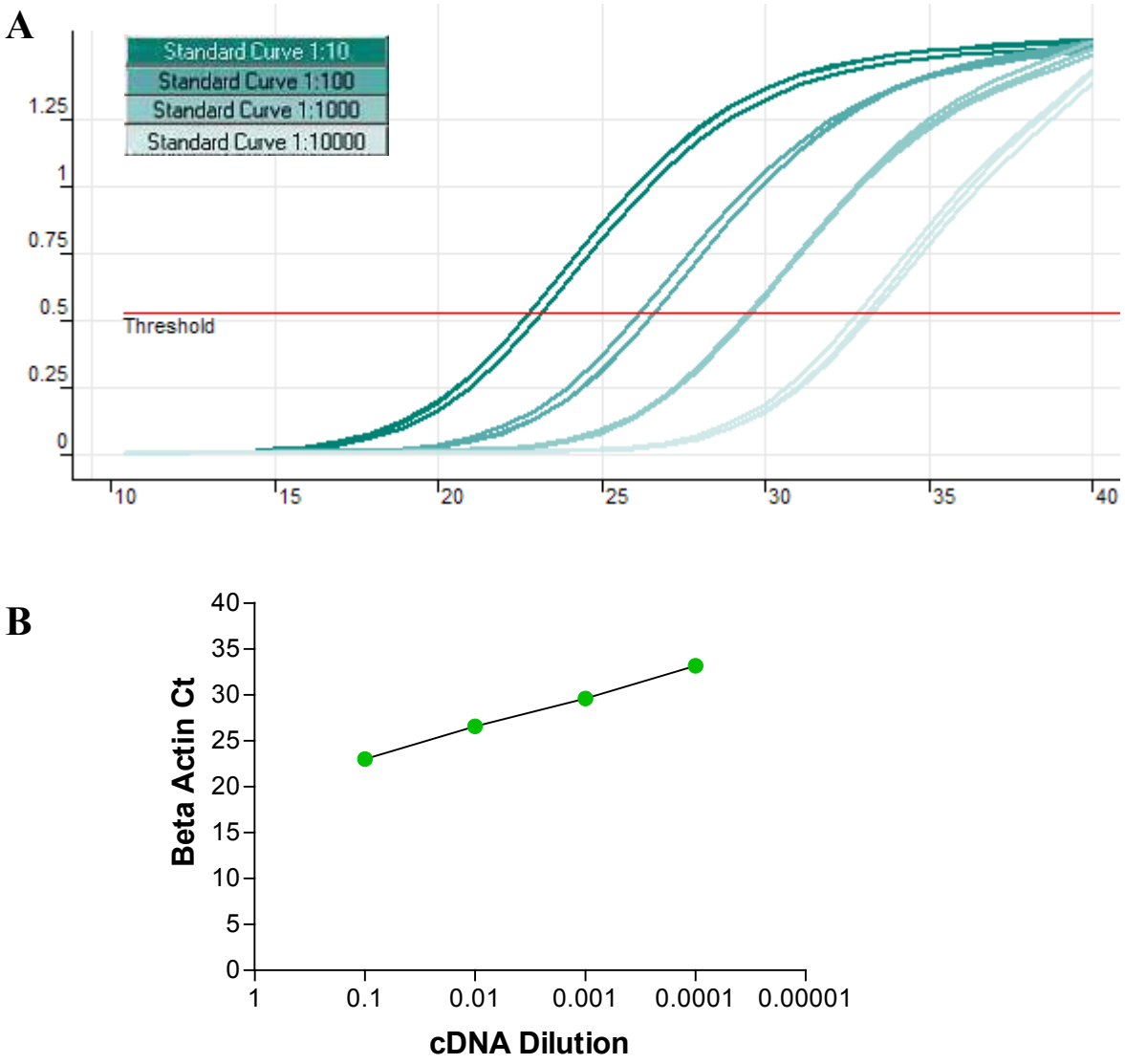

Figure 2.6 β-actin standard curve for real-time PCR analysis. A) Output of Rotor Gene 6 software. The H69 control cDNA was serially diluted from 1:10 to 1:10000 in deionised water and used as the template in the PCR reaction described in section 2.12.3. B) β-actin standard curve. A Ct value is calculated by Rotor Gene 6 for each standard (•) analysed for β-actin. The mean and standard deviation of the Ct value for triplicate reactions is shown.

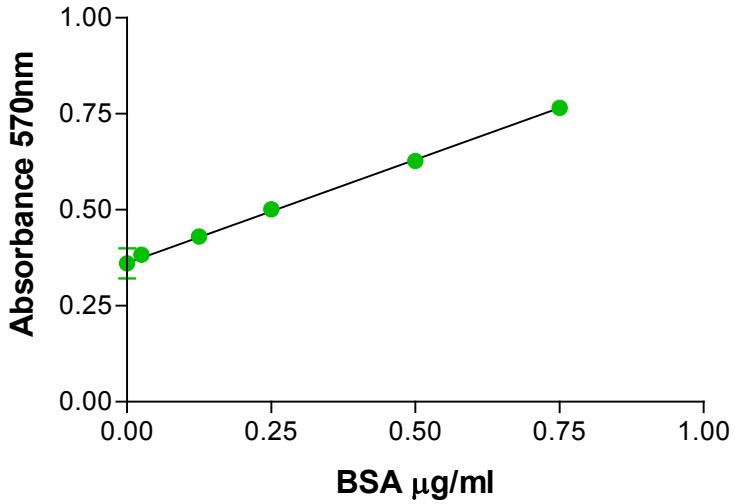

Figure 2.7 Pierce protein assay standard curve. BSA standards (•) ranging from 0-0.75 μg/ml of protein was prepared in deionised water and analysed as described in section 2.13.1. Means and standard deviations are shown for duplicate wells.

diluted samples were aliquoted in duplicate into a flat-bottomed 96-well microtitre plate. 200 µl of coomassie reagent (Pierce) was then added to each well, samples were mixed for 1 minute and the absorbance of the wells read at 570 nm using a Biotek Synergy HT microplate reader. Linear regression and interpolation of protein concentrations from the standard curve was then performed by Graphpad Prism software.

2.13.2 Preparation of cell fractions for soluble/polymerised tubulin analysis

Hypertonic buffer

1 mM $MgCl_2$, 2 mM EGTA, 20 mM TrisHCl, 2 mM PMSF, 0.5% NP40 pH 6.8

The following method was adapted from Kavallaris et al. 2001. 5 x 10^6 cells were centrifuged at 800 g for 5 minutes at room temperature, and then washed in 10 ml room temperature PBS. The cells were resuspended in 200 µl of hypertonic buffer with 10 µl complete protease inhibitor (Roche) and incubated at 37°C in the dark for 15 minutes to lyse the cells. The remainder of the preparation was conducted at room temperature. The cells were sonnicated using a Sonifer® C Cell Disruptor B-30 (SmithKline) for 40 pulses at 10V and checked microscopically to confirm disruption of cells. The samples were centrifuged at 14,000 rpm for 10 minutes. The supernatant was transferred to a new eppendorf tube, this was the soluble protein fraction. The pellet was then resuspended in 200 µl of hypertonic buffer, this was the polymerised fraction. Both fractions were then re-sonnicated for 10 pulses. 10 µl of each fraction was combined with laemmli sample buffer and run on an SDS-PAGE gel as described below in section 2.13.3

2.13.3 Sodium dodecyl sulphate - polyacrylamide gel electrophoresis (SDS-PAGE)

Laemmli sample buffer

1.25 mM Tris pH 6.8, 10% glycerol, 2% SDS, 0.04 mM 2-mercaptoethanol and bromophenol blue for visualisation, stored at –20°C.

12% Tris/glycine separating gel (2 x 0.75 mm gels)

2.4 ml 40% acrylamide, 2 ml 1.5 M Tris pH 8.8, 2.72 ml H_2O, 40 µl 20% SDS mixed together. 40 µl 10% ammonium persulfate (AMPS) and 8 µl tetramethylethylenediamine (TEMED) were added immediately prior to pouring to set the acrylamide.

4% Tris/glycine stacking gel (2 x 0.75 mm gels)

0.4 ml 40% acrylamide, 1 ml 0.5 M Tris pH 6.8, 2.56 ml H_2O, 20 µl 20% SDS mixed together. 20 µl 10% AMPS and 4 µl TEMED were added immediately prior to pouring to set the acrylamide.

Electrophoresis running buffer

0.024 M Tris, 0.192 M glycine, 0.1% SDS pH 8.3, stored at 4°C.

Protein extracts were electrophoresised according to the method of Laemmli (Laemmli, 1970). The samples were diluted in Laemmli sample buffer, boiled for 3 minutes to dissociate proteins and cooled on ice. Samples were pulse spun and 20 µg total protein was then loaded onto 12% Tris/glycine gels with a 4% stacking gel. Samples were then electrophoresised for 90 minutes at 100 V in a Biorad Mini-protean II system using 400 ml electrophoresis running buffer. 5 µl Molecular weight markers (Biorad broad range) were also electrophoresised on all gels.

2.13.4 Western blotting

Transfer buffer

25 µM Tris/glycine pH 8.2, 20% methanol, stored at 4°C.

The gels were electrotransferred to 0.45 µm nitrocellulose membranes (Biorad) for 90 minutes at 100 V using the Biorad Mini-protean II Trans Blot system in cold transfer buffer. The Western blots were then stained with ponceau-s-red solution (Sigma) to check the protein had transferred properly and to enable quantitation of loading in each lane.

2.13.4.1 Development of Western blots

Tris buffered saline (TBS)

Tris base (2.42 g/L) and NaCl (8.0 g/L), pH 7.6 stored at 4°C.

The nitrocellulose membranes were blocked with 5% defatted skim milk (Diploma Brand) in TBS/0.1% tween for 1 hour at room temperature, followed by three 10 minute washes in TBS/0.1% tween. All subsequent washes were also performed in TBS/0.1% tween. The membranes were then incubated at room temperature for 2 hours with primary antibody diluted in 0.5% defatted skim milk in TBS (5 ml) at the dilution specified in Table 2.6. The incubation was then followed by three 10 minute washes after which membranes were incubated for 1 hour with an alkaline phosphatase immunoglobin as per Table 2.6, diluted in 5 ml 0.5% defatted skim milk in TBS. The membranes were washed three times and protein bands visualised by 5 ml Sigma Fast^{TM} BCIP/NBT alkaline phosphatase substrate (Sigma).

Developed Western blots were scanned and saved as a *.tif file and analysed with Quantity One software (Biorad). Each blot was scanned with ponceau-s-red staining prior to development and the amount of ponceau staining was used to normalise for protein loading and transfer.

2.14 Immunocytochemistry

1.25 x 10^5 cells in 100 µl PBS were cytospun onto Superfrost® Plus slides (Menzel-Glasier) using reusable Shandon cytospin funnels and disposable filter cards (Thermoelectron). The slides were air dried and cells were then fixed by incubating the slides in 100% ice cold methanol for 5 minutes. The slides were air dried and stored at –20°C prior to analysis.

The slides were incubated with a serum free protein block (Dako) for 10 minutes at room temperature in a humidified atmosphere. All further incubations were also at room temperature in a humidified atmosphere. The blocking solution was tapped off and the appropriate dilution of primary antibody (Table 2.7) was added in antibody diluent (Dako) and incubated for 2 hours. The slides were then washed in D-PBS for 5

Table 2.6 Antibodies used for Western blotting.

Protein	**kDa**	**Antibody**	**Type**	**Epitope**	**Host**	**Supplier**	**Dilution**
β-actin	42	Anti-β-actin Clone AC-15	Monoclonal	N-terminal	Mouse	Sigma	1 : 20,000
ERCC1	33-36	ERCC1 Ab-1 (3H11) mAb	Monoclonal	Full Length	Mouse	Labvision	1 : 200
γGCS	73	γGCS	Polyclonal	aa295-313 Rat sequence	Rabbit	Labvision	1: 400
RAD51B	38	RAD51b Antibody [1H3/13]	Monoclonal	Full Length	Mouse	Abcam	1 : 1000
MSH2	100	Anti-MSH2 (Ab-1) (GB12)	Monoclonal	N-terminal	Mouse	Calbiochem	1 : 100
mTOR	290	Anti-mTOR/FRAP	Monoclonal	230-240	Mouse	Calbiochem	1 : 58
Thioredoxin	12	Anti-Thioredoxin	Polyclonal	Full Length	Rabbit	Abcam	1 : 5000
α-tubulin	50	Anti-α-tubulin Clone DMIA	Monoclonal	aa426-430	Mouse	Sigma	1 : 50,000
Mouse AP	N/A	Anti Mouse Immunoglobulin	Polyclonal IgG	N/A	Sheep	Chemicon	1 : 500
Rabbit AP	N/A	Anti Rabbit Immunoglobulin	Polyclonal IgG	N/A	Sheep	Chemicon	1 : 500

AP – alkaline phosphatase.

Table 2.7 Antibodies used for immunocytochemistry.

Protein	**Antibody**	**Type**	**Epitope**	**Host**	**Supplier**	**Dilution**
β-actin	Anti-β-actin Clone AC-15	Monoclonal	N-terminal	Mouse	Sigma	1 : 200
RAD51B	RAD51b Antibody [1H3/13]	Monoclonal	Full Length	Mouse	Abcam	1 : 100
Thioredoxin	Anti-Thioredoxin	Polyclonal	Full Length	Rabbit	Abcam	1 : 500
α-tubulin	Anti-α-tubulin Clone DMIA	Monoclonal	aa426-430	Mouse	Sigma	1 : 100
Mouse FITC	Anti Mouse Immunoglobulin	Polyclonal IgG	N/A	Sheep	Chemicon	1 : 300
Rabbit FITC	Anti Rabbit Immunoglobulin	Polyclonal IgG	N/A	Sheep	Chemicon	1 : 300

FITC - Fluorescein isothiocyanate

minutes. A 1: 300 dilution of FITC conjugated anti-mouse or anti-rabbit secondary antibody in antibody diluent was then added (Table 2.7) and incubated for 1 hour in the dark. The slides were then washed in D-PBS for 5 minutes. Slides were incubated with a DAPI counterstain (1:50 of 5 mg/ml stock solution in D-PBS) for 5 minutes in the dark and then again washed in D-PBS for 5 minutes. Slides were air dried and then coverslipped using PermaFlour^{TM} Aqueous Mounting Medium (Thermoelectron) which enhances FITC intensity and reduces fading.

Slides were photographed at x 600 magnification using a Nikon Eclipse 80i Microscope. Two photographs were taken of each region of interest, one FITC image for the stained primary antibody of interest and one DAPI image for the nuclei. The scale bar on each photograph indicates 20 μm. The FITC secondary antibodies were used alone as a control to determine the amount of background staining. The mouse-FITC antibody showed virtually no staining apart from in apoptotic or dead cells. The rabbit-FITC antibody showed a low level staining over all cells. This staining was apparent with a longer exposure time than that used for photographing the stronger signals obtained in combination with the specific primary antibodies.

2.15 Statistics

All experiments were repeated at least twice. Statistical analysis performed using the Student's t-test in Microsoft excel using a two tailed analysis and two samples of equal variance settings.

CHAPTER 3.0

DEVELOPMENT OF PLATINUM-RESISTANT SMALL CELL LUNG CANCER CELL LINES

3.1 Introduction

The majority of studies in platinum-resistant cell lines do not discuss the development of the cell lines in detail. Most describe the dose of drug, length of exposure and number of treatments but do not elaborate on the success or failure of various treatment strategies. The failure of a treatment strategy to produce a resistant cell line in the lab may be unfortunate for the researcher trying to understand mechanisms of resistance, but may be useful information for a clinician planning successful cancer therapy. The failure to produce resistance in cell models is rarely published in the literature. However, anecdotal evidence from researchers in the field suggest that the inability to produce resistance in the laboratory is common. A comparative analysis between different developmental strategies is required to prove that the failure to produce resistance was related to the chemotherapeutic and not human error.

The cell lines developed as part of this project were developed in parallel allowing a comparative study of cisplatin and oxaliplatin and their ability to induce resistance in the human H69 SCLC cell line when administered repeatedly as either a 4 day or 2 hour pulse. Treatment doses were chosen in the range of $IC_{10} - IC_{40}$ and are consistent with doses used in the clinical setting. Pharmacokinetic studies show that plasma platinum levels peak at a range of 1-10 μg/ml in 2 hours with a rapid drop to the ng/ml range and then a slow decrease over the next 48 hours (Sockalingam et al., 2002; Liu et al., 2002a). Two time and dose strategies were chosen to reflect these differing pharmacokinetic phases of the administration of platinum drugs; 2 hour treatments at 1000-8000 ng/ml and 4 day treatments at 200-1600 ng/ml. These doses were also chosen with the hope of obtaining low-level resistant cell lines with clinically relevant mechanisms of resistance. The two stably resistant cell lines produced (H69CIS200 and H69OX400) were then maintained in drug-free media.

This chapter compares the development of cisplatin and oxaliplatin resistance in SCLC. The patterns of cross resistance between cisplatin, oxaliplatin and other chemotherapeutics were also examined in this SCLC model. The resistance mechanisms of increased efflux/decreased uptake of platinum and detoxification by glutathione were also determined.

3.2 Development of platinum resistance

The H69 SCLC cells were treated as shown in Figure 3.1 with cisplatin for 4 days at doses of 200, 400 or 800 ng/ml; with cisplatin for 2 hours at doses of 1000, 2000 or 4000 ng/ml; with oxaliplatin for 4 days at doses of 400, 800 or 1600 ng/ml; or with oxaliplatin for 2 hours at doses of 2000, 4000 or 8000 ng/ml. Following treatment cells were transferred to drug-free culture conditions for recovery and the treatment was repeated either at the same drug dose or at higher doses as indicated in Figure 3.1. Eight consecutive treatment cycles were performed on cultures over an 8 month period.

Of the 12 different initial treatments, only the lowest drug concentrations produced surviving cells (Figure 3.1). These lowest drug concentration treatments all produced between 20 and 30% cell death and growth arrest. On drug treatment cells increased in size and did not aggregate in typical SCLC clumping morphology. Surviving cultures were then re-treated when their normal growth rate and clumping morphology had returned. Cultures were treated with the same drug and dose as well as with twice and four times that dose. All cultures again survived the lowest dose but none survived the higher doses except for those treated with 4000 ng/ml oxaliplatin for 2 hours. The results of the third treatment with the same and with escalated doses produced cultures that survived the same dose, none of the cultures treated with increased cisplatin doses survived while increased oxaliplatin produced two surviving cultures (Figure 3.1). Subsequent treatments with increased doses of cisplatin were performed out to treatment 4 which produced one culture that survived treatment with 400 ng/ml cisplatin for 4 days. Cultures therefore appeared to survive oxaliplatin dose escalation more easily than cisplatin dose escalation. However, those cultures surviving dose escalation were not more resistant than the cultures from which they were derived as determined by the standard 5 day MTT cytotoxicity assay suggesting that this resistance may be associated with growth delay.

Dose escalation of platinum drugs rarely occurs as part of SCLC treatment (Sandler, 2003). It was therefore decided to concentrate on characterising the development of resistance in the cultures repeatedly treated with the same lowest dose schedule. The initial treatments with cisplatin and oxaliplatin for 4 days produced a growth arrest

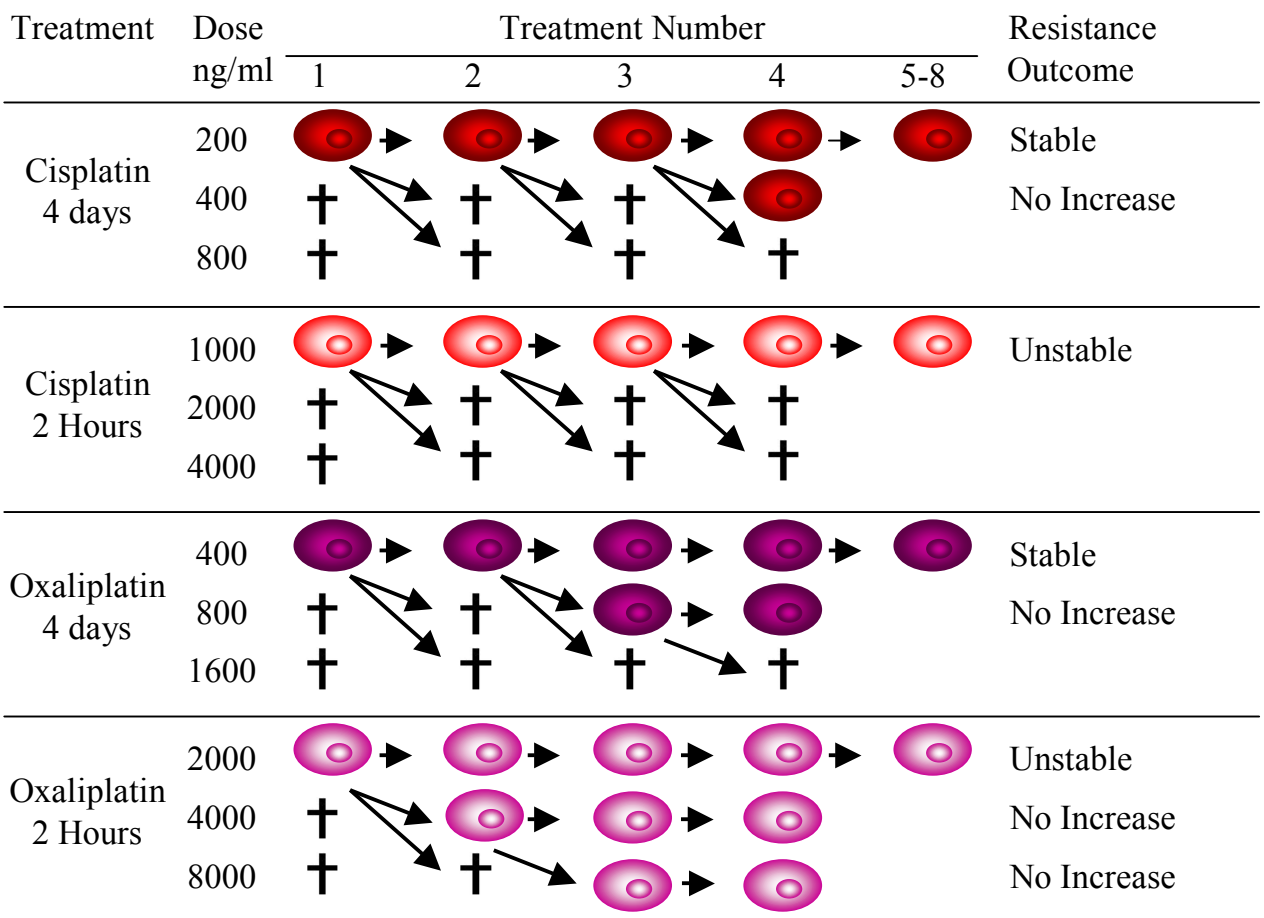

Figure 3.1. Drug treatment regimens and the development of resistance. The H69 SCLC cell line was treated with 12 different regiments as indicated. Cultures surviving a treatment are represented by a cell image while unsuccessful treatments are represented by a cross.

and a time-to-doubling of 21 days while the 2 hour treatments resulted in a 17 day recovery (Figure 3.2). A similar growth arrest occurred in all schedules for the first five treatments. For the sixth, seventh and eighth treatments, the recovery period was reduced to 6 days in all except the 2 hour cisplatin schedule. The cell sublines resulting from 8 treatments of the 4 day cisplatin schedule were designated H69CIS200; the 2 hour cisplatin schedule, H69CIS1000; the 4 day oxaliplatin schedule, H69OX400 and the 2 hour oxaliplatin schedule, H69OX2000. The resistant cells were of the same size and morphology as the parental cells and grew at a similar growth rate in drug-free media (Figure 3.3A, B and C).

The level of resistance to cisplatin and oxaliplatin was monitored after each treatment at weekly intervals after recovery by performing a 5 day MTT cytotoxicity assay comparing the developing cells to the parental cell line. The results in Figure 3.4 show that for the 4 day cisplatin and oxaliplatin schedules, low-level (approximately 2-fold), stable resistance developed following the eighth treatment. A similar level and pattern of stable cross-resistance to the non-selecting platinum drug was also evident. Although the 2 hour cisplatin and oxaliplatin schedules showed similar trends to those of the 4 day schedules (Figure 3.4), they did not produce stable resistance after the eighth treatment and therefore they were not included in further studies. The instability of the H69CIS1000 cell line was not determined by repeating additional MTT assays. Its instability was assumed from the initial loss of resistance and the failure of this cell line to reduce its growth arrest period like the other cell lines (Figure 3.2).

Resistance to oxaliplatin was detected earlier than resistance to cisplatin in both sublines. A higher level of oxaliplatin resistance was also detected in comparison to cisplatin resistance in both resistant sublines. Resistance appeared to be greatest in the second week after recovery. However this resistance was transient as the level of resistance was usually lower in the third week. This variation was largest for the oxaliplatin treatments as compared to the cisplatin treatments and it was most evident at treatment 7. This increased variation may be related to the drop in doubling time at treatment 6 but may not be part of the progression to stable resistance as it did not re-occur at treatment 8.

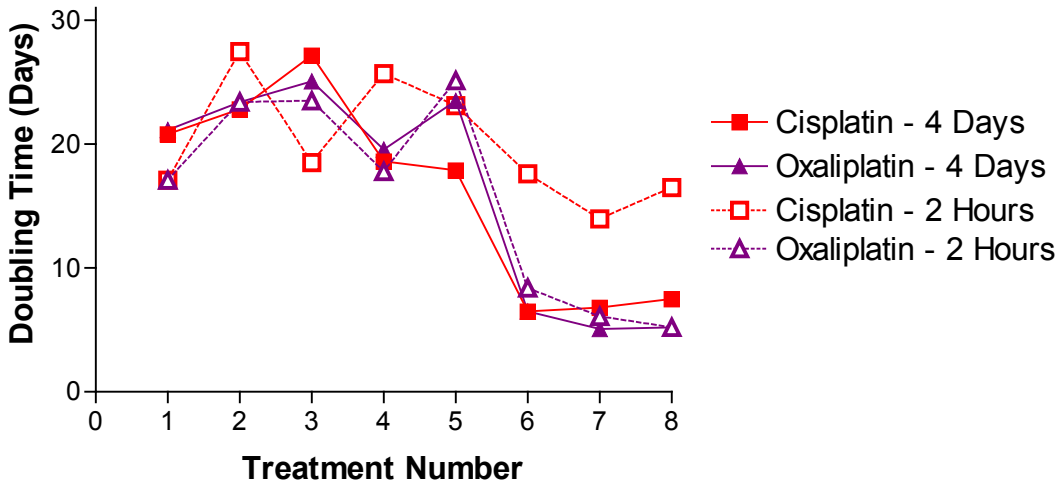

Figure 3.2. The recovery time following each treatment. Cells were exposed at a cell density of 5 x 10^5 cells/ml, for either 2 hours or 4 days to the doses of drugs as outlined in Figure 3.1, then resuspended in fresh media and left to recover. This produced the following cell lines H69CIS200 (■), H69CIS1000 (□), H69OX400 (▲) and H69OX2000 (△). The number of cells that exclude trypan blue were counted twice a week following treatment and the time taken to double cell number after each treatment was determined.

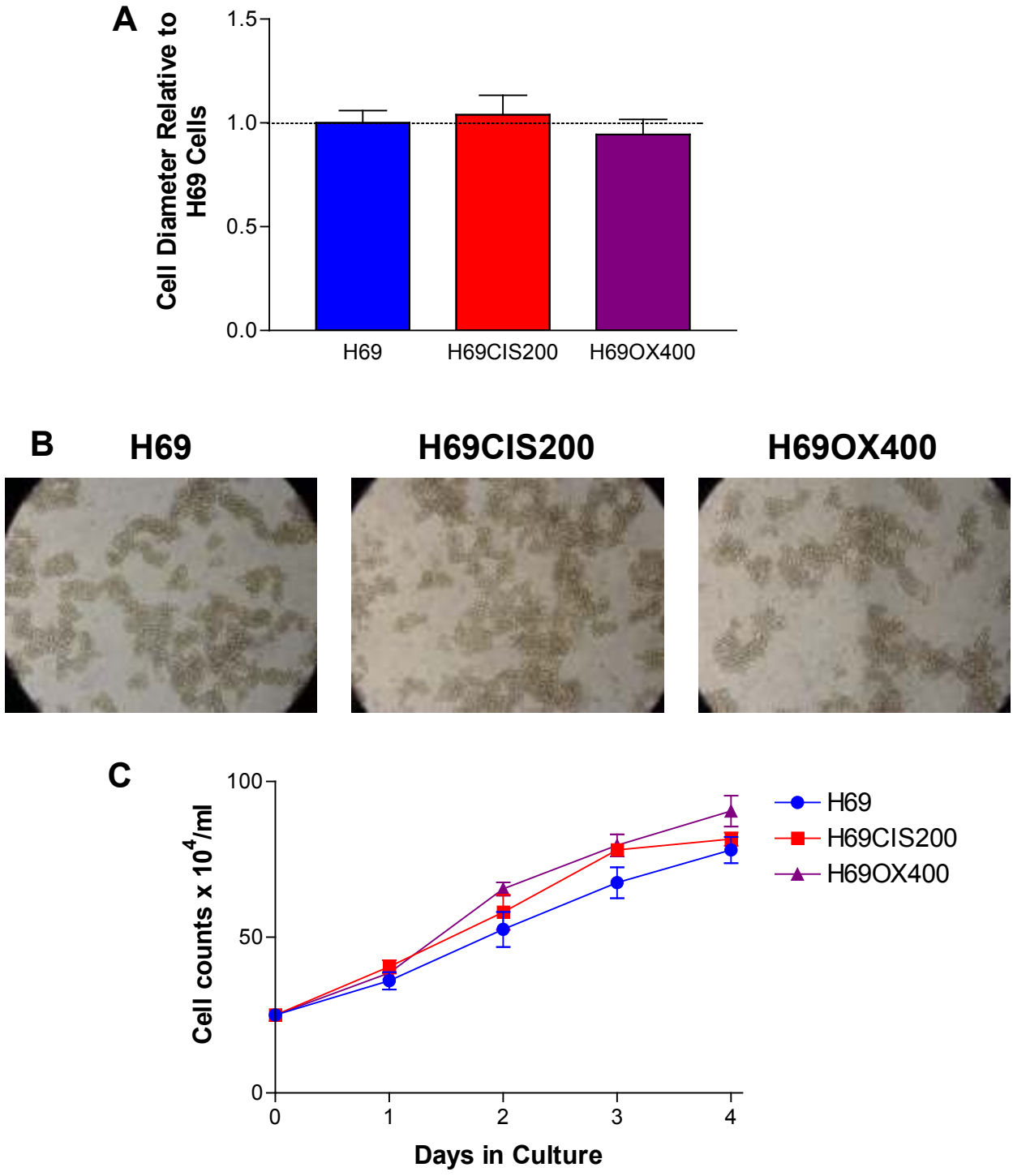

Figure 3.3. Size, morphology and growth rate of resistant cell lines. A) Cell size was determined by measuring cell diameter on printed photographs of cells photographed on a haemocytometer. Two measurements were taken for each cell at 90° angles. Cell diameter is presented for the resistant cell lines relative to the parental H69 cells. B) Morphology. Flasks of confluent cells were photographed at x10 magnification. C) Growth rate of H69 parental cells (●), H69CIS200 (■) and H69OX400 cells (▲). Cells were resuspended in 10 ml fresh media at a cell density of 2.5 x 10^5 cells/ml. Cells were sampled and counted microscopically with trypan blue staining, every day for 4 days.

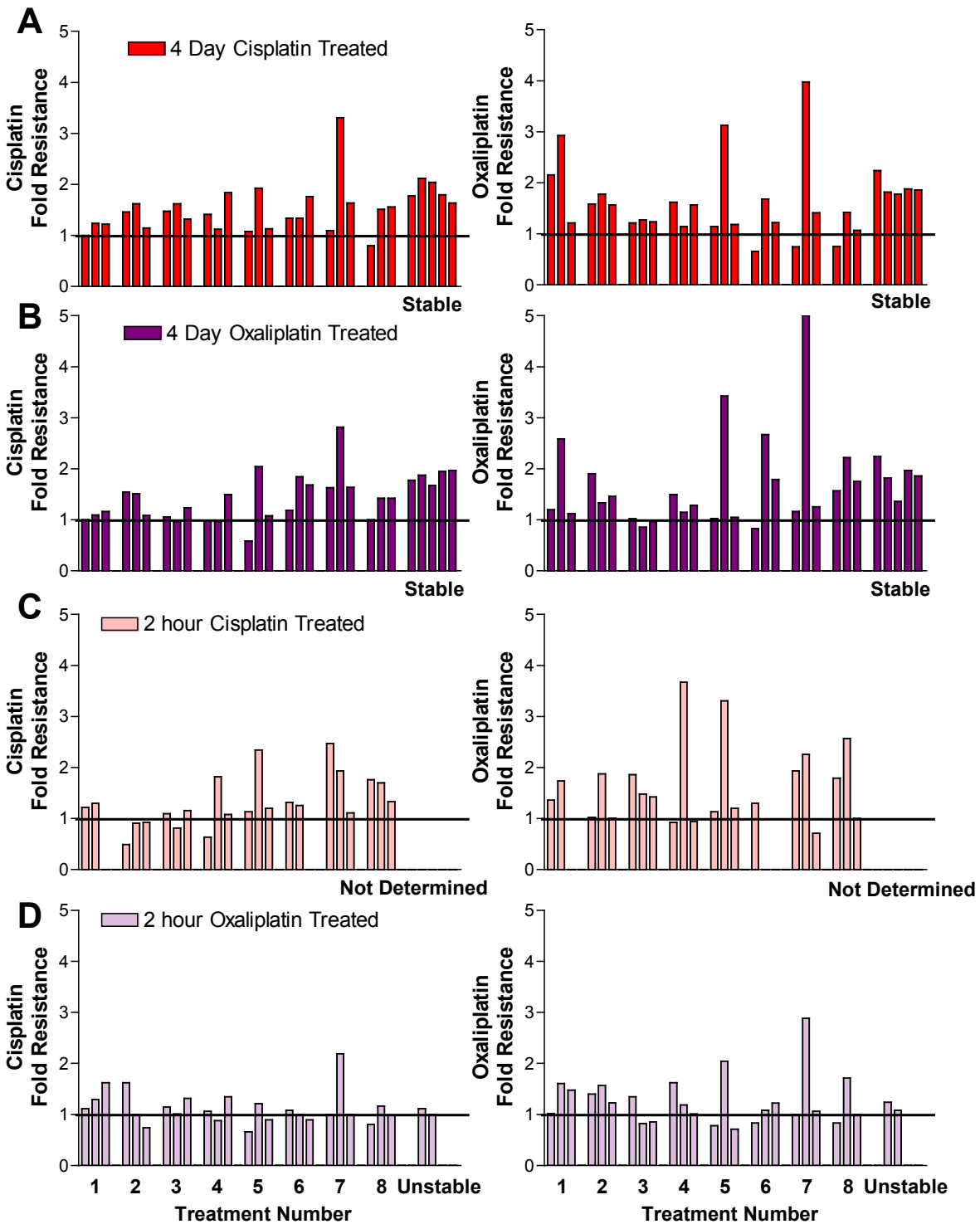

Figure 3.4. Resistance to cisplatin and oxaliplatin following each treatment. The resistance to cisplatin and to oxaliplatin was determined for 3 consecutive weeks following recovery from each treatment using a 5 day cytotoxicity assay in which viability was determined by the MTT assay as described in section 2.3. After 8 treatments the resistance was monitored for stability. A) 4 day treatment with 200 ng/ml cisplatin B) 4 day treatment with 400 ng/ml oxaliplatin C) 2 hour treatment with 1000 ng/ml cisplatin D) 2 hour treatment with 2000 ng/ml oxaliplatin.

3.3 Cell cycle changes associated with platinum resistance

The effect of an acute drug treatment on recovery time was determined by counting cells microscopically following treatment of the H69 cells and the H69CIS200 subline with 1000 ng/ml cisplatin for 2 hours and the H69 cells and the H69OX400 subline with 2000 ng/ml oxaliplatin for 2 hours. Figure 3.5 shows that the doubling time after cisplatin treatment for the H69CIS200 subline was 10 days compared to 18 days for the H69 cells. The doubling time after oxaliplatin treatment was even shorter for the H69OX400 subline (5 days) compared to greater than 21 days for the H69 cells. These shorter doubling times were reflected in the time for the cell cycle to return to normal (Figure 3.6). When the H69 and H69CIS200 cells were treated with 1000 ng/ml cisplatin for 2 hours; the time for the recovery of the sub-G_0 phase from 25% to a normal 4% and for the return of the G_0/G_1 phase to a normal 60% was faster for the H69CIS200 cells than the H69 cells. There was also an increase in the proportion of H69 cells in the G_2/M phase, but there was no such change for the H69CIS200 subline. The H69OX400 subline treated with 2000 ng/ml oxaliplatin for 2 hours showed little change in the cell cycle relative to those changes seen in the H69 cells. Even though 1000 ng/ml cisplatin and 2000 ng/ml oxaliplatin produced a more dramatic change in cell cycle in the H69 cells than in both the resistant sublines, when the H69CIS200 subline was acutely treated with double the dose (2000 ng/ml cisplatin for 2 hours) and the H69OX400 subline with 4 times the dose (8000 ng/ml oxaliplatin for 2 hours), the cell cycle profiles of the sublines resembled those for the H69 cells (Figure 3.7). The cell cycle kinetics were also determined during the development of the sublines following treatment cycle 4 and found to be the same as for the parental H69 cells (Figure 3.8).

3.4 Cross resistance to other chemotherapeutics

The H69CIS200 and H69OX400 cell sublines were equally resistant to cisplatin and oxaliplatin but they were not significantly resistant to carboplatin (Figure 3.9). Neither subline showed resistance to daunorubicin, epirubicin, etoposide, irinotecan, selenium or copper. However both the resistant sublines showed increased sensitivity to taxol and taxotere. This increase in sensitivity was not associated with other mitotic spindle poisons such as vinblastine or navelbine. Rather the H69OX400 subline was

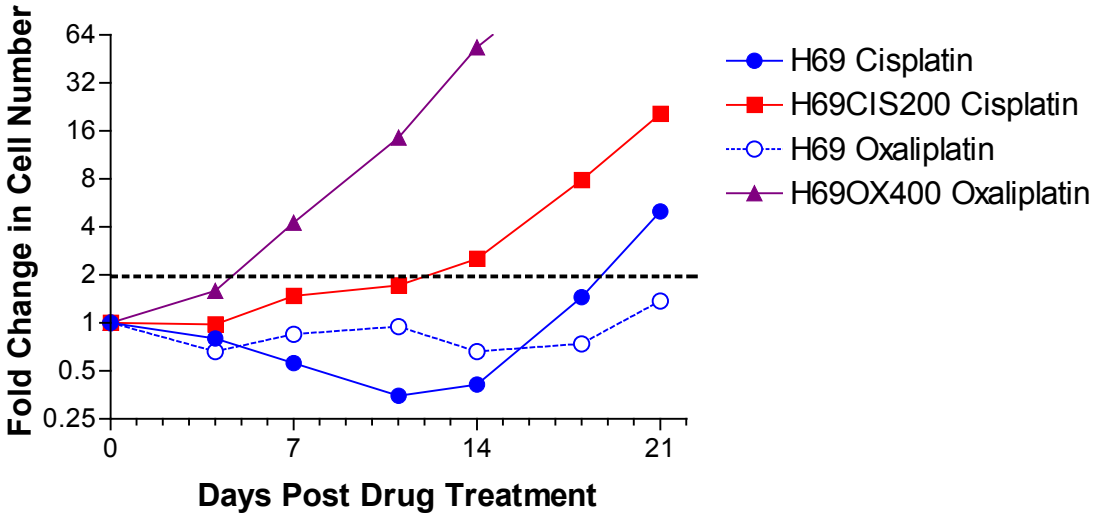

Figure 3.5. Effect of acute platinum drug treatment on cell growth. The H69CIS200 (■) and H69 (●) cells were treated with 1000 ng/ml cisplatin for 2 hours and the H69OX400 (▲) and H69 (○) cells were treated with 2000 ng/ml oxaliplatin for 2 hours. The number of cells that exclude trypan blue were counted twice a week and the fold change was plotted vs. time after treatment. The experiment was repeated twice and a representative experiment is shown.

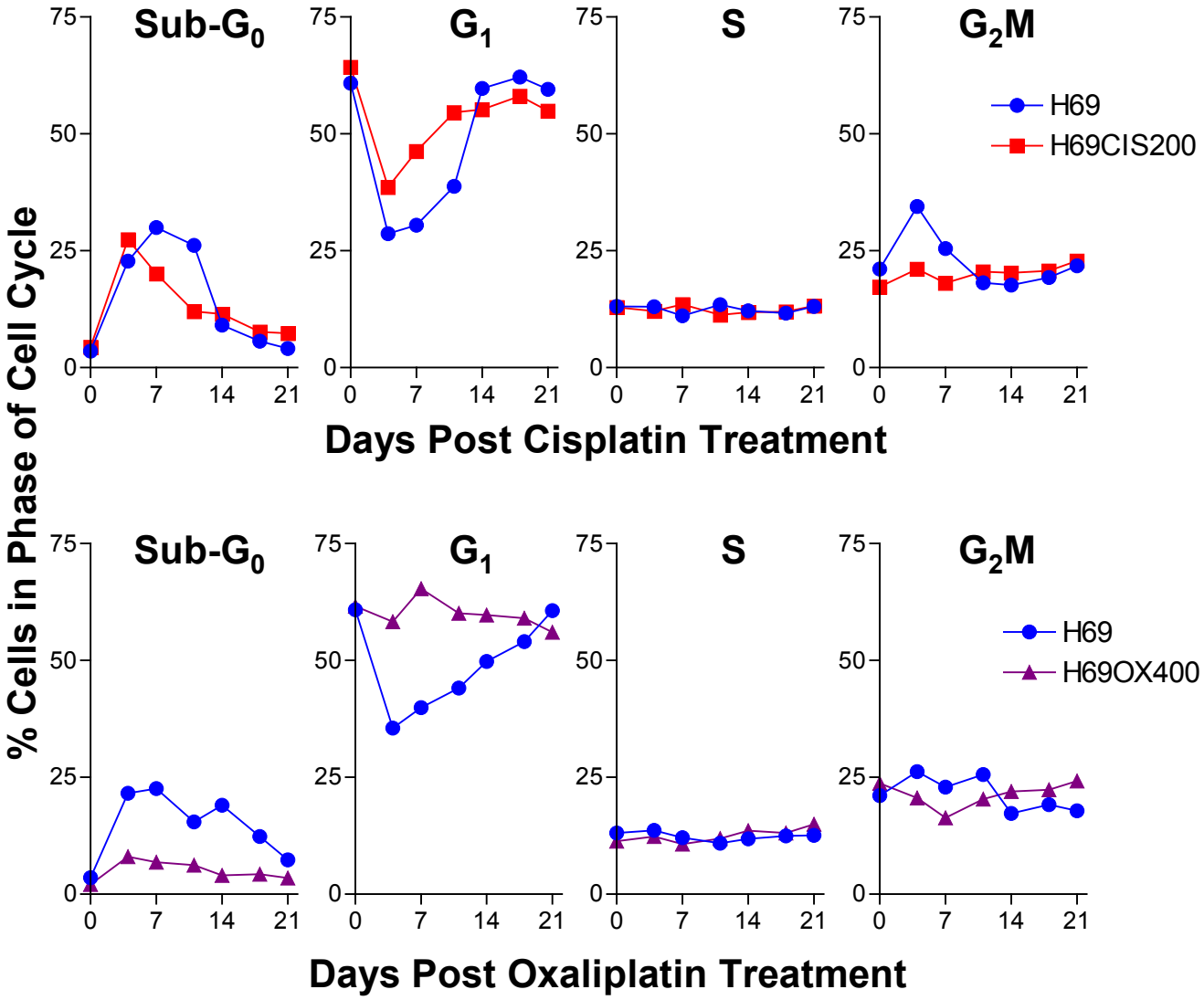

Figure 3.6. Effect of acute platinum drug treatment on cell cycle. The H69CIS200 (■) and H69 (●) cells were treated with 1000 ng/ml cisplatin for 2 hours and the H69OX400 (▲) and H69 (●) cells were treated with 2000 ng/ml oxaliplatin for 2 hours and the proportion of cells in each phase of the cell cycle was determined by propidium iodide flow cytometry twice a week as described in section 2.4. The experiment was repeated twice and a representative experiment is shown.

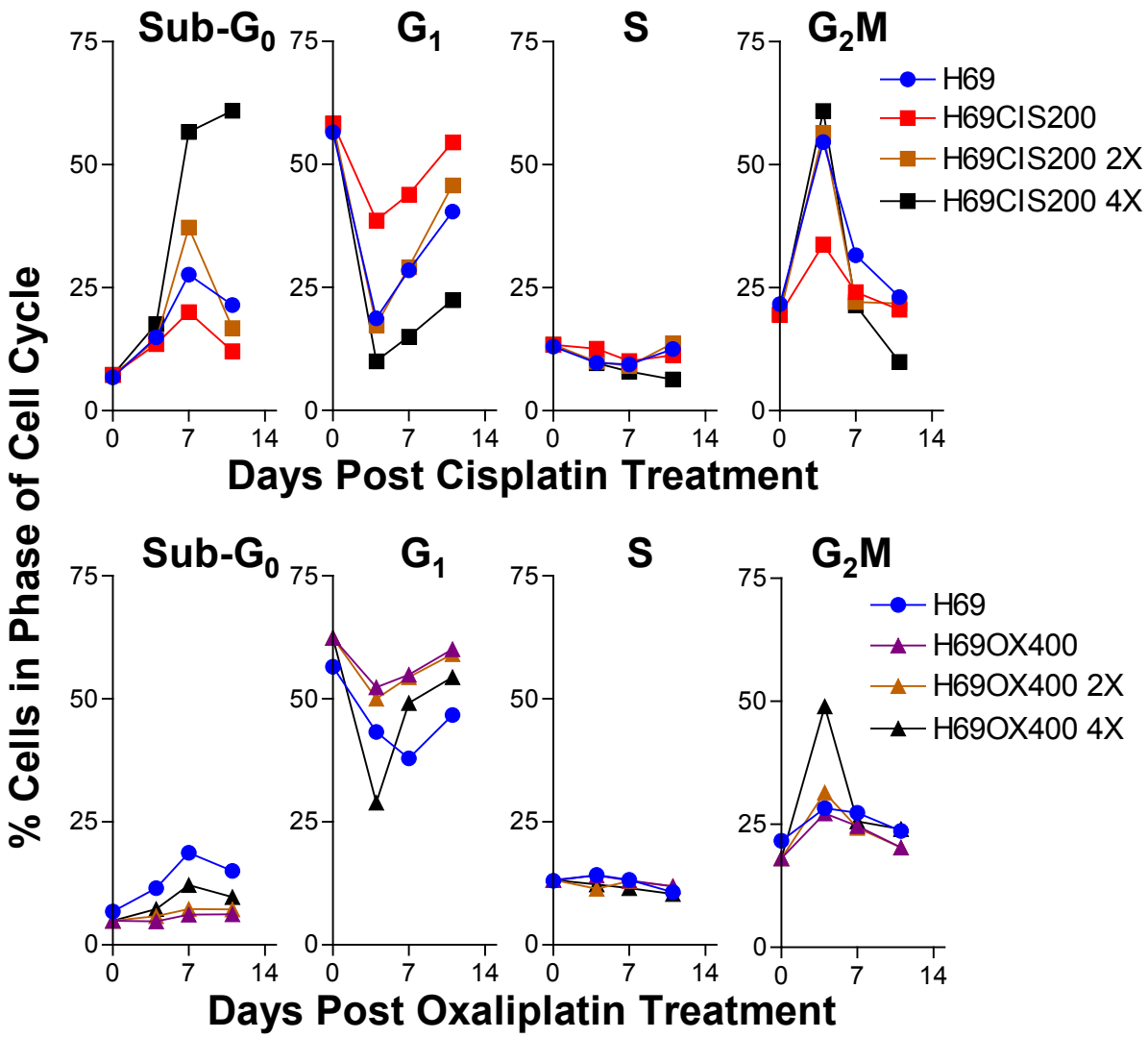

Figure 3.7. Effect of dose escalation on cell cycle. The cells were treated with the same doses as Figure 3.6 as well as 2X and 4X the dose of drug for 2 hours and the proportion of cells in each phase of the cell cycle was determined by propidium iodide flow cytometry twice a week as described in section 2.4. The experiment was repeated twice and a representative experiment is shown.

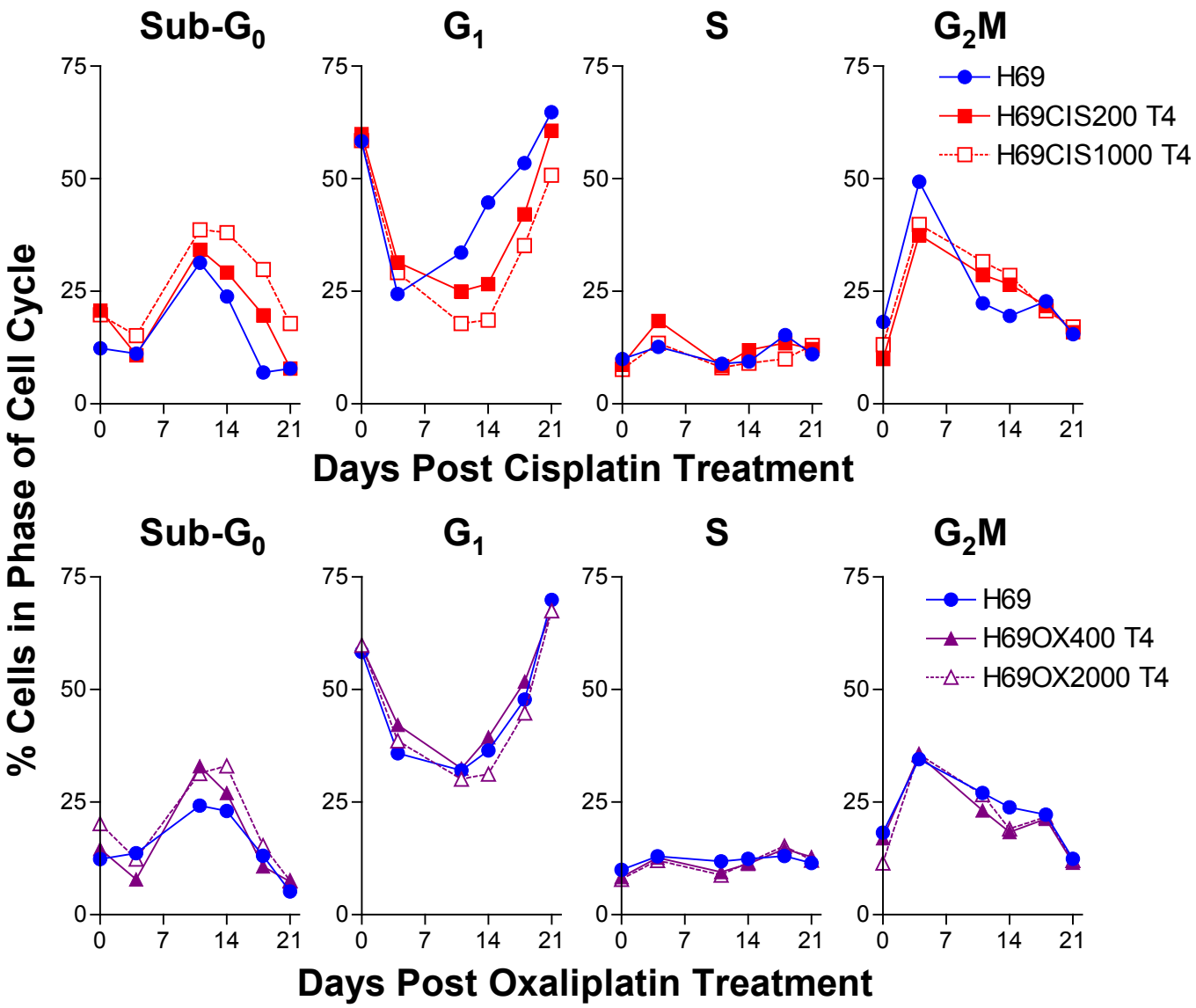

Figure 3.8. Effect of acute drug treatment on cell cycle at treatment 4. The H69CIS200(T4) (■), H69CIS1000(T4) (□) and H69 (●) cells were treated with 1000 ng/ml cisplatin for 2 hours and the H69OX400(T4) (▲), H69OX2000(T4) (△) and H69 (●) cells were treated with 2000 ng/ml oxaliplatin for 2 hours and the proportion of cells in each phase of the cell cycle was determined by propidium iodide flow cytometry twice a week as described in section 2.4. The experiment was repeated twice and a representative experiment is shown.

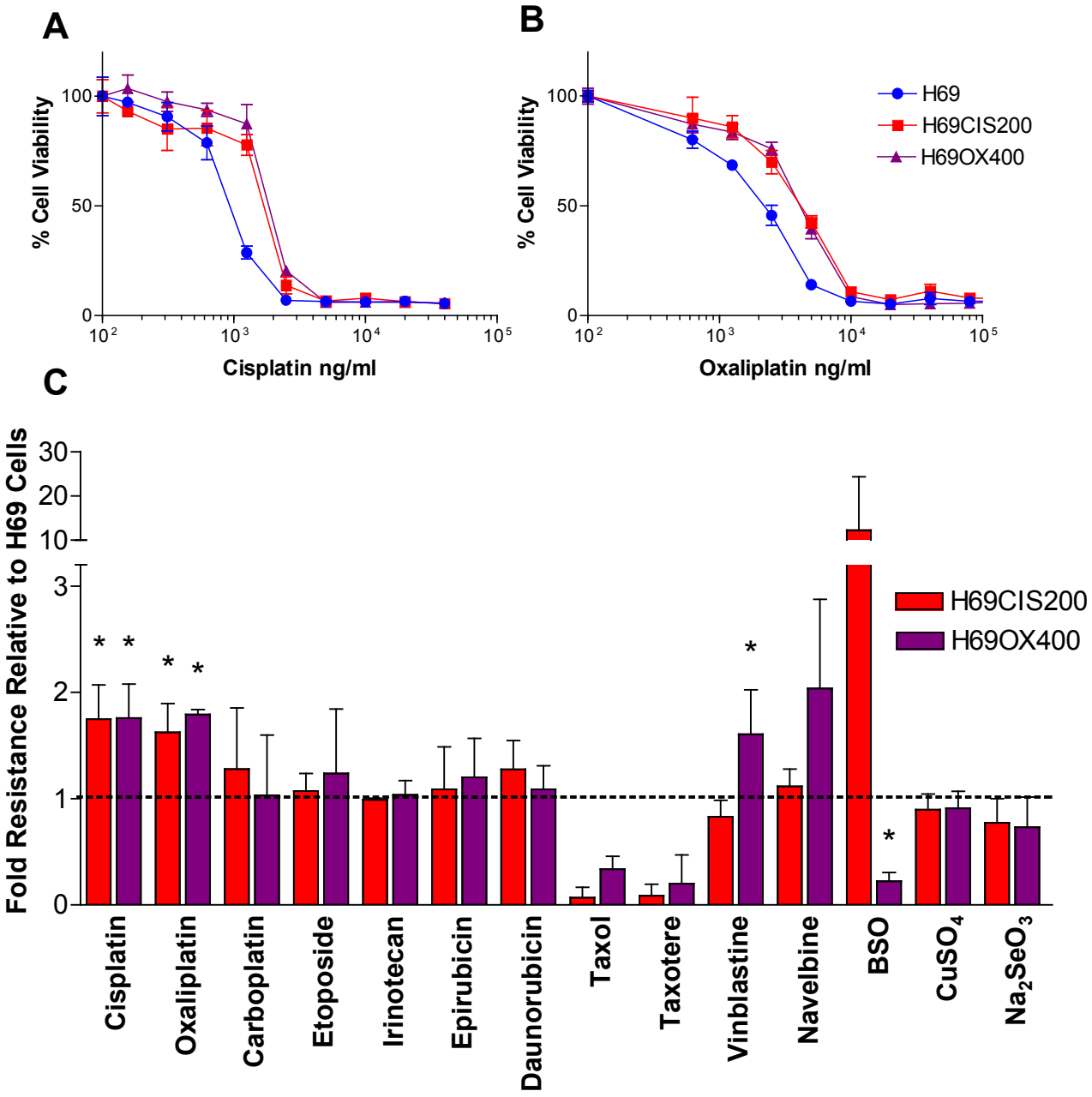

Figure 3.9. Resistance and cross resistance of the H69 sublines. A) Resistance to cisplatin B) Resistance to oxaliplatin C) The cross resistance of the H69CIS200 and H69OX400 sublines to the indicated drugs was determined using a 5 day MTT cytotoxicity assay as described in section 2.3. The mean fold resistance and standard deviation relative to the H69 cells for at least two independent experiments is shown. Significant differences from the H69 parental as determined by a student's t-test $p<0.05$ and is represented by a *****.

resistant to vinblastine. The H69CIS200 subline was resistant to buthionine sulfoximine (BSO) while the H69OX400 subline was sensitive to BSO.

3.5 Cellular glutathione and resistance

To further investigate this differential effect of BSO, the levels of cellular glutathione was determined. The level of cellular glutathione changes over the period of each subculture, glutathione rapidly increases with the fresh media then drops over the next several days in all cell lines (Figure 3.10A). The glutathione levels were quite variable on the first day of culture so glutathione levels were examined 48 hours after subculture. There was no significant difference in glutathione levels between the sublines without drug treatment. Platinum drug treatment increased glutathione levels significantly (Figure 3.10B). However, this response was the same in all cell lines, indicating that the resistant cells cannot upregulate glutathione any better than the parental cells (Figure 3.10B). There was a trend for cisplatin to increase the levels of glutathione more than oxaliplatin, this was significant as indicated by # for the response in H69 cells only.

Fifty μM BSO depleted glutathione in all the cell lines to a similar extent of approximately 2% of the untreated level (Figure 3.10C). The effect of depleting cellular glutathione on cell growth and on resistance was determined by culturing the H69 cells and the resistant sublines in media containing 50 μM BSO. Figure 3.11A shows that BSO treatment reduced the growth of the H69 cells to 65% of untreated cells, for the H69CIS200 subline the reduction was similar but for the H69OX400 subline growth was further inhibited. BSO tended to sensitise all cells to oxaliplatin, but had little effect on cisplatin resistance (Figure 3.11B,C).

3.6 Platinum accumulation

There were no significant changes in the level of cell-associated platinum in the H69CIS200 or H69OX400 sublines relative to the H69 cells following a 2 hour exposure to 1000 ng/ml cisplatin, 2000 ng/ml oxaliplatin or a 4-day exposure to 200

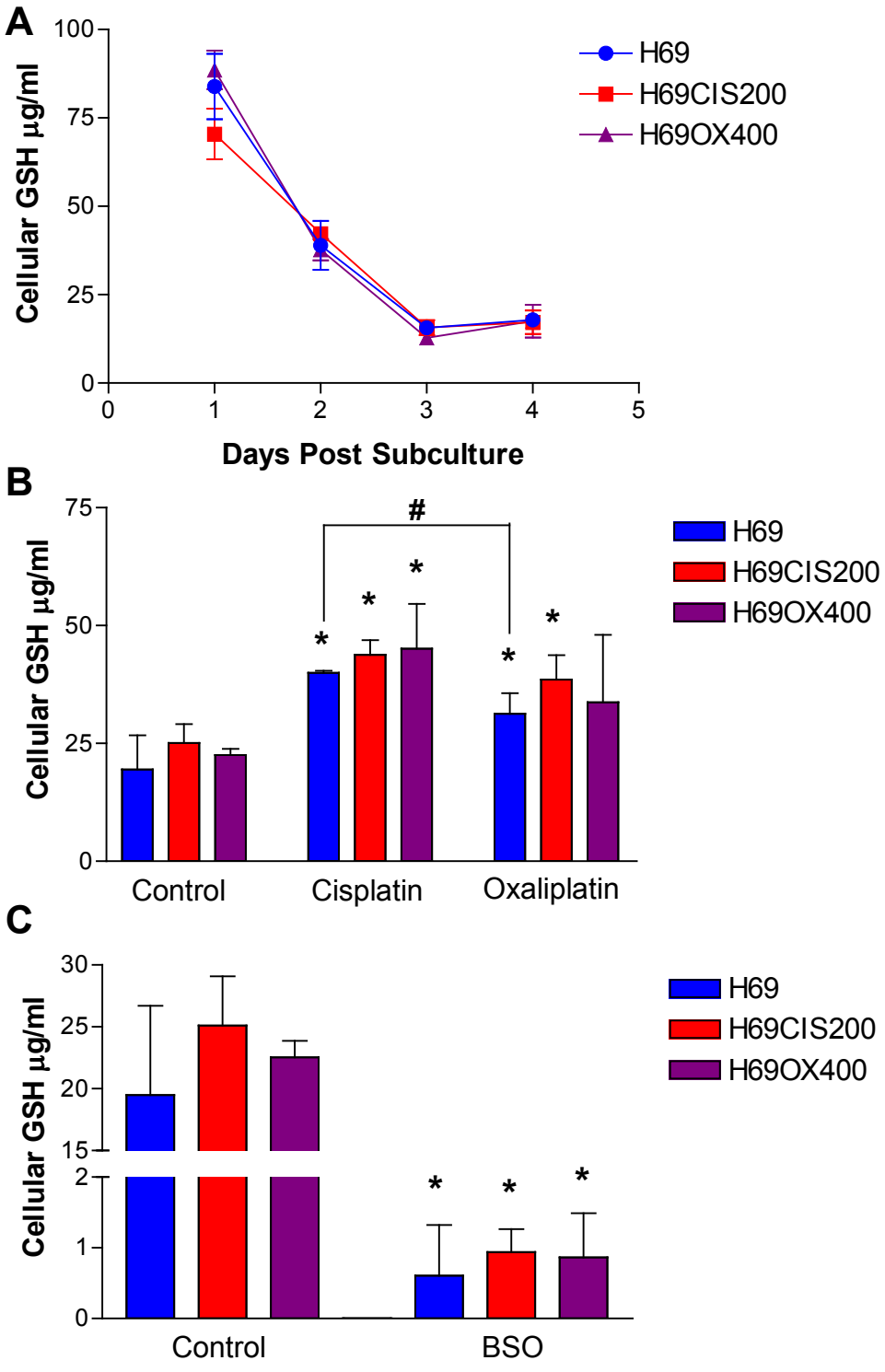

Figure 3.10. Cellular glutathione. A) Change in cellular glutathione over the drug-free subculture period in H69 cells (●), H69CIS200 (■) and H69OX400 cells (▲). B) Glutathione levels in control cells and cells treated with 200 ng/ml cisplatin and 400 ng/ml oxaliplatin for 48 hours. C) Glutathione levels in control cells and cells treated with 50 µM BSO for 48 hours. Glutathione was assayed as described in section 2.5. The mean glutathione level for two independent experiments is shown. * - significant difference from control samples, # - significant difference between the response to cisplatin and oxaliplatin as determined by a student's t-test $p<0.05$.

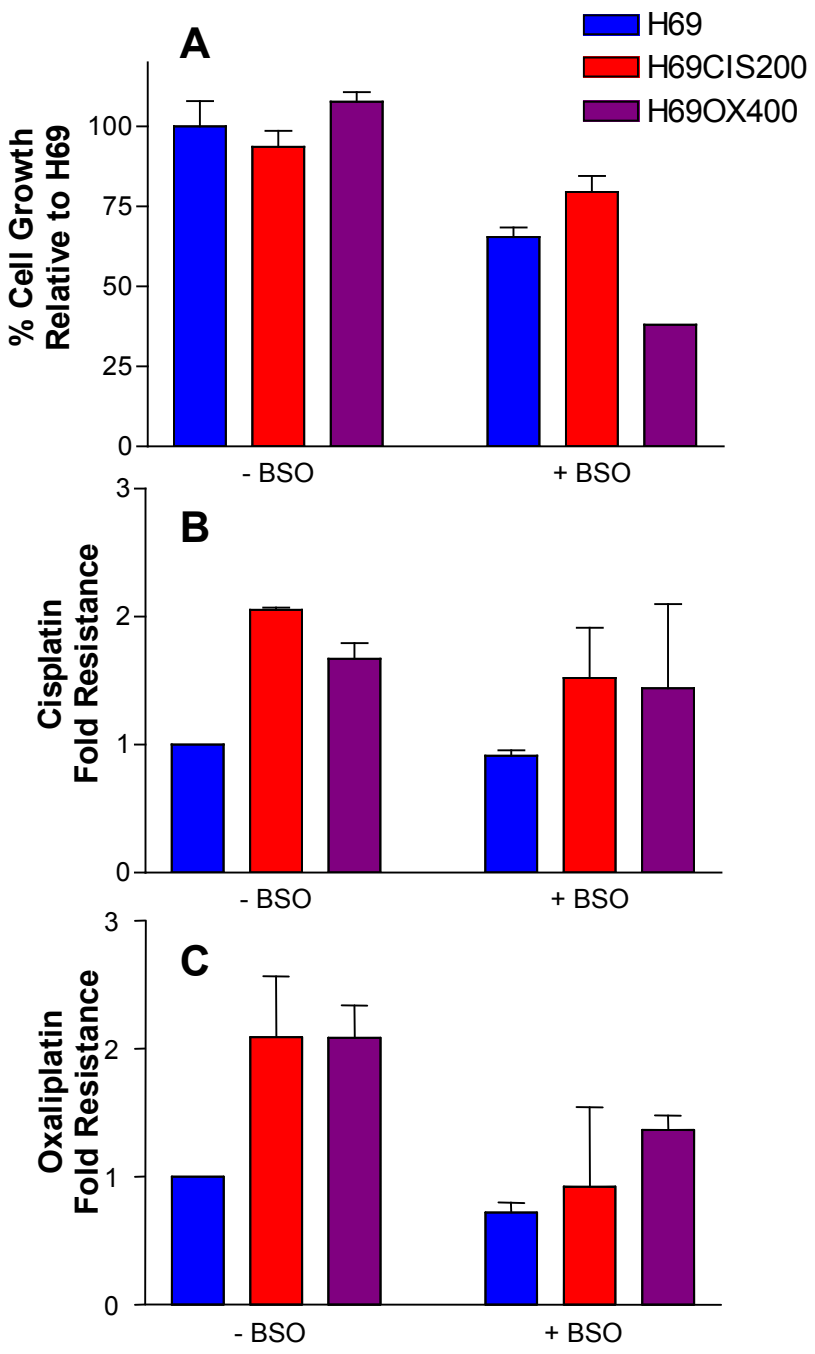

Figure 3.11. Effect of glutathione depletion on cell growth and drug resistance. A) The number of cells which exclude trypan blue was determined after 3 days in culture +/- 50 μM BSO. The IC_{50} for B) cisplatin and C) oxaliplatin was determined for a 5 day MTT cytotoxicity assay as described in section 2.3 in the presence and absence of 50 μM BSO. The fold resistances were calculated relative to the H69 cells in the absence of BSO. The means and standard deviations of 2 separate experiments is shown.

ng/ml cisplatin or 400 ng/ml oxaliplatin (Figure 3.12A). This suggests that changes in drug efflux or drug uptake were not contributing to the platinum resistance.

There was a significantly higher level of residual platinum in the resistant cells before drug treatment (Figure 3.12A). When platinum accumulation was studied at treatment 4 during the development of the cell lines there was a significant increase in the resistant cell lines. This significant increase is due to the recent drug treatment (Figure 3.12B). However, the stably resistant cell lines examined in Figure 3.12A were grown for an average of 7 weeks in drug-free culture after platinum drug treatment. The exponentially growing cell lines complete cell division 3-4 times per week (Figure 3.3) The residual platinum therefore seemed too high for cells which had divided up to 28 times in drug-free culture which would theoretically dilute the amount of cell associated platinum from drug treatment by a factor of 2^{28}.

There could be another explanation for the high levels of platinum in the resistant cell lines. Sodium ions in an atomic absorption sample can potentially interfere with platinum analysis as there is a sodium peak near the wavelength for platinum at 265.9 nm. The cell lines were analysed for changes in sodium or other electrolytes which could contribute to a higher platinum background in the resistant cell lines. However, there was no significant difference in Na, K or Cl concentrations in the resistant cell lines (Figure 3.12C). There was a trend towards decreased sodium rather than an increase that would contribute to the high platinum background. There was also no significant difference in cell size (Figure 3.3C) that could explain the higher levels of platinum background in the resistant cells.

When the platinum accumulation data in Figure 3.12A was adjusted for the background platinum levels before drug treatment, there was still no difference in platinum accumulation between the sensitive and resistant cell lines. This suggests that the initial conclusion was correct, that no changes in uptake or efflux of platinum is contributing to the mechanism of platinum resistance in these cell lines. However, there is no explanation for the high levels of residual platinum in the resistant cell lines. The rate of decrease of platinum after drug treatment should be further analysed in this cell model to fully understand the metabolism of the drug and to explain the background levels of Pt in the resistant cells.

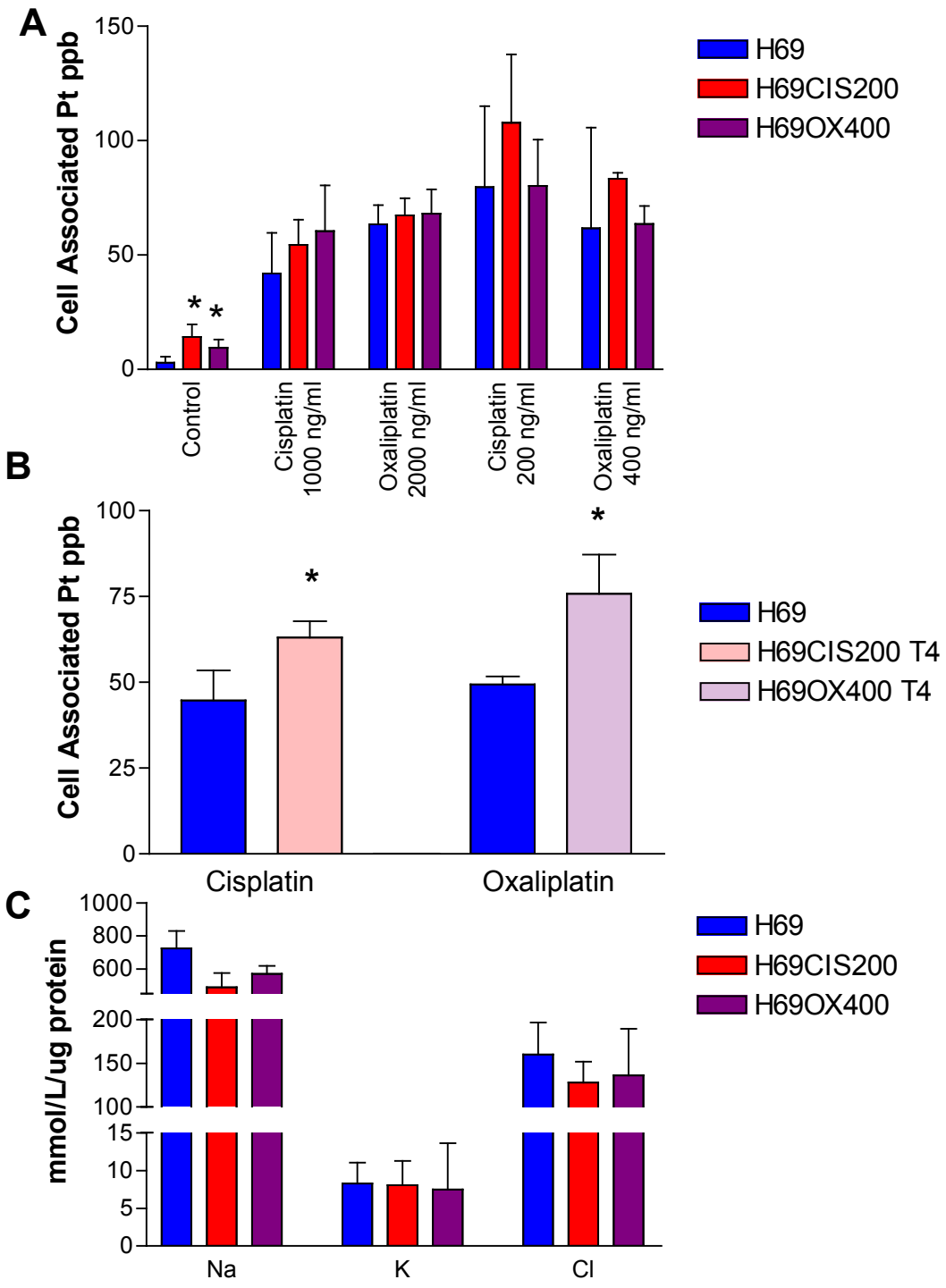

Figure 3.12. Platinum accumulation. A) H69, H69CIS200 and H69OX400 cells were treated with 1000 ng/ml cisplatin, 2000 ng/ml oxaliplatin for 2 hours, 200 ng/ml cisplatin for 4 days or 400 ng/ml oxaliplatin for 4 days. The amount of platinum accumulated after a drug exposure was determined by atomic absorption spectroscopy as described in section 2.6. B) H69, H69CIS200(T4) and H69OX400(T4) cells were treated with 1000 ng/ml cisplatin, 2000 ng/ml oxaliplatin for 2 hours and analysed for platinum as in part A. C) Na, K and Cl concentrations in the cell lines were analysed as described in section 2.6.1.The mean platinum, Na, K and Cl levels for two independent experiments is shown. * - significant difference from the H69 cells as determined by a student's t-test $p<0.05$.

3.7 Discussion

Studies of cellular drug resistance mainly focus on the molecular mechanisms contributing to the resistance rather than how the cells became resistant and the factors that promote its development. In this study the H69 SCLC cells were treated either for 4 days or 2 hours with an IC_{20} dose of cisplatin or oxaliplatin to determine the impact of cisplatin versus oxaliplatin and the length of drug exposure on the development of resistance. The time taken to develop stable resistance was approximately 8 months and this compares with the range of 4 months to 24 months reported for other cisplatin-resistant SCLC sublines (Table 1.4). The rate of development of resistance appeared similar between the 2 hour and 4 day treatment schedules. However, the 4 day schedule produced stable resistance while the 2 hour schedule produced unstable resistance suggesting that a shorter pulse may be more effective against cancer than continuous exposure or longer pulse times. This is similar to what was observed in the development of a cisplatin-resistant ovarian carcinoma, which yielded stable resistance from a continuous exposure but not from a series of 1 hour pulses (Kuppen et al., 1988). However, other studies have produced stable cisplatin resistance with 1-2 hour pulses in murine ovarian reticulosarcoma (Belvedere et al., 1996), human ovarian adenocarcinoma (Poulain et al., 1998) and non-SCLC (Lai et al., 1995) using higher doses of drug (μmolar) than used in this study.

The results of this comparative study show that SCLC cells develop resistance to oxaliplatin more easily than they develop resistance to cisplatin. There appear to be no other studies of oxaliplatin selected SCLC cells, however, there are many reports for other types of carcinoma cells. Commonly reported mechanisms of resistance to oxaliplatin include increased cellular glutathione (El-akawi et al., 1996) and decreased platinum accumulation (Hector et al., 2001; Mishima et al., 2002; Rennicke et al., 2005) similar to what is seen in cisplatin resistance. The H69CIS200 and H69OX400 sublines appear not to have decreased platinum accumulation (Figure 3.12A) nor increased glutathione (Figure 3.9B) but may rely on altered cell cycle kinetics as a means of resistance (Figures 3.5, 3.6 and 3.7).

During the first five treatment cycles there was no measurable drug resistance yet the treated cells survived and regrew. Survival of these early treatment cycles involved a reversible cell cycle arrest followed by regrowth. Regrowth resistance has previously been reported as a mechanism that allows cells to survive drug treatment via proliferation rather than increased drug resistance (Preisler et al., 1994). Regrowth resistance arose from the observation that there are many tumours in which complete remission but not cure can be achieved fairly easily. Upon relapse some tumours will respond very well when retreated with the agents with which they were initially treated. It is therefore difficult to envisage classical drug resistance as being the sole cause of treatment failure in this scenario. Regrowth resistance is one possible explanation for the recurrence of disease despite continued drug sensitivity. Depending on the rate of proliferation and the sensitivity of the malignancy to therapy, the effects of tumour regrowth can range from insignificant to the complete offsetting of the effects of treatment (Preisler, 1995). Regrowth resistance may therefore be an initial response before more permanent resistance mechanisms develop.

After six treatment cycles the response of the resistant cells changed. There was a shorter time to doubling for 3 out of the 4 resistant sublines and this change in response was accompanied by a change in the cell cycle kinetics following drug treatment (Figure 3.5). This is comparable to the resistance observed after 6 treatment cycles in cisplatin-resistant SCLC (Locke et al., 2003) and 6 treatment cycles in oxaliplatin-resistant ovarian carcinoma (Mishima et al., 2002). Earlier in the development of resistance (treatment cycle 4) treated cells showed a similar cell cycle recovery as the H69 cells (Figure 3.8). A similar pattern of growth arrest and recovery was observed in the development of cisplatin-resistant IGROV1 ovarian carcinoma cells (Poulain et al., 1998). IGROV1 cells were exposed to cisplatin for 2 hours and allowed to recover for several weeks. Development of resistance to cisplatin was associated with the ability of the treated cells to progress through the cell cycle beyond the G_1/S checkpoint; although most cells died by apoptosis, a few surviving cells proliferated and recolonised the cultures. The authors suggested that this was not resistance to drug induced cell death, rather an increased propensity to proliferate after cytotoxic treatment (Poulain et al., 1998), in other words regrowth resistance. It is likely that regrowth resistance is initially used as a survival

mechanism that also provides the time for a more permanent protective mechanism to develop.

Regrowth resistance is difficult to measure using a conventional 5 day MTT cytotoxicity assay. The main reason for this is that regrowth does not occur within the time of the assay. Also the cytotoxicity assay depends on their being a change in growth rate or survival with changing dose of test drug. For regrowth resistance, growth arrest can occur over a wide drug concentration range effectively producing no change in growth or survival for the cytotoxicity assay to detect. The sublines which survived dose escalation showed no increase in resistance in a conventional 5 day cytotoxicity assay (Figure 3.1), however their survival is indicative of regrowth resistance.

As to whether oxaliplatin is more effective than cisplatin, there is little in the way of direct comparisons in cellular resistance studies. Resistance developed in a similar manner in response to cisplatin and oxaliplatin in this SCLC cell model. Both platinum drugs produced similar levels of resistance (Figure 3.4), patterns of drug cross-resistance (Figure 3.9C) and stability of the resistance (Figure 3.4). However, it was easier to escalate the dose of oxaliplatin compared to cisplatin**.** A two-fold higher dose of cisplatin was cytotoxic to low-level resistant cells while a two-fold higher dose of oxaliplatin still resulted in viable cells. This suggests oxaliplatin may be less effective than cisplatin. This is also supported by the quicker recovery of growth from a single drug treatment for the H69OX400 subline compared to the H69CIS200 subline (Figure 3.5).

A possible explanation for the faster recovery from oxaliplatin treatment and the greater number of oxaliplatin surviving sublines, is the greater efficiency of bypassing of oxaliplatin-DNA adducts than cisplatin-DNA adducts by DNA polymerases (Chaney et al., 2005). There is also further evidence to suggest that at equimolar concentrations oxaliplatin forms fewer but more cytotoxic DNA lesions than cisplatin (Woynarowski et al., 1998; Woynarowski et al., 2000). This may explain the response of the sublines to equally cytotoxic doses of drug, in the case of oxaliplatin there may be fewer lesions with a better chance of being bypassed by DNA polymerases. This combination leads to a greater chance of the oxaliplatin treated cell dividing, despite

the presence of DNA lesions. The cell division will dilute out the number of lesions per cell and these surviving cells are likely to have additional attributes contributing to their mechanism of resistance to the platinum drug.

There is evidence to suggest that oxaliplatin is active against highly cisplatin-resistant cell lines, however there is just as much evidence to suggest that cisplatin is active in highly oxaliplatin-resistant cell lines (Figure 1.2). In this study of H69 SCLC cells, oxaliplatin did not have activity against the cisplatin-resistant H69CIS200 cells and there are similar reports in ovarian carcinoma (Hector et al., 2001). This also complements the clinical studies showing a lack of activity of oxaliplatin in cisplatin-resistant ovarian carcinoma (Chollet et al., 1996; Soulie et al., 1997; Dieras et al., 2002). Oxaliplatin may only be effective in highly cisplatin-resistant cells with different mechanisms to the regrowth resistance observed in the H69CIS200 cells. This study questions the effectiveness of oxaliplatin in cisplatin-resistant cancer and suggests that more research into the mechanisms of low-level platinum resistance is needed to resolve this issue.

Even though oxaliplatin had little activity against cisplatin resistance in this study, taxol and taxotere showed increased activity against both the H69CIS200 and H69OX400 sublines relative to the H69 cells (Figure 3.9C). There are previous reports of cisplatin-resistant SCLC cells being sensitised by pretreatment with a low dose of taxol (Locke et al., 2003) and there are many examples of other cisplatin-resistant cell lines that are sensitive to taxanes (Christen et al., 1993; Jekunen et al., 1994; Johnson et al., 1996; Yamamoto et al., 2000a; Burns et al., 2001). Taxanes bind to and stabilise microtubules and block cell cycle progression through centrosomal impairment, induction of abnormal spindles and suppression of spindle microtubule dynamics (Abal et al., 2003). The mechanism of platinum resistance in these resistant sublines may involve tubulin abnormalities which then render the cells sensitive to subsequent taxol treatment. This is supported by the report of cisplatin resistance being associated with decreased levels of β-tubulin and tubulin abnormalities (Christen et al., 1993; Ohta et al., 1993). Another possible explanation could involve survivin since this is increased in cisplatin-resistant ovarian cancer cells and taxol treatment reduces survivin levels in these cells (Wang et al., 2005b). This important

issue of taxane sensitivity being associated with platinum resistance is further investigated in Chapter 6.

The H69CIS200 and H69OX400 cells are not cross-resistant to topoisomerase poisons daunorubicin, etoposide and epirubicin which target topoisomerase II (Hande, 1998; Fedier et al., 2001). The cell lines are also not cross-resistant to irinotecan which targets topoisomerase I (Figure 3.9C) (Xu et al., 2002). This suggests that there are no changes in the expression of topoisomerase I or II associated with the mechanism of platinum resistance.

The H69CIS200 and H69OX400 cells are not cross-resistant to copper (Figure 3.9C). Suggesting that the copper efflux proteins CTR1, ATP7A and ATP7B are not associated with resistance in this cell model unlike other models of cisplatin resistance with cross resistance to copper (Katano et al., 2002). The cells also show similar levels of platinum accumulation (Figure 3.12A), suggesting that no mechanisms of increased efflux or decreased uptake are associated with platinum resistance in this cell model.

Increases in intracellular glutathione has been previously associated with platinum resistance in many studies (El-akawi et al., 1996; Jansen et al., 2002; Kawai et al., 2002). The level of glutathione remains unchanged between the cell lines (Figure 3.10B) and treatment with 50 μM BSO tended to sensitise all cells to oxaliplatin, but had little effect on cisplatin resistance (Figure 3.11B & C). This suggests that a depletion of glutathione is not enough to overcome the platinum resistance in this model. All the cell lines show a drop in growth rate in response to 50 μM BSO (Figure 3.11A), however the H69OX400 cells show the most inhibition and the H69CIS200 cells grow more than the parental cells under these conditions. This corresponds to what was found in the BSO toxicity assay, the H69CIS200 cells are resistant and the H69OX400 cells are sensitive to BSO (Figure 3.9). How this difference in response to BSO treatment relates to platinum resistance will be examined further in this cell model in Chapter 7.

3.8 Conclusions

Cisplatin and oxaliplatin treatment both cause the development of resistance in the H69 SCLC cell line in similar ways that initially involves growth arrest-regrowth resistance followed by more permanent resistance mechanisms that appear not to involve decreased platinum accumulation or increased glutathione levels. Oxaliplatin resistance was induced more rapidly than cisplatin resistance and oxaliplatin-resistant cell lines survived dose escalation to a greater extent than the cisplatin-resistant cell lines. Oxaliplatin was not effective against cisplatin resistance in this cell model however both resistant sublines were more sensitive to taxol and taxotere suggesting the taxanes should be further investigated for their potential against platinum-resistant SCLC.

CHAPTER 4.0

CHROMOSOMAL CHANGE ASSOCIATED WITH PLATINUM RESISTANCE

4.1 Introduction

The karyotypic abnormalities of drug-resistant cells have been studied extensively with the hope of gaining insight into the drug-resistant phenotype. Changes in gene copy number at loci associated with drug resistance have provided links between changes in the genotype of a cell line and its resistant phenotype. These changes have also provided clinical markers used to monitor the development of resistance over the course of treatment. The increase in gene copy number for ABC transporters MRP1 at 16p13.1 (Cole et al., 1992) and P-glycoprotein (P-gp) at 7q36 (Bell et al., 1987) have been associated with resistance to doxorubicin and vinblastine respectively. The increase in copy number of dihydrofolate reductase has also been associated with the development of methotrexate resistance in human and animal cell lines (Fougere-Deschatrette et al., 1984) as well as clinically in the treatment of leukemia (Horns, Jr. et al., 1984).

Chromosomal rearrangement has been studied in many cisplatin-resistant cancer cell lines (Table 4.1) in the hope of discovering a unique marker of platinum resistance. Many rearrangements have been observed, including amplifications and deletions on almost every chromosome, as summarised in Figure 4.1. There are more amplifications (57.4%) than deletions (42.6%) associated with cisplatin resistance, and the number of changes in a cell line does not correlate with the level of cisplatin resistance. Chromosomal changes have also been studied in tumour samples from patients who have received platinum-based therapy with a similarly large array of changes found (Rao et al., 1998; Kudoh et al., 1999; Cullen et al., 2003). Chromosomal changes have not been previously studied in cisplatin-resistant small cell lung cancer (SCLC) or in oxaliplatin-resistant cell lines.

Very few links to the platinum-resistant phenotype have been established by examining the changes in chromosomes. A wide ranging study examining many types of tumours resistant to several drugs, looked for changes in copy number at known drug resistance loci. It established several links to the resistant phenotype for etoposide and camptothecin but not for any of the cisplatin-resistant cell lines examined (Yasui et al., 2004). From the literature review (Table 4.1), the only study which has successfully linked changes in genotype to the platinum-resistant

Table 4.1 Cisplatin-resistant cell lines previously analysed for chromosomal changes.

Cell Line	Cancer	Analysis	Fold Cisplatin Resistance	References	Amplifications	Deletions
RT112-CP	Bladder	Karyotype	4.6	(Walker et al., 1990)	4	10
KK47/DDP10	Bladder	CGH	9.3	(Kotoh et al., 1997; Yasui et al., 2004)	4	1
KK47/DDP20	Bladder	CGH	18.7	(Kotoh et al., 1997; Yasui et al., 2004)	2	1
T24/DDP5	Bladder	CGH	2.2	(Kotoh et al., 1994; Yasui et al., 2004)	1	1
T24/DDP7	Bladder	CGH	5.2	(Kotoh et al., 1994; Yasui et al., 2004)	1	0
T24/DDP10	Bladder	CGH	8.4	(Yasui et al., 2004)	6	2
HT-29/cDDP	Colon	CGH	5	(Yamada et al., 1996; Yasui et al., 2004)	4	2
YES-2/CDDP	Oesophageal	CGH	7.5	(Toshimitsu et al., 2004)	13	2
St-4/cDDP	Gastric	CGH	7	(Yamada et al., 1996; Yasui et al., 2004)	0	0
MeWo/Cis1	Melanoma	CGH	6	(Kern et al., 1997; Wittig et al., 2002)	2	3
BMI/BMIR2	Neuroblastoma	CGH	17	(Yasuno et al., 1999)	3	3
IMR/CP.17	Neuroblastoma	Karyotype	6.6	(Ireland et al., 1994)	1	1
SK/CP.12	Neuroblastoma	Karyotype	3.8	(Ireland et al., 1994)	4	0
2008/C8	Ovarian	CGH	4	(Wasenius et al., 1997)	9	5
2008/C13*5.25	Ovarian	CGH	15	(Wasenius et al., 1997)	11	9
2008/A	Ovarian	CGH	17	(Wasenius et al., 1997)	7	8
A2780/CP	Ovarian	CGH	11	(Wasenius et al., 1997)	0	5
CH1: CisR	Ovarian	CGH	6.4	(Leyland-Jones et al., 1999)	3	0
41M: CisR	Ovarian	CGH	4.7	(Leyland-Jones et al., 1999)	5	5
A2780: CisR	Ovarian	CGH	16	(Leyland-Jones et al., 1999)	3	2
KF28/KFr13	Ovarian	CGH	4.72	(Takano et al., 2001)	1	2
A2780/2780CP8	Ovarian	Karyotype	7.3	(Behrens et al., 1987)	0	3
GCT27cisR	Testicular	Microarray	5.6	(Kelland et al., 1992a; Wilson et al., 2005)	4	8
833K/64CP	Testicular	Microarray	7	(Reilly et al., 1993; Wilson et al., 2005)	12	5
Susa-CP	Testicular	Microarray	4.2	(Walker et al., 1990; Wilson et al., 2005)	8	2
				Total	108	80

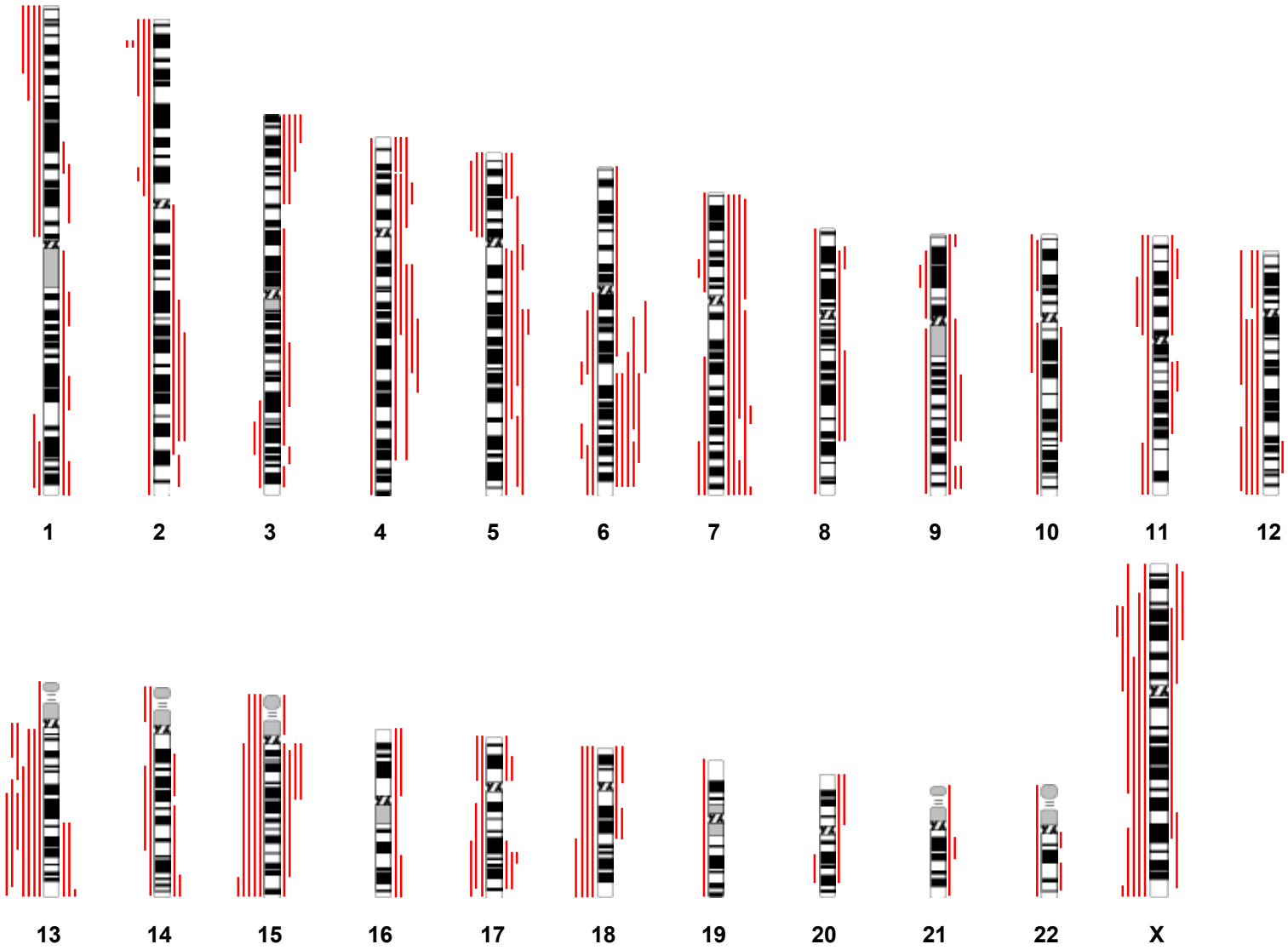

Figure 4.1 Literature review of chromosomal changes in cisplatin-resistant cell lines. Lines to the left indicate a deletion, lines to the right indicate an amplification. Papers used in the preparation of this diagram are presented in Table 4.1.

phenotype involved an amplification of 11q13 and overexpression of GSTP1 which was associated with cisplatin resistance in tumours of the head and neck in both cell lines and tumour biopsies (Cullen et al., 2003).

A large number of chemotherapeutics including platinum drugs achieve cytotoxicity through DNA damage. The platinum drug binds to the DNA strand hindering DNA transcription and replication and sometimes causing chromosome breakage. The chromosomal aberrations caused by this DNA damage are thought to be non-random in their genomic distribution (Meyne et al., 1979). Platinum drugs bind to GC-rich areas but not specific DNA sequences. Therefore, it is not clear which regions of the genome are more susceptible to damage. Chromosomal aberrations can in theory lead to the development of a drug-resistant phenotype. However, most chromosomal changes caused by DNA damaging drugs will not involve loci associated with drug resistance and will not contribute to the resistant phenotype. Amplifications and deletions can often arise in a single exposure to drug, and it is difficult to determine if it is the amplification of one gene or the loss of another that is responsible for resistance. Chromosomal changes accumulated in response to treatment with platinum drugs could be a part of the mechanism of drug resistance or they could be nothing more than a by-product of exposure to DNA damaging chemotherapeutics and not responsible for the resistance.

The contribution of any particular chromosomal change to the resistant phenotype is difficult to study. However, the analysis of chromosomal change in the H69CIS200 and H69OX400 platinum-resistant cell lines may provide a unique insight. The H69CIS200 and H69OX400 cells are stably 2-fold resistant and cross-resistant to both platinum drugs for 6-8 weeks in drug-free culture. After this period their resistant phenotype fades in the absence of drug as determined by an MTT cytotoxicity assay. These drug-sensitive revertant cell lines have been designated H69CIS200-S and H69OX400-S.

An Affymetrix 10K SNP array was performed to characterise the chromosomal changes in the resistant cell lines during their period of stable resistance and again after the resistant phenotype spontaneously faded. Through this novel approach it can be determined which chromosomal rearrangements are associated with the drug

resistance phenotype and which are random DNA damage. This study is the first SNP array analysis of the H69 SCLC cell line. This is also the first SNP array and cytogenetic analysis of either a cisplatin-resistant SCLC cell line or an oxaliplatin-resistant cell line of any carcinoma.

4.2 Affymetrix 10K SNP Array

Genomic DNA was extracted from the H69, H69CIS200 and H69OX400 cell lines and analysed with an Affymetrix 10K SNP array. The results of the array were then analysed with the Affymetrix chromosomal copy number tool. The Affymetrix system compares the chromosomal copy number tool data to a pool of normal samples in order to determine SNPs that have changed. This method was inappropriate to analyse cytogenetically abnormal samples to each other. The resistant samples were compared to the drug-sensitive parent by the following method. The chromosomal copy number data for each chromosome was smoothed by averaging a window of 20 SNPs. The chromosomal copy number data for all chromosomes is presented in Figures 4.2-4.7. Significant differences, indicating amplifications or deletions in the resistant cell lines were defined as any smoothed region which had at least 3 SNPs in a row in which the resistant cell line differed from that of the parental by a gene copy number of at least 0.5. A summary of the changes found in the H69CIS200 and H69OX400 cell lines compared to the parental H69 cell line is presented in Figure 4.8, deletions to the left of the chromosome, amplifications to the right.

4.3 H69 parental cell line

The Affymetrix 10K SNP array analysis of the H69 parental cell line revealed many changes in copy number associated with the cancerous phenotype. The highest copy number amplifications were on chromosome 8 (Figure 4.3) and 14 (Figure 4.5). The H69 cell line and all its sublines were quasi-tetraploid each cell having around 60 chromosomes per cell, including 3 structurally normal copies of chromosome 8 (Figure 4.9A). The gross amplification of chromosome 8 sequences was confirmed to be the c-myc gene by FISH (Figure 4.10). Cytogenetically, the c-myc amplification was seen within a homogenously staining region located on a derivative fusion

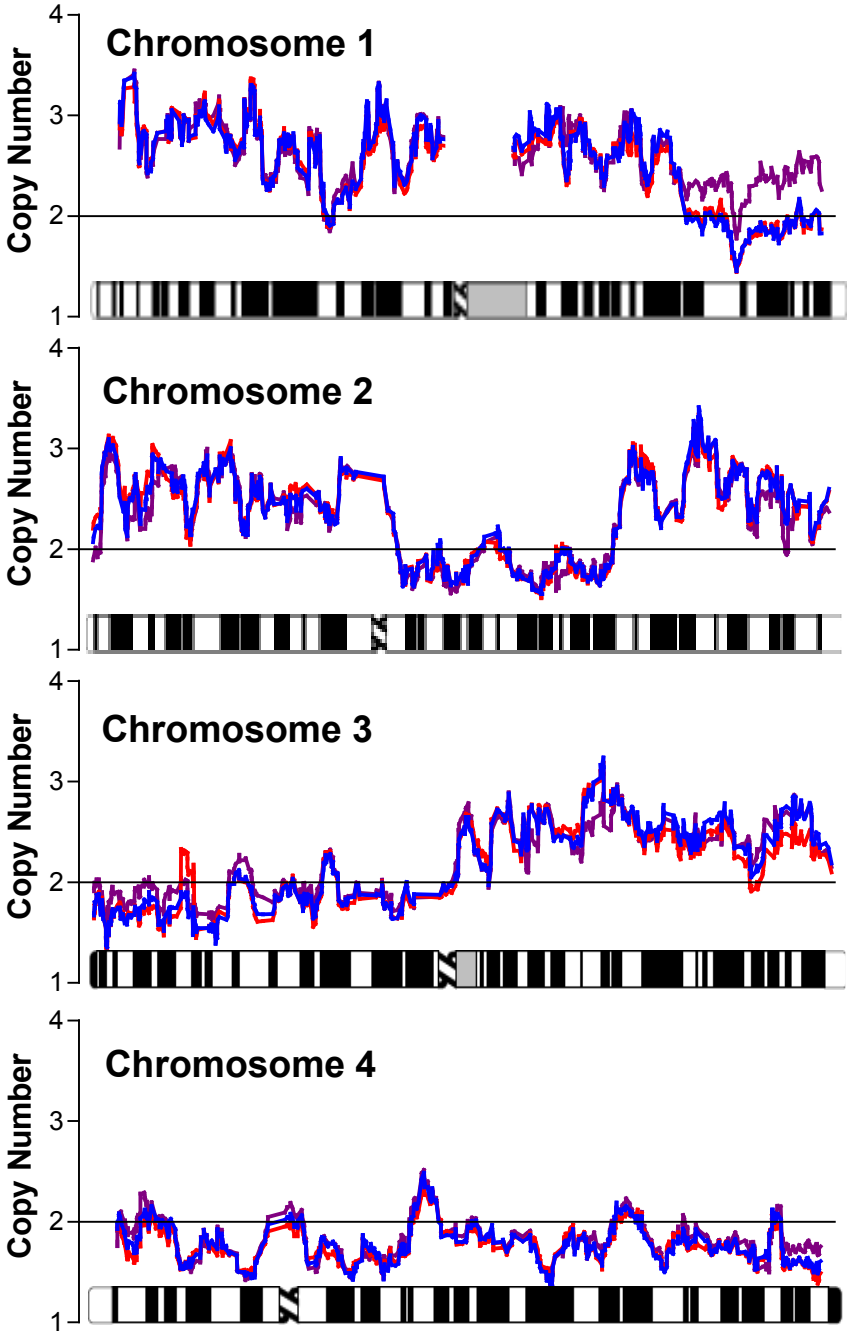

Figure 4.2 Chromosomal copy number of chromosomes 1, 2, 3 and 4. Genomic DNA was extracted from the H69 (——), H69CIS200 (——) and H69OX400 (——) cell lines and analysed by Affymetrix 10K SNP array and Affymetrix chromosomal copy tool as described in sections 2.7 and 2.8. Data was smoothed by averaging a window of 20 SNPs.

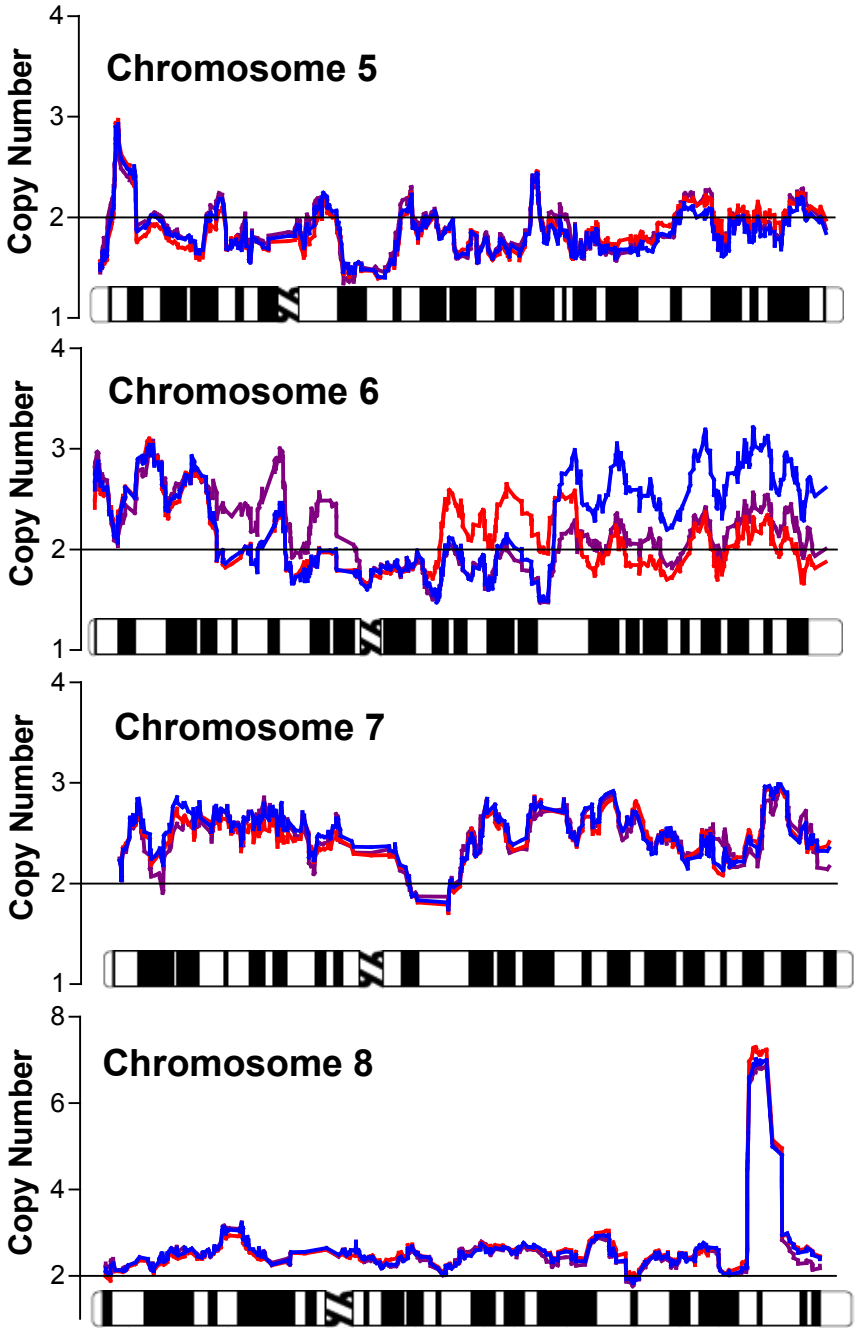

Figure 4.3 Chromosomal copy number of chromosomes 5, 6, 7 and 8. Genomic DNA was extracted from the H69 (——), H69CIS200 (——) and H69OX400 (——) cell lines and analysed by Affymetrix 10K SNP array and Affymetrix chromosomal copy tool as described in sections 2.7 and 2.8. Data was smoothed by averaging a window of 20 SNPs.

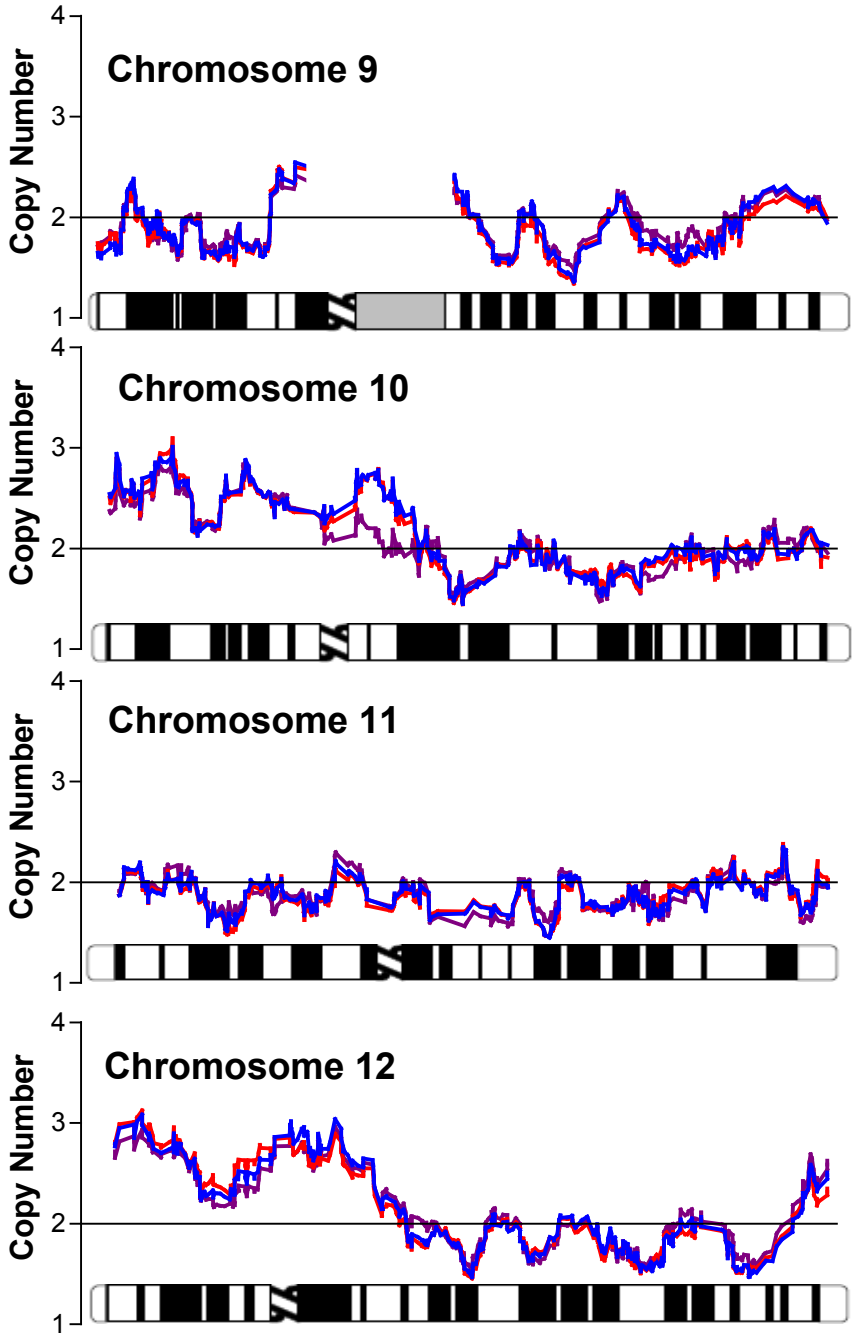

Figure 4.4 Chromosomal copy number of chromosomes 9, 10, 11 and 12. Genomic DNA was extracted from the H69 (——), H69CIS200 (——) and H69OX400 (——) cell lines and analysed by Affymetrix 10K SNP array and Affymetrix chromosomal copy tool as described in sections 2.7 and 2.8. Data was smoothed by averaging a window of 20 SNPs.

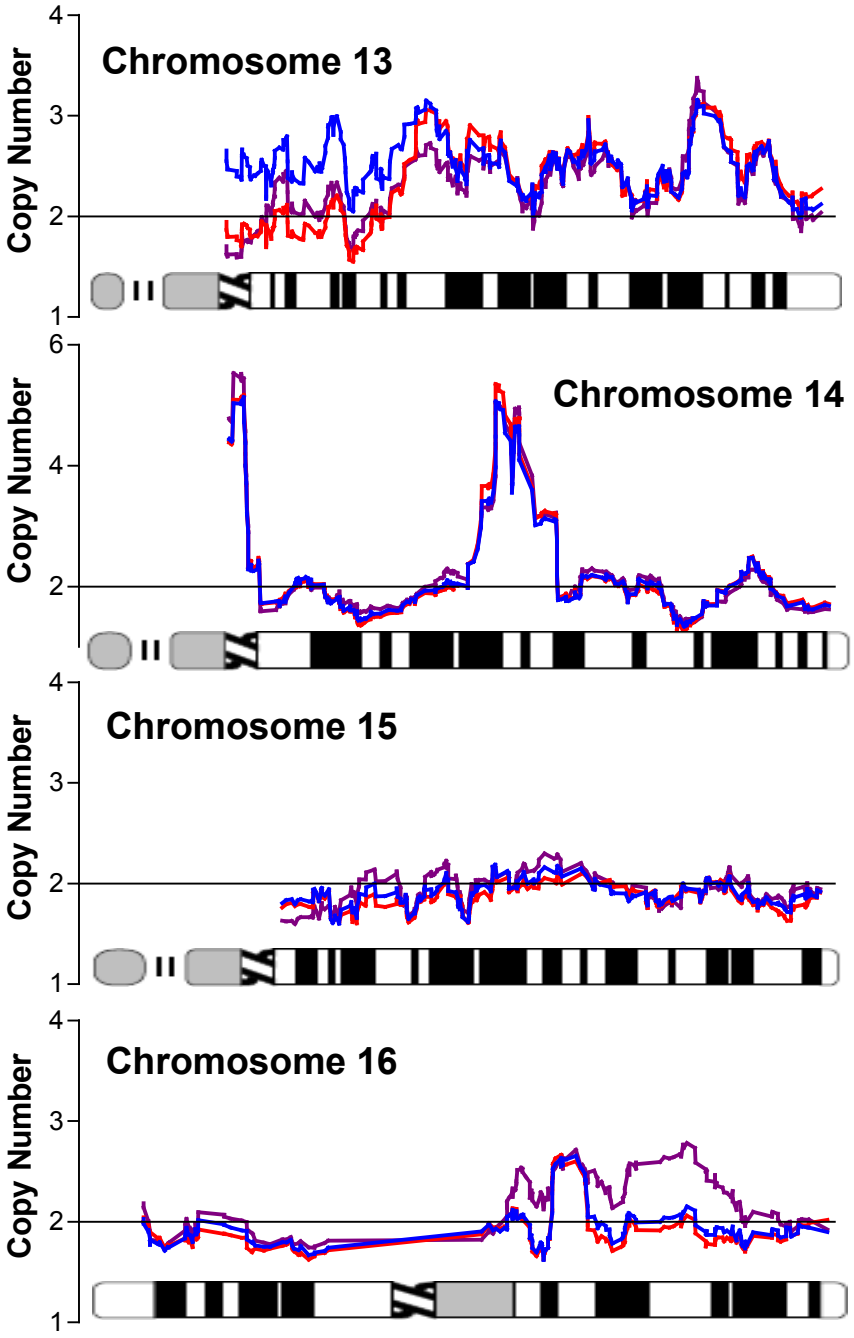

Figure 4.5 Chromosomal copy number of chromosomes 13, 14, 15 and 16. Genomic DNA was extracted from the H69 (——), H69CIS200 (——) and H69OX400 (——) cell lines and analysed by Affymetrix 10K SNP array and Affymetrix chromosomal copy tool as described in sections 2.7 and 2.8. Data was smoothed by averaging a window of 20 SNPs.

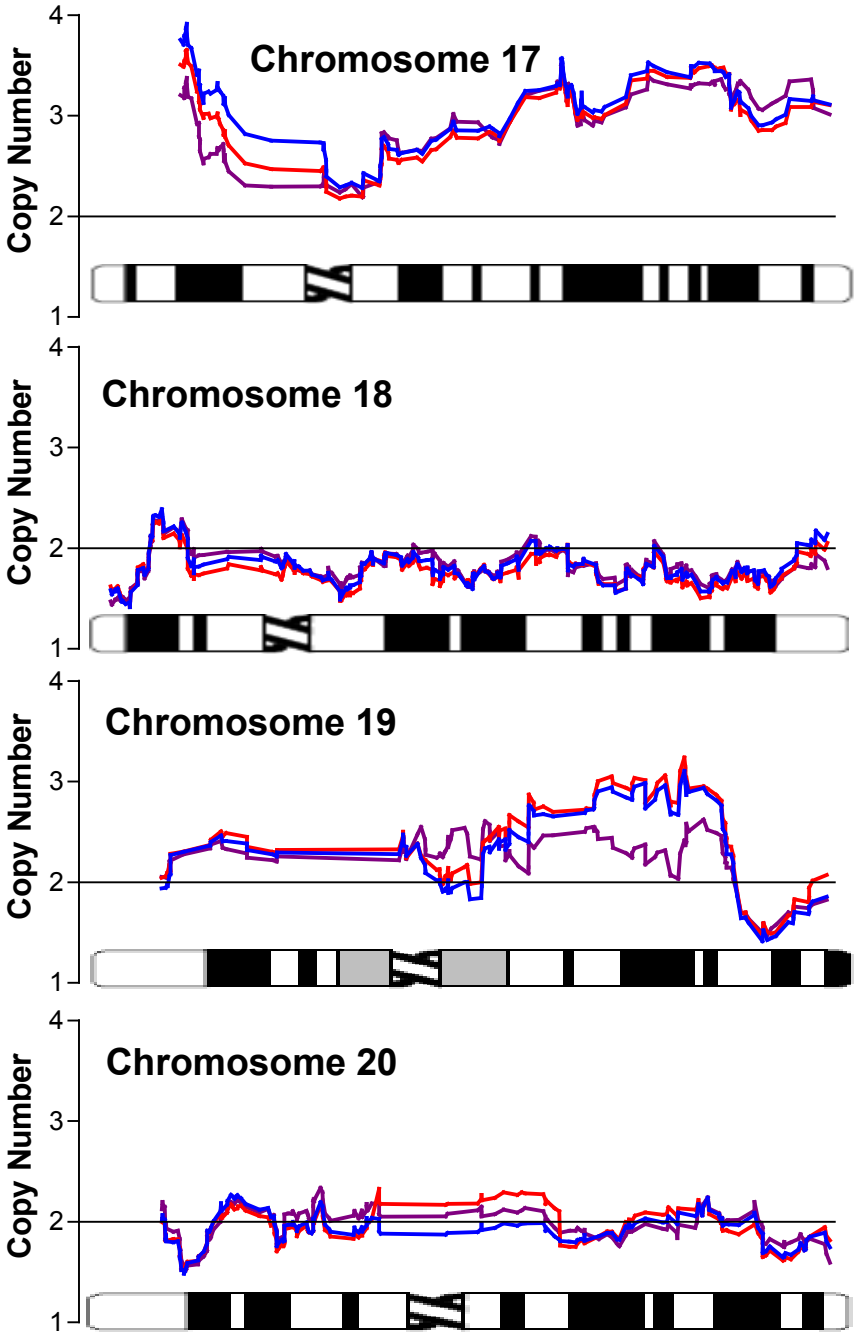

Figure 4.6 Chromosomal copy number of chromosomes 17, 18, 19 and 20. Genomic DNA was extracted from the H69 (——), H69CIS200 (——) and H69OX400 (——) cell lines and analysed by Affymetrix 10K SNP array and Affymetrix chromosomal copy tool as described in sections 2.7 and 2.8. Data was smoothed by averaging a window of 20 SNPs.

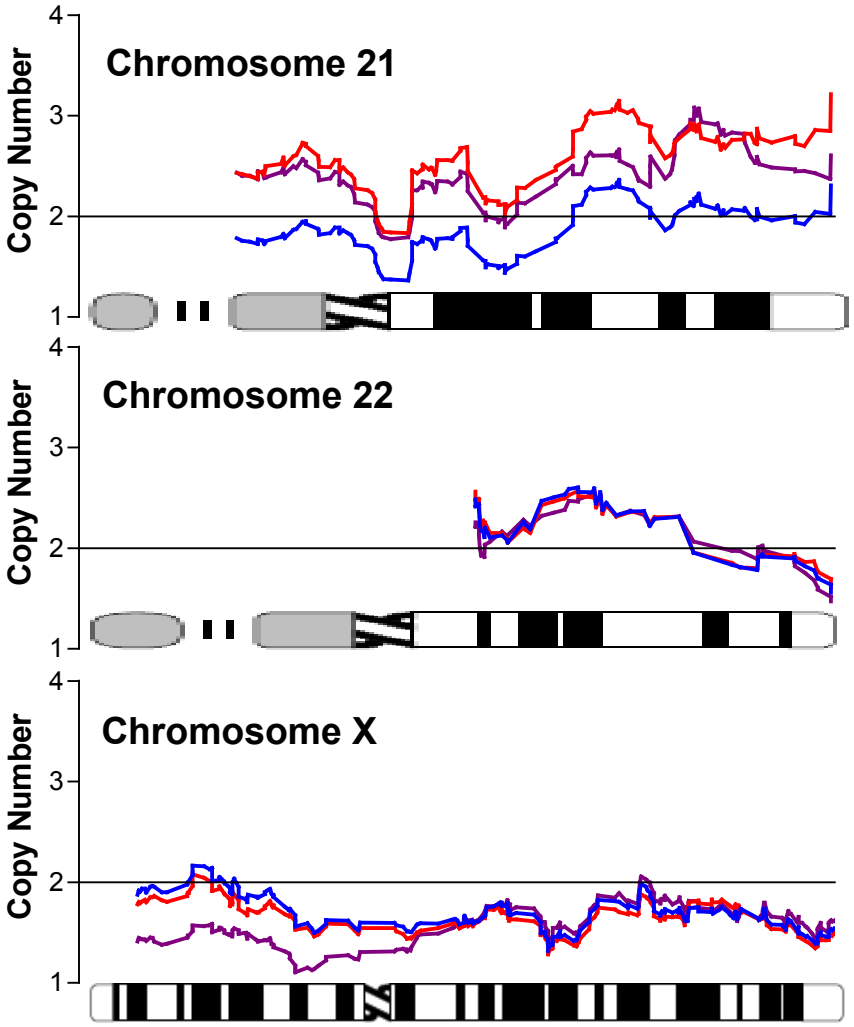

Figure 4.7 Chromosomal copy number of chromosomes 21, 22, and X. Genomic DNA was extracted from the H69 (——), H69CIS200 (——) and H69OX400 (——) cell lines and analysed by Affymetrix 10K SNP array and Affymetrix chromosomal copy tool as described in sections 2.7 and 2.8. Data was smoothed by averaging a window of 20 SNPs.

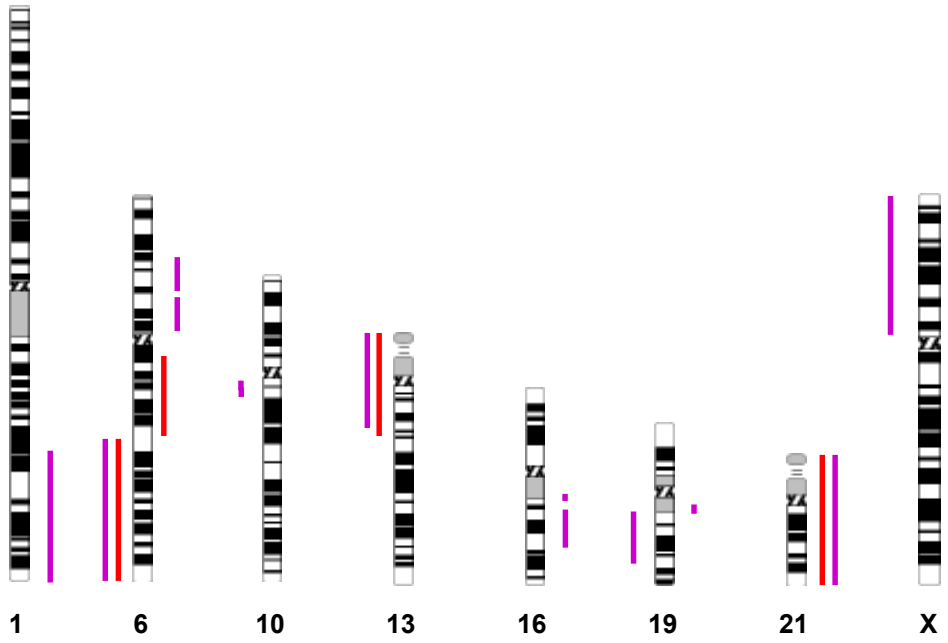

Figure 4.8 Summary of chromosomal copy number changes in the resistant cell lines. Genomic DNA from the H69CIS200 (——) and H69OX400 (——) cells were analysed with an Affymetrix 10K SNP array and Affymetrix chromosomal copy number tool as described in sections 2.7 and 2.8. Segments of change compared to the parental H69 cell line are presented, deletions to the left of the chromosome, amplifications to the right.

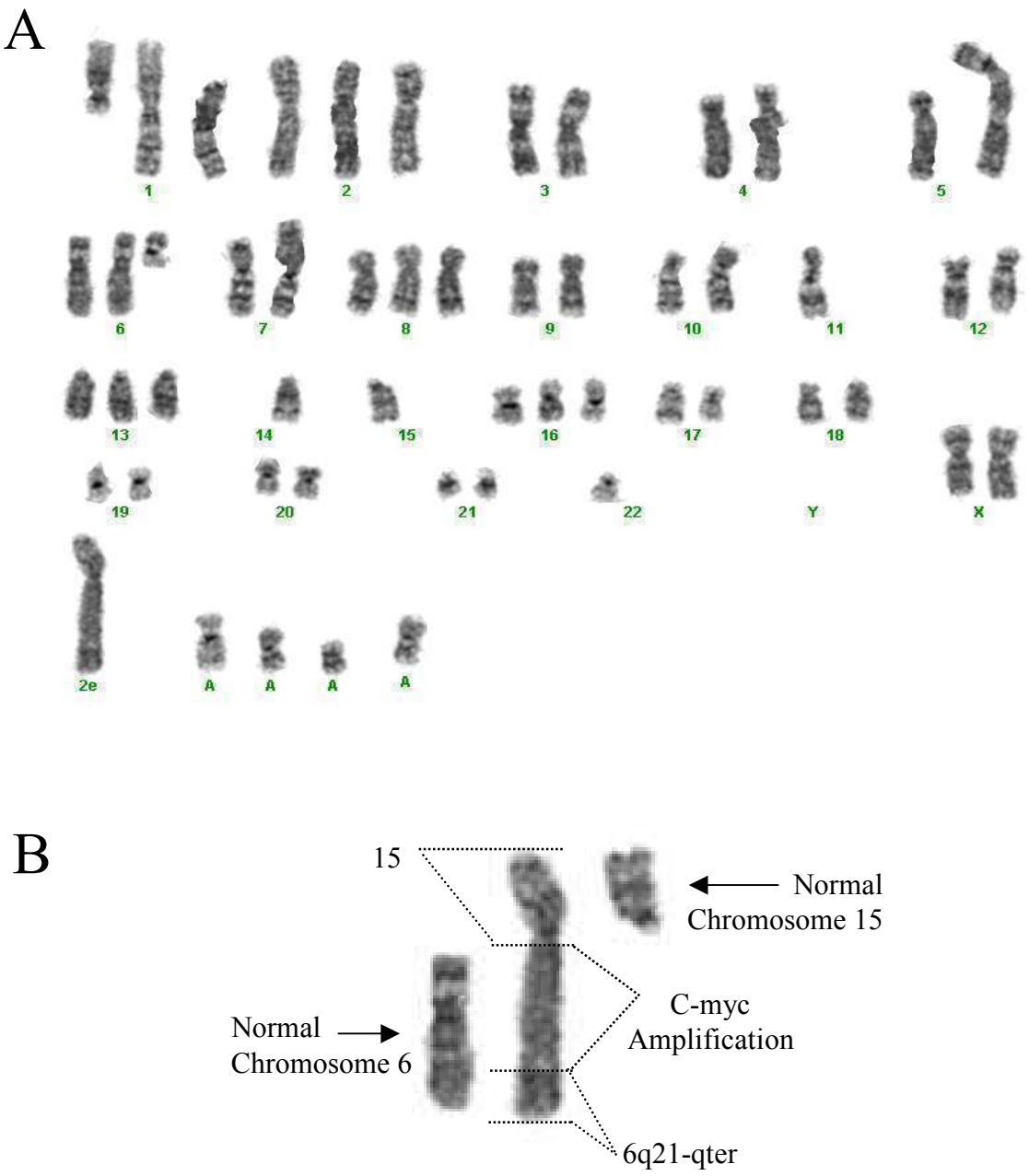

Figure 4.9 Karyotype of the H69 SCLC cell line. Metaphase spreads were prepared from H69 cells and stained for G-banding as described in section 2.9. A) A representative H69 karyotype. B) The c-myc derivative chromosome. The c-myc amplification within a homogenously staining region was flanked by a copy of chromosome 15 providing the centromere and one telomere. The other end of this derivative chromosome is a copy of 6q21-qter providing a second telomere.

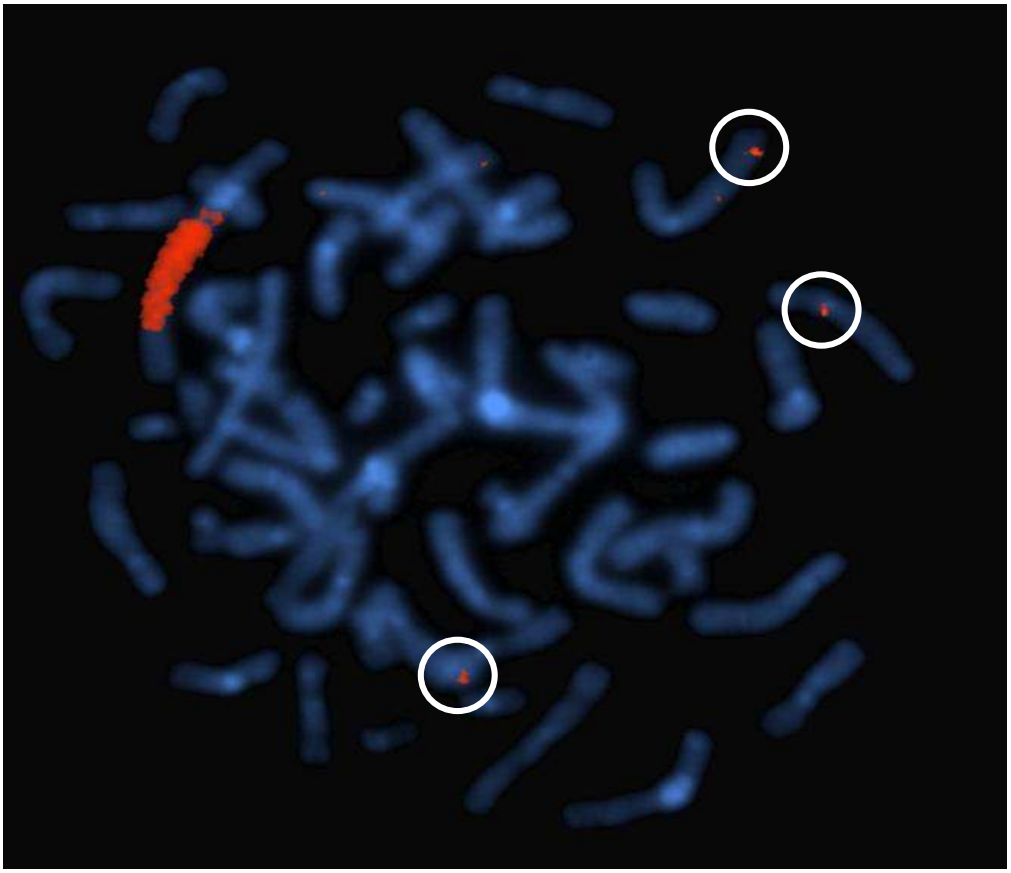

Figure 4.10 H69 metaphase stained with c-myc FISH probe. Metaphase chromosomes stained with c-myc (red), as described in section 2.9, reveal a large c-myc amplified region and 3 normal copies of c-myc on chromosome 8 indicated with circles.

chromosome much larger than chromosome 1 (Figure 4.9B). There were also 3 copies of c-myc on normal copies of chromosome 8 (circled) (Figure 4.10). The c-myc amplification within the large chromosome was flanked by a copy of chromosome 15 providing the centromere and one telomere. The other end of this derivative chromosome is a copy of 6q21-qter providing a second telomere (Figure 4.10B). This c-myc amplification and the large undefined amplifications on chromosome 14, did not alter with the development of drug resistance as both were present at the same level of amplification in the H69CIS200 and H69OX400 resistant sublines.

4.4 H69CIS200 and H69OX400 resistant cell lines

The platinum-resistant cell lines had many genotypic changes from the parental cell line as determined by the Affymetrix 10K SNP array (Figure 4.8). Some changes observed were very similar in the H69CIS200 and H69OX400 cells despite their independent treatments with different platinum drugs. The similarities were a deletion of segments 6q21-qter and 13pter-13q14.11 and duplication of chromosome 21 (Figure 4.8). There was a greater number of smaller changes due to oxaliplatin treatment than due to cisplatin treatment. The most change occurred on chromosome 6, where the resistant cell lines shared a deletion of 6q21-qter but had different duplications. The H69CIS200 cells have an amplification of segment 6q12-q21 and the H69OX400 cells have an amplification of segment 6p12.3-21.2. These chromosome 6 changes were further examined by FISH.

The duplication of segment 6q12-q21 in the H69CIS200 cells was examined using a single-locus FISH probe RP11-124K9 at 6q15 (Figure 4.11). Metaphase preparations of H69, H69CIS200 and H69OX400 cells were stained with a 6q15 probe (green) and a 6p subtelomere control probe (red) to indicate which chromosomes were chromosome 6. The H69CIS200 cells (Figure 4.11B) showed a normal copy of chromosome 6 and a copy of chromosome 6 with a tandem duplication of 6q15. In contrast, the H69 parental cells (Figure 4.11A) and the H69OX400 (Figure 4.11C) cells showed normal dosage for 6q15 on both copies of chromosome 6 as predicted by the Affymetrix data. There is also a small metacentric chromosome which has a segment of 6p which is stained red with the control probe (Figure 4.11A and 4.11C). This metacentric chromosome is absent in this particular metaphase of the

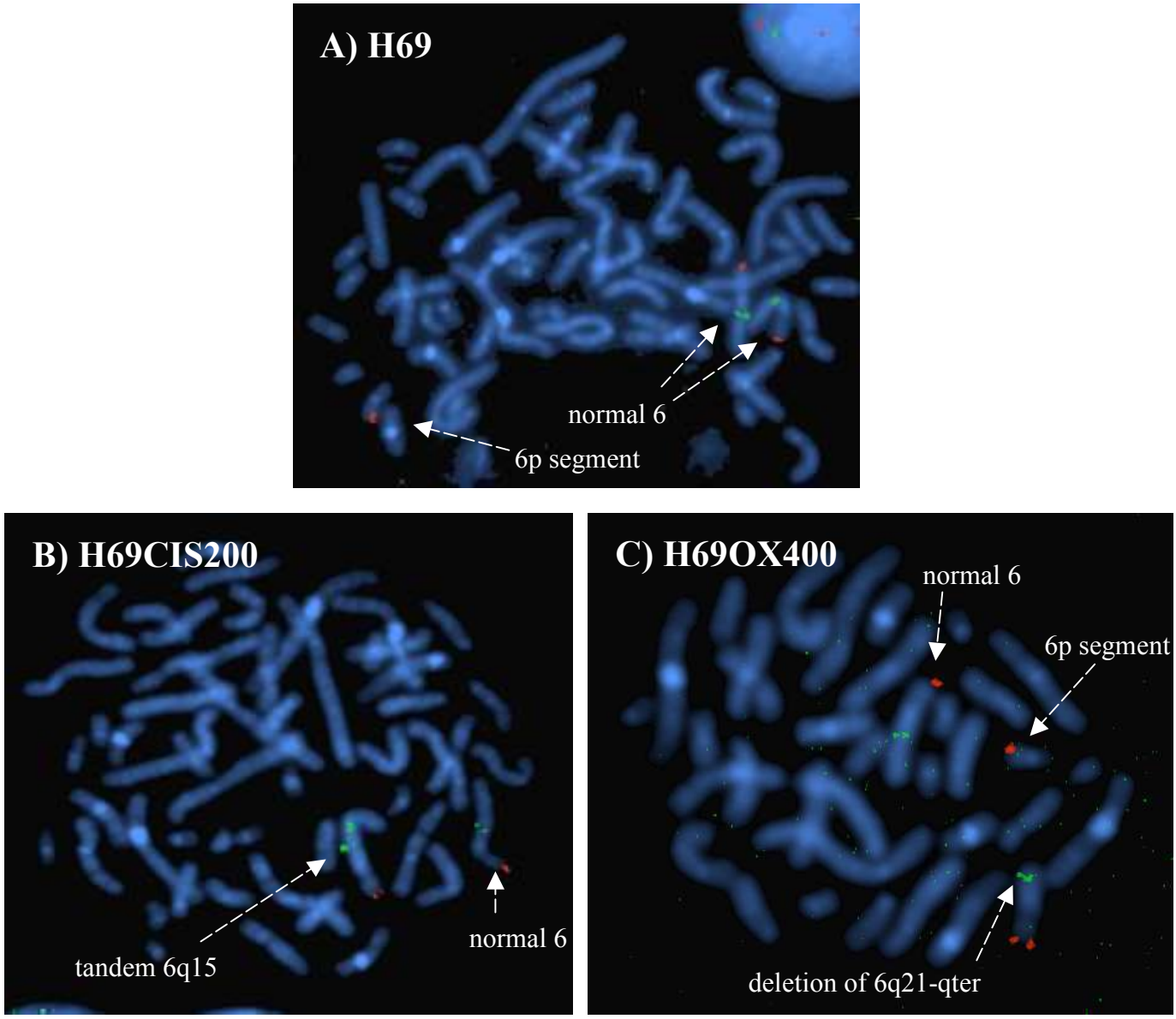

Figure 4.11 H69, H69CIS200 and H69OX400 metaphases stained with 6q15 probe. Metaphase chromosomes were stained with a 6q15 probe (green) and 6p sub telomere control (red) as described in section 2.9. A) H69 cells have normal dosage for 6q15 on both copies of chromosome 6 and 6p staining on a small metacentric chromosome. B) H69CIS200 cells have a normal copy of chromosome 6 and a copy of chromosome 6 with a tandem duplication of 6q15, the 6p metacentric chromosome is missing from this metaphase. C) H69OX400 cells have normal dosage for 6q15 on both copies of chromosome 6, the deletion from 6q21-qter is evident on one copy of chromosome 6 as the 6q15 probe appears near the end of this chromosome.

H69CIS200 cells indicating an incomplete metaphase, which is quite common. In H69OX400 cells the deletion of 6q21-qter is evident on one copy of chromosome 6 as the 6q15 probe is near the end of the chromosome rather than in the middle (4.11C). The deletion of 6q21-qter in the H69CIS200 cells is not visually apparent with the 6q15 staining as in the H69OX400 cells, this may be due to a translocation to another chromosome associated with the deletion.

Metaphase preparations of H69, H69CIS200 and H69OX400 cells were stained with a whole chromosome 6 paint (green) (Figure 4.12). The chromosome paint showed 4 separate regions of staining in each cell line. All cell lines had a copy of 6q21-qter on the large c-myc derivative chromosome and a small segment of 6p on a metacentric chromosome. The H69 cells showed two normal copies of chromosome 6 (Figure 4.12A). The H69CIS200 cells showed a normal copy of chromosome 6 and a larger copy of 6 with 6q12-q21 duplication and fused to another chromosome at 6q21 (Figure 4.12B). The H69OX400 cells showed a normal copy of chromosome 6 and a shorter copy with 6q21-qter deleted (Figure 4.12C)

The duplication in 6p in the H69OX400 cells was examined using single locus probes for RP11-262E12 at 6p21.2 (green) and RP11-876F11 at 6p12.3 (red) which were bands corresponding to the peak of the amplifications as identified by the Affymetrix SNP array. The amplification in the H69OX400 cells could not be detected in the metaphases seen via FISH but could be observed in 26.5% of interphase nuclei on the same slide, (Figure 4.13A). This indicates that the H69OX400 cells are mosaic for this abnormality. Figure 4.13B shows two interphase cells from the H69OX400 cell line. The cell on the left has three copies of the 6p21.2 and 6p12.3 probes, whereas the cell on the right has the normal two copies. The additional copy was not detectable in either the parental H69 cells or the H69CIS200 cells, showing that this duplication was specific to the H69OX400 cells as predicted from the Affymetrix analysis.

The loss of heterozygosity (LOH) analysis revealed a LOH in regards to the 6q21-qter deletion for the H69CIS200 cells but not for the H69OX400 cells. The LOH analysis is limited in its power to detect changes between the H69 cells and the resistant cell lines because of the large amount of LOH already present in the H69 cells compared to a normal non-cancerous sample. The Affymetrix array gives a call of AA, AB or

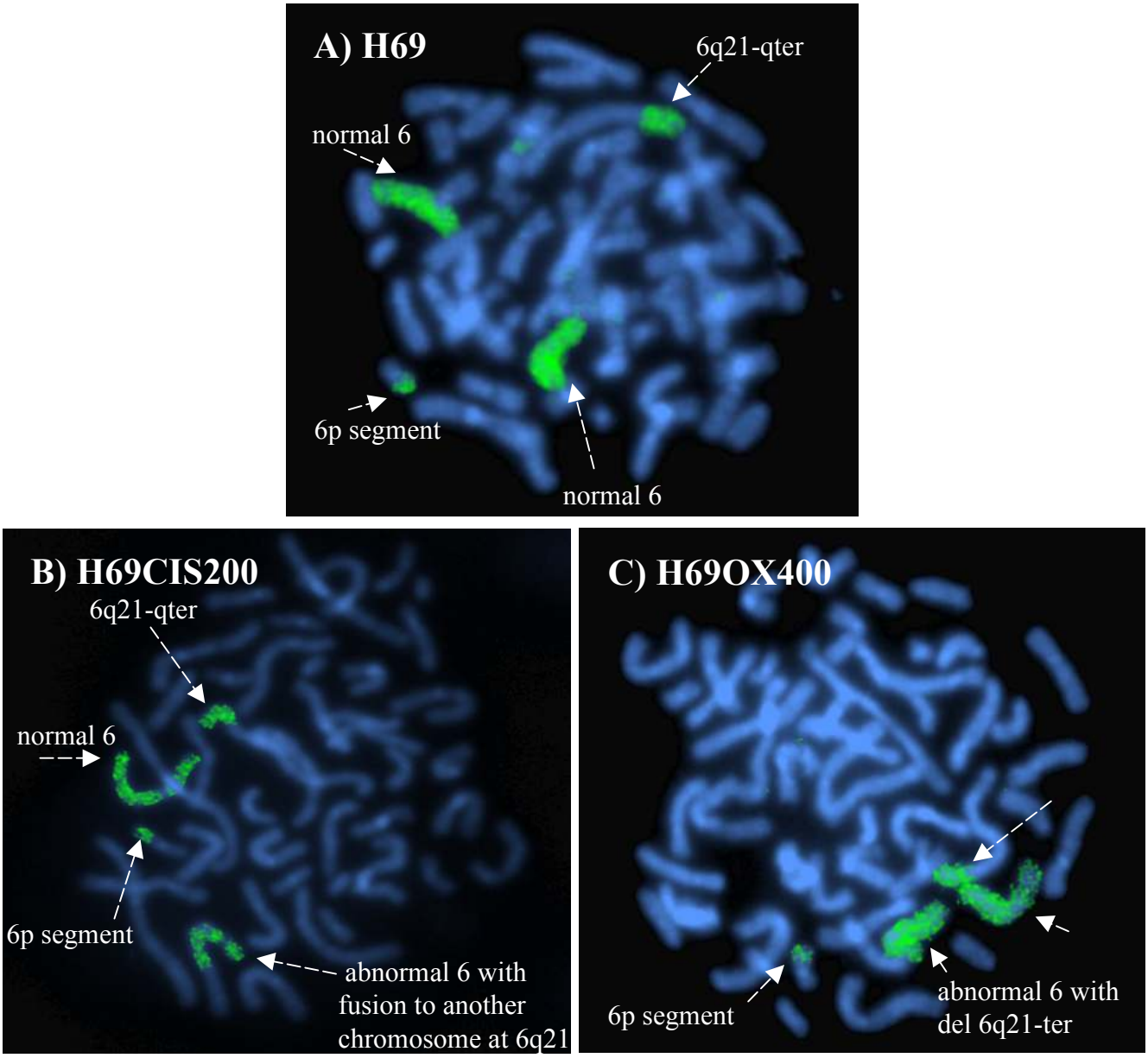

Figure 4.12 H69, H69CIS200 and H69OX400 metaphases stained with chromosome 6 paint. Metaphase chromosomes were stained with whole chromosome 6 paint as described in section 2.9. A) H69 cells have two normal copies of chromosome 6 B) H69CIS200 have a normal copy of chromosome 6, a copy of 6 with 6q12-q21 duplication, and fused to another chromosome at 6q21. C) H69OX400 have a normal copy of chromosome 6, a shorter copy of 6 with the region 6q21-qter deleted. All cell lines had a copy of 6q21-qter on the c-myc derivative chromosome and a small segment of 6p on a metacentric chromosome.

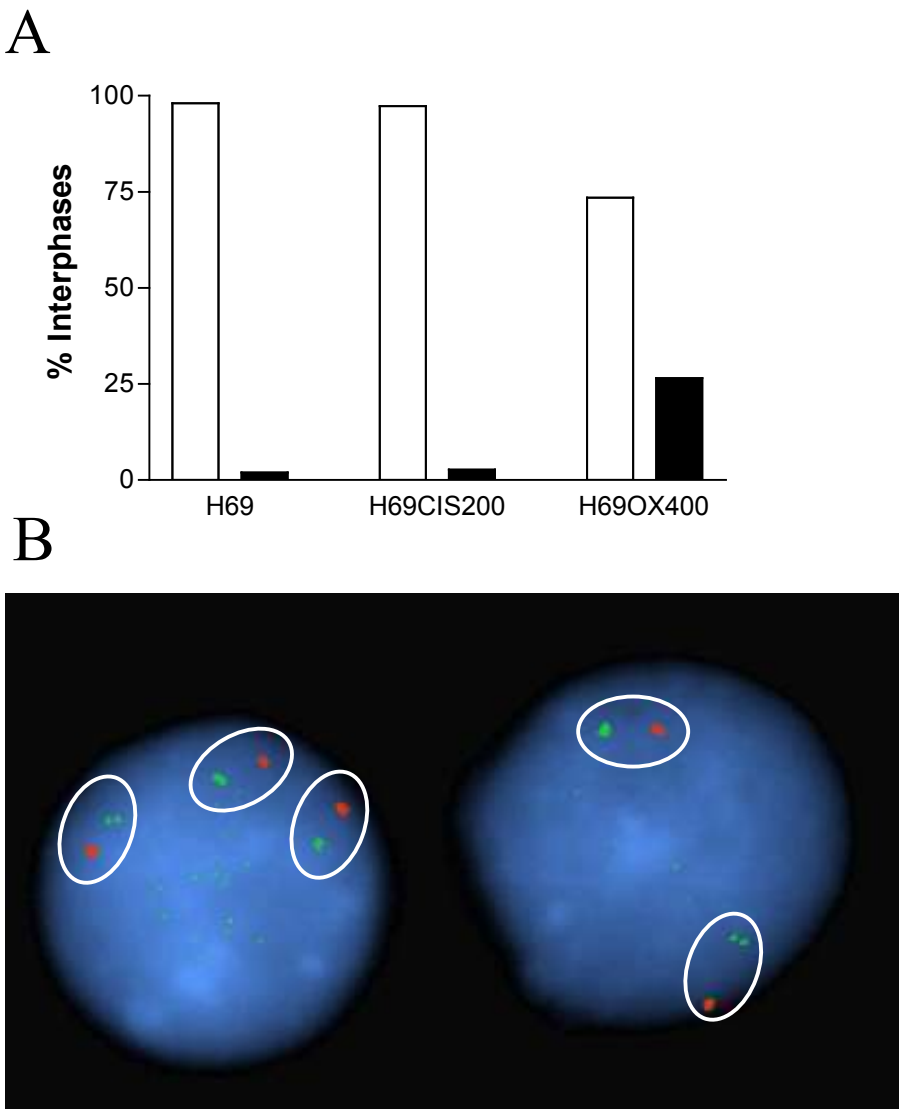

Figure 4.13 Number of copies of 6p probes in interphase nuclei. Interphase nuclei were stained with two FISH probes 6p21.2 (green) and 6p12.3 (red) as described in section 2.9 A) At least 100 interphase cells for each of the cell lines were scored for their number of 6p probes (□) 2 copies or (■) 3 copies and a percentage calculated. B) Interphases from the H69OX400 cell line, the cell on the left has 3 copies of each probe the cell on the right the normal 2 copies.

BB for each SNP. A shift from an AB call to an AA or BB indicates a LOH. This can mean the second copy has been lost and the locus is hemizygous. Alternatively, in a quasi-polyploid cell line such as the H69 cells, it can mean that one of three copies has been lost and the two that remain are of the same parental origin. A LOH can also occur if DNA damage has occurred in a locus and it has been repaired by referring to the other copy. The H69 cells have AB calls for only 12.33% of the SNPs assayed in the 10K array. This is quite low compared to normal non-cancerous samples which usually have 30% of the genome as AB calls (Wong et al., 2004). The AB calls for the H69CIS200 cells is 11.51% and this difference is primarily due to the LOH associated with the deletion of 6q21-qter. The AB calls for the H69OX400 cells remains similar to the parental H69 cell line at 12.35%.

4.5 H69CIS200-S and H69OX400-S sensitive revertant cell lines

The H69CIS200 and H69OX400 cells were stably 2-fold resistant and cross-resistant to cisplatin and oxaliplatin for 6-8 weeks in drug-free culture as determined by an MTT cytotoxicity assay. Over a further 6-8 weeks their resistant phenotype fades (Figure 4.14), at the end of this drug-free period the revertant cell lines were denoted H69CIS200-S and H69OX400-S.

The H69CIS200-S and H69OX400-S cell lines were analysed by Affymetrix 10K SNP array. Also analysed were H69 parental cells that were grown over the same period during which the revertant cell lines were losing their resistance. The H69 parental cell line sampled here showed very similar results to the first experiment, indicating that the chromosomes of this cell line were stable in drug-free culture. The H69CIS200-S and H69OX400-S sensitive cells however, showed many differences from the resistant cell lines from which they were derived. Figures 4.15 and 4.16 shows the copy number profile of chromosomes 1, 6, 10, 13, 16, 19, 21 and X in both the drug-resistant and revertant drug-sensitive cell lines. Some of the changes developed with resistance are absent in the revertant cell lines suggesting that these changes may contribute to the resistant phenotype. Figure 4.17A summarises the chromosomal changes that were lost with the loss of resistance and may therefore be associated with the resistant phenotype. Figure 4.17B summarises those changes still

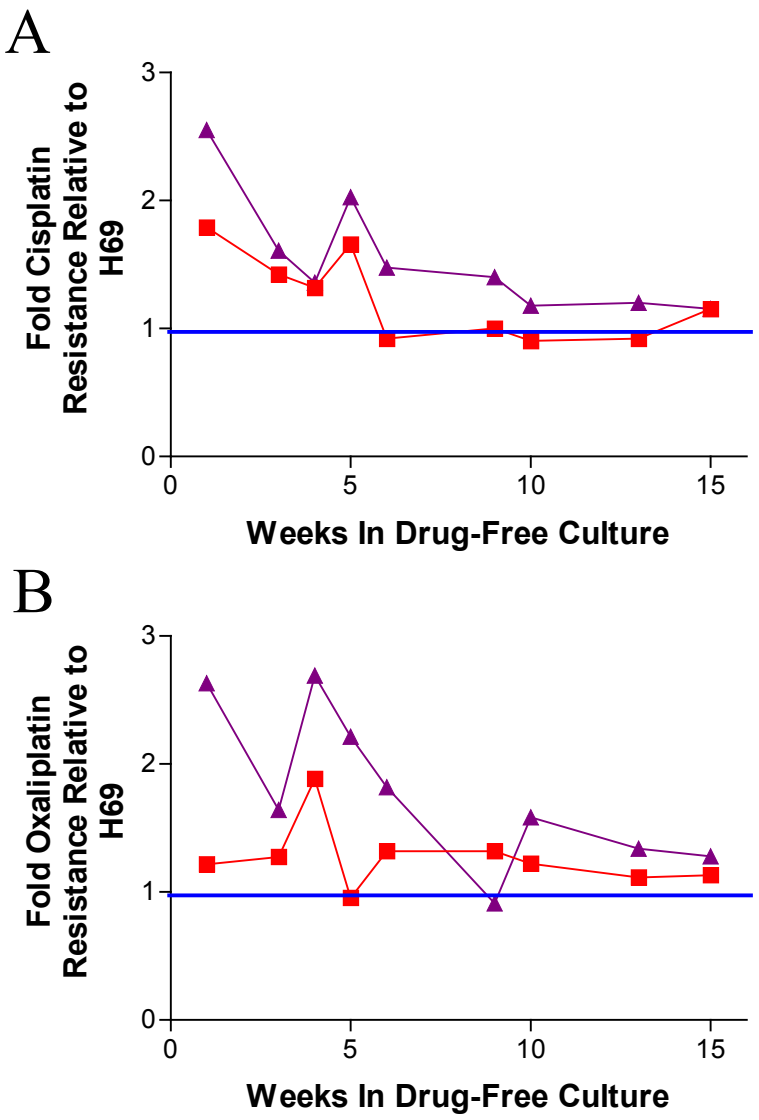

Figure 4.14 Loss of the platinum-resistant phenotype in the H69CIS200 and H69OX400 cells. The H69CIS200 (■) and H69OX400 (▲) cells were grown in drug-free media and their resistance monitored weekly using an MTT cytotoxicity assay as described in section 2.3. At the end of this drug-free period the revertant cell lines were denoted H69CIS200-S and H69OX400-S.

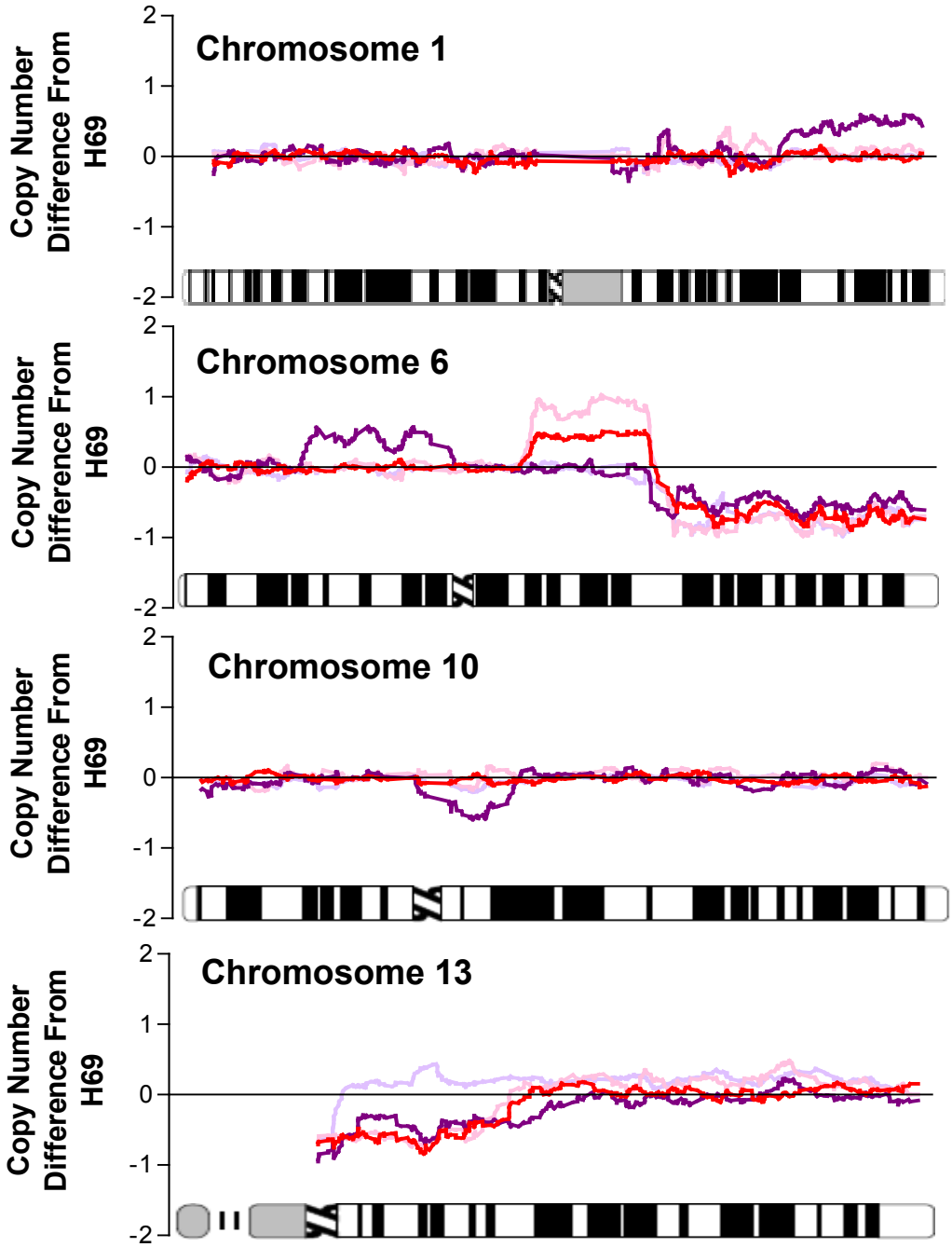

Figure 4.15 Comparison of chromosomal copy number of chromosomes 1, 6, 10 and 13 before and after the loss of resistance. Genomic DNA was extracted from the H69, H69CIS200 (—), H69OX400 (—), H69CIS200-S (—) and H69OX400-S (—), cell lines and analysed by Affymetrix 10K SNP array and Affymetrix chromosomal copy tool as described in sections 2.7 and 2.8. Data was smoothed by averaging a window of 20 SNPs. The difference in copy number from the parental H69 cells is presented for each cell line.

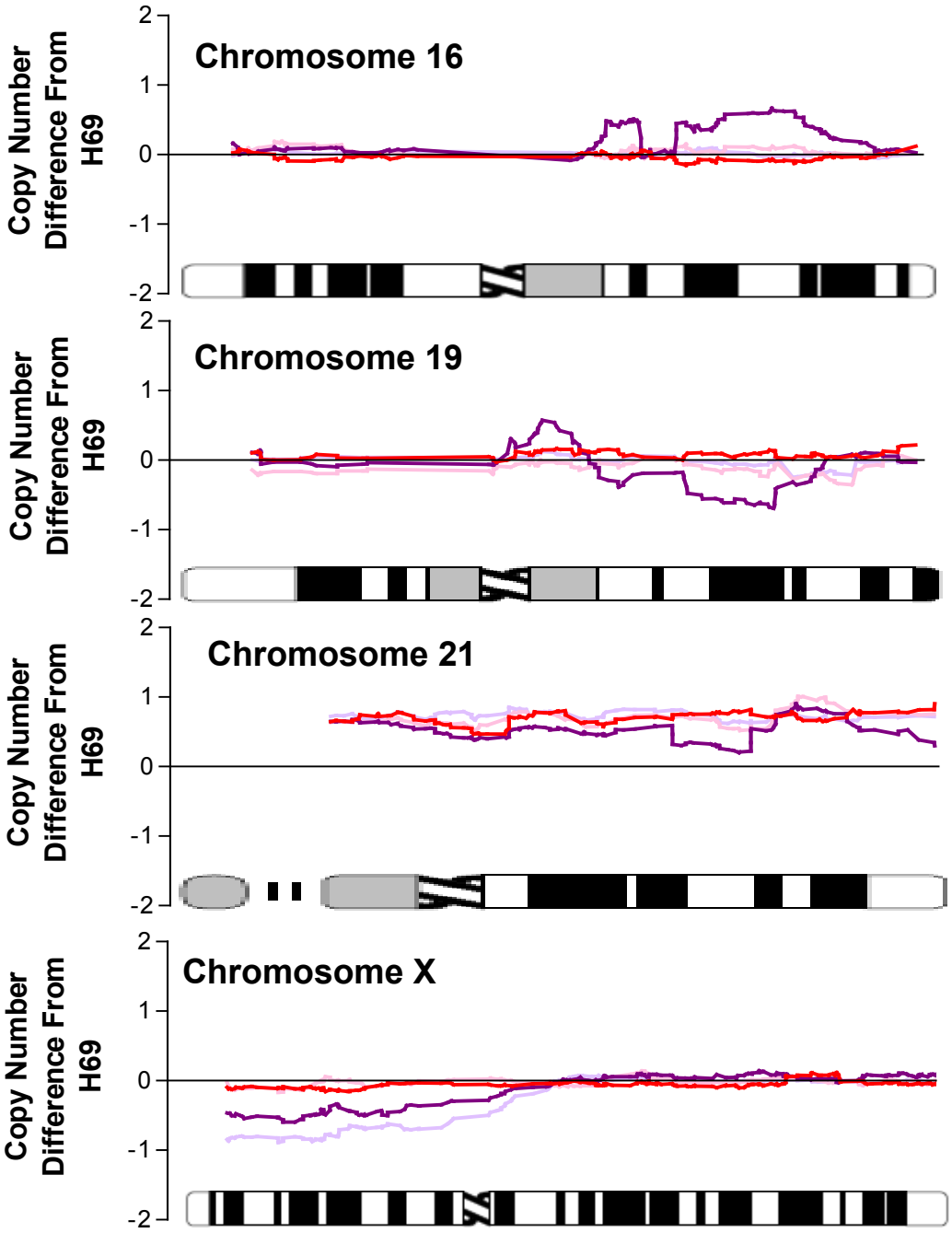

Figure 4.16 Comparison of chromosomal copy number of chromosomes 16, 19, 21 and X before and after the loss of resistance. Genomic DNA was extracted from the H69, H69CIS200 (—), H69OX400 (—), H69CIS200-S (—) and H69OX400-S (—), cell lines and analysed by Affymetrix 10K SNP array and Affymetrix chromosomal copy tool as described in sections 2.7 and 2.8. Data was smoothed by averaging a window of 20 SNPs. The difference in copy number from the parental H69 cells is presented for each cell line.

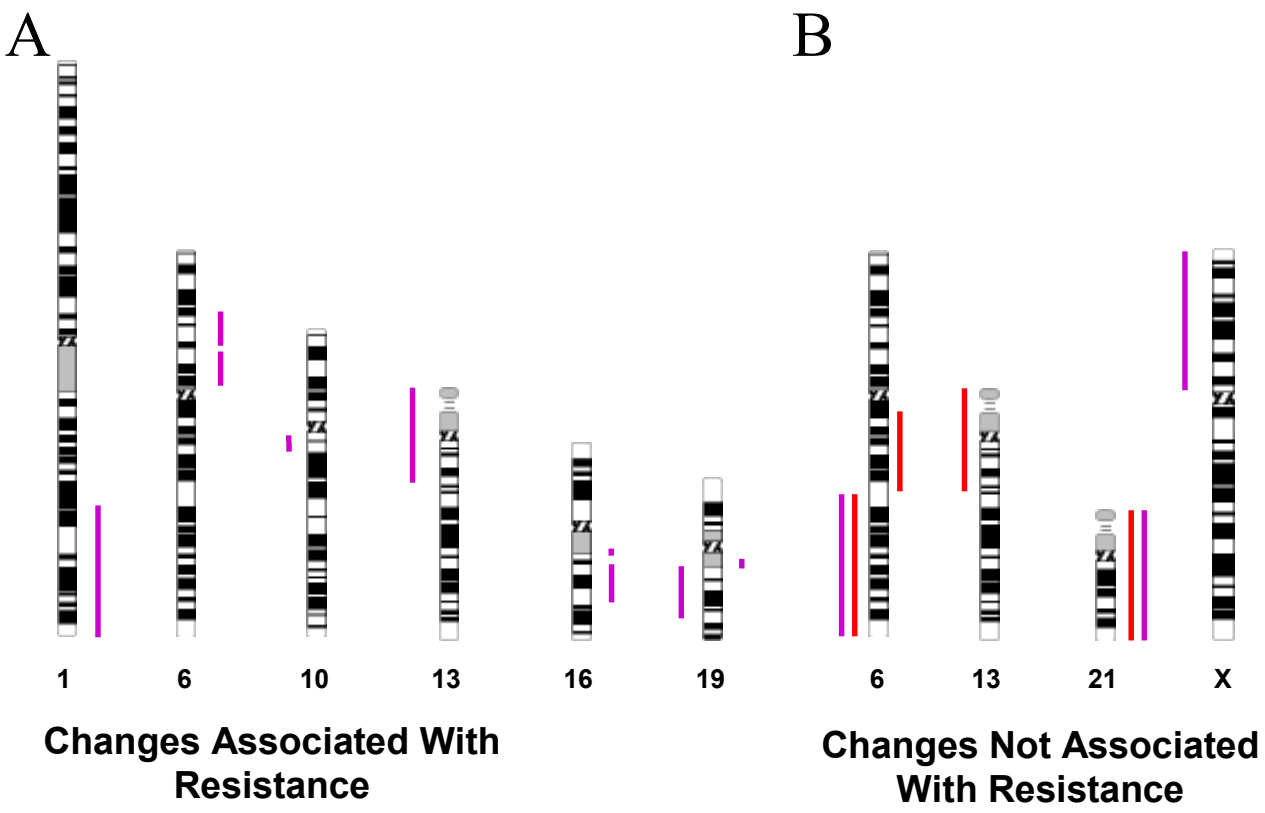

Figure 4.17 Summary of chromosomal copy number changes associated and not associated with resistance. From the analysis of the revertant cell lines (Figures 4.15 and 4.16) the changes in the resistant cell lines H69CIS200 (——) and H69OX400 (——) were divided into two groups A) those associated with the mechanism of resistance and B) those not associated with the mechanism of resistance. Segments of change compared to the parental H69 cell line are presented, deletions to the left of the chromosome, amplifications to the right.

present with the loss of resistance and are therefore not associated with the resistant phenotype.

The amplification of 6q12-q21 in the H69CIS200-S cells has increased with the loss of the resistant phenotype (Figure 4.15). The H69OX400-S cells also have two other segments of change associated with the loss of resistance, duplication of 4q34.3-qter and 12pter-12p13.31 (Figure 4.18). However, these regions are not associated with the mechanism of resistance as these changes arose in conjunction with a loss rather than a gain of resistance. This data suggests that the genome of the resistant cells was more dynamic than that of the parental cell line which had no changes over the 3 month culture period.

The H69CIS200-S and H69 parental cells grown for 3 months in drug-free culture show no major changes in LOH compared to the original analysis (11.70% and 12.40% AB calls respectively). However, the H69OX400-S cells have dropped their AB calls to 11.83%. This is due in part to a new region of LOH at 6q21-qter not associated with a change in copy number. This is the same region which experienced a LOH with the deletion of a copy in the H69CIS200 cells. Clearly this is a very unstable region in this cell line. It is possible that the H69OX400-S cells experienced some damage to, or a complete deletion of this region over the 3 months in culture and repaired it by duplicating a remaining copy without altering the copy number for this region. Hence a new region of LOH arose without a change in gene copy number.

4.6 Discussion

4.6.1 Inherent chromosomal changes in the H69 cells

The H69 SCLC cell line is a near-tetraploid cell line with up to 87 chromosomes per cell (Whang-Peng et al., 1982). The c-myc amplification in SCLC has been shown previously by Affymetrix 10K SNP array (Zhao et al., 2004) but has not been visualised by FISH before (Figure 4.9). *In vivo*, overexpression of c-myc leads to uncontrolled cell growth and proliferation, and so this amplification most likely occurred *in vivo* before the cell line was established. This probably contributed to the cancerous phenotype of the original tumour. The c-myc homogenously staining

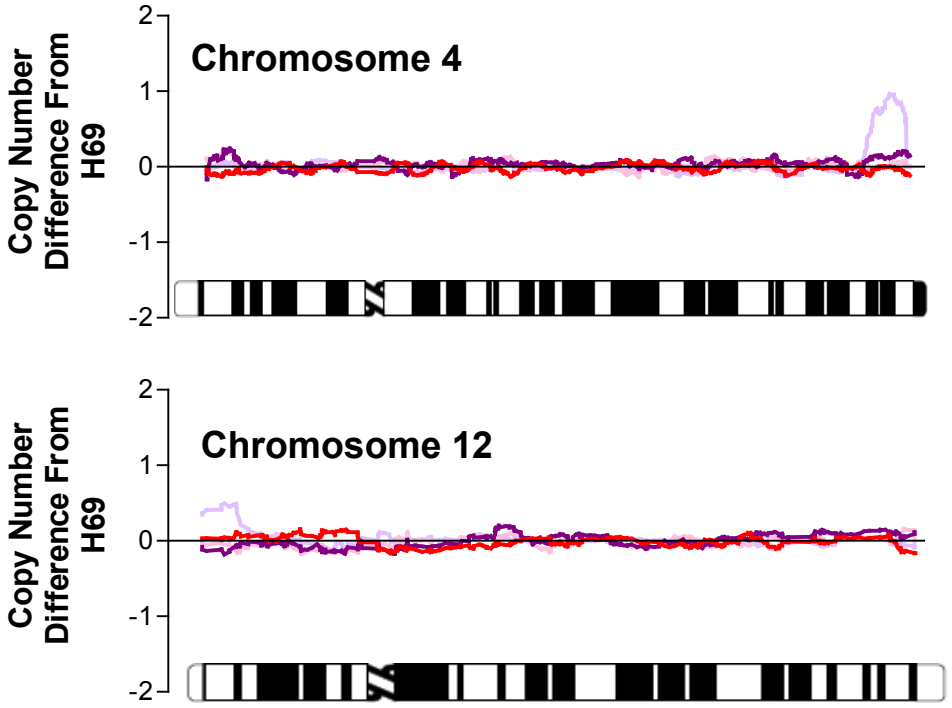

Figure 4.18 Additional chromosomal copy number changes associated with the loss of resistance on chromosome 4 and 12. Genomic DNA was extracted from the H69, H69CIS200 (——), H69OX400 (——), H69CIS200-S (——) and H69OX400-S (——), cell lines and analysed by Affymetrix 10K SNP array and Affymetrix chromosomal copy tool as described in sections 2.7 and 2.8. Data was smoothed by averaging a window of 20 SNPs. The difference in copy number from the parental H69 cells is presented for each cell line.

region is flanked by an almost complete copy of chromosome 15 including the centromere and a copy of segment 6q21-qter (Figure 4.10B). These occurrences of 15 and 6q21-qter confer stability to this large derivative chromosome but are unlikely in themselves to contribute to the cancerous phenotype.

The large amplifications on chromosome 14 did not alter with the development of drug resistance, but could have been associated with the initial cancerous phenotype. Amplifications in the region 14q12-q21 were also found in other SCLC cell lines but any specific association with malignancy is unknown (Ashman et al., 2002). The H69 cells also had a loss of 3p which is characteristic of SCLC cells (Whang-Peng et al., 1982).

4.6.2 Changes induced by cisplatin and oxaliplatin treatment

The Affymetrix 10K SNP array (Figure 4.8) revealed many similar changes in both resistant sublines relative to the parental sensitive cell line. The question remains as to whether these similarities are due to the similar nature of the two chemotherapeutics used in drug treatment or because these breakpoints are places of inherent vulnerability in the parental cell line.

There were more changes in the oxaliplatin-resistant cell line than in the cisplatin-resistant cell line even though the doses used in development were equivalent in cytotoxicity. Cisplatin and oxaliplatin form the same types of DNA adducts at the same sites on the DNA strand (Woynarowski et al., 1998; Chaney et al., 2005) which may explain some of the similarities in chromosomal changes shared by the resistant cell lines. However, oxaliplatin is more cytotoxic per DNA lesion than cisplatin (Woynarowski et al., 1998); which may in part explain why there was an increase in chromosomal rearrangement in the oxaliplatin-resistant cell line in comparison to the cisplatin-resistant cell line.

The cisplatin and oxaliplatin-resistant cell lines both have a breakpoint at 6q21 and a subsequent deletion of 6q21-qter. The H69 parental cell line has a duplication of the same region (6q21-qter) seen on the derivative chromosome carrying the c-myc amplification. Therefore the resistant cells have copy numbers of chromosome 6 that

are closer to that of a normal cell than their drug-sensitive parent. The LOH analysis also revealed that the loss of 6q21-qter was on different copies of chromosome 6 (differing in respect of parental origins) in the two resistant cell lines. Similarly, a cisplatin-resistant ovarian carcinoma and its parental cell line (A2780/A2780CP8) both share changes in 6q21. The parental has a translocation with 1q23 and the resistant cell line has a deletion of 6q21 (Behrens et al., 1987). This suggests that if a chromosomal region is altered in the process of oncogenesis it may again be altered in the development of drug resistance. There are also several other studies which have reported a correcting of the genome with cisplatin resistance (Walker et al., 1990; Yasuno et al., 1999), where amplifications in the parental cell line are deleted in the resistant subline.

Cisplatin-induced DNA damage in normal cells is to some extent non-random, having 'hot spots' where damage is most likely to occur (Meyne et al., 1979). The preferential assignment of chemically induced breakpoints to lightly staining G-bands has also been reported with particular reference to the junction point between a light and dark G-band (Meyne et al., 1979). However, this could also be due to systematic observer bias as G-band junctions are easier to see. The chromatin within certain bands may be more prone to damage by a variety of DNA damaging chemical agents (Brogger, 1977), this includes the lightly staining band 6q21 of interest in this study. There are many changes on chromosome 6 observed in other cisplatin-resistant cell lines, summarised in Figure 4.1. In the region 6q21-qter most changes previously reported are duplications rather than deletions as found in this study. However, the large number of chromosomal changes around 6q21 seen in many studies suggest this region is a 'hot spot' for chromosomal breakage due to platinum.

There are many possibilities to explain why a particular region may be more prone to damage and breakage from treatment with platinum. The region may be particularly GC-rich which means a platinum adduct is more likely to occur in the region. There may be a known fragile site at that locus, although their involvement is controversial. A loss in chromatin methylation may also render the region more open and therefore more exposed to DNA damage.

The %GC content of the regions associated with chromosomal breakage in the resistant cell lines was analysed (Figures 4.19 - 4.22), using the %GC content maps available at http://genomat.img.cas.cz. (Paces et al., 2004). While breakages tend to occur in regions of %GC content 40% or greater they do not occur at the most GC-rich areas of the genome. Chromosomes 16, 17, 19, 20 and 22 are very GC-rich and it is clear from the summary of breakage due to platinum in the literature (Figure 4.1), and the results of this study, that these chromosomes are some of the least damaged by platinum. High GC-rich regions are also the regions containing the most genes and when transcriptionally active are more open to chemical attack. Perhaps some mechanisms of DNA repair such as transcription-coupled nucleotide excision repair, which repairs actively transcribing genes (Sancar et al., 2004) efficiently repairs the damage to these %GC-rich small chromosomes.

4.6.3 Changes associated with reversion of resistance

The mechanism of loss of resistance of a cell line has not been studied extensively. Some resistant cell lines are stable for long periods in drug-free culture (Slovak et al., 1993), some require the presence of drug either constantly (Burns et al., 2001) or regular short treatments to maintain their resistant phenotype (Locke et al., 2001). There are two broad hypotheses for what could be causing a loss of the resistant phenotype in the resistant cell lines:-

A) There is a homogenously resistant population and the loss of the resistant phenotype is due to a downregulation of stress response pathways as the cells grow for many weeks in drug-free culture leading to a sensitive phenotype. The chromosomal changes previously detected in the resistant cell line will still be present and were not part of the mechanism of resistance.

B) There is a mixed population of resistant and sensitive cells. Initially the resistant cells dominate as the population has been recently exposed to a chemotherapeutic, as weeks pass in drug-free culture the sensitive cells dominate the culture as they tend to grow faster. This may be due to the taxing nature of the resistance mechanism on cell growth. The chromosomal changes previously detected will be absent as the sensitive

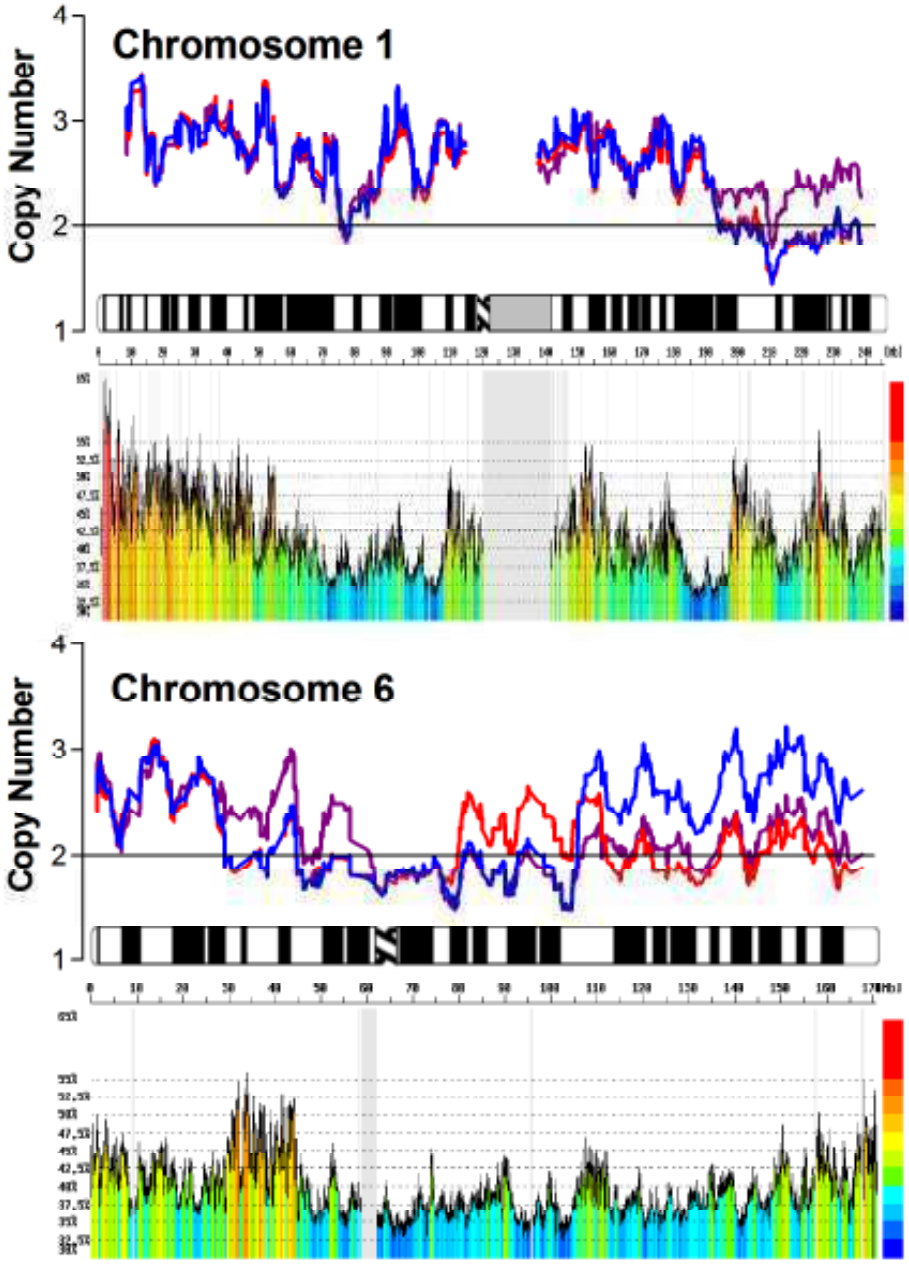

Figure 4.19 %GC content maps of chromosomes 1 and 6. %GC content of the regions associated with chromosomal breakage in the resistant cell lines was analysed using the %GC content maps available at http://genomat.img.cas.cz as described in Paces et al., 2004.

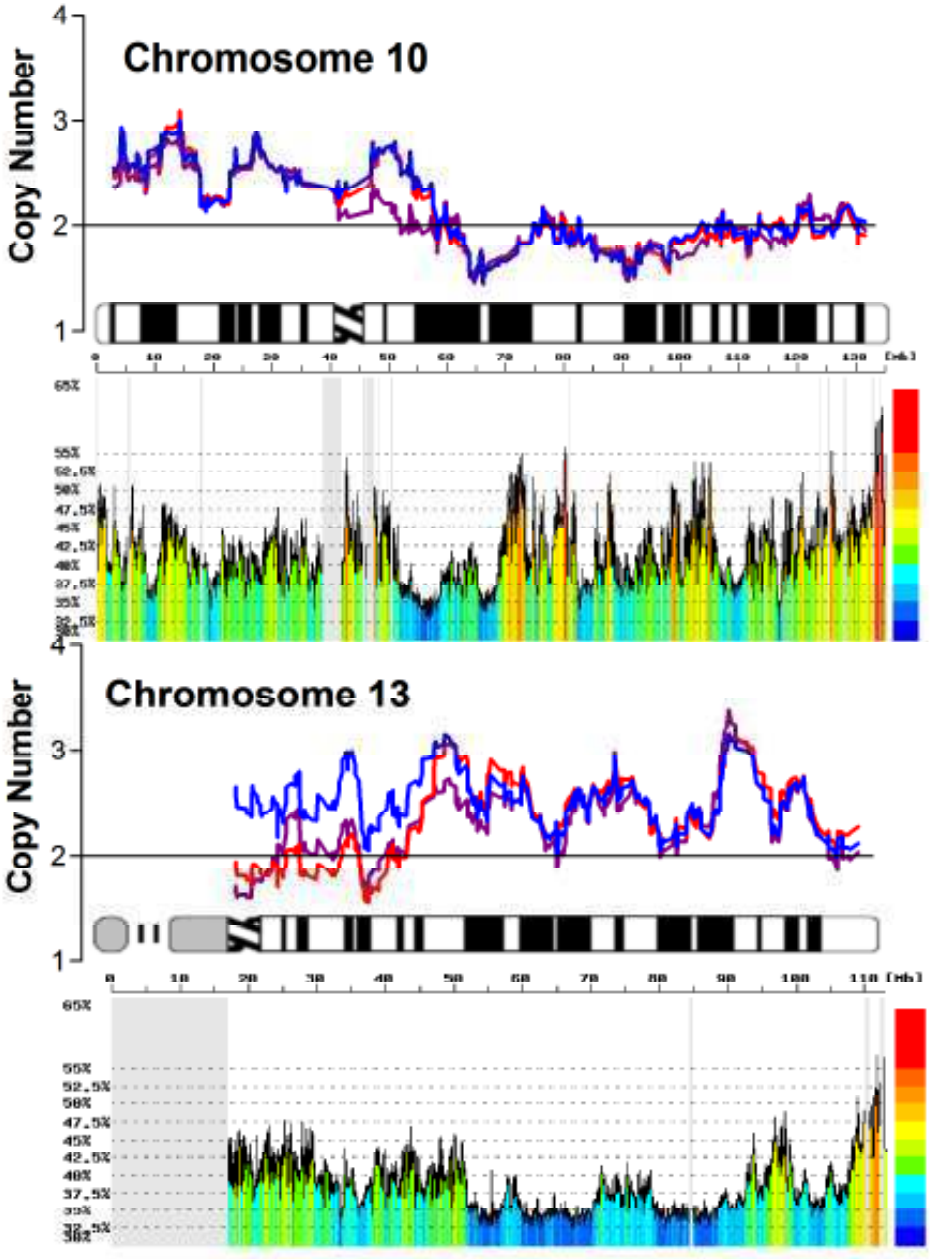

Figure 4.20 %GC content maps of chromosomes 10 and 13. %GC content of the regions associated with chromosomal breakage in the resistant cell lines was analysed using the %GC content maps available at http://genomat.img.cas.cz as described in Paces et al., 2004.

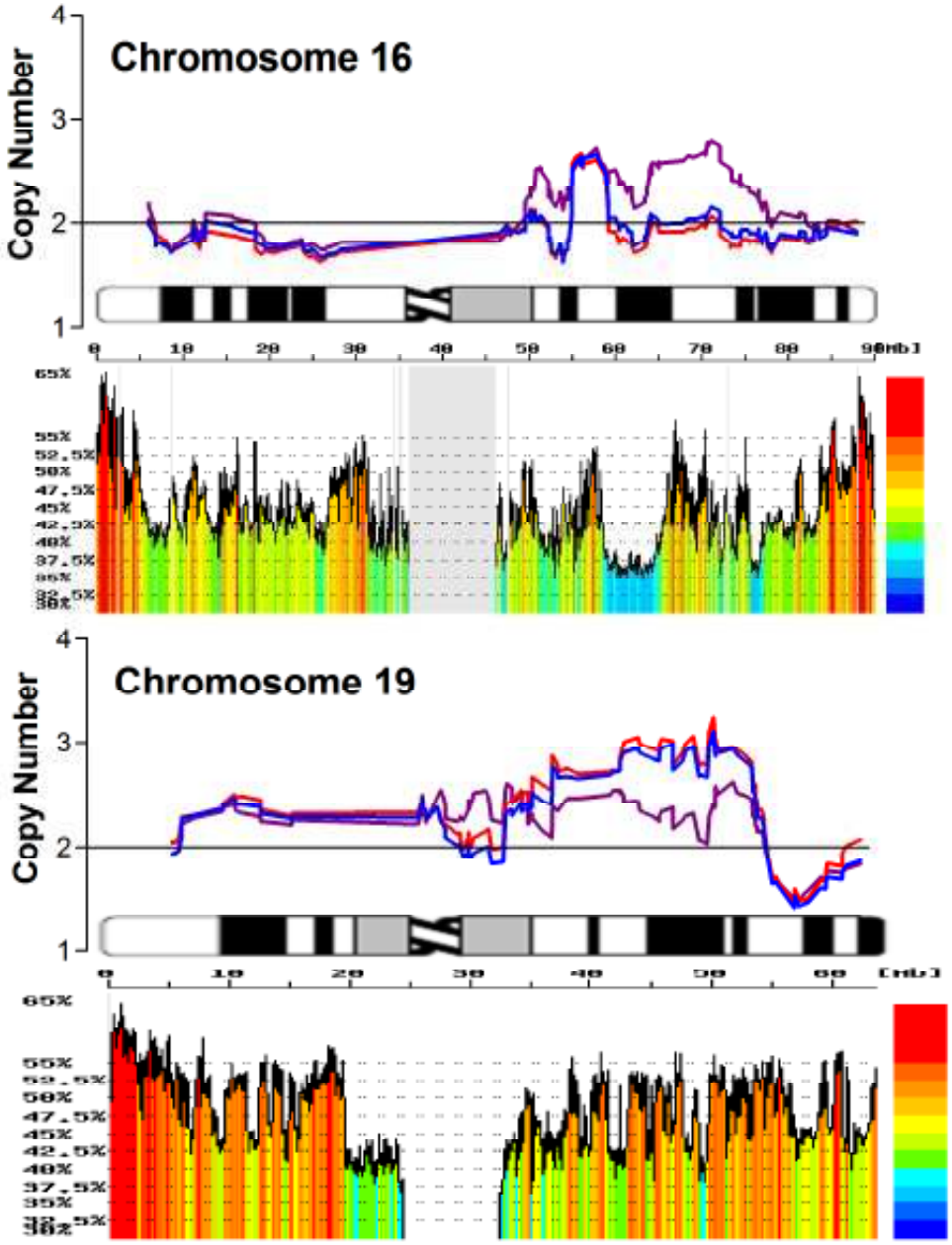

Figure 4.21 %GC content maps of chromosomes 16 and 19. %GC content of the regions associated with chromosomal breakage in the resistant cell lines was analysed using the %GC content maps available at http://genomat.img.cas.cz as described in Paces et al., 2004.

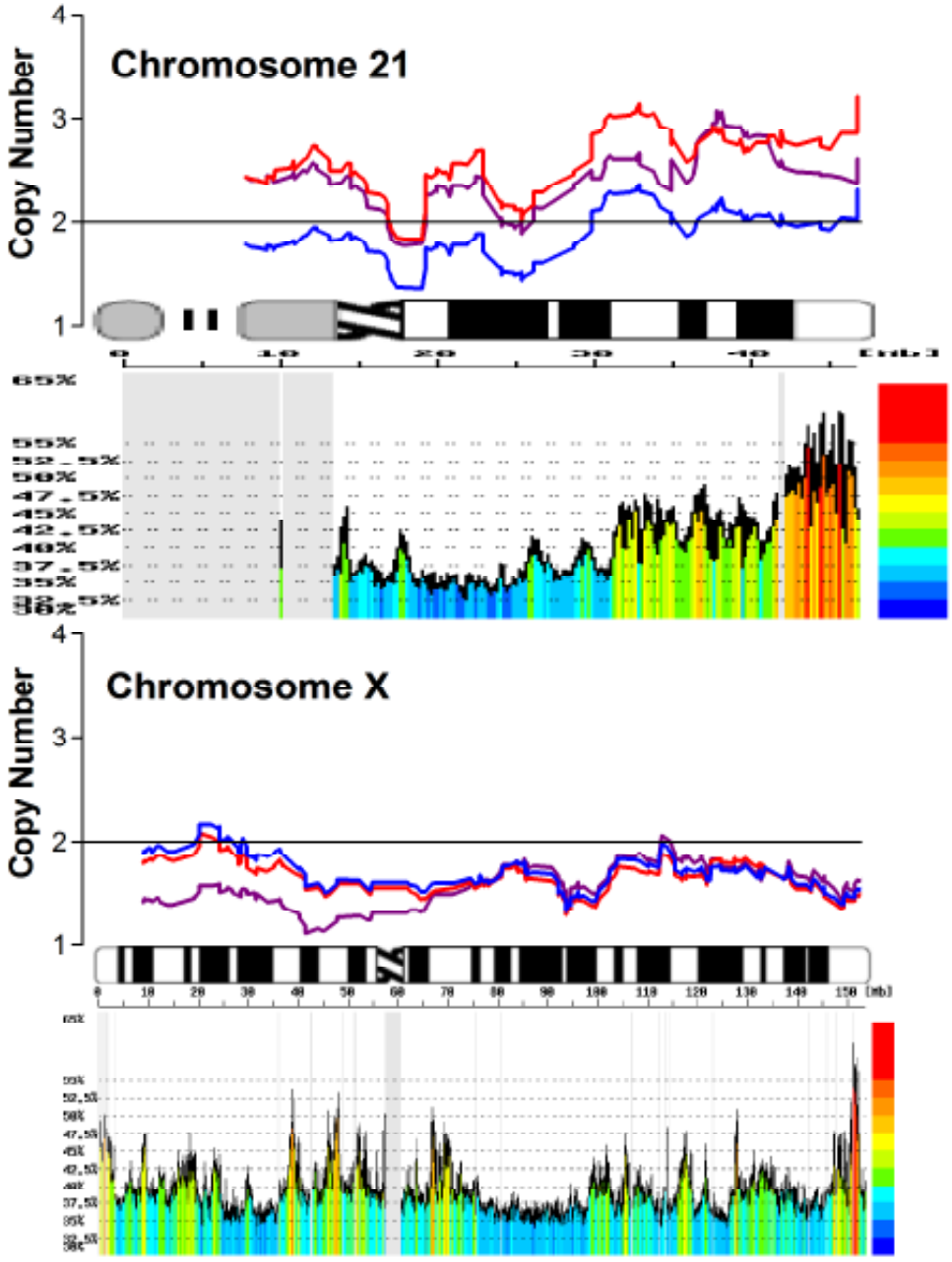

Figure 4.22 %GC content maps of chromosomes 21 and X. %GC content of the regions associated with chromosomal breakage in the resistant cell lines was analysed using the %GC content maps available at http://genomat.img.cas.cz as described in Paces et al., 2004.

cells without the changes associated with the resistance mechanism have dominated the culture.

From the FISH analysis it was determined that all chromosomal changes seen in the H69CIS200 cells were non-mosaic. From the results of the Affymetrix array on the sensitive revertant cells the H69CIS200 cells appear to fit hypothesis A. All the chromosomal changes detected in the resistant cell lines were still present in the sensitive revertant cells. A downregulation of stress response pathways is the most likely explanation for the loss of the resistance mechanism. The chromosomal changes may have been involved in the development of resistance but their presence is not sufficient to maintain the resistant phenotype.

However, the H69OX400 cells were generally non-mosaic but were mosaic for the 6p duplication as it was detected in 26.5% of interphase nuclei (Figure 4.13). This suggests a mixed population of cells in the H69OX400 cell line. The H69OX400 cells appear to fit hypothesis B as many of the changes associated with the resistant phenotype are absent in the revertant cell lines. This suggests that these particular chromosomal changes, combined with the upregulation of stress response pathways, were part of the resistance mechanism. However, three changes did not revert in the H69OX400-S cells, the loss of segments 6q21-ter and Xp and gain of chromosome 21. These changes were therefore not associated with the mechanism of resistance.

It is interesting to note that out of the three large changes that were seen in both the cisplatin and oxaliplatin-resistant cell lines, two of them (loss of the segment 6q21-ter and gain of chromosome 21) were not associated with the mechanism of resistance. The other large change, loss of segment 13pter-13q14.11 was associated with oxaliplatin resistance but not cisplatin resistance (Figure 4.17). This suggests that these regions are inherently vulnerable in H69 cells and are not part of the mechanism of platinum resistance.

The reversion of chromosomal changes associated with the loss of resistance has been shown previously in H69 cells resistant to doxorubicin. Chromosomal amplification of MRP1 (16p13.1) in the form of both a homogenously staining region and double minute chromosomes led to doxorubicin resistance in H69AR cells (Cole et al., 1992).

However, these MRP1 double minutes were no longer present in H69PR cells which had partially reverted to a drug-sensitive phenotype over 36 months in culture (Slovak et al., 1993). This demonstrates that a resistant cell line grown in culture without the selective pressure of drug can revert to a more drug-sensitive phenotype and genotype. The authors used this as further evidence for the amplifications being responsible for the drug-resistant phenotype. The authors didn't speculate on the reasons for the reversion to a sensitive phenotype. It seems likely that the maintenance of the MRP1 amplification in the double minutes became a burden for the resistant cells. However, it should be noted that double minutes are a special case as they lack centromeres and are spontaneously lost in the absence of selective pressure from drug treatment. The H69PR cells seem to be an example of hypothesis B, like the H69OX400 cells, where with time without selective pressure a more sensitive sub-population dominates the culture.

Another study which showed a small amplification in the gene for P-gp in a doxorubicin-resistant sarcoma reported interesting results for their revertant cell lines. Their revertants were selected for by flow cytometry-sorting for high or low P-gp expression. The revertant cell line had low-level P-gp expression but carried the same amplifications observed in the parental cells (Chen et al., 2002a). This indicates that the amplification alone was not sufficient to produce resistance in these cell lines, upregulation of the transcription of the gene was also required. This is similar to the H69CIS200 cells, where chromosomal change alone was not enough to maintain resistance, the upregulation of the stress response was also required to maintain resistance.

4.7 Conclusion

Cisplatin and oxaliplatin promote genomic rearrangement in low-level platinum-resistant SCLC cells. Oxaliplatin is better than cisplatin at promoting chromosomal change and changes that may be associated with resistance. However, the major changes in common between the two platinum drugs seem not to be associated with resistance, but rather reflect the vulnerability of the genome to platinum drugs. Many studies have found the same karyotypic abnormalities in multiple cisplatin-resistant cell lines and have logically concluded that these changes were part of the resistant

phenotype. However, from the search of the literature there does not appear to be any phenotypic link between 'hot spots' of chromosomal change due to platinum and platinum resistance. This study suggests that finding similar chromosomal changes in multiple platinum-resistant cell lines may not reflect the platinum-resistant phenotype. These 'hot spots' must therefore be viewed with caution when considering potential markers for the diagnosis of clinical platinum resistance.

CHAPTER 5.0

IDENTIFICATION OF GENES ASSOCIATED WITH PLATINUM RESISTANCE AND PLATINUM CYTOTOXICITY

5.1 Introduction

In order to identify which mechanisms of resistance are present in the platinum-resistant cell lines an Atlas toxicology nylon array (BD Biosciences) was performed. This nylon array assays for 1000 genes associated with the stress response to drug treatment. The genes on this array represent many divergent stress response pathways. The toxicology array will therefore be a good screening method to see which genes are transcriptionally active in the resistant cell lines and which genes are activated with the stress response to platinum drug treatment. This will narrow down the list of genes and pathways associated with both the cytotoxic response to platinum and mechanism of platinum resistance.

5.2 Atlas toxicology array results

RNA was prepared from the H69, H69CIS200 and H69OX400 cell lines under 3 different conditions, a drug-free control, 200 ng/ml cisplatin or 400 ng/ml oxaliplatin for 4 days in culture. These doses and length of exposure of cisplatin and oxaliplatin were the treatment conditions that were used in the development of these cell lines. Looking at other time points such as the initial response to drug or different doses of drug may lead to the expression of a different and interesting subset of genes. However, as a screening method to determine which genes and pathways are associated with both the development of resistance and the stable resistance mechanism these were the most appropriate doses and exposure times. Figure 5.1 shows 6 example Atlas nylon arrays of the H69, H69CIS200 and H69OX400 cells treated with cisplatin or oxaliplatin. Many spots are different between the different arrays.

The differences in gene expression were compared between untreated H69 parental cells and untreated H69CIS200 and H69OX400 resistant cells. Differences in gene expression here would indicate changes which are maintained in the resistant cell lines. The differences in gene expression between the H69 parental cells and H69CIS200 and H69OX400 cells were also compared in response to both cisplatin and oxaliplatin treatment. Drug treatment is likely to produce larger differences in gene expression, particularly in the subset of stress response genes analysed by the

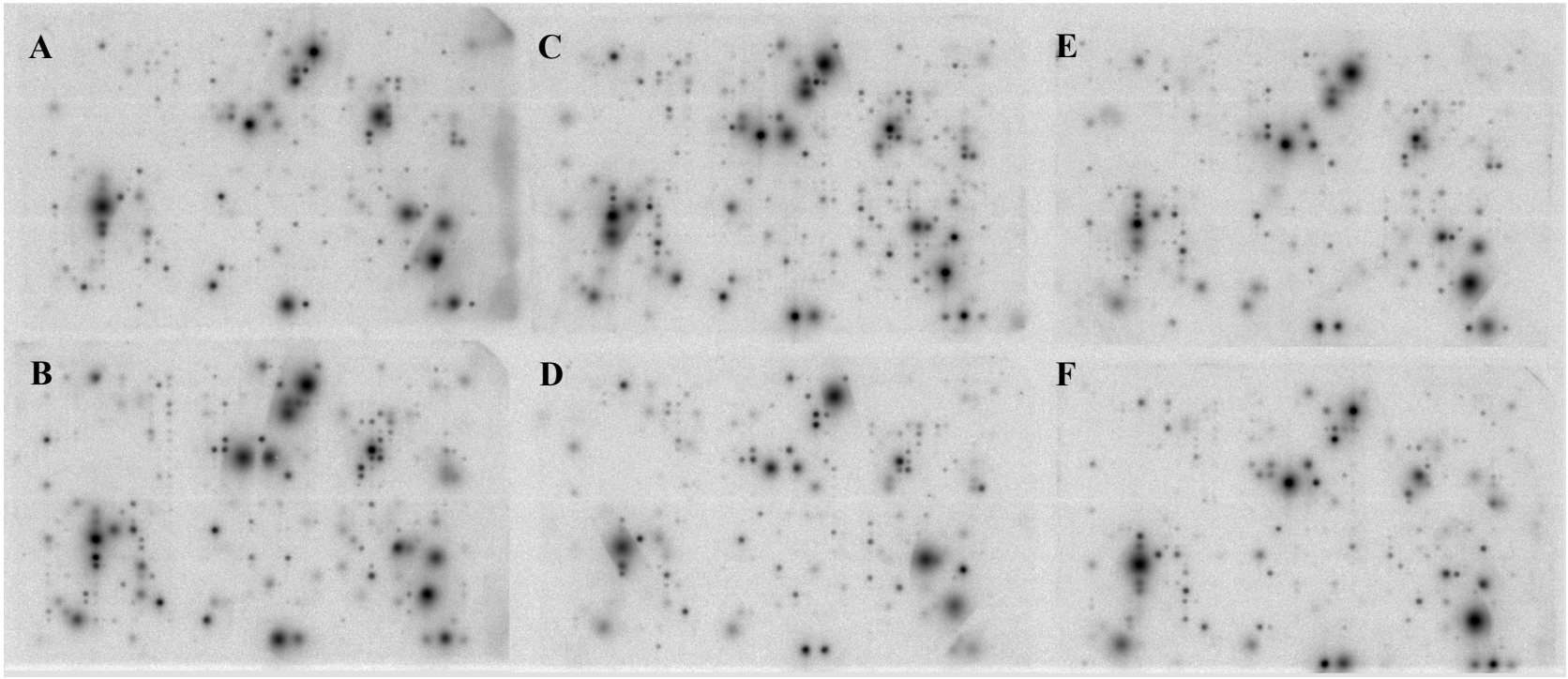

Figure 5.1 Atlas toxicology 1.2 nylon arrays. Examples of Atlas toxicology nylon array hybridised with P^{32} labelled cDNA and exposed to a phosphoimaging screen as described in section 2.11 A) H69 + cisplatin B) H69CIS200 + cisplatin C) H69OX400 + cisplatin D) H69 + oxaliplatin E) H69CIS00 + oxaliplatin F) H69OX400 + oxaliplatin.

Atlas toxicology array. Genes upregulated in the resistant cell lines and not in the parental cell lines in response to platinum drug treatment may be part of the mechanism of platinum resistance

The changes in gene expression levels were relatively small between the sensitive and resistant cell lines and in response to platinum drug treatment. This is because low clinically relevant doses of drug were used in developing the cell lines and in re-treating the cell lines for assessing the stress response to platinum chemotherapeutics. As the level of change in mRNA expression was low and the number of genes assayed relatively small compared to other array based methods, the criteria for the selection of candidate genes had to be specially designed to compensate (Figure 5.2). Spots were defined as any region which reached 1500 units above the background intensity of the array. This value was determined by examining the array by eye and determining the lowest value in which a spot rather than background could be seen. A gene would have to be present above the 1500 unit threshold on more than 1 array, all other genes were excluded from the analysis.

The intensity value for each gene was normalised to the total intensity of genes in an individual array to adjust for differences in radioactive probe intensity between samples. The changes in expression levels were then compared between the duplicate experiments. The data obtained from the Atlas nylon array analysis was viewed as qualitative rather than quantitative. Each gene in each repeat of the experiment was called as either increased expression or decreased expression in relation to the parental cell line. Each gene in the drug treated sample was also called as either increased expression or decreased expression in comparison to its untreated control. The up or down calls were compared over duplicate experiments and genes with consistent up or down calls were tabulated. The total number of up or down calls was calculated for each gene, those genes with the highest number of calls became candidate genes for quantitative real-time PCR analysis. The top 40 candidate genes and their respective up and down calls are presented in Table 5.1. Those genes highlighted in yellow were chosen for real-time PCR analysis. In general the genes with the highest differential expression score were chosen and some genes which I had a prior interest in. The ribosomal gene with the highest score from each subunit were also chosen for analysis.

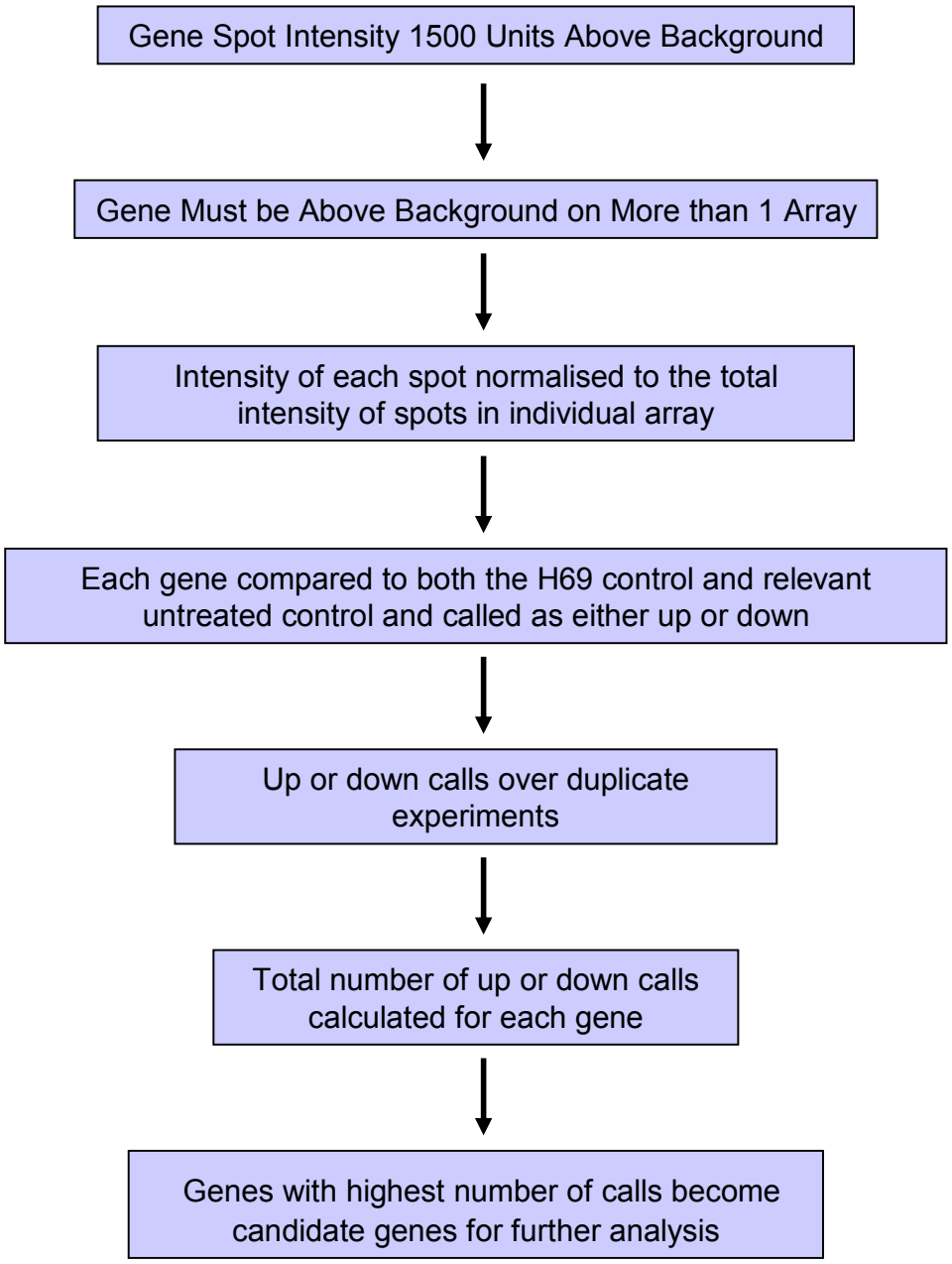

Figure 5.2 Flow chart of the selection of candidate genes from Atlas toxicology nylon array data.

Rank	Gene Name	Abrev.	Genbank	Up	Down	Total	Chromosome
1	mutY homolog	MutY	NM012222	7	1	8	1p32.1-1p34.3
2	glutathione S-transferase theta 1	GSTT1	NM000853	6	1	7	22q11.23
3	retinoic acid receptor alpha	RAR-A	NM000964	5	1	6	17q21
4	DNA repair protein RAD 51 Homolog 2	RAD51B	NM002875	6	0	6	14q23-q24.2
5	60S ribosomal protein L39	RPL39	NM001000	3	3	6	Xq22-q24
6	60S ribosomal protein L3	RPL3	NM00967	3	3	6	22q13
7	40S ribosomal protein S3	RPS3	NM001005	5	0	5	11q13.3-q13.5
8	40S ribosomal protein S30	RPS30	NM001997	4	1	5	11q13
9	liver cytochrome c oxidase VIa	COX6A	NM004373	1	4	5	12q24.2
10	RAN-binding protein 1	RANBP1	NM002882	3	2	5	22q11.21
11	protein-tyrosine phosphatase 1E	PTPL1	NM080685	4	1	5	4q21.3
12	retinoblastoma-like protein 1	p107	NM002895	4	1	5	20q11.2
13	40-kDa heat shock protein 1	HSP401	NM006145	3	2	5	19p13.2
14	CD81 antigen	TAPA1	NM004356	5	0	5	11p15.5
15	xeroderma pigmentosum group A complementing	XPA	NM000380	2	3	5	9q22.3
16	glutathione reductase	GSR	NM000637	4	1	5	8p21.1
17	40S ribosomal protein S5	RPS5	NM001009	4	1	5	19q13.4
18	insulin-like grow th factor-binding protein 2	IGFBP2	NM000597	3	2	5	2q33-q34
19	metastasis inhibition factor NM23	NM23-H1	NM198175	3	1	4	17q21.3
20	90-kDa heat-shock protein beta	HSP90B	NM007355	4	0	4	6p12
21	DNA polymerase delta catalytic subunit	POLD1	NM002691	4	0	4	19q13.3
22	48-kDa FKBP-associated protein	FAP48	NM007070	3	1	4	1p22.1
23	excision repair deficiency complementation group 1	ERCC1	NM001983	2	2	4	19q13.2-q13.3
24	DNA mismatch repair protein MSH2	MSH2	NM000251	1	3	4	2p22-p21
25	N-oxide-forming dimethylaniline monooxygenase 4	FMO4	NM002022	2	2	4	1q23-q25
26	fibrillarin; 34-kDa nucleolar scleroderm antigen	FBL	NM001436	3	1	4	19q13.1
27	macrophage-specific colony-stimulating factor	CSF-1	NM000757	1	3	4	1p21-p13
28	glutathione synthetase	GSH-S	NM000178	3	1	4	20q11.2
29	plasma glutathione peroxidase	GPX3	NM002084	2	2	4	5q23
30	DNA-(apurinic or apyrimidinic site) lyase	APE1	NM001641	3	1	4	14q11.2-q12
31	xeroderma pigmentosum group G complementing	XPG	NM000123	2	2	4	13q33
32	DNA-3-methyladenine glycosylase	ADPG	NM002434	3	1	4	16p13.3
33	chaperonin containing TCP1 subunit 6A	CCT6A	NM001762	2	2	4	7p11.2
34	prosaposin	PSAP	NM002776	2	1	3	10q21-q22
35	glutathione S-transferase pi	GSTP1	NM000852	2	1	3	11q13
36	grow th arrest & DNA damage-inducible protein	GADD45	NM001924	3	0	3	1p31.2-p31.1
37	liver/heart cytochrome c oxidase polypeptide VIII	COX8	NM004074	1	2	3	11q12-q13
38	mitogen-activated protein kinase kinase 2	MAPKK2	NM030662	2	1	3	19p13.3
39	glutathione S-transferase mu 1	GSTM1	NM000561	2	1	3	1p13.3
40	histone 2AX	H2AX	NM002105	1	2	3	11q23.2-q23.3

Table 5.1 Top 40 candidate genes selected from Atlas array data. Data was processed from the nylon array experiments as outlined in Figure 5.2. The top 40 candidate genes are presented with their respective up and down calls and chromosomal location. Genes that were chosen to be further analysed with real-time PCR are highlighted in yellow.

5.3 Functional classification of candidate genes

Table 5.2 presents the top 40 candidate genes and classifies them into functional groups. The functional groupings for each gene were those allocated by the manufacturer of the Atlas toxicology array. The groupings for each gene are indicated in red, some genes appear in more than one category. Functional groups which do not have any genes in the top 40 are indicated in pale blue. Firstly, it is interesting to see which functional groupings do not appear in the top 40 most differentially expressed genes. Cell adhesion proteins, extracellular transport proteins, channels and transporters, extracellular matrix proteins, protein turnover and cytoskeleton/motility genes do not feature in the most differentially expressed genes. This does not mean that resistance and drug treatment has not altered these pathways, rather that other pathways have been affected to a greater and possibly more significant extent.

The transporter proteins included on the Atlas toxicology array included P-gp and MRP1 which do not transport platinum drugs. Therefore it is not surprising that no transporter genes were found to be differentially expressed. Unfortunately, MRP2 and copper transporter CTR1 were not included on the array, these transporters are known to transport platinum drugs. However, it is unlikely that changes in the uptake or efflux of platinum are associated with the mechanism of resistance in these cell models as there was no changes in the cellular accumulation of platinum (Figure 3.12). The lack of cytoskeletal/motility genes is also interesting considering that the resistant cell lines have become more sensitive to taxol (Figure 3.9) which targets the cytoskeleton. The majority of cytoskeletal/motility genes on the array were collagen, crystallin, myosin and actin genes. Two of the cytoskeletal housekeeping genes on the nylon array showed differential expression between samples, α-tubulin and β-actin, these genes will be included in the real-time PCR analysis.

The functional groupings with the greatest number of differentially expressed genes include the very broad category of stress response proteins (15), DNA synthesis and repair (11), apoptosis associated proteins (8), metabolism (6), oncogenes and tumour suppressors (5) and translation (5). The broad category of stress response proteins includes glutathione-related proteins, heat shock proteins and some DNA repair proteins. DNA synthesis and repair genes form just over one quarter of the

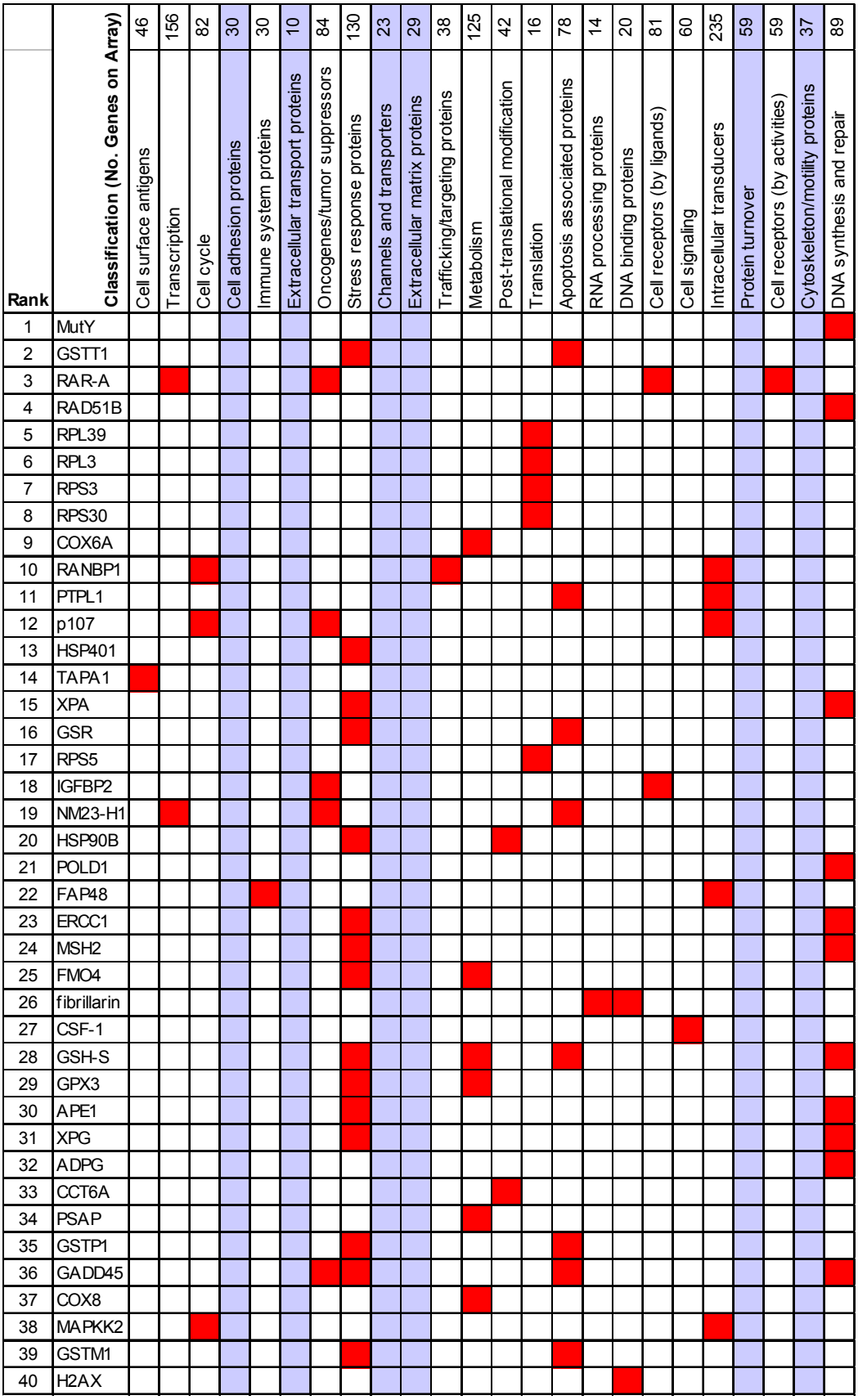

Table 5.2 Analysis of functional classification of candidate genes. Each functional group that a candidate gene is classified in is indicated in red. Genes appear in more than one category. Functional groupings that did not have genes in the top 40 candidate genes are indicated in pale blue.

differentially expressed genes, therefore DNA repair may be a major resistance mechanism in these cell lines with some help from changes in glutathione related genes. There are a moderate number of hits in the apoptosis associated proteins category. Six of these genes are involved in glutathione synthesis and metabolism. Glutathione plays an important role in apoptosis, but what is interesting is the lack of any other genes more commonly associated with apoptosis such as the Bcl-2 family and the Fas/FasL extrinsic mechanism of apoptosis (Figure 1.6) all of which were on the array. The expression of these apoptosis associated genes may have changed in the cell lines but the level of expression was below that detected by the array.

5.4 Chromosomal location of candidate genes

The chromosomal location of the candidate genes were analysed to determine if any occur in close proximity in the genome. If genes that showed increased levels of expression were in the same chromosomal segment, their overexpression may be due to an amplification in this segment. Conversely, decreased expression of genes in close proximity may indicate a deletion in a chromosomal segment. The H69CIS200 and H69OX400 cell lines have many amplifications and deletions compared to the H69 parental cells (Figure 4.8). If these rearrangements have led to a change in gene expression, this would be a link between the changes in genotype and the resistant phenotype of the resistant cell lines.

The chromosomal location of the candidate genes are listed in Table □.1. The 40 candidate genes are spread across the genome, but there are more hits on chromosome 1, 11, 19 and 22. In order to determine if this is a larger number of hits than one would expect by chance, the distribution of genes across the genome and distribution of genes on the array by chromosome have been graphed in Figure □.3A. The distribution in the genome and on the nylon array are relatively similar. This shows that by picking 1000 genes of interest the manufacturers of the nylon array have not skewed the distribution of genes analysed per chromosome. However, when looking at the chromosomal distribution of the candidate genes there is a greater number of genes on chromosomes 1, 11, 19 and 22 than one would expect by chance.

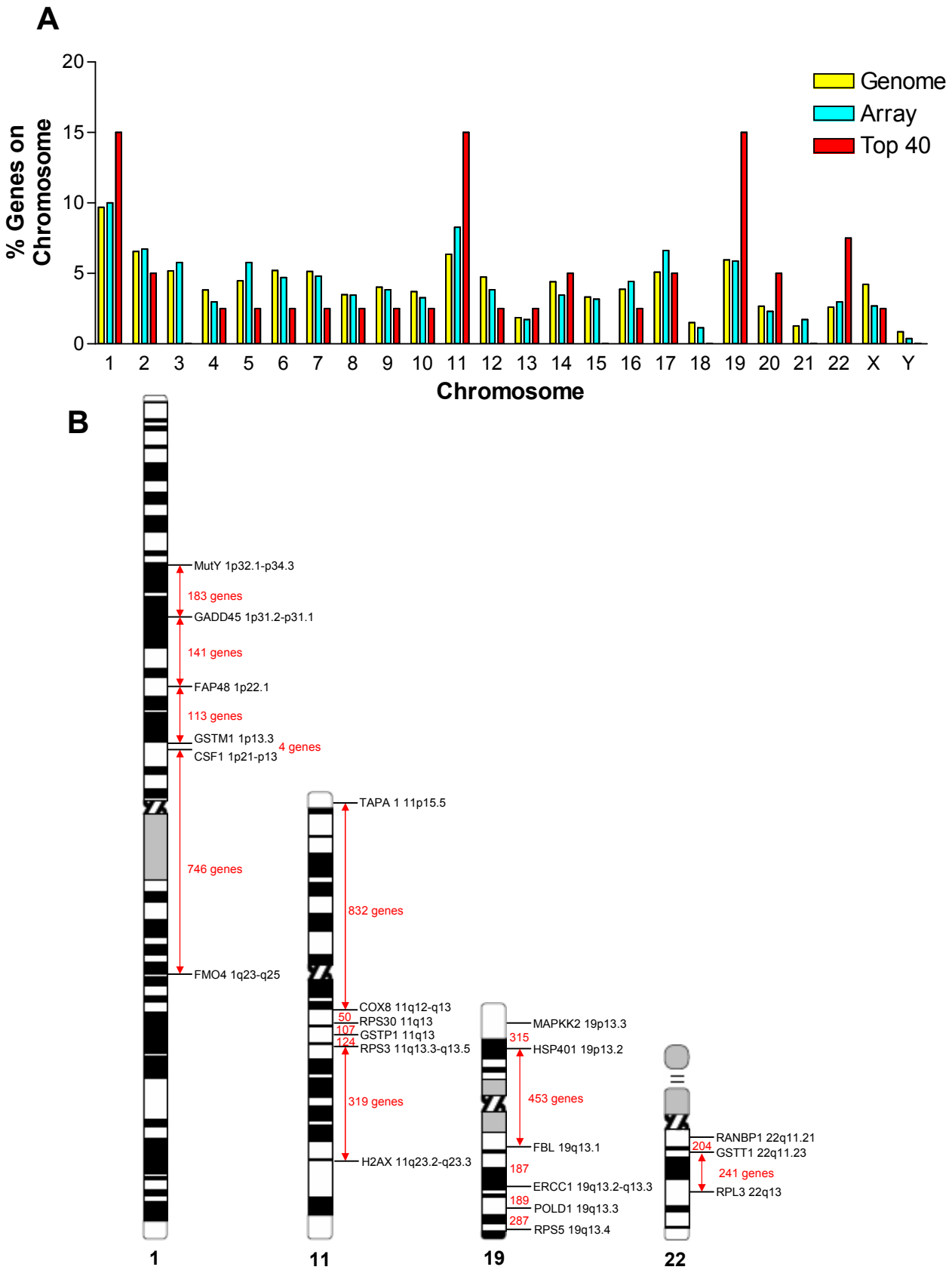

Figure 5.3 Analysis of chromosomal location of candidate genes. A) Distribution of genes by chromosome in the genome, 1000 genes on nylon array and 40 candidate genes. B) Location of candidate genes on chromosomes 1, 11, 19 and 22.

The location of the genes on chromosomes 1, 11, 19 and 22 and the number of genes in between each pair is shown in Figure 5.3B. From this analysis it is clear that the genes are not located in close proximity even though they are on the same chromosome. However, on chromosome 1 there are only 4 genes which separate GSTM1 and CSF1, 3 of these intervening genes are also members of the glutathione-S-transferase family. This raises the possibility of an increase in gene expression due to an increase in copy number. The Affymetrix data in Chapter 4 shows that there is no change in the copy number of any of the segments containing these differentially expressed genes, including the segment on chromosome 1 where GSTM1 and CSF1 are located (Figure 4.8). The changes in DNA copy number are therefore not contributing to the differential expression of the candidate genes. A whole genome mRNA array approach would be needed to associate changes in expression with the chromosomal changes observed in the resistant cell lines.

5.5 Real-time PCR results for candidate genes

A total of twenty-seven genes were analysed by real-time PCR. Twenty-one were from the candidate genes chosen from the nylon array. Another six genes were chosen based on the cross resistance data presented in Chapter 3. Gamma-glutamyl cysteine synthetase (γGCS) catalytic and regulatory subunits were chosen due to the interesting BSO cytotoxicity data (Figure 3.10). γGCS is the rate limiting enzyme in glutathione synthesis and BSO is an inhibitor of this enzyme (Figure 1.5). The γGCS regulatory subunit was on the Atlas array but its spot intensity was below the level of detection. The γGCS catalytic subunit was not on the array. GSTO1 was chosen for analysis because of its high spot intensity on the array suggested it was very abundant, there also appeared to be differences between samples. Cytoskeletal genes, β-actin, α-tubulin and microtubule associated protein 4 (MAP4) were chosen due to the relative sensitivity of the cell lines to taxanes (Figure 3.9). β-actin and α-tubulin were on the Atlas toxicology array, classified as housekeeping genes, both genes showed differential expression between samples. MAP4 was not on the array.

The real-time PCR analysis was conducted on the same mRNA samples used for the Atlas nylon array analysis. Figure 5.4 presents the average expression of each assayed

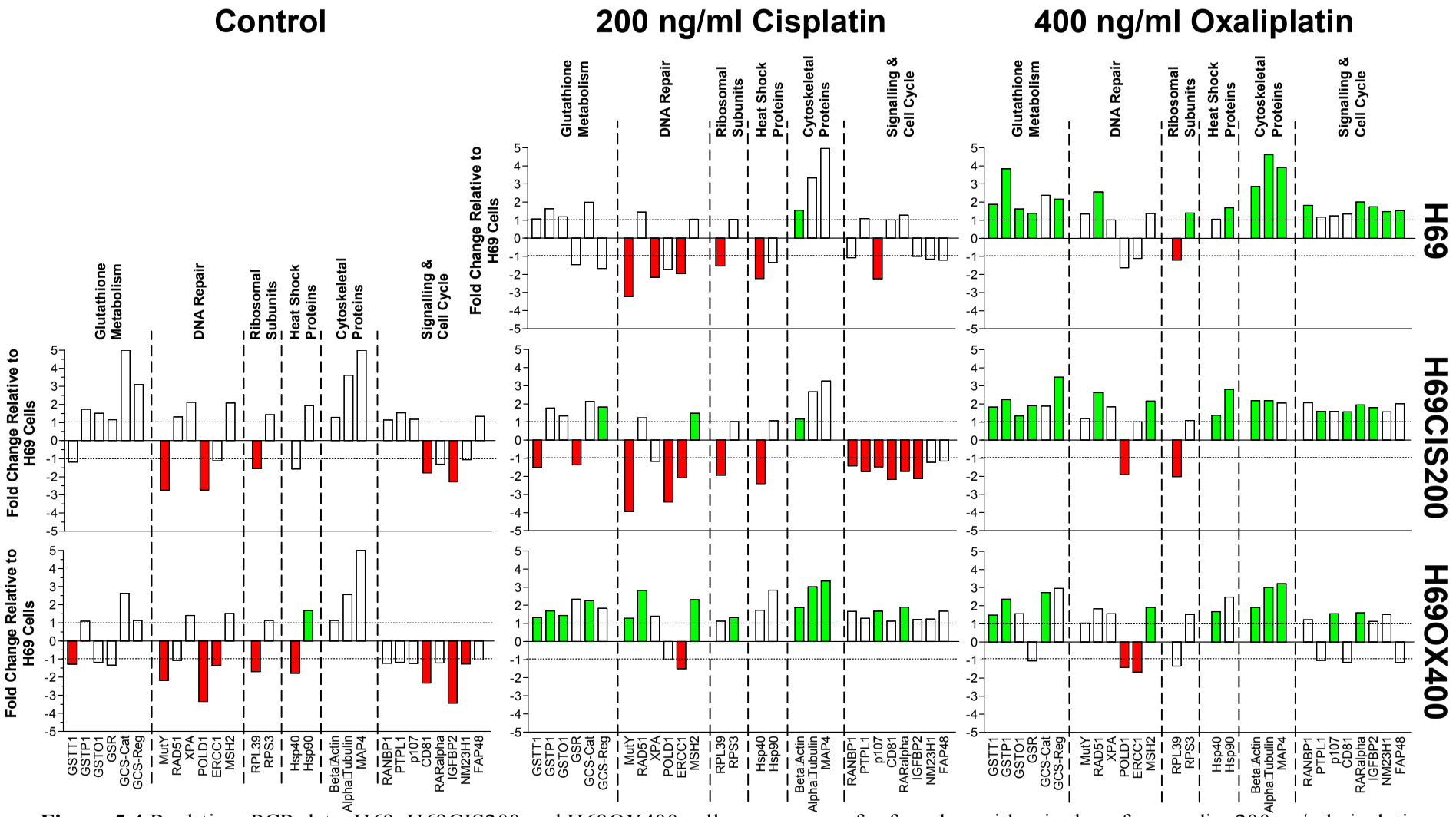

Figure 5.4 Real-time PCR data. H69, H69CIS200 and H69OX400 cells were grown for four days either in drug-free media, 200 ng/ml cisplatin or 400 ng/ml oxaliplatin. mRNA was extracted, converted to cDNA and assayed by real time PCR for the genes indicated as described in section 2.12. The mean fold change for each gene relative to the H69 control is presented. Standard deviations have been omitted for clarity. Significant increases are indicated in green, significant decreases are indicated in red. Significant differences were determined using a student's t-test $p < 0.05$.

gene expressed relative to the H69 control. Significant increases are indicated in green, significant decreases are indicated in red. The gene expression pattern for the H69CIS200 and H69OX400 control samples were quite similar showing many significant decreases in expression. The H69 + cisplatin and H69CIS200 + cisplatin showed a similar pattern of gene expression. In contrast the H69OX400 + cisplatin resembled the response to oxaliplatin in all cell lines. This suggests that the response to oxaliplatin is quite different to the response to cisplatin in this cell model. The H69OX400 cell line responds to the stress of cisplatin treatment in a similar way as it responds to oxaliplatin which may explain the cross resistance in this cell line (Figure 3.9). However, the H69CIS200 cell line responds to cisplatin and oxaliplatin in different ways, yet there is still cross resistance between the two compounds in this cell line (Figure 3.9).

5.6. Discussion

The cellular function of each gene examined by real-time PCR and any known association with platinum resistance is presented in Tables 5.3A and B. Many of these genes will be discussed in the more detailed analysis of pathways in later chapters and the relevant chapter is listed. The relationship between the genes identified in this chapter has been summarised in a biological association network (BAN). Figures 5.5-5.8 show BAN maps for all the samples analysed by real-time PCR. These network diagrams were created manually by literature searches and coloured to reflect the real-time PCR data from Figure 5.4. The literature used to create the biological association network is summarised in Tables 5.4A and B. The vast majority of links are well established in the literature and only one or two references are cited as examples. Pathways or groups of genes are indicated in blue. Some additional genes have been added where they help associate two or more candidate genes (indicated in grey). Dark green indicates a significant increase in gene expression, dark red a significant decrease in gene expression. Light green indicates a trend of increased expression, light red indicates a trend of decreased expression and pale orange indicates no change.

Table 5.3A Candidate genes function and association with platinum resistance.

Gene	Function	Relationship to Platinum Resistance	Chapter
GSTT1	Conjugation of GSH (Figure 1.5)	Not previously associated	7
GSTP1	Conjugation of GSH and MAP kinase signalling (Townsend et al., 2003b)	↑GSTP1 leads to cisplatin resistance in primary tumours and cell lines (Cullen et al., 2003)	7
GSTO1	Conjugation of GSH (Figure 1.5)	Not previously associated	7
GSR	GSH Recycling (Figure 1.5)	↑GSR leads to cisplatin resistance (Ogawa et al., 1993)	7
γGCS-Reg	GSH Synthesis (Figure 1.5)	↑γGCS-Reg leads to cisplatin resistance (Godwin et al., 1992; Iida et al., 1999)	7
γGCS-Cat	GSH Synthesis (Figure 1.5)	↑γGCS-Cat leads to cisplatin resistance (Godwin et al., 1992; Iida et al., 1999)	7
MutY Homolog	Long patch BER repair pathway (Figure 1.11)	Not previously associated	9
RAD51B	Homologous recombonation (Figure 1.10A)	↓RAD51B leads to cisplatin sensitivity (Takata et al., 2000)	9
ERCC1	Nucleotide excision repair (Figure 1.9)	↑ERCC1 leads to cisplatin resistance (Ferry et al., 2000; Selvakumaran et al., 2003)	9
XPA	Nucleotide excision repair (Figure 1.9)	↑XPA clinical cisplatin resistance (Dabholkar et al., 1994)	9
POLD1	DNA polymerase involved in DNA replication and NER and long patch BER (Figure 1.9 and 1.11)	DNA polymerase δ cannot bypass Pt adducts Not previously associated	9
MSH2	Mismatch repair (Figure 1.13)	↓MSH2 leads to cisplatin resistance (Aebi et al., 1997)	9
RPL39 60S	Part of the large ribosomal subunit	↓RPL39 associated with cisplatin resistance (Toshimitsu et al., 2004)	-
RPS3 40S	Part of the small ribosomal subunit and plays a role in apoptosis (Jang et al., 2004) and BER (Kim et al., 1995; Hegde et al., 2004)	Not previously associated	9
Hsp40 Homolog	Stress protein with chaperone activity	Not previously associated	-

BER - base excision repair, GSH - glutathione, GST – glutathione-S-transferase, NER - nucleotide excision repair

Table 5.3B Candidate genes function and association with platinum resistance.

Gene	Function	Relationship to Platinum Resistance	Chapter
Hsp90β	Stress protein with chaperone activity	↓Hsp90β by antisense leads to cisplatin sensitivity (Huang et al., 2000)	-
β-actin	Component of the cytoskeleton and role in cell motility (Zeng et al., 1997)	↑ and ↓ in β-actin has been associated with cisplatin resistance in different studies (Whiteside et al., 2004; Shen et al., 2004)	6
α-tubulin	Structure of microtubules (Orr et al., 2003)	↑α-tubulin mRNA associated with cisplatin resistance (Toshimitsu et al., 2004)	6
MAP4	Binds to and stabilises microtubules (Kavallaris et al., 2001)	Not previously associated	6
RANBP1	Binding protein of Ran-GTP involved in nuclear-cytoplasmic transport and mitotic spindle assembly (Mattaj et al., 1998)	Not previously associated	6
PTPL1	Inhibition of PI3K/Akt pathway (Bompard et al., 2002) and involved in Fas mediated apoptosis (Ivanov et al., 2003)	Not previously associated	6
p107	Cell cycle transistion from G_1 to S phase (Kondo et al., 2001)	Not previously associated	9
CD81 Antigen	Differentiation and MAP kinase signalling (Carloni et al., 2004)	Not previously associated	-
RARα	Cell growth and differentiation (Brooks, III et al., 1997; Lehmann et al., 2001)	Not previously associated	-
IGFBP2	Regulator of Insulin-like growth factors(Busund et al., 2005)	↓IGFBP2 associated with cisplatin resistance in ovarian carcinoma (Sakamoto et al., 2001)	6
NM23H1(NDK1)	Differentiation factor (Lombardi et al., 2000) also involved in nucleotide synthesis and possibly in DNA repair (Yoon et al., 2005)	↓NM23H1 associated with cisplatin resistance (Iizuka et al., 1999)	9
FAP48	Interacts with FK506 binding proteins which bind to the drug rapamycin associated with the mTOR pathway (Krummrei et al., 2003)	Not previously associated	6

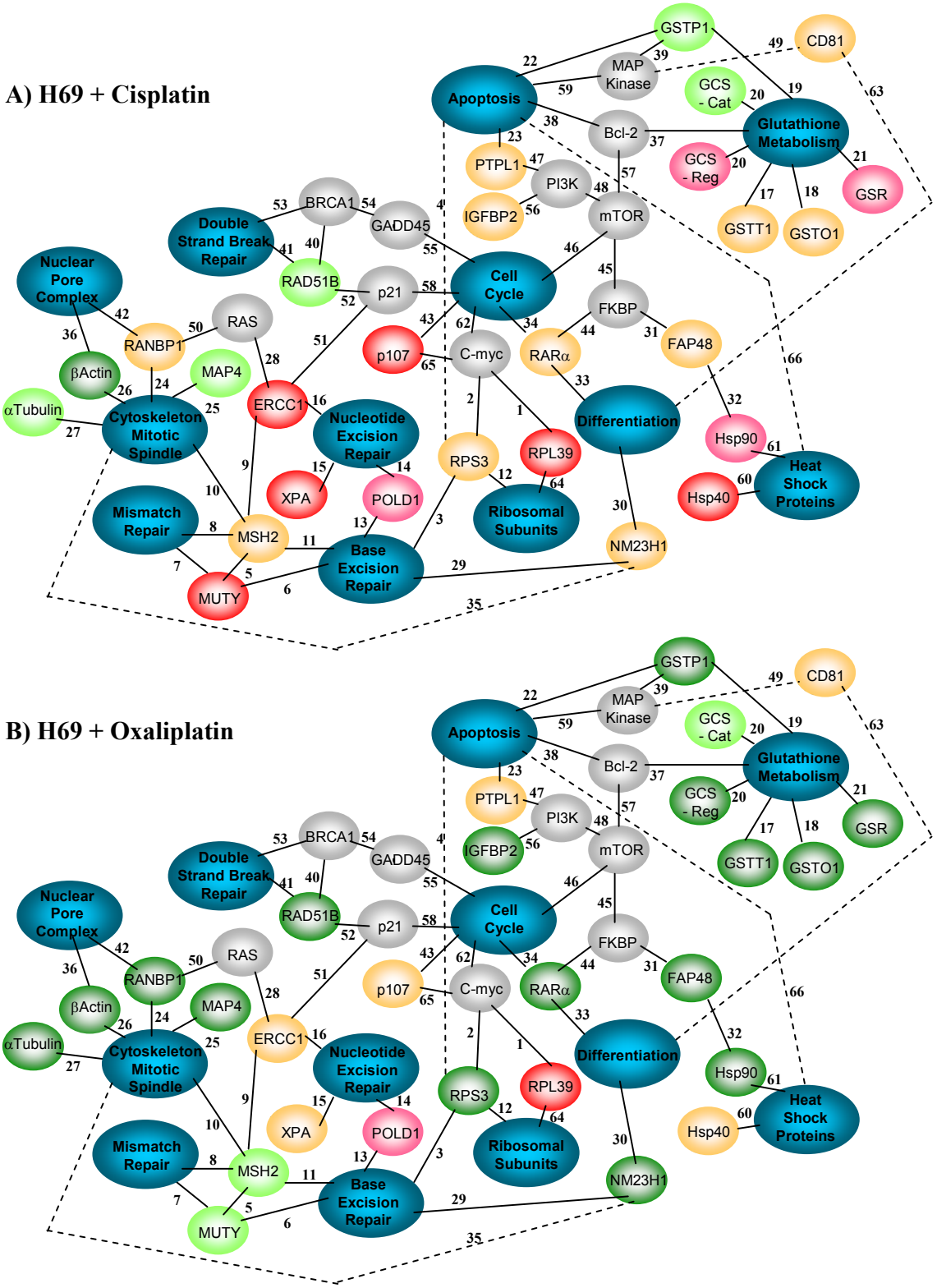

Figure 5.5 Biological association network of the H69 parental cell line treated with cisplatin and oxaliplatin. The real-time PCR data for the A) H69 cells + cisplatin and B) H69 + oxaliplatin has been taken from Figure 5.4 and arranged in a biological association network. Functional groups are blue, non assayed linking genes are grey. Significant increases are dark green, significant decreases are dark red. Trends to increase are pale green, trends to decrease are pale red. Genes with no change in expression are indicated in pale orange. Numbers refer to the reference for the connection (Table 5.4).

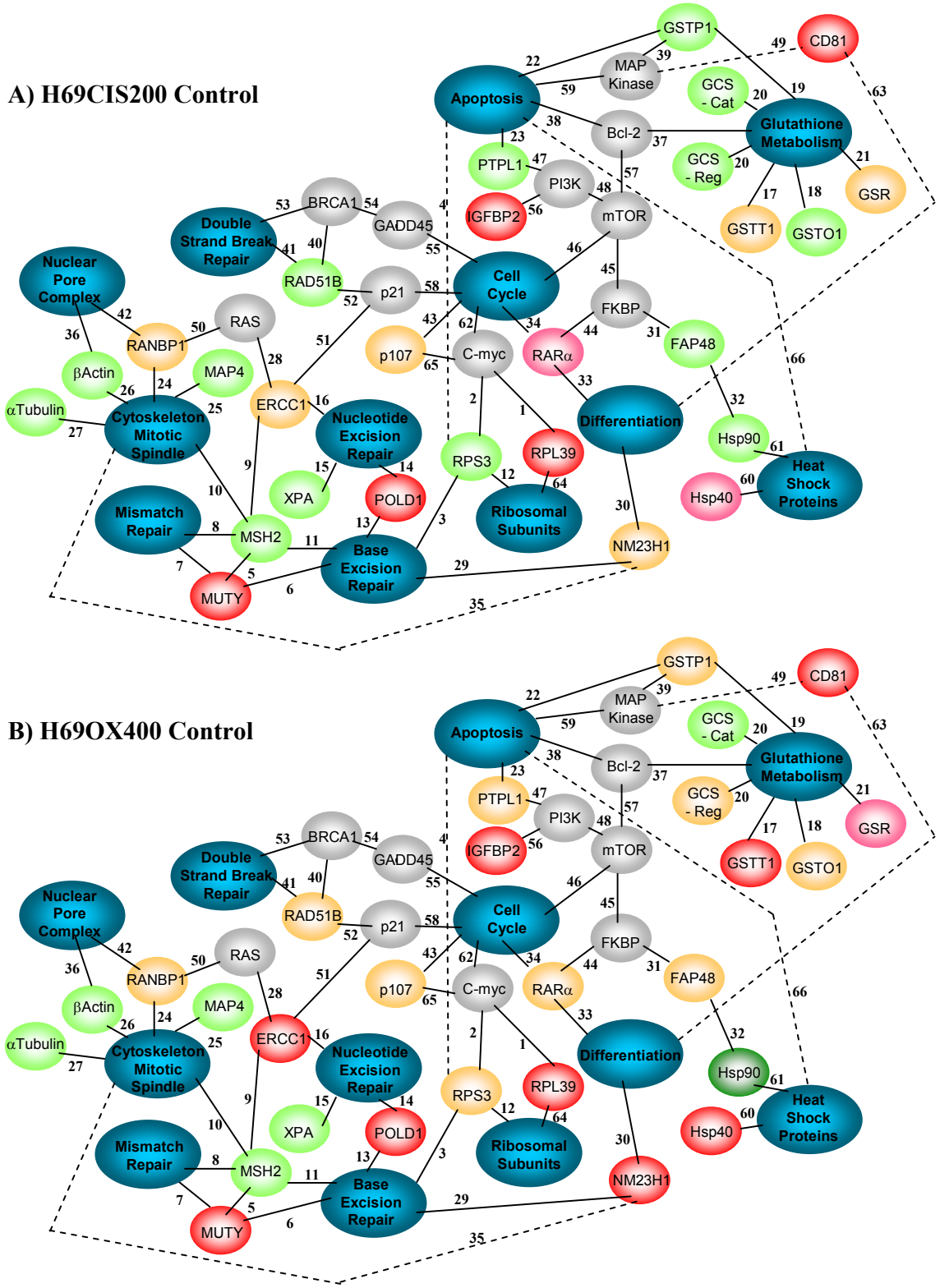

Figure 5.6 Biological association network of the H69CIS2□□and H69OX4□□control cells. The real-time PCR data for the A) H69CIS2□□control and B) H69OX4□□control has been taken from Figure 5.4 and arranged in a biological association network. Functional groups are blue, non assayed linking genes are grey. Significant increases are dark green, significant decreases are dark red. Trends to increase are pale green, trends to decrease are pale red. Genes with no change in expression are indicated in pale orange. Numbers refer to the reference for the connection (Table 5.4).

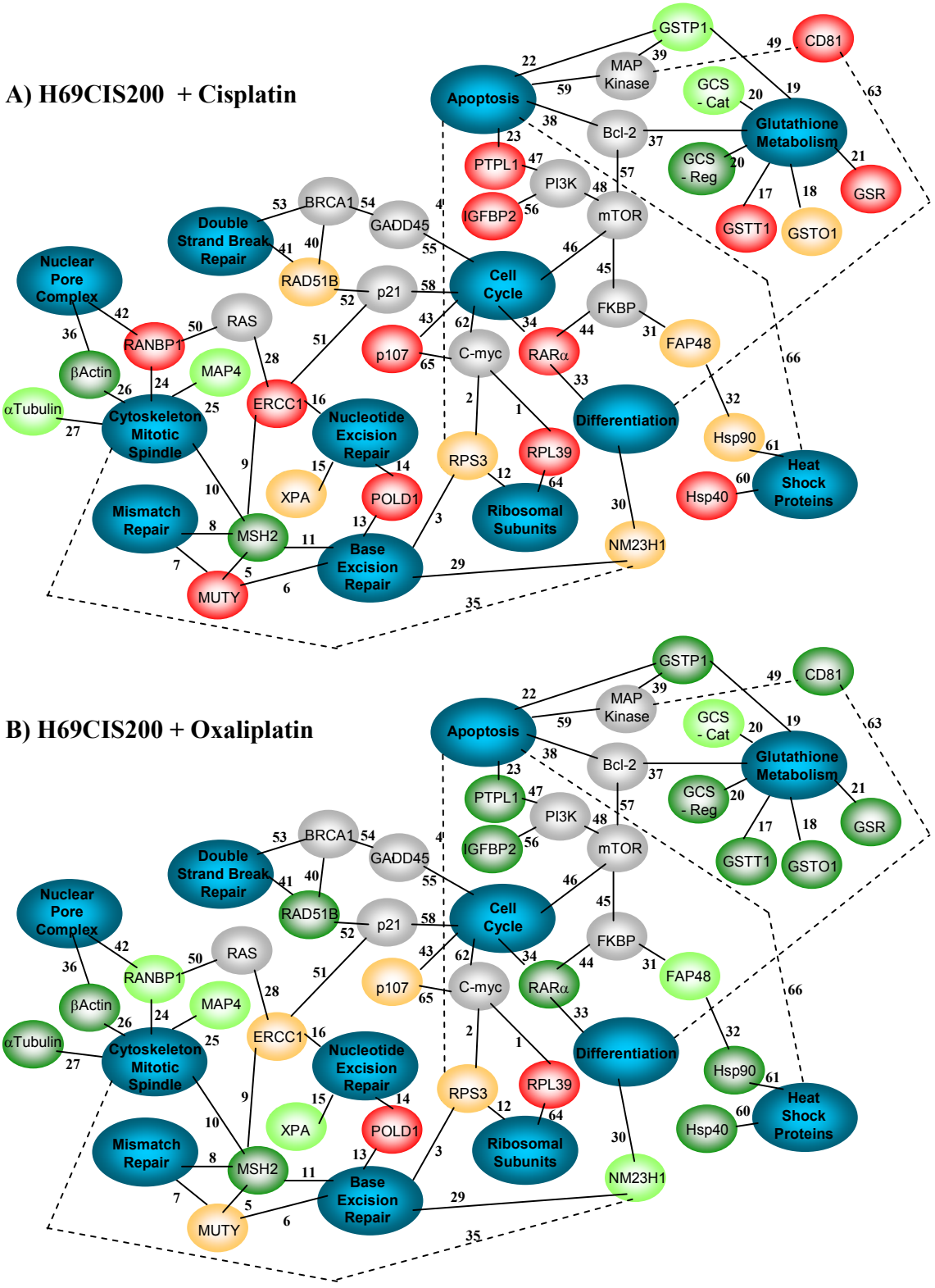

Figure 5.7 Biological association network of the H69CIS2□□cell line treated with cisplatin and oxaliplatin. The real-time PCR data for the A) H69CIS2□□cells + cisplatin and B) H69CIS2□□+ oxaliplatin has been taken from Figure 5.4 and arranged in a biological association network. Functional groups are blue, non assayed linking genes are grey. Significant increases are dark green, significant decreases are dark red. Trends to increase are pale green, trends to decrease are pale red. Genes with no change in expression are indicated in pale orange. Numbers refer to the reference for the connection (Table 5.4).

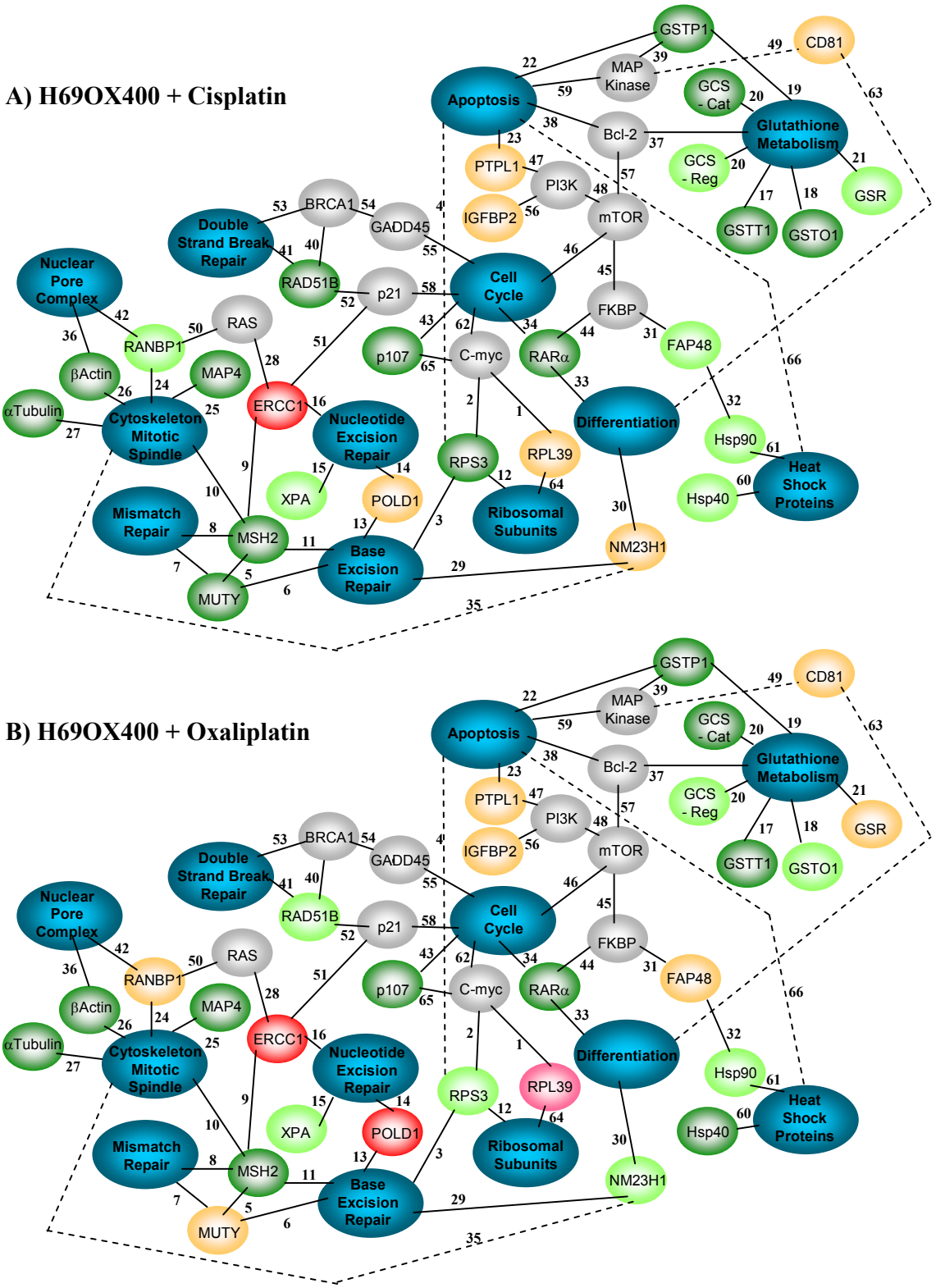

Figure 5.8 Biological association network of the H69OX4□□cell line treated with cisplatin and oxaliplatin. The real-time PCR data for the A) H69OX4□□cells + cisplatin and B) H69OX4□□+ oxaliplatin has been taken from Figure 5.4 and arranged in a biological association network. Functional groups are blue, non assayed linking genes are grey. Significant increases are dark green, significant decreases are dark red. Trends to increase are pale green, trends to decrease are pale red. Genes with no change in expression are indicated in pale orange. Numbers refer to the reference for the connection (Table 5.4).

Table 5.4A References for biological association network diagrams – Part 1.

Link	Genes	References
1	RPL39 and C-myc	(Ruggero et al., 2003)
2	RPS3 and C-myc	(Ruggero et al., 2003)
3	RPS3 and BER	(Kim et al., 1995; Hegde et al., 2004)
4	RPS3 and Apoptosis	(Jang et al., 2004)
5	MSH2 and MutY	(Gu et al., 2002)
6	MutY and BER	(Gu et al., 2002)
7	MutY and MMR	(Fourrier et al., 2003)
8	MSH2 and MMR	(Wozniak et al., 2002)
9	MSH2 and ERCC1	(Lan et al., 2004)
10	MSH2 and cytoskeleton	(Marquez et al., 2004)
11	MSH2 and BER	(Gu et al., 2002)
12	RP3S and Ribosomal	(Jang et al., 2004)
13	POLD1 and BER	(Sancar et al., 2004)
14	POLD1 and NER	(Sancar et al., 2004)
15	XPA and NER	(Sancar et al., 2004)
16	ERCC1 and NER	(Sancar et al., 2004) (Selvakumaran et al., 2003)
17	GSTT1 and Glutathione	(Townsend et al., 2003b)
18	GSTO1 and Glutathione	(Townsend et al., 2003b)
19	GSTP1 and Glutathione	(Townsend et al., 2003b)
20	γGCS and Glutathione	(Rahman et al., 1999)
21	GSR and Glutathione	(Rahman et al., 1999)
22	GSTP1 and Apoptosis	(Townsend et al., 2003b)
23	PTPL1 and Apoptosis	(Bompard et al., 2002)
24	RANBP1 and Cytoskeleton	(Mattaj et al., 1998; Dasso, 2002; Moore et al., 2002)
25	MAP4 and Cytoskeleton	(Orr et al., 2003)
26	β-actin and Cytoskeleton	(Shen et al., 2004)
27	α-tubulin and Cytoskeleton	(Orr et al., 2003)
28	ERCC1 and Ras	(Youn et al., 2004)
29	NM23H1 and BER	(Yoon et al., 2005)
30	NM23H1 and Differentiation	(Lombardi et al., 2000)
31	FAP48 – FKBP	(Krummrei et al., 2003)
32	FKBP – Hsp90	(Krummrei et al., 2003)
33	RARα - Differentiation	(Brooks, III et al., 1997; Lehmann et al., 2001)
34	RARα – Cell Cycle	(Bhatia et al., 1996; Walkley et al., 2004)
35	NM23H1 and microtubules	(Lombardi et al., 2000)
36	Actin and NPC	(Prat et al., 1996; Tonini et al., 1999)
37	Bcl-2 and Glutathione	(Celli et al., 1998)
38	Bcl-2 and Apoptosis	(Ghobrial et al., 2005)
39	GSTP1 and MAP kinase	(Townsend et al., 2003b)
40	RAD51B and BRAC1	(Zhou et al., 2005)

BER – base excision repair, MMR – mismatch repair, NER – nucleotide excision repair and NPC – nuclear pore complex.

Table 5.4B References for biological association network diagrams - Part 2.

Link	Genes	References
41	RAD51B and HRR	(Xu et al., 2005)
42	RANBP1 and NPC	(Mattaj et al., 1998)
43	p107 and cell cycle	(Kondo et al., 2001)
44	FKBP and RARα	(Kwok et al., 2006)
45	FKBP and mTOR	(Mita et al., 2003)
46	mTOR and cell cycle	(Mita et al., 2003)
47	PTPL1 and PI3K/AKT	(Bompard et al., 2002)
48	mTOR and PI3K/AKT	(Mita et al., 2003)
49	CD81 and MAP Kinase	(Carloni et al., 2004)
50	Ras and RANBP1	(Youn et al., 2004)
51	ERCC1 and p21	(Melton et al., 1998) (Nunez et al., 2000)
52	RAD51B and p21	(Raderschall et al., 2002)
53	BRCA1 and HRR	(Sancar et al., 2004)
54	BRCA1 and GADD45	(Mullan et al., 2001)
55	GADD45 and Cell Cycle	(Mullan et al., 2001)
56	IGFBP2 and PI3K	(Foulstone et al., 2005)
57	mTOR and Bcl-2	(Asnaghi et al., 2004a) (Calastretti et al., 2001)
58	p21 and Cell Cycle	(Sancar et al., 2004)
59	MAP Kinase and Apoptosis	(Ichijo et al., 1997)
60	Hsp40 and Heat Shock Proteins	(Santoro, 2000)
61	Hsp90 and Heat Shock Proteins	(Santoro, 2000)
62	C-myc and Cell Cycle	(Amati et al., 1998)
63	CD81 and Differentiation	(Carloni et al., 2004)
64	RPL39 and Ribosomal	(Uechi et al., 2001)
65	p107 and C-myc	(Chen et al., 2002b)
66	Heat Shock Proteins and Apoptosis	(Creagh et al., 2000)

HRR – homologous recombination repair, NPC – nuclear pore complex.

5.6.1 H69 parental cells response to cisplatin and oxaliplatin

The H69 parental cells were examined in response to cisplatin and oxaliplatin to see how sensitive cells respond to the stress of platinum drug treatment. By comparing the pattern of change in gene expression in both chemotherapy-sensitive cells and resistant cells, it can be determined which genes are changing only in the resistant cells contributing to the resistant phenotype. The gene expression pattern of the H69 parental cells respond very differently to drug treatment with cisplatin and oxaliplatin. Cisplatin treatment results in mostly significantly decreased expression of this subset of genes where as oxaliplatin treatment results in significantly increased expression as shown in Figure 5.5. The majority of these genes will be discussed in later chapters in further detail as listed in Tables 5.3A and B. This section is designed to analyse broad patterns of gene response with reference to previously reported mechanisms of platinum resistance.

Cisplatin treated H69 cells show no significant change in the glutathione associated genes studied. In contrast, many glutathione associated genes were upregulated in H69 cells in response to oxaliplatin, GSTP1, GSTO1, GSTT1, GSR and γGCS-Reg. This suggests that the glutathione pathway is more important in the response to oxaliplatin than cisplatin in this cell model. This fits with the platinum and BSO cytotoxicity data (Figure 3.11B,C). BSO, which depletes glutathione, tended to sensitise all cell lines to oxaliplatin, but had little effect on cisplatin resistance.

The H69 cells treated with cisplatin show decreased expression of DNA repair genes MutY, XPA and ERCC1 suggesting a downregulation of DNA repair in response to cisplatin drug treatment. However, oxaliplatin treated H69 cells do not have decreased expression of MutY, XPA or ERCC1. The oxaliplatin treated H69 cells also have increased expression of RAD51B which is associated with double-strand break DNA repair. This suggests that the expression of DNA repair genes is more important in the response to oxaliplatin than cisplatin in H69 cells.

The H69 cells treated with cisplatin and oxaliplatin both show a significant decrease in ribosomal subunit RPL39. A decrease in the mRNA expression of RPL39 has previously been associated with cisplatin resistance in oesophageal squamous cell

carcinoma cells (Toshimitsu et al., 2004). This study showed changes in 15 ribosomal subunits, of which the majority were decreases. However, the exact mechanism of how these genes confer resistance is unknown. Cisplatin has been shown to decrease the synthesis of rRNA by interfering with a ribosomal transcription factor UBF (Zhai et al., 1998; Jordan et al., 1998). Perhaps a decrease in one component of ribosomes, the rRNA signals a decrease in the mRNA of ribosomal protein subunits. The decrease in expression of ribosomal genes may therefore be part of the cytotoxic response to cisplatin treatment rather than a mechanism of resistance.

The H69 cells treated with oxaliplatin have a significant increase in ribosomal subunit RPS3. This gene has not been previously associated with the response to platinum but may play a role in other cellular processes. RPS3 has been associated with both apoptosis (Jang et al., 2004) and base excision DNA repair (Kim et al., 1995; Hegde et al., 2004).

The H69 cells treated with cisplatin show decreased expression of heat shock protein Hsp40 homolog. Hsp40 homolog has not been previously associated with platinum resistance. The H69 cells treated with oxaliplatin show increased expression of Hsp90β. Decreased expression of Hsp90β by antisense leads to cisplatin sensitivity in HeLa cells (Huang et al., 2000). Conversely, the increase in Hsp90β may confer platinum resistance by increasing the stability of proteins to which it acts as a chaperone. However, the precise mechanism for this relationship is unknown.

H69 cells treated with both cisplatin and oxaliplatin show increases in cytoskeletal proteins α-tubulin, β-actin and MAP4. Increased expression of α-tubulin mRNA has been associated with cisplatin resistance in oesophageal squamous cell carcinoma cells (Toshimitsu et al., 2004). Increased expression of β-actin mRNA has been associated with cisplatin resistance in lung cancer cells (Whiteside et al., 2004). However, decreased expression of β-actin protein has been associated with cisplatin resistance in epidermoid carcinoma cells (Shen et al., 2004). MAP4 has not been previously associated with platinum resistance. β-actin may play a role in the recognition and repair of platinum adducts and therefore by involved in the cytotoxic response to platinum treatment (Wozniak et al., 2002). The overall increase in

cytoskeletal genes may play a role in cellular transport in response to platinum drug treatment.

Cisplatin treatment of H69 cells decreased the expression of p107 which is involved in cell cycle transition from the G_1 to S phase (Kondo et al., 2001). p107 has not been previously associated with cisplatin resistance, and will be discussed in further detail in Chapter 8. Oxaliplatin treatment of H69 cells increased the expression of RANBP1 which is involved in mitotic spindle assembly (Mattaj et al., 1998), RARα which is involved in cell growth and differentiation (Brooks, III et al., 1997; Lehmann et al., 2001) and FAP48 which interacts with FK506 binding proteins which bind to the drug rapamycin associated with the mTOR pathway (Krummrei et al., 2003). These three genes have not been previously associated with platinum resistance.

Oxaliplatin treatment of H69 cells led to an increase in NM23H1 a differentiation factor (Lombardi et al., 2000) which is also involved in nucleotide synthesis and possibly in DNA repair (Yoon et al., 2005). In contrast a decrease in NM23H1 mRNA has been previously associated with cisplatin resistance in oesophageal squamous cell carcinoma patients (Iizuka et al., 1999). This difference may be due to the many roles of this gene in different pathways. Oxaliplatin treatment of H69 cells also led to an increase in IGFBP2 which is a regulator of insulin-like growth factors (Busund et al., 2005). In contrast, decreased IGFBP2 mRNA has been associated with cisplatin resistance in ovarian carcinoma (Sakamoto et al., 2001). The mechanism for this association is unknown.

5.6.2 H69CIS200 and H69OX400 control cells

The resistant cell lines in their untreated state have mostly decreases in gene expression compared to the untreated H69 cells and appear relatively similar in their patterns of gene expression as shown in Figure 5.6. Changes in gene expression in the untreated resistant cell lines are changes that the resistant cell lines maintain in the absence of the stress response of drug treatment. The H69CIS200 cisplatin-resistant cells did not have as many significant differences as the H69OX400 cell line. However the majority of genes in the H69CIS200 cells showed a trend towards change in the same direction as the H69OX400 cells. This suggests that the

expression pattern in the two resistant cell lines are quite similar in their resting state and this may contribute to the ability of these cells to be cross-resistant to both cisplatin and oxaliplatin.

The H69CIS200 untreated cells have a trend of increased expression of γGCS-Cat and γGCS-Reg, however this does not correspond to an increase in glutathione synthesis in this cell line (Figure 3.10). The H69OX400 untreated cells have decreased expression of GSTT1. This is surprising as an upregulation of this gene would be beneficial in a platinum-resistant cell.

The H69CIS200 and H69OX400 untreated cells share decreases in expression in DNA repair genes MutY and POLD1. The H69CIS200 and H69OX400 cells also share a decrease in ribosomal gene RPL39 and heat shock protein Hsp40 homolog. This pattern is the same as what was observed for the response to cisplatin treatment in the H69 cells (Figure 5.5A). The resistant cell lines also share an increase in Hsp90β expression, which is the same as what was observed in response to oxaliplatin treatment in the H69 cells (Figure 5.5B). The resistant cell lines also have increases in cytoskeletal genes α-tubulin, β-actin and MAP4, as was observed in response to both cisplatin and oxaliplatin in the parental H69 cells (Figure 5.5A and B). This suggests that the increased expression of these genes is part of the stress response to platinum treatment rather than the mechanism of resistance as the same pattern occurred in the sensitive and resistant cell lines. The cytoskeletal genes will be further examined in Chapter 6.

The untreated resistant cell lines both have decreased expression of CD81. Tetraspannin CD81 has been associated with differentiation as well as cell proliferation through interaction with MAP kinase signalling (Carloni et al., 2004). CD81 has not been previously associated with platinum resistance. The untreated resistant cell lines also have decreased expression of IGFBP2. Decreased IGFBP2 has been previously associated with cisplatin resistance in ovarian carcinoma (Sakamoto et al., 2001). The H69OX400 cell line also has a small but significant decrease in NM23H1.

5.6.3 H69CIS200 response to cisplatin and oxaliplatin

The H69CIS200 cells respond to cisplatin and oxaliplatin treatment in a differential fashion (Figure 5.7). This is similar to the differential response seen in the parental H69 cells (Figure 5.5). Cisplatin treatment of H69CIS200 cells results in mostly significantly decreased expression of this subset of genes where as oxaliplatin treatment of H69CIS200 results in mostly significantly increased expression (Figures 5.7).

Cisplatin treatment of the H69CIS200 cells significantly decreased the expression of glutathione genes GSTT1 and GSR. Whereas oxaliplatin treatment increased expression of GSTT1, GSTO1, GSTP1 and GSR. This suggests a differential response of glutathione metabolism to cisplatin and oxaliplatin treatment in this cell line. The response of glutathione metabolism will be further examined in Chapter 7.

Cisplatin treatment of the H69CIS200 cells induced decreased expression of DNA repair genes ERCC1 and MutY, whereas oxaliplatin treatment did not alter the expression of these genes. This suggests that the DNA repair pathways respond differently to cisplatin and oxaliplatin in the H69CIS200 cells. However, there was increased expression of MSH2 and decreased expression of POLD1, suggesting some similarity in the DNA repair response to cisplatin and oxaliplatin in H69CIS200 cells. The response of DNA repair pathways will be further analysed in Chapter 8.

The ribosomal genes responded in the same manner in response to both cisplatin and oxaliplatin treatment in the H69CIS200 cells. There was no change in the expression of RPS3 and a significant decrease in RPL39. This was the same pattern as in the H69 parental cells treated with cisplatin (Figure 5.5).

Cytoskeletal genes show the same increased expression in response to cisplatin and oxaliplatin in the H69CIS200 cells. This is the same as observed in the H69 cells in response to cisplatin and oxaliplatin (Figure 5.5) and in the untreated resistant cell lines (Figure 5.6). This suggests that cellular transport is important both in the untreated resistant cell lines and in response to platinum drug treatment. These

cytoskeletal changes will be further examined in Chapter 6 in association with the analysis of the mechanism of sensitivity to taxanes in the resistant cell lines.

Heat shock proteins Hsp90β and Hsp40 homolog are significantly increased in response to oxaliplatin treatment in the H69CIS200 cells. In contrast, Hsp40 homolog is significantly decreased in expression in response to cisplatin treatment.

Cell signalling and cell cycle genes PLPL1, IGFBP2, p107 and RARα show a differential response between cisplatin and oxaliplatin treatment in the H69CIS200 cells. Cisplatin treatment causes a significant decrease in all these genes whereas oxaliplatin treatment causes a significant increase. This suggests a difference in cell cycle response between cisplatin and oxaliplatin treatment in the H69CIS200 cells. These changes may play a role in the regrowth resistance phenotype of this cell model and will be further discussed in Chapters 6 and 8.

However, despite the broad differential response of the H69CIS200 cells to cisplatin and oxaliplatin there were five significant changes in common to both cisplatin and oxaliplatin treatment in the H69CIS200 cells. These were increased expression of γGCS-Reg, MSH2 and β-actin, and decreased expression of POLD1 and RPL39 (Figure 5.7). The significantly increased expression of β-actin and decreased expression of RPL39 also occurred in the H69 sensitive cells in response to cisplatin and oxaliplatin treatment (Figure 5.5). The expression of POLD1 was also decreased in the response of the H69 cells to cisplatin and oxaliplatin but these changes were not significant. This suggests that changes in these genes are not associated with the mechanism of resistance but are rather reflective of the stress response to platinum drug treatment in both the H69 and H69CIS200 cell lines.

The expression of γGCS-Reg has shifted from a decrease in H69 cells treated with cisplatin (Figure 5.5) to a significant increase in H69CIS200 cells treated with cisplatin. However, γGCS-reg was significantly increased in both H69 and H69CIS200 cells in response to oxaliplatin. This suggests that this gene may be involved in the resistance to cisplatin in the H69CIS200 cells but not to oxaliplatin. γGCS will be further discussed in chapter 7.

The expression of MSH2 has significantly increased in response to both cisplatin and oxaliplatin drug treatment in the H69CIS200 cells (Figure 5.7) compared to the parental H69 cells (Figure 5.5). Suggesting that this gene may be involved in resistance to both cisplatin and oxaliplatin in the H69CIS200 cells. However, an increase in the mismatch repair protein MSH2 may increase the cytotoxicity of platinum adducts which would not promote platinum resistance. MSH2 will be further examined in Chapter 8.

5.6.4 H69OX400 response to cisplatin and oxaliplatin

In contrast to the H69CIS200 cells the H69OX400 cells respond to cisplatin and oxaliplatin in a very similar manner, with increased gene expression of most of the genes analysed (Figure 5.8). This is similar to the pattern of gene expression of the H69 parental cells and H69CIS200 cells treated with oxaliplatin (Figure 5.5).

Significant increases in common between cisplatin and oxaliplatin treatment in the H69OX400 cells include GSTT1, GSTP1, γGCS-Cat, MSH2, β-actin, α-tubulin, MAP4, p107 and RARα. The only significant decrease in common was ERCC1. The H69OX400 cells have learned to respond to cisplatin treatment like oxaliplatin treatment. In contrast, the H69 and H69CIS200 cells respond to these drugs in a differential manner. However, the similar expression of these genes in the H69OX400 cells may not be part of the platinum resistance mechanism as the expression of GSTT1, GSTP1, MSH2, β-actin, α-tubulin, MAP4 and RARα were all increased in the H69 parental cells treated with oxaliplatin. Cell cycle gene p107 was not increased and DNA repair gene ERCC1 was not decreased in the H69 cells response to oxaliplatin and therefore may be associated with the shift to a platinum-resistant phenotype. The expression of both of these genes and their role in resistance are discussed in Chapter 8.

5.6.5 Consistency between Atlas nylon array and real-time PCR data

For the top 40 candidate genes there were 104 up or down calls from the nylon array data which were used to rank them into order of most differentially expressed. Some of these genes were examined in the real-time PCR analysis. 66.67% of the real-time PCR analysis agreed with the nylon array analysis; an up call from the array was a statistically significant increase in the real-time data and a down call was a significant decrease. While the real-time data did not correspond exactly with the array, it did correspond in the majority of significant differences found. The array has also proven itself as a general screening method firstly to determine the subset of highly expressed genes, in this case those with spots with an intensity of over 1500 units. The ranking of differentially expressed genes has also proven successful as all 21 genes chosen from this method had significant differences in expression as determined by real-time PCR.

The differences that the nylon array and real-time PCR disagreed upon tended to cluster based on which two data sets were being compared. Some would all correspond to the real-time and others would all be in the opposite direction. This suggests differences between different batches of array experiments. There were 18 nylon arrays used for the 18 mRNA samples in this study and the experiments were conducted in 4 different batches as all could not be completed in the same day. However, the real-time experiment was conducted in the one day in the same PCR run for all 18 samples. This combined with the more quantitative nature of the real-time PCR experiment probably accounts for the discrepancies between data sets.

5.7 Conclusion

The Atlas toxicology array has successfully screened many stress response genes and identified key pathways involved in the response to platinum in this cell model. When analysed with real-time PCR these genes had many significant changes. Patterns detected in the real-time PCR data give us insight into the similarity of gene expression in response to cisplatin and oxaliplatin which may relate to the cross resistance between the two drugs. The parental cell line and the H69CIS200 cells respond in a differential manner to the two drugs whereas the H69OX400 cells

respond in a largely similar manner. This screening has allowed the identification of glutathione associated genes, DNA repair genes and cytoskeleton associated genes as pathways of interest in this cell model. These pathways and their role in the mechanism of platinum resistance will be the subject of the remaining chapters of this thesis.

CHAPTER 6.0

THE INVERSE RELATIONSHIP BETWEEN PLATINUM AND TAXANE RESISTANCE

6.1 Introduction

In developing resistance to the platinum drugs cisplatin and oxaliplatin, the H69CIS200 and H69OX400 cells have become more sensitive to taxane drugs taxol and taxotere (Figure 3.9). There have been many studies in drug-resistant cell models showing an inverse relationship between cisplatin and taxol resistance which are summarised in Figure 6.1. This phenomena occurs in many types of cancer cell lines including ovarian, breast, lung, cervical, prostate, leukemia and osteosarcoma. This pattern also occurs with acquired resistance to other platinum drugs such as carboplatin and oxaliplatin and other taxane drugs such as taxotere. This pattern also occurs in response to selection with many different kinds of drugs not just selection with platinums and taxanes, but other chemotherapeutics including, doxorubicin, etoposide and 5-FU.

Cell lines selected for acquired resistance to a drug can be divided into three groups based on their resistance to cisplatin and taxol; the hypersensitive cell lines (green), non-cross-resistant cell lines (orange) and cross-resistant cell lines (red) as shown in Figure 6.1. The literature used in preparation of Figure 6.1 is presented in Tables 6.1 for the hypersensitive cell lines, 6.2 for the non-cross-resistant cell lines and 6.3 for the cross-resistant cell lines. The major mechanisms of resistance for either platinum or taxanes for each cell line are also listed if known. The hypersensitive cell lines have resistance to the selecting drug, either cisplatin or taxol, but have become more sensitive to the other drug with a fold resistance to the other drug of less than 1 (Table 6.1A and B). The level of resistance that constitutes cross resistance is a matter of debate in the literature. For the purposes of this study cross resistance is defined as resistance above the level of clinical resistance, that is 2-fold. The non-cross-resistant group therefore has resistance to one drug and their fold resistance to the second drug is between 1 and 2-fold (Table 6.2A and B). The cross-resistant group has greater than 2-fold resistance to both drugs (Table 6.3).

It is clear from this survey of cell lines with acquired resistance that cross resistance to both cisplatin and taxol are in the minority of cases 13% compared to the 87% of cell lines that are resistant to one drug and not to the other. Out of these 87% of cell lines which are not cross-resistant to cisplatin and taxol, cell lines which have become

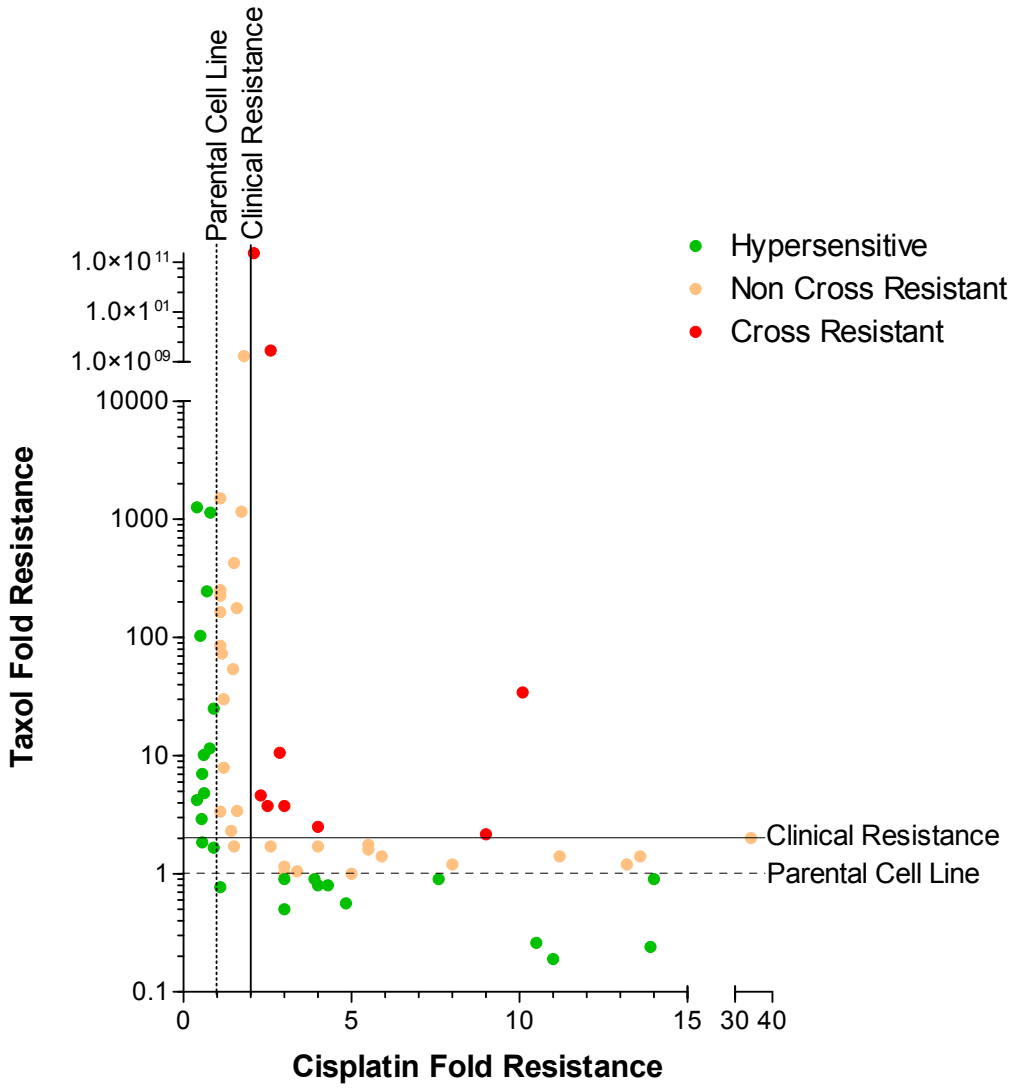

Figure 6.1 A summary of reported relationships between cisplatin and taxol resistance in cell lines. Cell lines selected for acquired resistance to a drug can be divided into three groups based on their resistance to cisplatin and taxol; the hypersensitives (●), non-cross-resistants (●) and cross-resistants (●). Literature used in the preparation of this figure is summarised in Tables 6.1, 6.2 and 6.3.

Table 6.1A Hypersensitive cell lines with resistance to either cisplatin or taxol and hypersensitivity to the other drug – Developed with either cisplatin or taxol.

Cell Line	Cancer	Selecting Agent	Fold Cisplatin Resistance	Fold Taxol Resistance	Reference	Resistance Mechanism
7404-CP1	Hepatoma	Cisplatin	3.9	0.9	(Johnson et al., 1996)	↓Acc(Cis) , ↓Adducts
7404-CP2.5	Hepatoma	Cisplatin	7.6	0.9	(Johnson et al., 1996)	↓Acc(Cis), ↓Adducts
CEM/CP800	Leukemia	Cisplatin	4	0.8	(McCann, 2003)	↑GSH
CEM/CP5000	Leukemia	Cisplatin	3	0.5	(McCann, 2003)	↑GSH
2008/C13*5.25	Ovarian	Cisplatin	11	0.19	(Christen et al., 1993)	↓Acc(Cis), ↓β-tubulin, ↑microtubule bundles (Tax)
2008/C13*	Ovarian	Cisplatin	12	0.06	(Parekh et al., 1996)	↑GSH
IGROV-1/Pt 0.5	Ovarian	Cisplatin	10.5	0.26	(Perego et al., 1998)	↑Mutant p53, ↑ GSH, ↓GST
IGROV-1/Pt 1	Ovarian	Cisplatin	13.9	0.24	(Perego et al., 1998)	↑Mutant p53, ↑ GSH, ↓GST
41McisR	Ovarian	Cisplatin	4.3	0.8	(Kelland et al., 1992b)	↓Acc(Cis)
KFr13	Ovarian	Cisplatin	4.84	0.56	(Yamamoto et al., 2000a)	↓Acc(Cis)
H69-CP	SCLC	Cisplatin	3	0.9	(Locke, 2001)	↑GSH, ↑GSTP1
TE-85TXL	Osteosarcoma	Taxol	0.4	1260	(Burns et al., 2001)	↑P-gp ↓Acc(Dox)
2008/17/0.5	Ovarian	Taxol	0.9	25	(Parekh et al., 1997)	↑P-gp
2008/13/2	Ovarian	Taxol	0.7	245	(Parekh et al., 1997)	↑P-gp
KFr28TX	Ovarian	Taxol	0.78	11.5	(Yamamoto et al., 2000a)	↑P-gp
KFr13TX	Ovarian	Taxol	0.62	4.8	(Yamamoto et al., 2000a)	↑P-gp

Acc – accumulation of drug, Cis – cisplatin, Dox – doxurubicin, GSH – glutathione, GST- glutathione-S-transferase, P-gp – P-glycoprotein, Tax – Taxol

Table 6.1B Hypersensitive cell lines with resistance to either cisplatin or taxol and hypersensitivity to the other drug – Developed with other compounds.

Cell Line	Cancer	Selecting Agent (Fold Resistance)	Fold Cisplatin Resistance	Fold Taxol Resistance	Reference	Resistance Mechanism
TE-85TXR	Osteosarcoma	Taxotere (878)	0.8	1139	(Burns et al., 2001)	↑P-gp
H69/DAU	SCLC	Daunorubicin (nd)	0.56	7	(Jensen et al., 1997)	↑P-gp ↓TopoIIα
H69AR	SCLC	Doxurubicin (21)	0.559	1.84	(Cole et al., 1990; Cole et al., 1992; Heuser et al., 2005)	↑MRP1, no P-gp, ↓GSH
H69/VP	SCLC	Etoposide (2)	0.54	2.9	(Jensen et al., 1997)	↑P-gp, ↑MRP1
NYH/VM	SCLC	VM-26 (14.6)	0.9	1.66	(Jensen et al., 1997)	↓TopoIIα
H69/BCNU	SCLC	BCNU (nd)	1.10	0.77	(Jensen et al., 1997)	↑O^6-methylguanine-DNA methyltransferase
MCF7/Mitox	Breast	Mitoxantrone (8)	0.5	103	(Ark-Otte et al., 1998)	No P-gp ↑MRP and LRP
H69/R38	SCLC	Radiation (2)	14	0.9	(Henness et al., 2002)	↓Acc(Cis), ↑MRP1, MRP2 and TopoII ↓Bcl-2, GSTP1 no change GSH
ME180/TNF	Cervical	TNF (nd)	0.4	4.2	(Ling et al., 2001)	↑EGFR, No P-gp
H69/VDS	SCLC	Vindesine (11.6)	0.61	10.1	(Ohta et al., 1993)	No P-gp, No ↓Acc(Vin & Dox), ↓Total α-tubulin

Acc – accumulation of drug, BCNU - 1,3-Bis(2-chloroethyl)-1-nitrosourea, Cis – cisplatin, Dox – doxurubicin, EGFR - epidermal growth factor receptor, GSH – glutathione, GST- glutathione-S-transferase, LRP – Lung resistance protein, nd – not determined, P-gp – P-glycoprotein, MRP1 – multidrug resistance associated protein 1, MRP2 – multidrug resistance associated protein 2, TNF – tumour necrosis factor , TopoII – Topoisomerase II, Vin – Vindesine.

Table 6.2A Non-cross-resistant cell lines showing an inverse relationship between cisplatin and taxol resistance – Developed with cisplatin or taxol.

Cell Line	Cancer	Selecting Agent	Fold Cisplatin Resistance	Fold Taxol Resistance	Reference	Resistance Mechanism
ME180/Pt	Cervical	Cisplatin	5.5	1.6	(Ling et al., 2001)	↓EGFR, No P-gp
A431/CDDP2	Epidermoid	Cisplatin	3	1.15	(Sawada et al., 2003)	Not Determined
7404-CP7.5	Hepatoma	Cisplatin	13.6	1.4	(Johnson et al., 1996)	↓Acc(Cis), ↓Adducts
7404-CP20	Hepatoma	Cisplatin	34.3	2.0	(Johnson et al., 1996)	↓Acc(Cis), ↓Adducts
CH1cisR	Ovarian	Cisplatin	5.9	1.4	(Kelland et al., 1992b)	↑DNA Repair, ↑Adduct tolerance
2780/C70	Ovarian	Cisplatin	8	1.2	(Parekh et al., 1996)	↑GSH
SKOV3-cis	Ovarian	Cisplatin	4.0	1.7	(Li et al., 2004)	↓Acc(Cis), ↓P-gp
LNCaP/C3	Prostate	Cisplatin	22	1.4	(Nomura et al., 2005)	No P-gp, ↑survivin, ↑Bcl-2
H82-CP	SCLC	Cisplatin	3.38	1.05	(Locke, 2001)	↑GSH, ↑GSTP1, ↑Bcl-2
SBC-3/CDDP	SCLC	Cisplatin	13.2	1.20	(Ikubo et al., 1999)	No P-gp, ↑GSH, ↑GSTP1
NYH/CIS	SCLC	Cisplatin	5.5	1.75	(Jensen et al., 1997)	↑GSH
NTUB/T	Bladder	Taxol	1.10	3.36	(Pu et al., 2001)	Not Determined
RPM1-2650/TX	Nasal Septum	Taxol	1.1	226	(Liang et al., 2001)	↑↑P-gp, ↓MRP1, ↓Tubulin
2008/17/1	Ovarian	Taxol	1.2	30	(Parekh et al., 1997)	↑P-gp
2008/17/2	Ovarian	Taxol	1.5	425	(Parekh et al., 1997)	↑P-gp
2008/17/4	Ovarian	Taxol	1.1	1500	(Parekh et al., 1997)	↑P-gp
2008/13/0.05	Ovarian	Taxol	1.2	7.9	(Parekh et al., 1997)	↑P-gp
2008/13/0.5	Ovarian	Taxol	1.1	85	(Parekh et al., 1997)	↑P-gp
2008/13/1	Ovarian	Taxol	1.1	164	(Parekh et al., 1997)	↑P-gp
2008/13/4	Ovarian	Taxol	1.1	252	(Parekh et al., 1997)	↓P-gp

Acc – accumulation of drug, Cis – cisplatin, EGFR - epidermal growth factor receptor, GSH – glutathione, GST- glutathione-S-transferase, P-gp – P-glycoprotein, MRP1 – multidrug resistance associated protein 1.

Table 6.2B Non-cross-resistant cell lines showing an inverse relationship between cisplatin and taxol resistance – Developed with other compounds.

Cell Line	Cancer	Selecting Agent (Fold Resistance)	Fold Cisplatin Resistance	Fold Taxol Resistance	Reference	Resistance Mechanism
SNU638-F1	Gastric	5-flourouricil (881)	1.48	53.9	(Chung et al., 2000)	No Change P-gp, ↑Hsp27
OVCAR-3carboR	Ovarian	Carboplatin (8)	11.2	1.4	(Kelland et al., 1992b)	Not Determined
SKOV3-car	Ovarian	Carboplatin(3.4)	1.5	1.7	(Li et al., 2004)	↓Acc(Car), ↓P-gp
KBC5-8	Adenocarcinoma	Colchicine (nd)	1.14	73.04	(Heuser et al., 2005)	↑P-gp
SW1573/2R120	NSCLC	Doxorubicin (864)	1.8	$1.3x10^9$	(Ark-Otte et al., 1998)	No P-gp, ↑MRP1 and LRP
SBC-3/ADM	SCLC	Doxurubicin (74.3)	1.73	1160	(Ikubo et al., 1999)	↑↑P-gp, ↑GSH, ↑GSTP1
H69-EPR	SCLC	Epirubicin (6)	3	1.0	(Locke, 2001)	↑MRP1
H69-VP1	SCLC	Etoposide (12)	5	1.0	(Locke, 2001)	Not Determined
SBC-3/ETP	SCLC	Etoposide (49)	1.59	177	(Ikubo et al., 1999)	↑P-gp, No change GSH, ↑GSTP1
HCT116/8FP	Colon Cancer	Flavopiridol (8)	1.42	2.3	(Smith et al., 2001)	No P-gp or MRP1, ↓Acc(Flav),
RPMI-2650/M1	Nasal Septum	Melphalan (11)	2.6	1.7	(Liang et al., 2001)	↑P-gp, MRP1, MRP2, ↓Tubulin
SF188/TR	Glioma	Temozolomide (6)	1.6	3.4	(Ma et al., 2002)	↓GSH

Acc – accumulation of drug, Car – carboplatin, Flav – Flavopiridol, GSH – glutathione, GST- glutathione-S-transferase, LRP – Lung resistance protein, nd – not determined, P-gp – P-glycoprotein, MRP1 – multidrug resistance associated protein 1, MRP2 – multidrug resistance associated protein 2.

Table 6.3 Cross-resistant cell lines resistant to both cisplatin and taxol.

Cell Line	Cancer	Selecting Agent (Fold Resistance)	Fold Cisplatin Resistance	Fold Taxol Resistance	Reference	Resistance Mechanism
NTUB1/P	Bladder	Cisplatin	10.1	34.3	(Pu et al., 2001) (Pu et al., 1996)	No change GSH, ↑P-gp
A2780-cis	Ovarian	Cisplatin	3.0	3.75	(Li et al., 2004)	↓Acc(Cis), ↑P-gp
WR	Rat Lymphoma	Cisplatin	9	2.15	(Parekh et al., 1996)	↑P-gp ↑GSH
A2780-pac	Ovarian	Taxol	2.5	3.75	(Li et al., 2004)	↓Acc(Tax), ↑P-gp
SNU638-F2	Gastric	5-flourouricil (2117)	2.87	10.54	(Chung et al., 2000)	↓P-gp, ↑Hsp27
A2780-car	Ovarian	Carboplatin(4.0)	4.0	2.5	(Li et al., 2004)	↓Acc(Car), ↑P-gp
MCF7/DOX40	Breast	Doxorubicin (200)	2.6	$1.7x10^{9}$	(Ark-Otte et al., 1998)	↑↑P-gp, ↑MRP1 and LRP, ↓Acc(Tax)
SW1573/2R160	NSCLC	Doxorubicin (1300)	2.1	$1.5x10^{11}$	(Ark-Otte et al., 1998)	↑↑P-gp, ↑MRP1 and LRP, ↓Acc(Tax)
AG6000	Ovarian	Gemcitabine (30,000)	2.3	4.6	(Bergman et al., 2000)	↓dCK, No change GSH, ↓DNA damage(Cis&Tax), No P-gp or MRP1

Acc – accumulation of drug, Car – carboplatin, Cis - cisplatin, dCK - deoxycytidine kinase, GSH – glutathione, LRP – lung resistance-related protein, P-gp – P-glycoprotein, MRP1 – multidrug resistance associated protein 1, Tax – taxol.

hypersensitive make up 45% and non-cross-resistant cell lines make up the remaining 55%. This suggests that when cells become resistant to cisplatin, something is altered that renders the cells sensitive to taxol and vice versa. This pattern has also been demonstrated in animal models (Yamamoto et al., 2000a; Yamamoto et al., 2000b). This pattern is more difficult to study in clinical trials as platinums and taxanes are often given in combination with other chemotherapeutics (Rosell et al., 2001). Despite the large number of studies showing this pattern of resistance and hypersensitivity between cisplatin and taxol, relatively little is understood about the molecular mechanism of this phenomena. If more could be learnt about this pattern, particularly what governs the shift from non-cross resistance to hypersensitivity then markers could be identified to predict a patient's response to a drug and hopefully improve clinical cancer therapy.

As this inverse relationship occurs in so many resistant cell models the individual mechanisms of resistance are many and varied. The major mechanisms of cisplatin resistance in cells with a lack of cross resistance to taxol include, increased glutathione (McCann, 2003), decreased accumulation of the drug (Johnson et al., 1996) and increased DNA repair (Kelland et al., 1992b). This suggests that cisplatin-resistant cell lines are sensitive to taxol irrespective of their major mechanism of platinum resistance. The ABC transporter P-glycoprotein transports taxol out of a cell but does not transport cisplatin. Many of the taxol-resistant cell lines, with a sensitivity to cisplatin, have increased P-glycoprotein expression leading to increased efflux of taxol (Parekh et al., 1997), but others do not (Ohta et al., 1993). This suggests that the sensitivity to cisplatin is independent of P-glycoprotein mediated resistance. The inverse relationship between cisplatin and taxol resistance occurs in a diverse range of carcinomas, with many different mechanisms of resistance to cisplatin and taxol. This suggests that there is a fundamental molecular process underpinning this relationship that is yet to be elucidated. An understanding of this response could lead to improved treatment strategies for both cisplatin- and taxol-resistant cancer.

Pre-treatment with a low dose of taxol can also sensitise platinum-resistant cells to platinum treatment (Su et al., 1998; Locke et al., 2001; Locke et al., 2003). Maximal sensitisation was achieved with a low 10 ng/ml dose of taxol, whereas a taxol induces

a G_2/M block at doses greater than 12.5 ng/ml. The sensitisation due to taxol was therefore independent of the cell cycle mediated effect of the drug (Locke et al., 2001). This suggests that other signalling pathways, independent of the cell cycle effects of taxol, may be involved in the sensitisation to cisplatin treatment.

The H69CIS200 and H69OX400 cell lines are two-fold resistant to both cisplatin and oxaliplatin but are hypersensitive to taxol and taxotere. This chapter examines possible mechanisms for this hypersensitivity with the aim of understanding the wider phenomena of the inverse relationship between these two drugs.

6.2 Analysis of α-tubulin

α-tubulin was identified as being differentially expressed in the Atlas nylon array analysis (Chapter 5). The chemotherapeutic drug taxol binds to and stabilises tubulin in its polymerised state leading to mitotic arrest. Alterations in the expression levels, polymerisation or cellular distribution of tubulin could explain the hypersensitivity of the H69CIS200 and H69OX400 cell lines to taxol. Decreases in tubulin proteins have been associated with cisplatin resistance in cell lines which have a sensitivity to taxol (Christen et al., 1993; Liang et al., 2001).

6.2.1 α-tubulin mRNA and protein expression

The expression of α-tubulin mRNA and protein was examined in the H69, H69CIS200 and H69OX400 cell lines in their resting state and in response to 200 ng/ml cisplatin and 400 ng/ml oxaliplatin drug treatment for 4 days. The mRNA expression of α-tubulin was increased in the untreated resistant cell lines and in response to cisplatin and oxaliplatin treatment in all cell lines, the majority of these increases were significant (Figure 6.2). However, when the total amount of α-tubulin protein was examined by Western blot under the same experimental conditions (Figure 6.3), there were no significant changes and a trend of decreased α-tubulin expression in the untreated resistant cell lines and in response to platinum drug treatment.

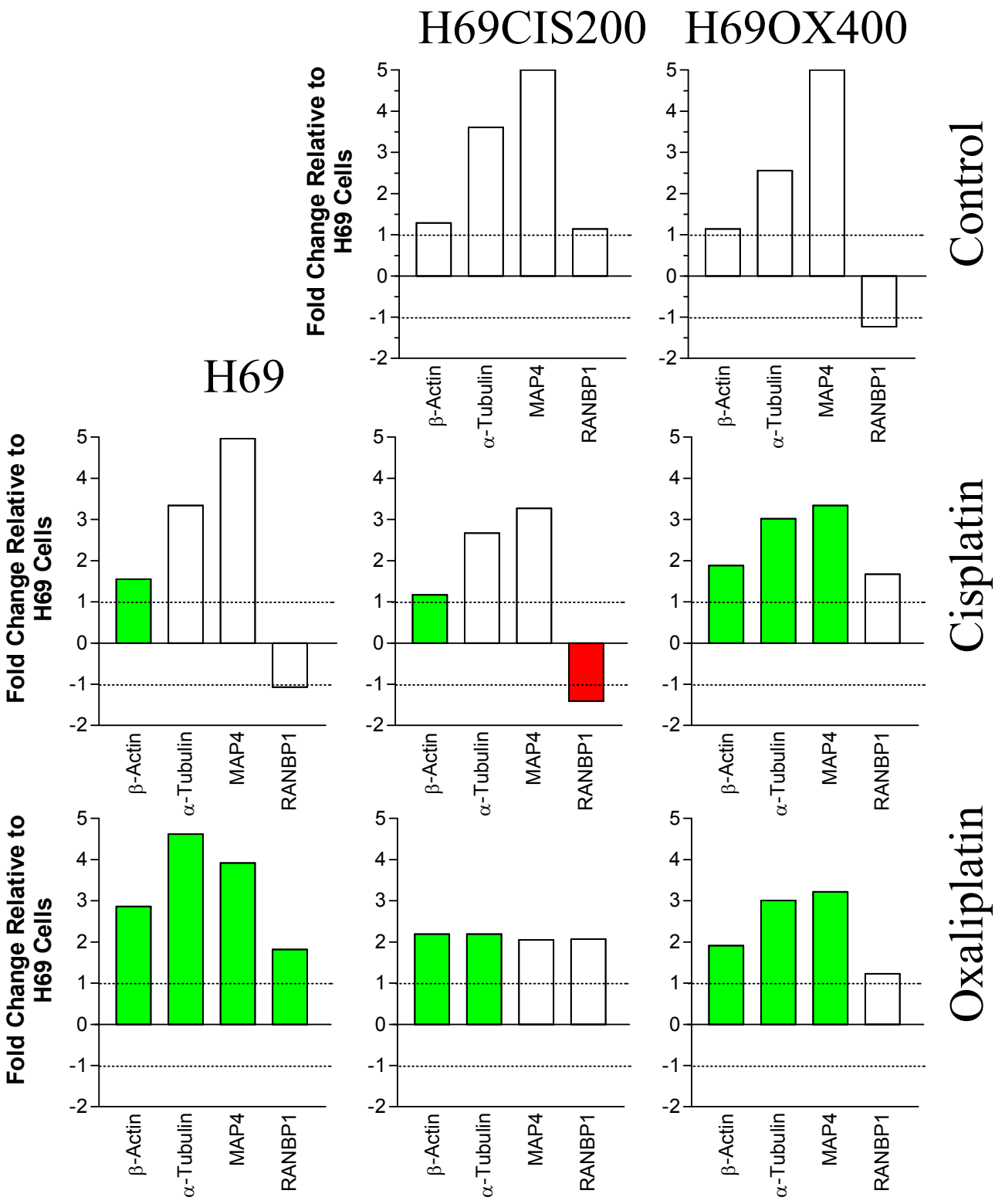

Figure 6.2 mRNA expression data for cytoskeletal genes. H69, H69CIS200 and H69OX400 cells were grown for four days either in drug-free media, 200 ng/ml cisplatin or 400 ng/ml oxaliplatin as indicated. mRNA was extracted, converted to cDNA and assayed by real time PCR as described in section 2.12. Means of duplicate experiments are presented, standard deviations have been omitted for clarity. Significant increases from the H69 control are indicated in green, significant decreases in red. Significant differences were determined using a student's t-test $p < 0.05$. Replotted from Figure 5.4.

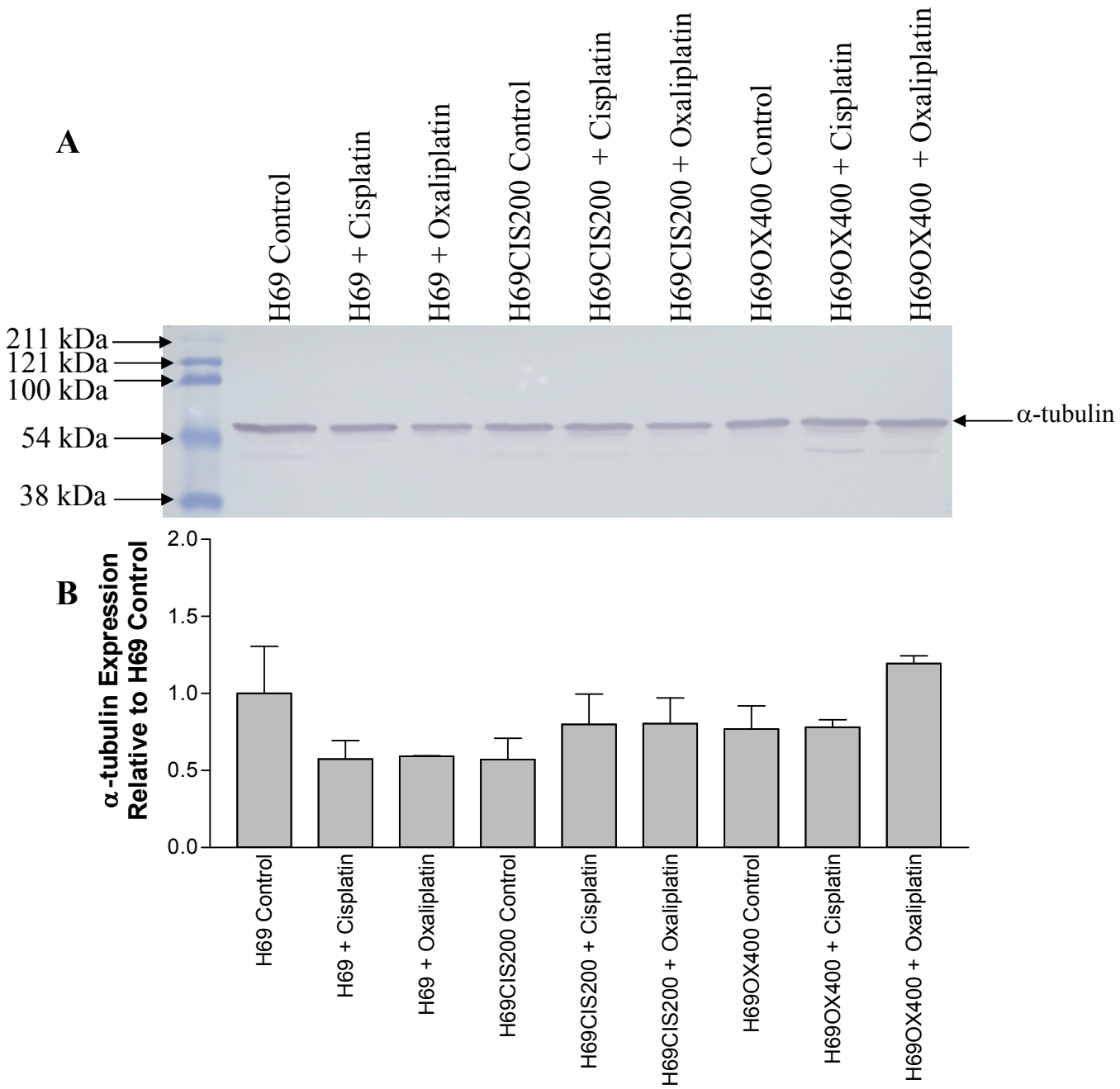

Figure 6.3 α-tubulin total protein expression determined by Western blot. A) H69, H69CIS200 and H69OX400 cells were grown for four days either in drug-free media, 200 ng/ml cisplatin or 400 ng/ml oxaliplatin. Total protein was extracted and 20 μg subjected to SDS-PAGE and Western blotting as described in section 2.13. α-tubulin was detected with a primary antibody and an alkaline phosphatase labelled secondary antibody as described in section 2.13.4.1 B) Quantitation of the α-tubulin bands was determined by Quantity-one software and adjusted for protein loading by ponceau staining. The mean and standard deviation of two independent experiments are presented.

6.2.2 α-tubulin protein soluble to polymerised ratio

The ratio of soluble to polymerised tubulin was examined by Western blot in untreated H69, H69CIS200 and H69OX400 cell lines (Figure 6.4). No change in the soluble to polymerised ratio was detected in the untreated cells. 5 μg□ml of taxol for 4 days (IC_{80}) was required to see a consistent increase in the polymerisation of tubulin (Figure 6.5). All cell lines increased their polymerisation of tubulin, the H69CIS200 cell line showed the largest increase in polymerisation but this change was not significant. This suggests that there are differences between the H69CIS200 and H69OX400 resistant cell lines as they respond differently to high dose taxol treatment.

Figure 6.3 shows a Western blot for total α-tubulin protein. α-tubulin protein tended to decrease in the untreated H69CIS200 and H69OX400 cells compared to untreated H69 cells. Figure 6.4 also shows a α-tubulin Western blot for the same cell lines except that the α-tubulin protein has been divided into soluble and polymerised fractions. The trend of decreased α-tubulin in the resistant cell lines is not obvious from this Western blot of soluble and polymerised fractions. This is probably due to the different experimental conditions used in the preparation of the proteins between the two analyses. The total protein was prepared on ice from sonnicated cells and a protein assay performed, 20 μg of protein was loaded in each lane. The soluble and polymerised tubulin fractions were prepared at room temperature and equal volumes of each fraction was loaded to determine a ratio of α-tubulin protein between fractions. No protein assay was performed to correct for the amount of protein between samples.

6.2.3 α-tubulin immunocytochemistry

The morphology of α-tubulin was examined in the H69, H69CIS200 and H69OX400 cell lines. Cytospun preparations were stained with a FITC conjugated α-tubulin antibody and the nuclei counterstained with DAPI. H69 cells and the resistant sublines are largely nuclear as can be seen from the DAPI staining, the tubulin forms a ring around the nucleus of each cell (Figure 6.6). There appeared to be no difference

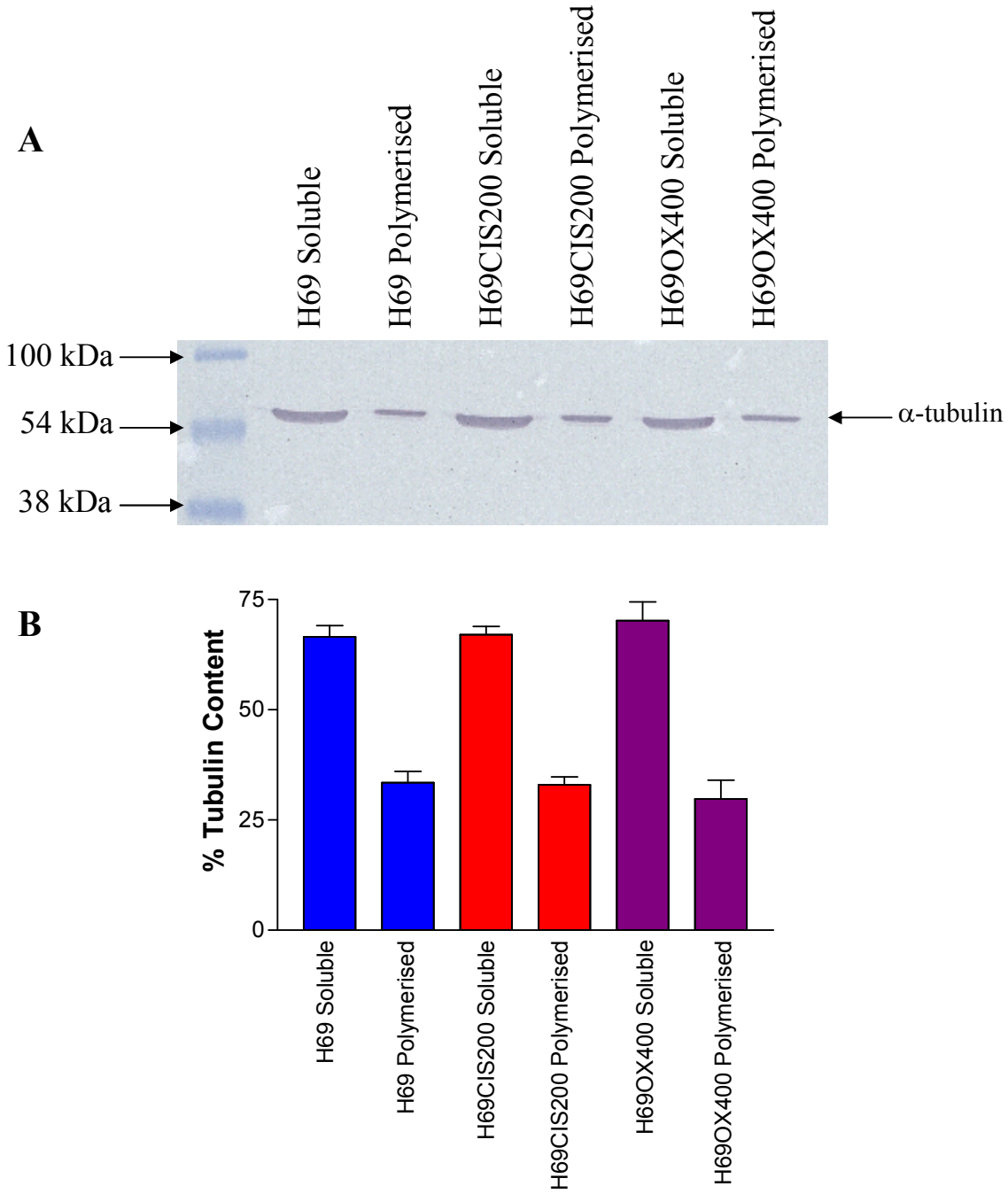

Figure 6.4 α-tubulin soluble and polymerised fractions determined by Western blot. A H69, H69CIS200 and H69OX400 cells were grown for four days in drug-free media. Soluble and polymerised fractions were prepared and equal volumes were subjected to SDS-PAGE and Western blotting as described in section 2.13. α-tubulin was detected with a primary antibody and an alkaline phosphatase labelled secondary antibody as described in section 2.13.4.1. B Quantitation of the α-tubulin bands was determined by Quantity-one software and the mean and standard deviation of two independent experiments are presented.

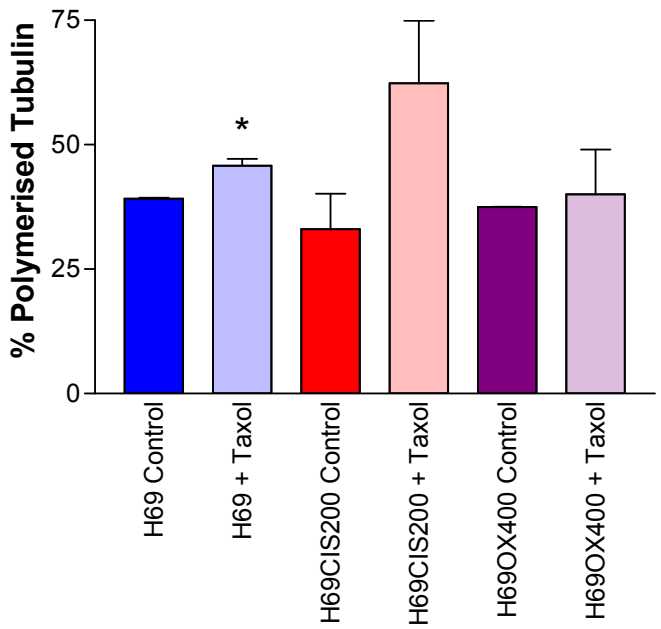

Figure 6.5 α-tubulin polymerised fractions in response to high dose taxol determined by Western blot. H69, H69CIS200 and H69OX400 cells were grown for four days in 5 μg/ml taxol. Soluble and polymerised fractions were prepared and equal volumes were subjected to SDS-PAGE and Western blotting as described in section 2.13. α-tubulin was detected with a primary antibody and an alkaline phosphatase labelled secondary antibody as described in section 2.13.4.1. Quantitation of the α-tubulin bands was determined by Quantity-one software and the mean and standard deviation of two independent experiments are presented. * - Significant increase in polymerisation in response to taxol compared to control, student's t-test $p<0.05$.

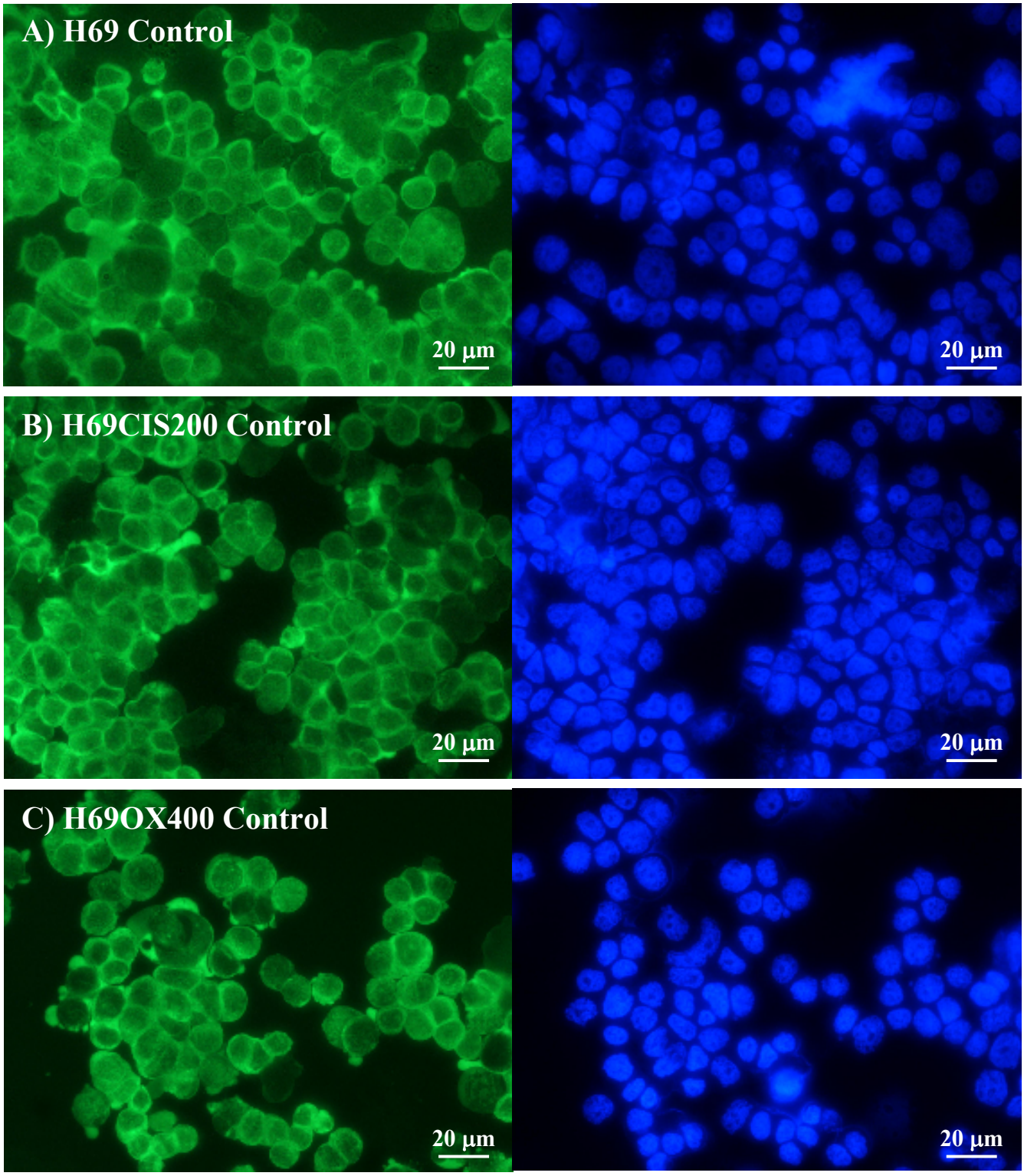

Figure 6.6 α-tubulin immunocytochemistry control cells. A) H69 B) H69CIS200 and C) H69OX400 cells were grown for 4 days in drug-free culture and prepared as cytospins. Slides were stained with an α-tubulin FITC labelled antibody shown on the left and counterstained with DAPI shown on the right as described in section 2.14.

in tubulin morphology, cellular distribution, cell size or shape between the sensitive and resistant cell lines.

α-tubulin morphology was assessed at the same cisplatin and oxaliplatin doses used to examine the mRNA and protein expression, 200 ng/ml and 400 ng/ml respectively. Figures 6.7 and 6.8 show an increase in cell size in all cell lines in response to both drugs. There was no morphological difference in α-tubulin between the cell lines in response to platinum drug treatment.

α-tubulin morphology was examined in response to taxol treatment under two different treatment conditions 10.7 ng/ml for 24 hours and 5 μg/ml for 4 days. This higher dose was the same as used to examine tubulin polymerisation. There was increased formation of microtubule bundles in the nuclei of the resistant cell lines compared to the H69 cells in response to 10.7 ng/ml taxol (Figure 6.9). This change was significant in the H69OX400 cell line (Figure 6.10). The higher dose of taxol increased the size of the cell lines and caused the microtubule fibers to aggregate into clusters opposing the nucleus of the cells (Figure 6.11). The microtubule bundles have also increased in size with the nucleus and collapsed into star shaped patterns. Again the resistant cells sustaining more damage than that of the parental cells to the same dose of taxol. There were also a higher proportion of apoptotic cells in response to taxol in the resistant cell lines as judged by the fragmented DAPI stained nuclei.

6.3 Analysis of β-actin

β-actin was identified as being differentially expressed in the Atlas nylon array analysis (Chapter 5). β-actin is a major cytoskeletal protein like tubulin (Zeng et al., 1997). Changes in cytoskeletal proteins such as β-actin may effect how taxol interacts with its molecular target tubulin and consequently influence the resistance to this drug. Changes in both actin and tubulin proteins have been associated with resistance to vincristine, another tubulin binding drug, in lung cancer cells (Chan et al., 1998).

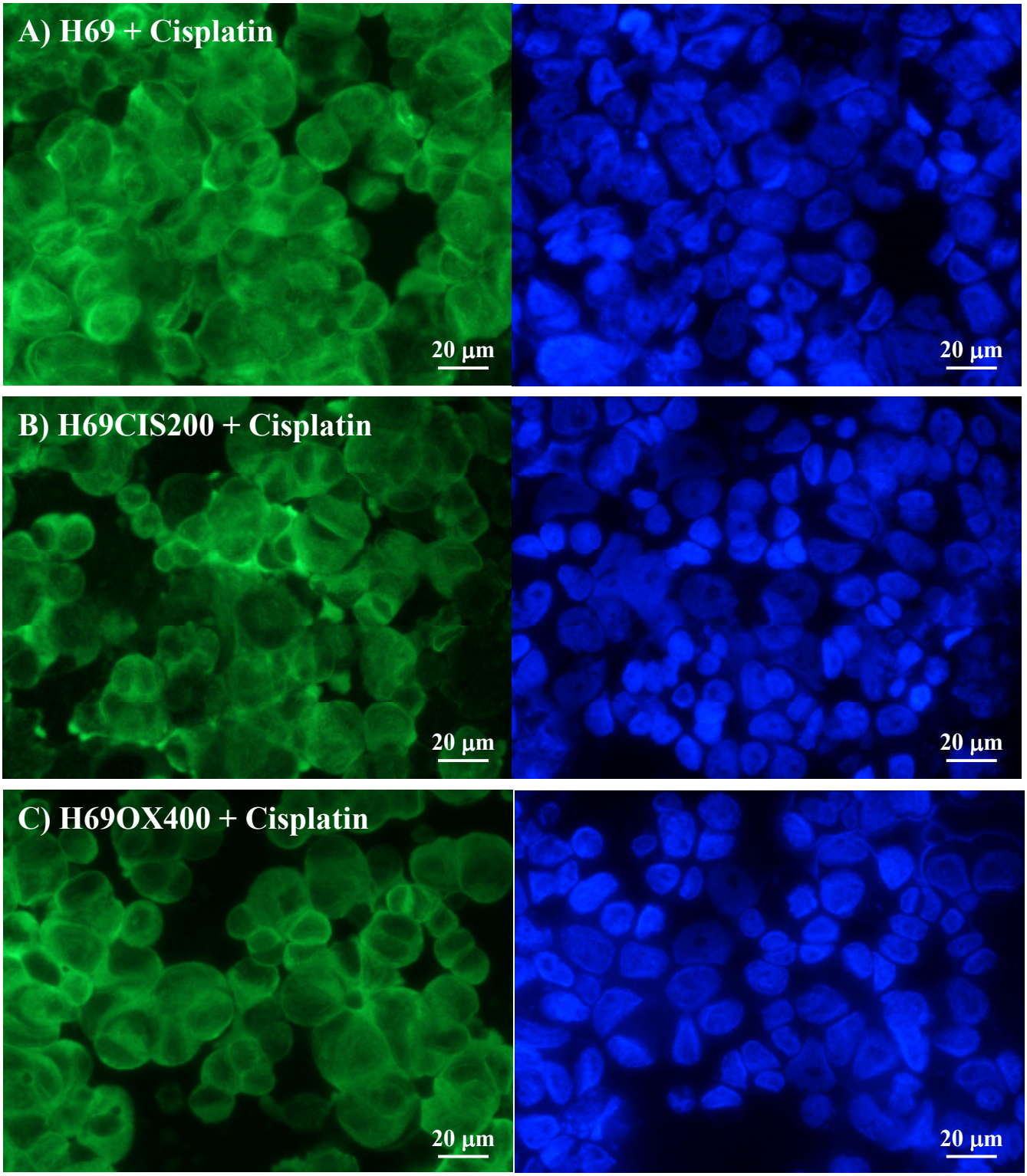

Figure 6.7 α-tubulin immunocytochemistry cisplatin treated cells. A) H69 B) H69CIS200 and C) H69OX400 cells were grown for 4 days in 200 ng/ml cisplatin and prepared as cytospins. Slides were stained with an α-tubulin FITC labelled antibody shown on the left and counterstained with DAPI shown on the right as described in section 2.14.

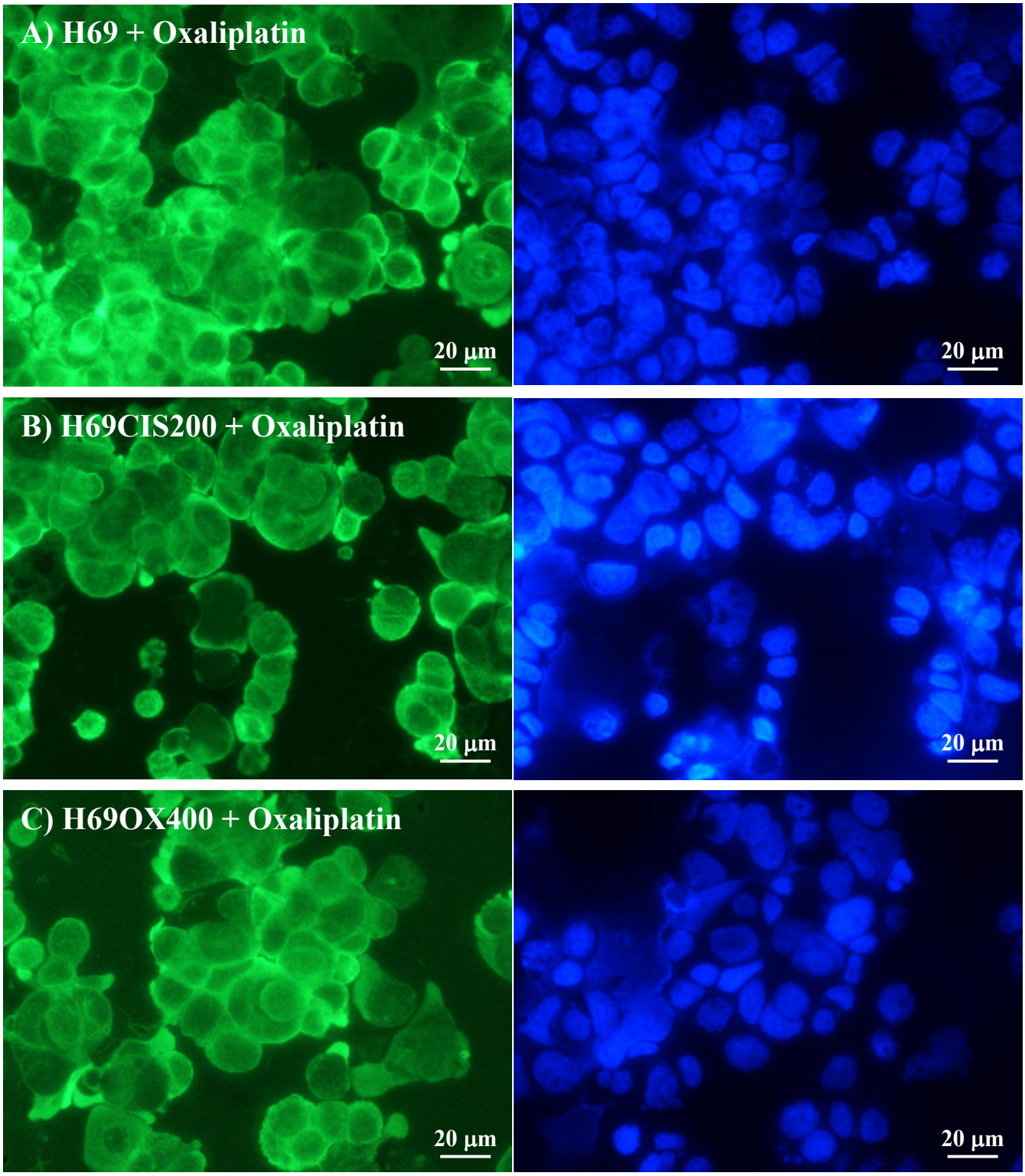

Figure 6.8 α-tubulin immunocytochemistry oxaliplatin treated cells. A) H69 B) H69CIS200 and C) H69OX400 cells were grown for 4 days in 400 ng/ml oxaliplatin and prepared as cytospins. Slides were stained with an α-tubulin FITC labelled antibody shown on the left and counterstained with DAPI shown on the right as described in section 2.14.

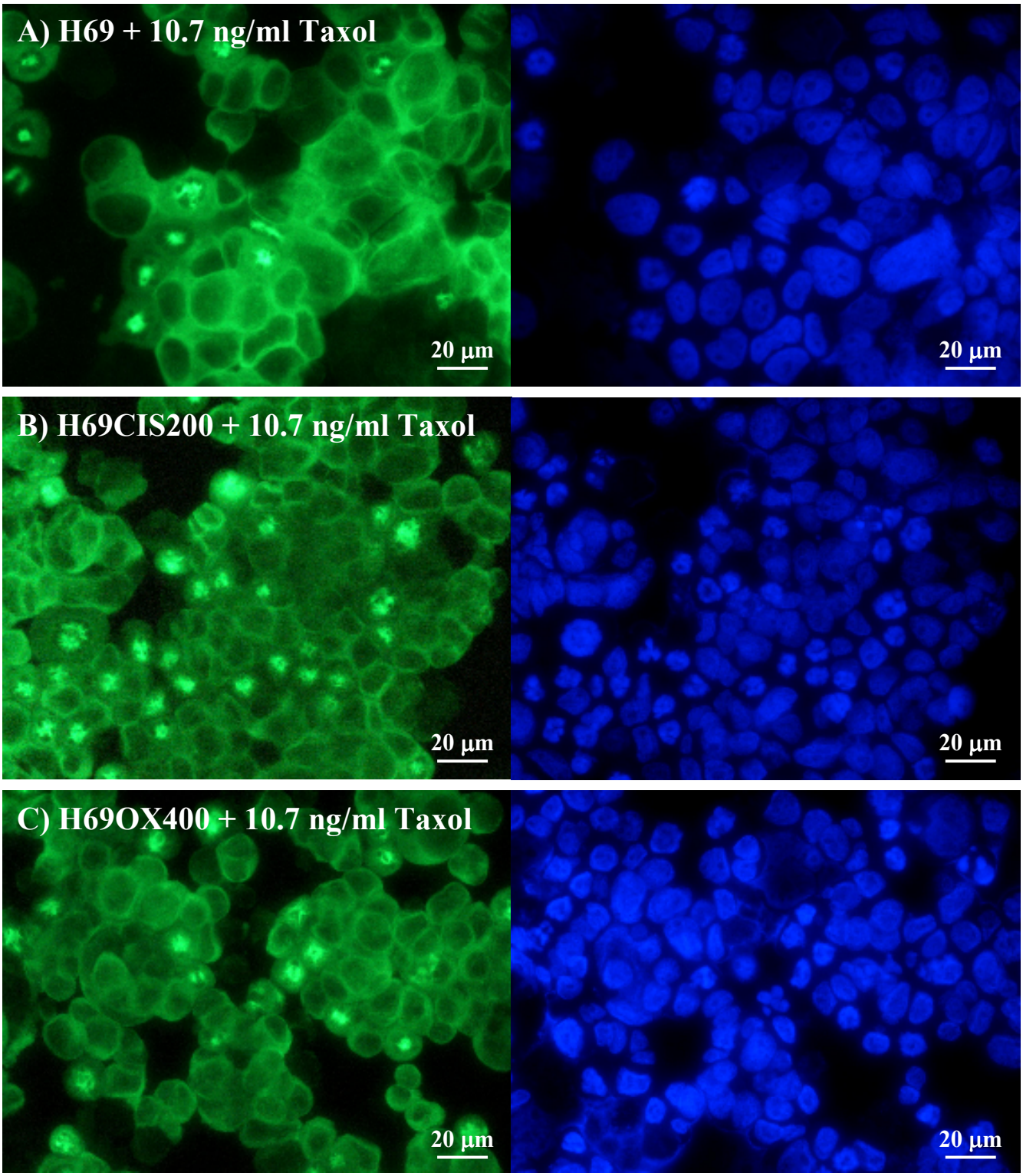

Figure 6.9 α-tubulin immunocytochemistry low dose taxol treated cells. A) H69 B) H69CIS200 and C) H69OX400 cells were grown for 24 hours in 12.5 nM taxol and prepared as cytospins. Slides were stained with an α-tubulin FITC labelled antibody shown on the left and counterstained with DAPI shown on the right as described in section 2.14.

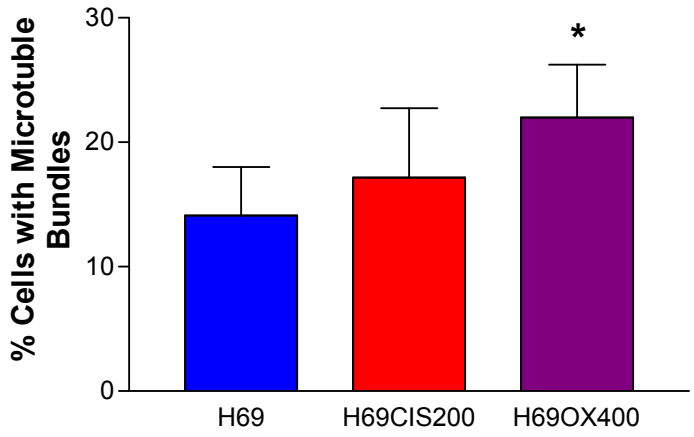

Figure 6.10 Percentage of cells with microtubule bundles in response to 12.5 nM taxol for 24 hours. The number of cells with microtubule bundles and total number of cells was counted for 6 images of each cell line and a percentage calculated. The mean and standard deviation of two independent experiments are presented. * - Significant increase in microtubule bundles from H69 cells, student's t-test $p<0.05$.

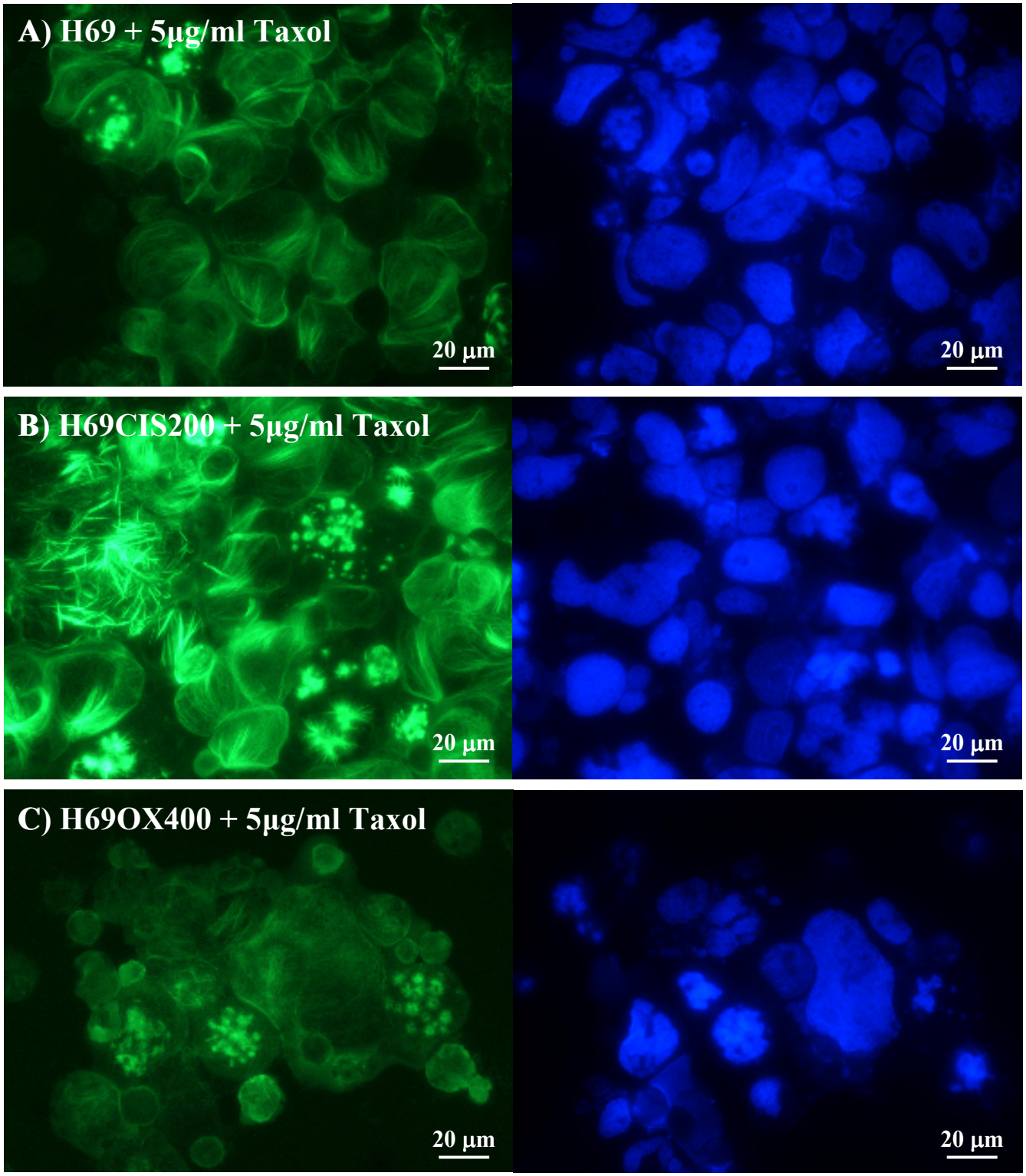

Figure 6.11 α-tubulin immunocytochemistry high dose taxol treated cells. A) H69 B) H69CIS200 and C) H69OX400 cells were grown for 4 days 5 µg/ml taxol and prepared as cytospins. Slides were stained with an α-tubulin FITC labelled antibody shown on the left and counterstained with DAPI shown on the right as described in section 2.14.

6.3.1 β-actin mRNA and protein expression

β-actin mRNA and protein expression was examined in the H69, H69CIS200 and H69OX400 cell lines in their resting state and on 200 ng/ml cisplatin and 400 ng/ml oxaliplatin drug treatment for 4 days. The H69CIS200 and H69OX400 cells in their resting state showed a trend towards a small increase in β-actin mRNA but these changes were not significant. β-actin mRNA was significantly increased in all cell lines in response to cisplatin and oxaliplatin drug treatment (Figure 6.2). The fold increase was higher in response to oxaliplatin treatment H69 (2.86-fold), H69CIS200 (2.19- fold) and H69OX400 (1.91-fold), than cisplatin treatment H69 (1.55-fold), H69CIS200 (1.17-fold) and H69OX400 (1.88-fold). However, there was no significant changes in β-actin protein expression (Figure 6.12). The H69CIS200 control cells showed a trend of increased β-actin protein but this was not a significant increase.

6.3.2 β-actin immunocytochemistry

The cellular distribution of β-actin was examined by immunocytochemistry. β-actin was distributed throughout the cytoplasm and nucleus but was strongly associated with the cell membrane in many cells. There appear to be no difference in β-actin protein distribution between the untreated parental and the resistant cell lines (Figure 6.13). The distribution of β-actin was also examined in cells treated with 200 ng/ml cisplatin or 400 ng/ml oxaliplatin for 4 days, the same conditions used for the Western blot analysis (Figures 6.14 and 6.15). Platinum drug treatment caused an increase in cell size in all cell lines. However, there was no difference in β-actin distribution between the resistant and sensitive cell lines in response to platinum drug treatment.

6.4 MAP4

Microtubule associated protein 4 (MAP4) binds to and stabilises microtubules. MAP4 was chosen for analysis by real-time PCR as increased expression of MAP4 has been associated with resistance to agents that promote the depolymerisation of microtubules such as the *vinca* alkaloids and sensitivity to taxanes (Zhang et al.,

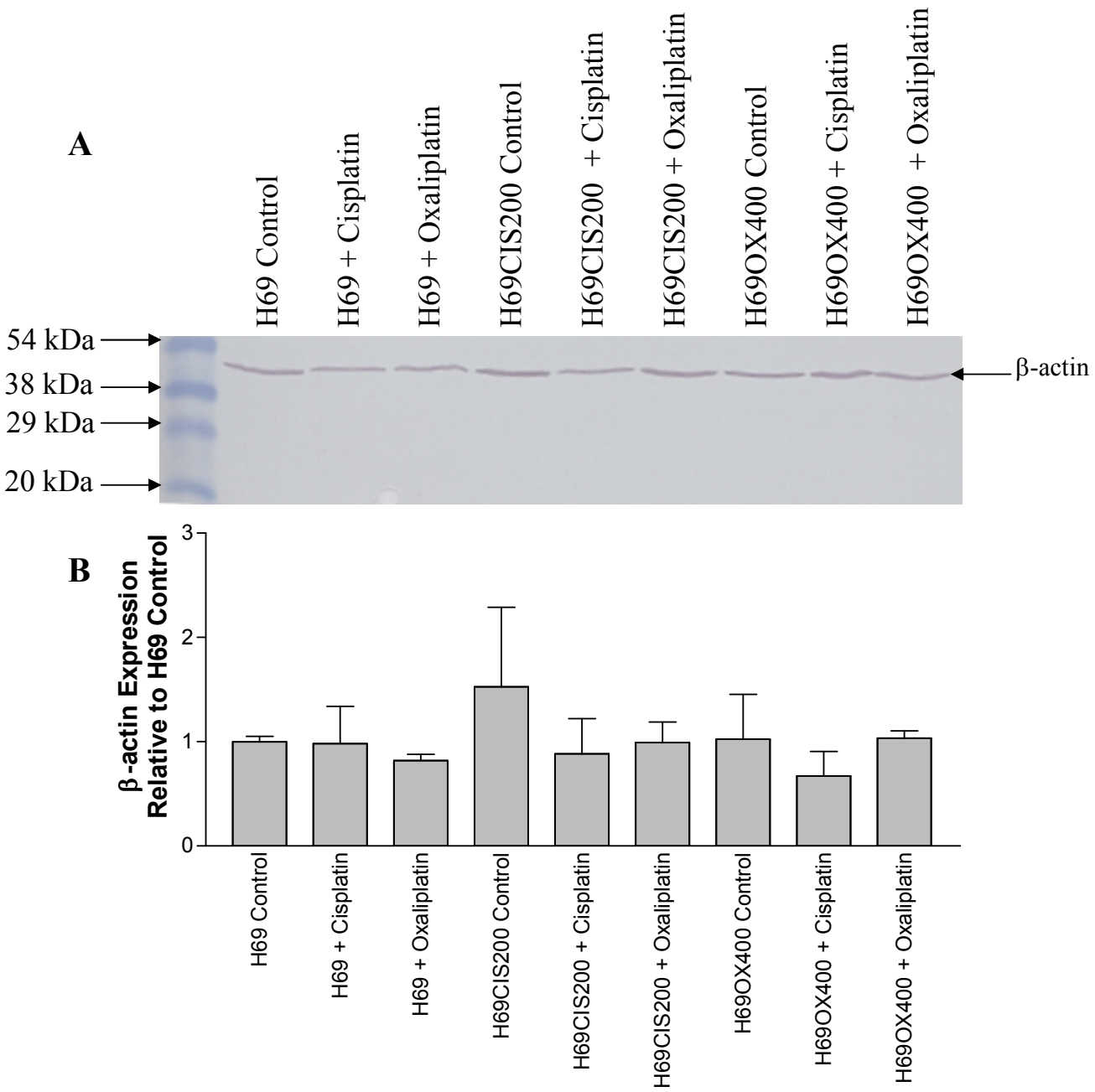

Figure 6.12 β-actin protein expression determined by Western blot. A) H69, H69CIS200 and H69OX400 cells were grown for four days either in drug-free media, 200 ng/ml cisplatin or 400 ng/ml oxaliplatin. Protein was extracted and 20 μg subjected to SDS-PAGE and Western blotting as described in section 2.13. β-actin was detected with a primary antibody and an alkaline phosphatase labelled secondary antibody as described in section 2.13.4.1. B) Quantitation of the β-actin bands was determined by Quantity-one software and adjusted for protein loading by ponceau staining. The mean and standard deviation of two independent experiments are presented.

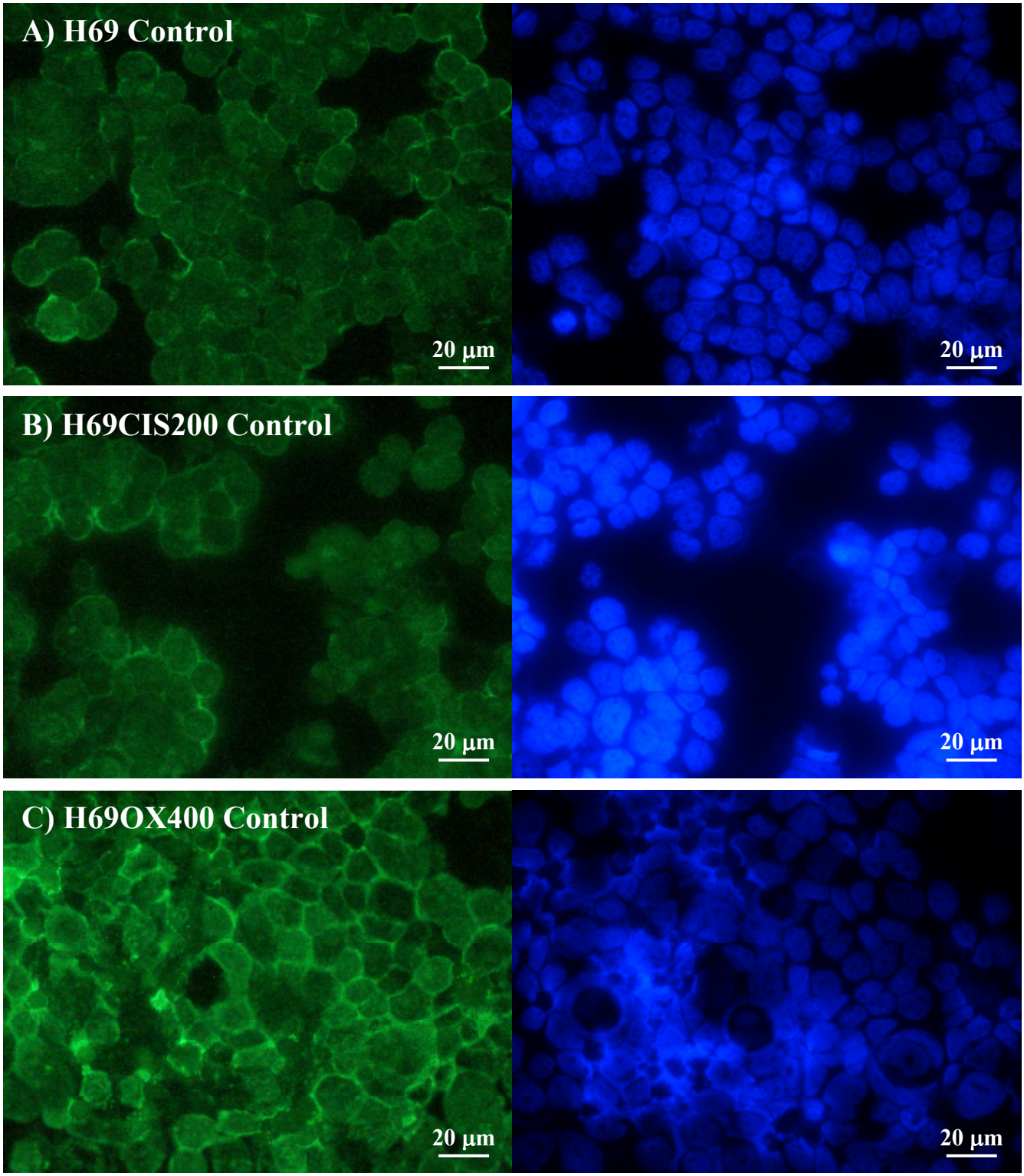

Figure 6.13 β-actin immunocytochemistry control cells. A) H69 B) H69CIS200 and C) H69OX400 cells were grown for 4 days in drug-free culture and prepared as cytospins. Slides were stained with a β-actin primary antibody and detected with a FITC labelled secondary antibody shown on the left and counterstained with DAPI shown on the right as described in section 2.14.

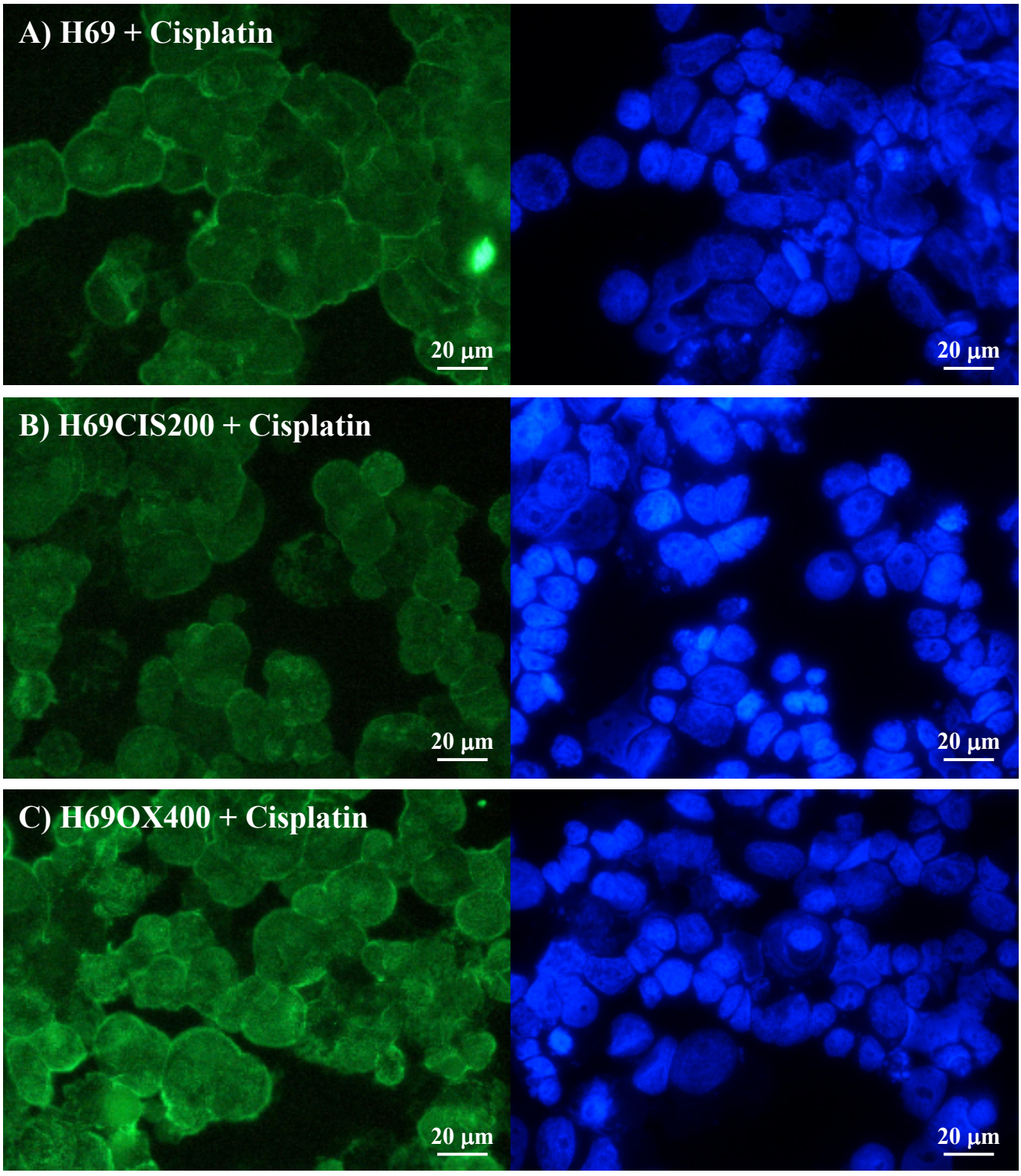

Figure 6.14 β-actin immunocytochemistry cisplatin treated cells. A) H69 B) H69CIS200 and C) H69OX400 cells were grown for 4 days in 200 ng/ml cisplatin and prepared as cytospins. Slides were stained with a β-actin primary antibody and detected with a FITC labelled secondary antibody shown on the left and counterstained with DAPI shown on the right as described in section 2.14.

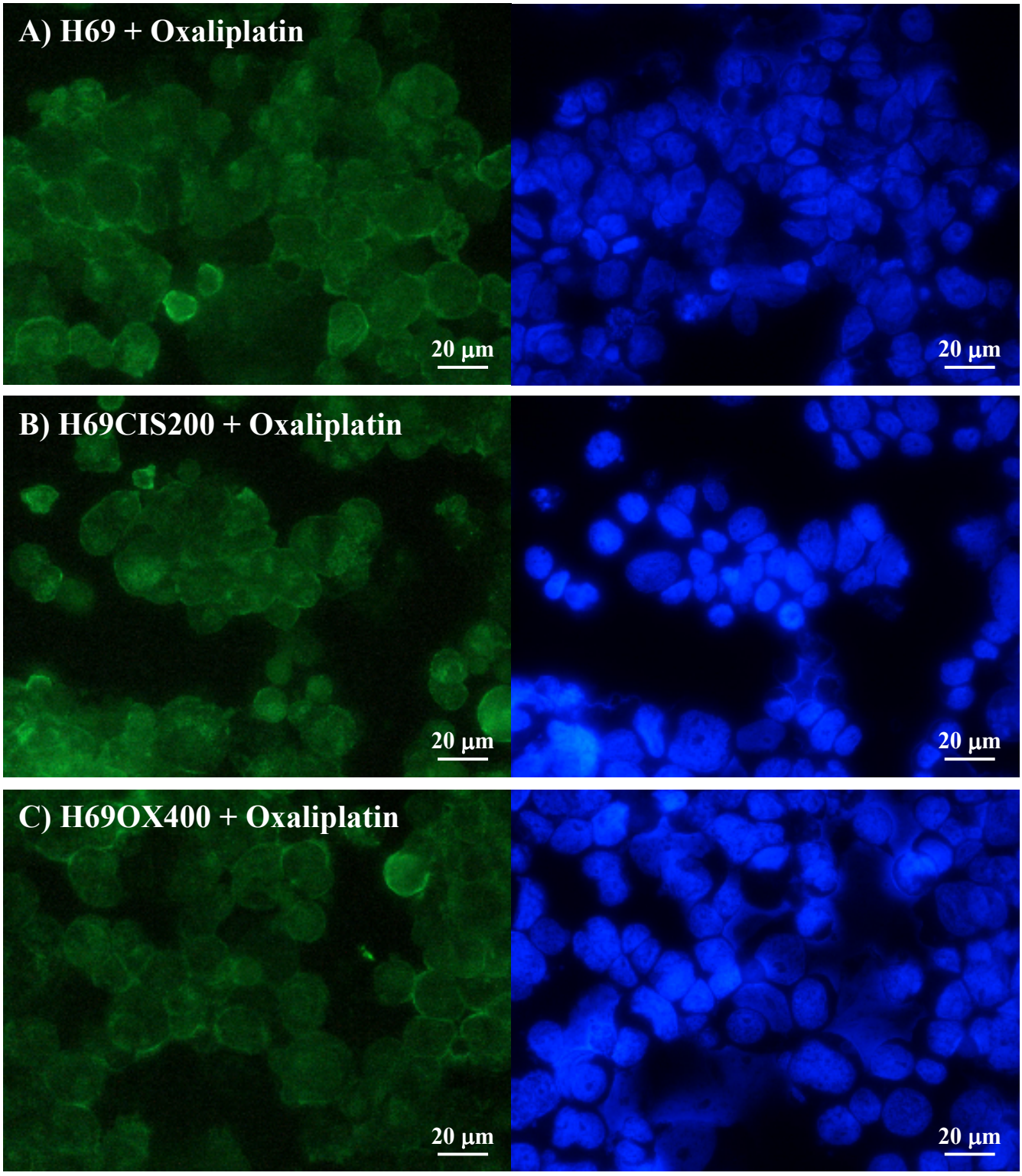

Figure 6.15 β-actin immunocytochemistry oxaliplatin treated cells. A) H69 B) H69CIS200 and C) H69OX400 cells were grown for 4 days in 400 ng/ml oxaliplatin and prepared as Slides were stained with a β-actin primary antibody and detected with a FITC labelled secondary antibody shown on the left and counterstained with DAPI shown on the right as described in section 2.14.

1998). This fits the phenotype of the H69OX400 cells which are sensitive to taxanes but also resistant to *vinca* alkaloids (Figure 3.9).

There was a trend of increased MAP4 mRNA expression in all samples, the untreated resistant cell lines and in response to platinum drug treatment in all cell lines (Figure 6.2). MAP4 mRNA was significantly increased in the H69 cells in response to oxaliplatin (3.92-fold) and in the H69OX400 cells in response to both cisplatin (3.34-fold) and oxaliplatin.

6.5 RANBP1

RANBP1 was identified as being differentially expressed by the Atlas nylon array analysis (Chapter 5). RANBP1 is a binding protein of Ran, a Ras-related GTPase that is involved in many cellular processes, including nuclear transport, mitotic spindle assembly, and post-mitotic nuclear assembly (Dasso, 2002). This system has been shown to be important for the fidelity of mitotic spindle assembly, defects in this system may therefore be associated with the sensitivity to taxanes in this model.

The untreated resistant cell lines showed no significant change in RANBP1 mRNA expression. RANBP1 was significantly decreased in the H69CIS200 cells in response to cisplatin (-1.41-fold). RANBP1 was significantly increased in the H69 parental cells in response to oxaliplatin (1.82-fold). There was a trend for increased RANBP1 mRNA expression in response to oxaliplatin in all cell lines and in the H69OX400 cell line in response to cisplatin (Figure 6.2).

6.6 Identification of genes associated with PI3K/Akt/mTOR signalling

The PI3K/Akt pathway regulates cell cycle progression and cell cycle checkpoints that control the cellular response to DNA damage. Several genes associated with PI3K/Akt signalling were found to be differentially expressed by the Atlas nylon array analysis. The identification PTPL1 and IGFBP2 as being differentially expressed by the Atlas nylon array suggested that PI3K signalling may be involved in the mechanism of platinum resistance in the H69CIS200 and H69OX400 cells.

Activation of the PI3K/Akt signalling pathway (Figure 1.7) has been previously associated with cisplatin resistance in ovarian carcinoma cells (Lee et al., 2005).

FAP48, a FKBP binding protein associated with the mTOR pathway, was also found to be differentially expressed by the Atlas nylon array analysis. PI3K/Akt signalling which has been associated with cisplatin resistance, activates mTOR. Downstream effects of mTOR signalling include control of growth and proliferation and the cell cycle (Asnaghi et al., 2004b Guertin et al., 2005). This suggested a role for mTOR signalling in the regrowth resistance phenotype of the H69CIS200 and H69OX400 cell lines. mTOR has also been associated with the stress response to microtubule damage, initiating the apoptotic response by inhibiting anti-apoptotic Bcl-2 by phosphorylation (Calastretti et al., 2001). It was therefore hypothesised that changes in PI3K/Akt/mTOR signalling could be involved in both the resistance to cisplatin and sensitivity to taxol in this cell model (Figure 6.16).

6.6.1 PTPL1

Protein tyrosine phosphatase L1 (PTPL1) was found to be differentially expressed by the Atlas nylon array analysis (Chapter 5). PTPL1 has been shown to inhibit the PI3K pathway and initiate apoptosis in breast cancer cells (Bompard et al., 2002). The H69CIS200 cells showed a significant decrease in PTPL1 mRNA expression in response to cisplatin treatment (-1.73-fold) but also showed a significant increase in response to oxaliplatin treatment (1.59-fold) (Figure 6.17).

6.6.2 IGFBP2

IGFBP2 was found to be differentially expressed by the Atlas nylon array analysis (Chapter 5). Insulin-like growth factor binding proteins (IGFBPs) act to modulate insulin-like growth factor (IGF) half-life, and bind with varying relative affinity to IGF-I and IGF-II (Foulstone et al., 2005). Phosphorylation of the insulin receptor and IGF-I receptor results in enhanced catalytic activity of the tyrosine kinase domain. Protein–protein interactions with insulin receptor substrates activate the PI3K pathway (Foulstone et al., 2005).

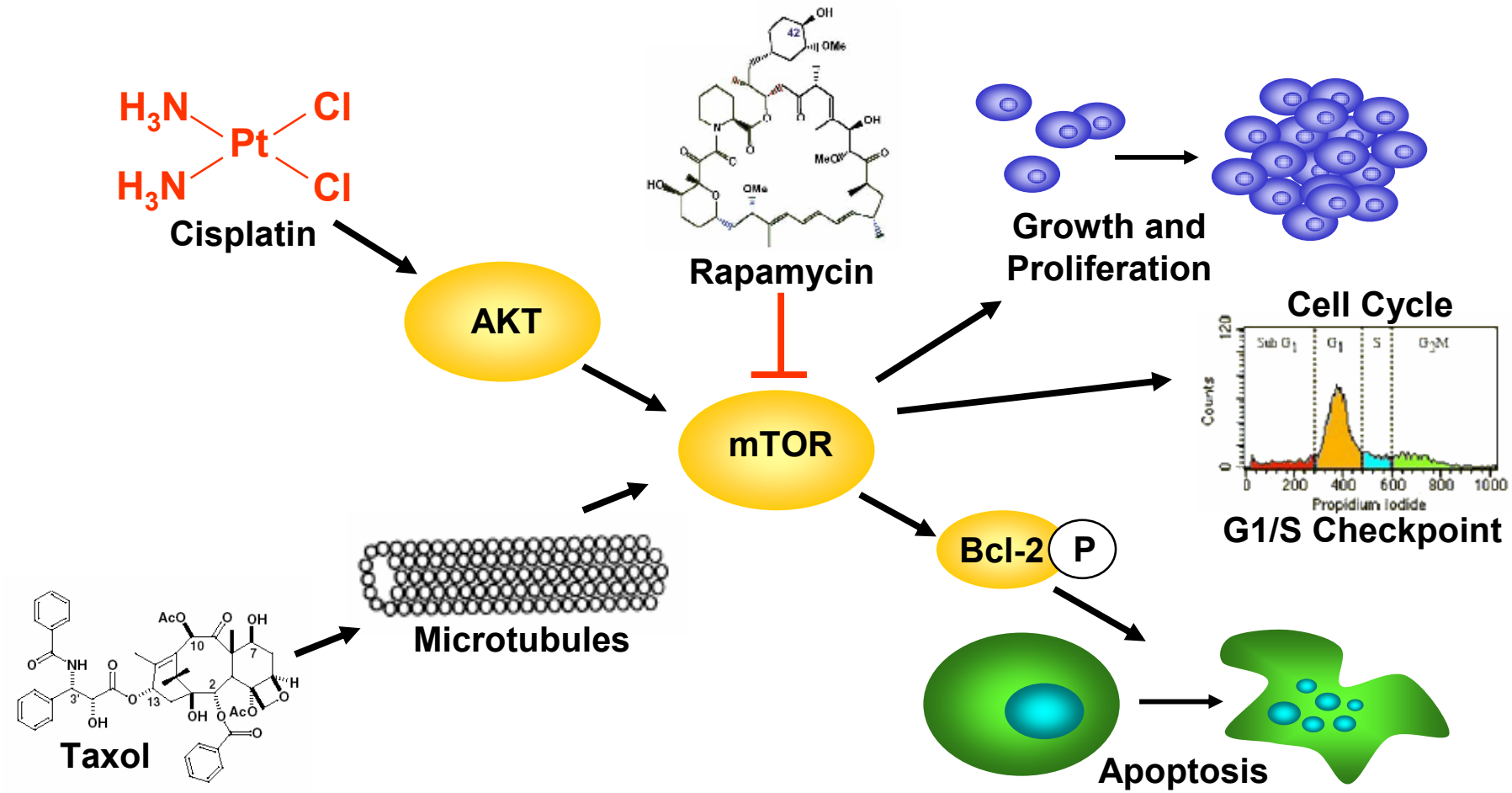

Figure 6.16 Interaction of cisplatin and taxol with mTOR signalling. Cisplatin activates mTOR signalling via Akt kinase. Downstream effects of mTOR include growth, proliferation and cell cycle control suggesting a role in the regrowth resistance phenotype of the H69CIS200 and H69OX400 cell lines. Taxol also stimulates mTOR signalling as part of the stress response to microtubule damage and this initiates the apoptotic response via mTOR's phosphorylation of anti-apoptotic Bcl-2. This led to the hypothesis that mTOR signalling is involved in both the platinum resistance and taxane sensitivity of the H69CIS200 and H69OX400 cell lines.

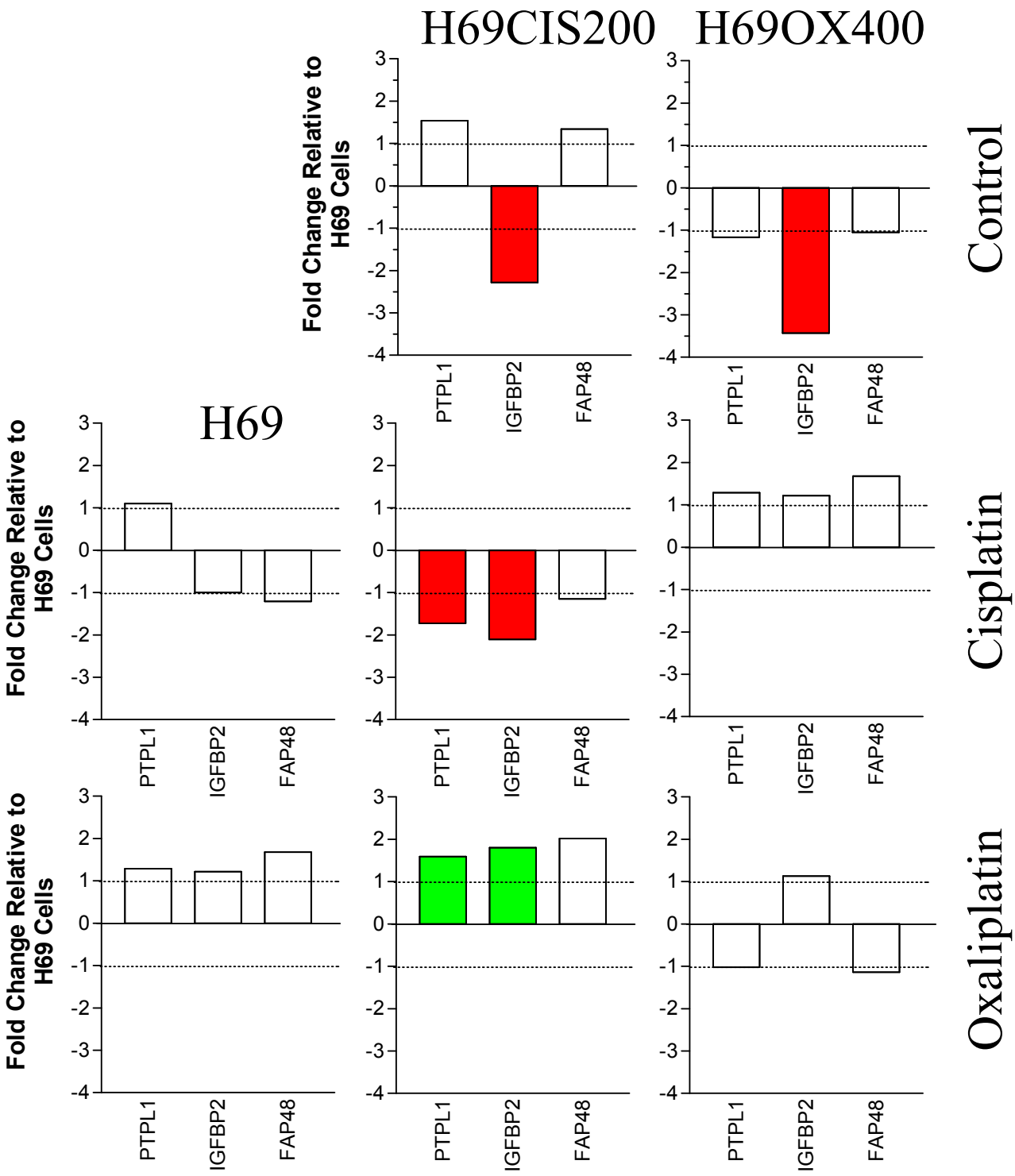

Figure 6.17 mRNA expression data for PI3K/Akt/mTOR signalling related genes. H69, H69CIS200 and H69OX400 cells were grown for four days either in drug-free media, 200 ng/ml cisplatin or 400 ng/ml oxaliplatin as indicated. mRNA was extracted, converted to cDNA and assayed by real-time PCR as described in section 2.12. Means of duplicate experiments are presented, standard deviations have been omitted for clarity. Significant increases from the H69 control are indicated in green, significant decreases in red. Significant differences were determined using a student's t-test $p < 0.05$. Replotted from Figure 5.4.

IGFBP2 mRNA was significantly decreased in both resistant cell lines –2.28-fold in the H69CIS200 cells and –3.43-fold in the H69OX400 cells. IGFBP2 was also significantly decreased in the H69CIS200 cells treated with cisplatin (-2.11-fold). However, IGFBP2 was significantly increased in the H69 (1.74-fold) and H69CIS200 cells (1.80-fold) in response to oxaliplatin treatment (Figure 6.17).

6.6.3 FAP48

FAP48 was identified as being differentially expressed by the Atlas nylon array analysis (Chapter 5). FAP48 interacts with FK506-binding proteins (FKBPs) such as FKBP52 and FKBP12, which belong to the large family of immunophilins that bind the immunosuppressant drugs FK506 and rapamycin. Rapamycin and FKBP12 associate and inhibit the activity of mTOR (Krummrei et al., 2003). FAP48 mRNA was not changed in the untreated H69CI200 and H69OX400 cells. FAP48 mRNA was found to be significantly increased in response to oxaliplatin treatment in H69 cells (1.54-fold) (Figure 6.17)

6.7 Response of cell lines to co-treatment with rapamycin

mTOR (mammalian target of rapamycin) was first characterised by its interaction with the drug rapamycin (Guertin et al., 2005). Rapamycin inhibits several of mTORs cellular functions associated with cell growth and proliferation. H69, H69CIS200 and H69OX400 cells were treated with 200 ng/ml cisplatin, 400 ng/ml oxaliplatin or 5 nM taxol for 4 days, in the presence or absence of 10 nM rapamycin. A dose of rapamycin which has been shown to inhibit mTOR in mammalian cells, but a dose which is non-cytotoxic to the cell lines (Figure 6.18A). Cells were stained with trypan blue and counted using a haemocytometer on the fourth day of treatment, Figure 6.18B shows the percentage cell growth compared to an untreated control for two independent experiments. The resistant cell lines show a higher level of growth compared to the parental H69 in response to both cisplatin and oxaliplatin. The resistant cells show a lower level of growth to taxol compared to the parental H69 cells, consistent with the cytotoxicity data (Figure 3.9). However when co-treated with 10 nM rapamycin the reverse pattern is seen. The H69 parental cells show the highest amount of growth compared to the resistant cells in response to both cisplatin and oxaliplatin. The

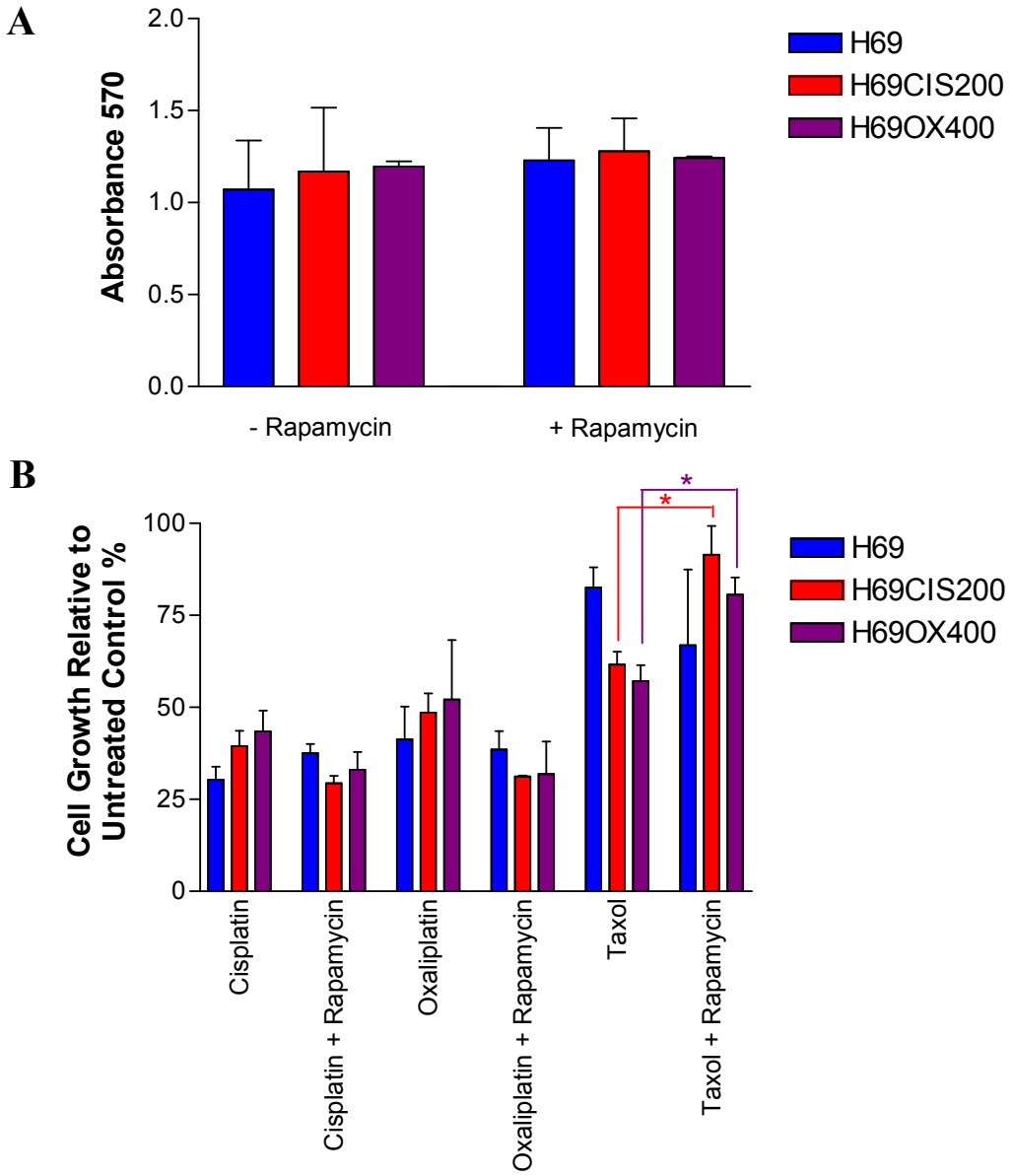

Figure 6.18 Cell growth in response to cisplatin, oxaliplatin and taxol in the presence or absence of rapamycin. A) A dose of 10 nM rapamycin had no effect on cell viability over 4 days as determined by MTT staining and reading of absorbance at 570 nM. B) H69, H69CIS200 and H69OX400 cells were grown for four days either in drug-free media, 200 ng/ml cisplatin, 400 ng/ml oxaliplatin, 5 nM taxol in either the presence or absence of 10 nM rapamycin. Cells were stained with trypan blue and counted microscopically. Presented is the percent cell viability compared to an untreated control for each cell line. Means and standard deviations of two independent experiments is presented. Significant differences as determined by a student's T-test $p<0.05$ is indicated by a * and lines to indicate the samples compared.

resistant cells also grow more than the parental cells when treated with taxol in the presence of rapamycin. There is a significant change in growth of the resistant cells in the response to taxol with the addition of rapamycin ($p<0.05$ students t-test).

6.8 Protein expression of mTOR

The expression of mTOR protein was examined by Western blot in the H69, H69CIS200 and H69OX400 cell lines in their resting state and in response to 200 ng/ml cisplatin and 400 ng/ml oxaliplatin drug treatment for 4 days (Figure 6.19). Platinum drug treatment reduced the expression of mTOR in all cell lines consistent with the cell lines being in growth arrest in response to platinum drug treatment. This decrease in expression was significant in the H69OX400 cells.

The phosphorylation of mTOR at Ser2448 opens the gate for the growth signals and closes the gate to the death signals. The inhibition of Ser2448 phosphorylation can allow the transmission of death signals (Asnaghi et al., 2004a). The mTOR Western blot shows a doublet in the untreated H69CIS200 and H69OX400 cells, suggesting that mTOR has been altered possibly by phosphorylation to become active in the resistant cell lines but not in the parental H69 cells (Figure 6.20). The mTOR doublet disappears upon platinum drug treatment, suggesting that phosphorylation and therefore activity has been inhibited in the cytotoxic response to platinum.

6.9 Discussion

The platinum-resistant cell lines are both sensitive to taxanes. The H69CIS200 cells are very sensitive to both taxol (16.6-fold) and taxotere (12.5-fold). The H69OX400 cells are also sensitive to taxanes but to a lesser extent □.0□-fold to taxol and 5.26-fold to taxotere (Figure □9). The H69OX400 cells are also different to the H69CIS200 cells as they are resistant to *vinca* alkaloids. Genes, proteins and pathways relating to the target of taxanes, the microtubules have been analysed in this chapter in the hope of understanding the sensitivity of taxanes.

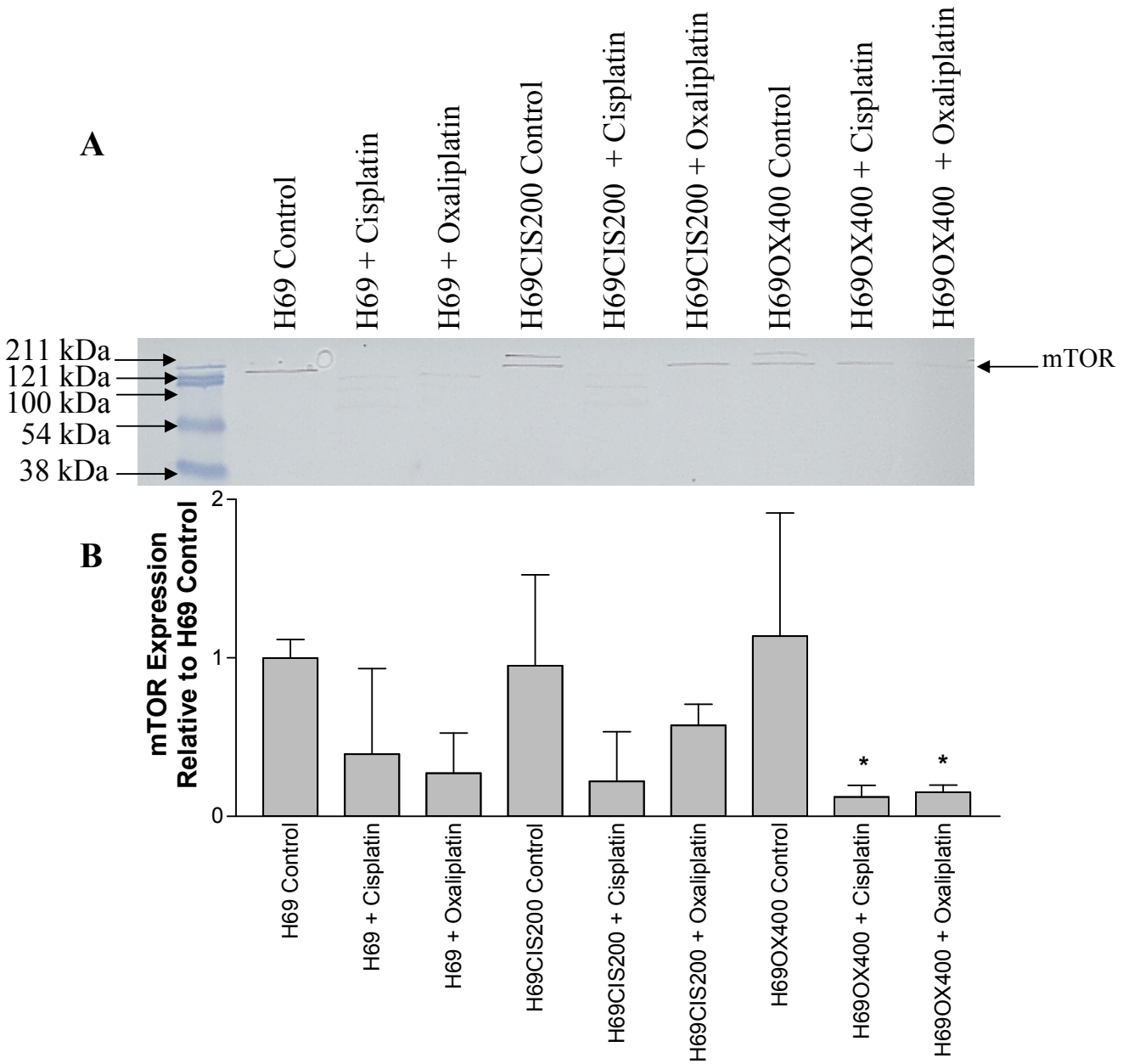

Figure 6.19 mTOR protein expression determined by Western blot. A) H69, H69CIS200 and H69OX400 cells were grown for four days either in drug-free media, 200 ng/ml cisplatin or 400 ng/ml oxaliplatin. Protein was extracted and 20 μg subjected to SDS-PAGE and Western blotting as described in section 2.13. mTOR was detected with a primary antibody and an alkaline phosphatase labelled secondary antibody as described in section 2.13.4.1. B) Quantitation of the mTOR bands was determined by Quantity-one software and adjusted for protein loading by ponceau staining. The mean and standard deviation of two independent experiments are presented. * = significant decrease from H69 control using the student's t-test $p < 0.05$.

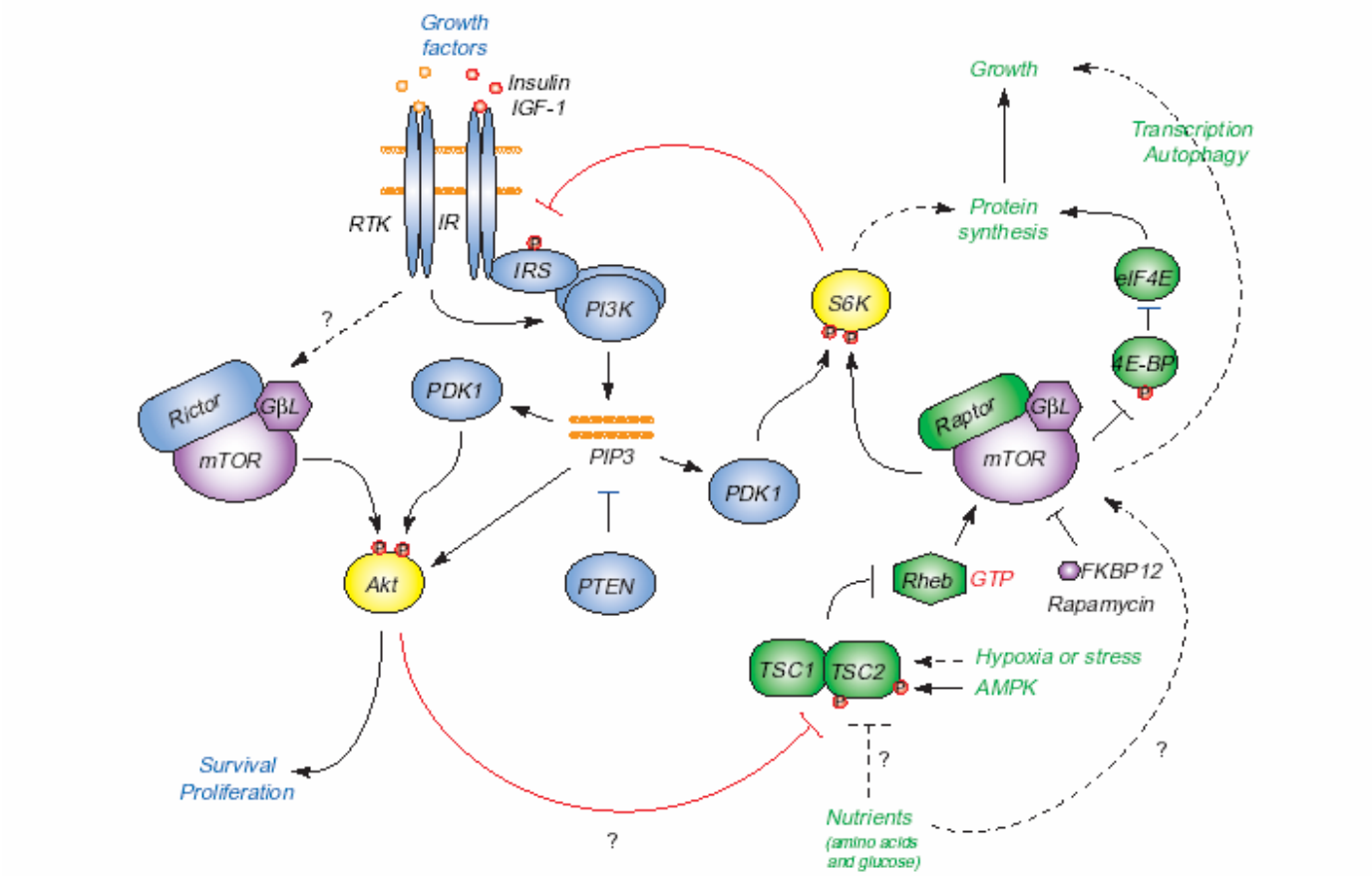

Figure 6.20 mTOR signalling in cell growth, proliferation and survival. Adapted from Guertin et al., 2005.

6.9.1 α-tubulin

α-tubulin was analysed to help understand the sensitivity of the H69CIS200 and H69OX400 cells to taxanes. The mRNA of α-tubulin was found to be increased in association with drug treatment (Figure 6.2) but no consequent increase in protein was found (Figure 6.3). There were no significant changes in α-tubulin protein levels, however drug treatment and resistance tended to lower the α-tubulin protein expression level. If the expression of α-tubulin protein was lower this could mean that it is easier to polymerise by taxol leading to sensitivity to this drug. However this small change alone is unlikely to cause the large sensitivity to taxol particularly in the H69CIS200 cells. Increased expression of α-tubulin mRNA has also been found in cisplatin-resistant oesophageal cancer, however, the level of protein expression was not examined in the study (Toshimitsu et al., 2004).

There was no change in the ratio of soluble to polymerised tubulin in the resistant cell lines compared to the parental cell line (Figure 6.4). However, the H69CIS200 cells were more likely to polymerise in response to high dose taxol treatment (Figure 6.5). Changes in the ratio of soluble to polymerised tubulin has been shown in cells resistant to *vinca* alkaloids vincristine and vinblastine, a shift to having a greater proportion of polymerised tubulin to compensate for the increased soluble tubulin from the vinca alkaloid treatment (Kavallaris et al., 2001). However, resistant variants of H69 cells were shown to have no change in the polymerisation of tubulin associated with taxol (Ohta et al., 1994) and vindesine (Ohta et al., 1993) resistance. Perhaps H69 resistant SCLC cells are less likely to alter their polymerisation of tubulin than other cell types.

There were no differences in the morphology of α-tubulin in the untreated cell lines or in response to platinum drug treatment. However, the relative amount of microtubule bundle formation in response to taxol treatment reflects the cytotoxicity data, the platinum-resistant cell lines having more microtubule bundles, that is arrested cells, compared to the parental cells in response to the same dose of taxol (Figure 6.10).

Mutations in β-tubulin have been associated with resistance to taxanes (Giannakakou et al., 1997) and *vinca* alkaloids (Kavallaris et al., 2001) in cell lines, although their contribution to clinical resistance remains controversial (Berrieman et al., 2004). Mutations in α-tubulin associated with resistance seem to be less common than mutations in β-tubulin, this is perhaps due to taxanes and *vinca* alkaloids both binding with the β-tubulin subunit (Verrills et al., 2005). A mutation in α-tubulin was associated with taxol resistance and alterations in the binding of MAP4 to the α-tubulin subunit (Martello et al., 2003). Mutations in tubulin have not been previously associated with sensitivity or resistance to platinum chemotherapeutics.

Few of the cell lines presented in Figure 6.1 with an inverse relationship between cisplatin and taxol resistance have reported changes in tubulin. This may be because changes in tubulin are a rare mechanism of resistance or that it has not been studied extensively. Decreases in tubulin proteins have been associated with both taxol resistance (Ohta et al., 1993; Liang et al., 2001) and cisplatin resistance (Christen et al., 1993; Liang et al., 2001) in cell lines which have an inverse response to cisplatin and taxol. Comparing this to the results of this study, there is a trend towards decreased α-tubulin protein expression and some changes in the amount of polymerisation of tubulin in response to high dose taxol in the H69CIS200 cells. However, this small change is unlikely to account for the 10-fold sensitivity to taxanes in this cell line. It therefore seems unlikely that changes in the expression or cellular distribution of α-tubulin is responsible for the large sensitivity to taxanes in the H69CIS200 and H69OX400 cells.

6.9.2 β-actin

β-actin mRNA was found to be increased on treatment with cisplatin and oxaliplatin in all cell lines (Figure 6.2). β-actin and MSH2 were the only two genes that were found to be increased in response to cisplatin and oxaliplatin drug treatment in both resistant cell lines. This suggests that β-actin may be involved in the cross resistance of cisplatin and oxaliplatin in this cell model. Similarly, an increase in the mRNA expression of β-actin has been associated with cisplatin resistance in squamous cell lung cancer (Whiteside et al., 2004). However, there was no consequent increase in β-

actin protein expression in the H69CIS200 and H69OX400 resistant cell lines or in response to platinum drug treatment (Figure 6.12).

Nuclear actin was found to be the major protein crosslinked to the DNA in cells treated with cisplatin (Miller, III et al., 1989). The involvement of actin in DNA–protein crosslinks induced by cisplatin can disturb the nuclear metabolism and the spatial organisation of chromatin leading to further cytotoxicity (Wozniak et al., 2002). Therefore the increase in β-actin mRNA expression in response to platinum treatment could be part of the cytotoxic response to platinum adduct formation. This response occurs in all cell lines (Figure 6.2). The cellular distribution of β-actin was examined by immunocytochemistry and found to be present throughout the cell in both the cytoplasm and nucleus. There were no differences in β-actin distribution in the resistant cell lines (Figure 6.13) or in response to platinum drug treatment (Figures 6.14 and 6.15), such as a shift to the nucleus. β-actin may become cross linked to Pt adducts, however there is no major shift in the cellular distribution of β-actin to reflect this.

β-actin was also found on the cell membrane in all cell lines, with higher expression in some individual cells than others in the same field of view (Figures 6.13, 6.14 and 6.15). Actins and tubulins have been found on the cell surface of cancer cells (Por et al., 1991) and have been associated with cell adhesion and migration (Azios et al., 2005). This suggests that β-actin may be involved in cell to cell adhesion which is important for the maintenance of clumps of cells required for growth in H69 cells. However, there was no change in the amount of membrane β-actin between the sensitive and the resistant cell lines.

It seems despite the increase in β-actin mRNA there is not a corresponding increase in protein or changes in protein distribution. It therefore seems unlikely that changes in β-actin are involved in the mechanism of platinum resistance and taxane sensitivity in this cell model.

6.9.3 *Vinca* alkaloid resistance and taxane sensitivity

The H69OX400 cells are sensitive to taxanes but are also resistant to *vinca* alkaloids.

Increased expression of MAP4 protein has been associated with *vinca* alkaloid resistance in leukemia cells (Kavallaris et al., 2001). There was a trend of increased MAP4 mRNA in the untreated resistant cell lines and on platinum drug treatment in all cell lines (Figure 6.2). However, the H69OX400 cells have significantly increased expression of MAP4 mRNA in response to both cisplatin and oxaliplatin treatment (Figure 6.2). If the H69OX400 cells upregulate MAP4 in response to cellular stress this may help explain their resistance to *vinca* alkaloids. The H69 cells also showed a significant increase in MAP4 expression in response to oxaliplatin treatment, this suggests that an upregulation of MAP4 mRNA may be more associated with the response to oxaliplatin than cisplatin in this cell model.

MAP4 has not only been associated with *vinca* alkaloid resistance but also sensitivity to taxanes in cells with mutant p53 (Zhang et al., 1998). The p53 pathway responds to a wide variety of cellular stress signals, including DNA damage, hypoxia, spindle damage and heat shock. p53 activation may result in cell cycle arrest (G_1 or G_2 arrest), senescence, or apoptosis (Levine et al., 2006). Cells with mutant p53 are less likely to enter a cell cycle arrest or apoptose in response to cellular stress, they are more likely to continue through the cell cycle despite the risk of further mutation. The H69 SCLC cell line has mutant p53 and the development of resistance in this cell line has been previously associated with an increase in the expression of mutant p53 (Davey et al., 2004). Cisplatin resistance has been associated with the mutation of p53 and sensitivity to taxol in ovarian carcinoma cells (Cassinelli et al., 2001). Conversely, cell lines expressing wild type p53 have been reported to be more sensitive to cisplatin and resistant to taxanes (Damia et al., 2001). MAP4 and p53 may therefore be involved in the sensitivity to taxanes in both platinum- resistant cell lines, and the resistance to *vinca* alkaloids in the H69OX400 cell line.

6.9.4 PI3K/Akt/mTOR signalling

The differential expression of genes FAP48, PTPL1 and IGFBP2 led to suspecting changes in the PI3K/Akt/mTOR signalling pathway were associated with platinum resistance in this cell model (Figure 6.17). Rapamycin treatment reversed both platinum resistance and taxol sensitivity in the H69CIS200 and H69OX400 cells (Figure 6.18). However, this difference was only significant in the response to taxol.

This suggests that the platinum resistance is multifactorial, involving components of the mTOR pathway as well as other mechanisms such as DNA repair and glutathione metabolism. However, a very low dose of rapamycin (10 nM) the minimum to inhibit mTOR activity, was used compared to other studies into mTOR. Perhaps by increasing the dose of rapamycin the reversal of platinum resistance would show a significant change. Doses of rapamycin up to 1 μM have been shown not to inhibit other protein kinases (Davies et al., 2000). The taxol sensitivity of the H69CIS200 and H69OX400 cell lines was reversed by rapamycin, suggesting that this sensitivity has been caused by changes in the PI3K/Akt/mTOR pathway.

There are two multiprotein complexes containing mTOR, only one is rapamycin sensitive (Figure 6.20). The two best characterised downstream targets of the rapamycin-sensitive mTOR complex are two families of proteins that control translation, the ribosomal protein S6 kinase (S6K) and the eukaryotic initiation factor eIF-4□ binding protein (4□-BP). S6K1 phosphorylates S6 which controls the translation of major components of the protein synthesis machinery such as ribosomal proteins and elongation factors. 4□-BP regulates the transcription factor eIF-4□ which controls the transcription of many mRNAs related to proliferation (Wu et al., 2005) (Figure 6.20). Therefore the reversal of platinum resistance by rapamycin in the H69CIS200 and H69OX400 cell lines is directly related to mTORs control of growth and proliferation factors. This suggests that mTOR is involved in the regrowth resistance mechanism of the H69CIS200 and H69OX400 cell lines. The rapamycin-sensitive mTOR complex is also involved in the sensitivity to taxol in the platinum-resistant cell lines as inhibition of this complex reverses taxol sensitivity.

The PI3K pathway is often activated in cancer through a mutation in PT□N. PT□N negatively regulates Akt activation through PIP3 dephosphorylation (Figure 1.7). A loss in PT□N activity either through mutation or chromosome deletion leads to permanent PI3K/Akt pathway activation (Vara et al., 2004). Around 20% of SCLC cell lines have a PT□N mutation, however the H69 SCLC cell line does not (Yokomizo et al., 1998). The gene for PT□N is located at 10q23.3, the H69 cells have the normal two copies of this segment and the H69CIS200 and H69OX400 cell lines show no change from the parental cell line (Figure 4.4). However, this does not exclude a new mutation in the PT□N gene in the resistant cell lines that doesn't

involve a change in copy number of the segment 10q23.3. Decreased expression of PT□N protein and consequent activation of PI3K/Akt has been associated with cisplatin resistance in ovarian carcinoma cells (Lee et al., 2005). Increased activity of PT□N and therefore suppression of PI3K/Akt signalling has also been associated with the response to increasing concentrations of both cisplatin and taxol treatment in cancer cells (Schondorf et al., 2001). This suggests that the PI3K/Akt pathway can be suppressed in a similar manner in response to both cisplatin and taxol treatment through PT□N. An inverse relationship between cisplatin and taxol resistance is therefore unlikely to be mediated by PT□N signalling.

Due to rapamycin's poor aqueous solubility it is inappropriate for use in the clinical treatment of cancer. Three rapamycin analogs, CCI-779, RAD001 and AP23573, with improved aqueous solubility, are currently in clinical trials and preliminary evidence suggest they are quite effective in tumours with PT□N inactivation (Guertin et al., 2005). The majority of clinical studies have examined CCI-779. CC1-779 showed little activity as a single agent in melanoma (Margolin et al., 2005) but showed some activity in glioblastoma (Galanis et al., 2005). CCI-779, RAD001 and AP23573 do not appear to have been trialed in combination with cisplatin or taxol.

6.9.5 PI3K/Akt/mTOR signalling and platinum

The platinum resistance in both the H69CIS200 and H69OX400 cells is reversed by rapamycin (Figure 6.19), suggesting that the rapamycin-sensitive mTOR complex is associated with the resistance mechanism (Figure 6.20). Downstream of the rapamycin-sensitive mTOR complex are transcription and translation factors which regulate cell growth. This suggests that the mTOR pathway may be part of the molecular mechanism responsible for the regrowth resistance phenotype described in Chapter 3; where resistance was characterised by the ability of a cell to survive and proliferate rather than increasing their level of resistance as determined by a 5-day MTT cytotoxicity assay.

There is another report of cisplatin resistance being associated with increased activity of the PI3K/Akt/mTOR pathway. Tsurutani et al. showed that adhering the normally suspension culture of H69 SCLC cells to an extracellular matrix composed of laminin,

fibronectin, and collagens I and IV increased their cisplatin resistance by activating the PI3K/Akt pathway (Tsurutani et al., 2005). Unfortunately the response to taxol was not investigated. The H69 SCLC cells grow as clumps of cells in suspension, when treated with platinum drugs many cells lose their ability to form clumps and die, those cells capable of re-clumping are the cells which survive and proliferate the culture and ultimately become platinum resistant. The work of Tsurutani et al. suggests that the ability of some cells to adhere to eachother may have induced the activity of the PI3K/Akt/mTOR pathway and promoted the development of platinum resistance in the H69CIS200 and H69OX400 cells.

Cisplatin resistance has been shown not to alter the level of protein expression of mTOR in SCLC cells (Wu et al., 2005). Similarly the H69CIS200 and H69OX400 cell lines do not have any change in mTOR protein expression compared to the parental cell line (Figure 6.19). However, when treated with cisplatin or oxaliplatin the level of mTOR expression is decreased in all cell lines, this decrease is significant in the H69OX400 cell line. The decrease in mTOR expression in response to drug treatment corresponds to the arrested cell cycle of the cell lines after a 4-day platinum drug treatment. Rapamycin reverses the platinum resistance in this model (Figure 6.18), perhaps by inhibiting the protective cell cycle arrest induced by platinum.

mTOR appears as a doublet in the H69CIS200 and H69OX400 untreated samples (Figure 6.19). The phosphorylation of mTOR at Ser2448 governs its activity. Phosphorylation at Ser2448 has been associated with growth signals whereas the inhibition of Ser2448 phosphorylation can allow the transmission of death signals (Asnaghi et al., 2004a). Phosphorylated mTOR has been associated with phosphorylated Akt in 87% of ovarian tumour samples, 55% of tumours also showed elevated levels of phosphorylated mTOR. This demonstrates the activity of this pathway in clinical specimens (Altomare et al., 2004). This suggests that the H69CIS200 and H69OX400 resistant cell lines have more active mTOR growth signals than the parental cell lines. An increase in mTOR activity as determined by activation of downstream signalling factors has been previously associated with cisplatin resistance in SCLC (Wu et al., 2005).

At the 4 day in drug time point analysed by the Western blot in Figure 6.19 drug treatment causes a decrease in mTOR protein expression in all cell lines and a reversal of phosphorylation in the resistant cell lines. It is possible that the resistant cell lines take longer to achieve this decrease in mTOR expression and drop in activity than the parental cell line. However this hypothesis remains to be examined.

6.9.6 PI3K/Akt/mTOR signalling and taxanes

The sensitivity of the H69CIS200 and H69OX400 cells to taxol is reversed by treatment with rapamycin (Figure 6.19). This suggests that both the platinum resistance and taxane sensitivity in the H69CIS200 and H69OX400 cells may be a result of changes in the mTOR pathway. The response of mTOR protein expression to taxol treatment remains to be studied. A possible explanation for this reversal of taxane sensitivity is the damaging of microtubules by taxol induces the phosphorylation of Bcl-2 and the initiation of apoptosis, a process which is dependent on mTOR signalling (Asnaghi et al., 2004a). Rapamycin can reverse this process through the inhibition of Bcl-2 phosphorylation, increasing the concentration of Bcl-2 by inhibiting the decay process (Calastretti et al., 2001).

Akt is directly upstream of mTOR and its activation has also been associated with resistance to both taxanes and *vinca* alkaloids (VanderWeele et al., 2004). Akt maintained an increased glycolytic rate in response to anti-microtubule treatment in murine hematopoietic cancer cells. Rapamycin inhibited the Akt-mediated maintenance of glycolysis and resistance to taxanes and *vinca* alkaloids, suggesting that these effects were dependent on mTOR signalling (VanderWeele et al., 2004). This implicates the activation of the PI3K/Akt/mTOR signalling pathway in both platinum and taxane resistance. However, the downstream activities of mTOR may differentiate between these two phenotypes.

mTOR may represent a crossing point between two different signaling pathways. The first is a survival pathway, activated by growth factors and involving PI3K and Akt. The second is an apoptotic pathway, activated by damaged microtubules and inducing downstream phosphorylation of Bcl-2 inhibiting its anti-apoptotic signalling (Asnaghi et al., 2004b). As mTOR activity is increased by phosphorylation in the H69CIS200

and H69OX400 cell lines this may lead to an increase in apoptotic signalling when exposed to taxol leading to hypersensitivity. mTOR activation by survival signals occurs in the G_1 phase of the cell cycle and damaged microtubules activate pro-apoptotic signals in G_2/M phase it has been suggested that mTOR might mediate these two different pathways in two different phases of the cell cycle (Asnaghi et al., 2004b).

6.10 Conclusion

The inverse relationship between platinum and taxane resistance in the H69CIS200 and H69OX400 cells appears to be mediated by the PI3K/Akt/mTOR signalling pathway. Changes in the expression of Bcl-2, MAP4 and p53 may also be involved in determining the final outcome of this signalling pathway. Changes in cytoskeletal proteins α-tubulin and β-actin seem not to play a role in this mechanism despite increases in mRNA expression. If molecular markers could be found to predict for sensitivity to platinum or taxanes in the clinic salvage chemotherapy could be more effectively planned.

CHAPTER 7.0

GLUTATHIONE METABOLISM AND PLATINUM RESISTANCE

7.1 Introduction

Cellular glutathione levels are often increased in platinum-resistant cell lines (Table 1.1). However, there was no change in glutathione levels in the H69CIS200 or H69OX400 resistant cell lines compared to the parental H69 cell line (Figure 3.10). Interestingly, there was a differential response to buthionine sulfoximine (BSO) treatment, an inhibitor of glutathione synthesis (Figure 1.4). The H69CIS200 cells were resistant to BSO and the H69OX400 cells were sensitive to BSO (Figure 3.9). The expression of genes and proteins associated with this pathway was therefore further analysed to understand this differential response to BSO treatment.

7.2 mRNA analysis of glutathione related genes

Analysis of mRNA expression was performed by real-time PCR on mRNA isolated from the H69, H69CIS200 and H69OX400 cell lines. Examined were untreated controls, cells treated with either 200 ng/ml cisplatin or 400 ng/ml oxaliplatin for 4 days.

7.2.1 Glutathione-S-transferases

Glutathione-S-transferases (GSTs) are a group of detoxification enzymes that catalyse the conjugation of glutathione to a wide variety of compounds including platinum drugs (Figure 1.4). The majority of previous studies on GSTs in relation to platinum therapy and cancer have been in clinical studies where gene polymorphisms have been assessed as prognostic markers.

7.2.1.1 Glutathione-S-transferase theta 1 (GSTT1)

GSTT1 was identified as being differentially expressed by the Atlas nylon array analysis (Chapter 5). GSTT1 has not been previously associated with platinum drug resistance. GSTT1 mRNA showed decreased expression in both the H69CIS200 and H69OX400 cell lines, this change was significant in the H69OX400 cells (-1.28-fold) (Figure 7.1). GSTT1 was also significantly decreased in cisplatin treated H69CIS200 cells (-1.5- fold) but in contrast was significantly increased in cisplatin treated

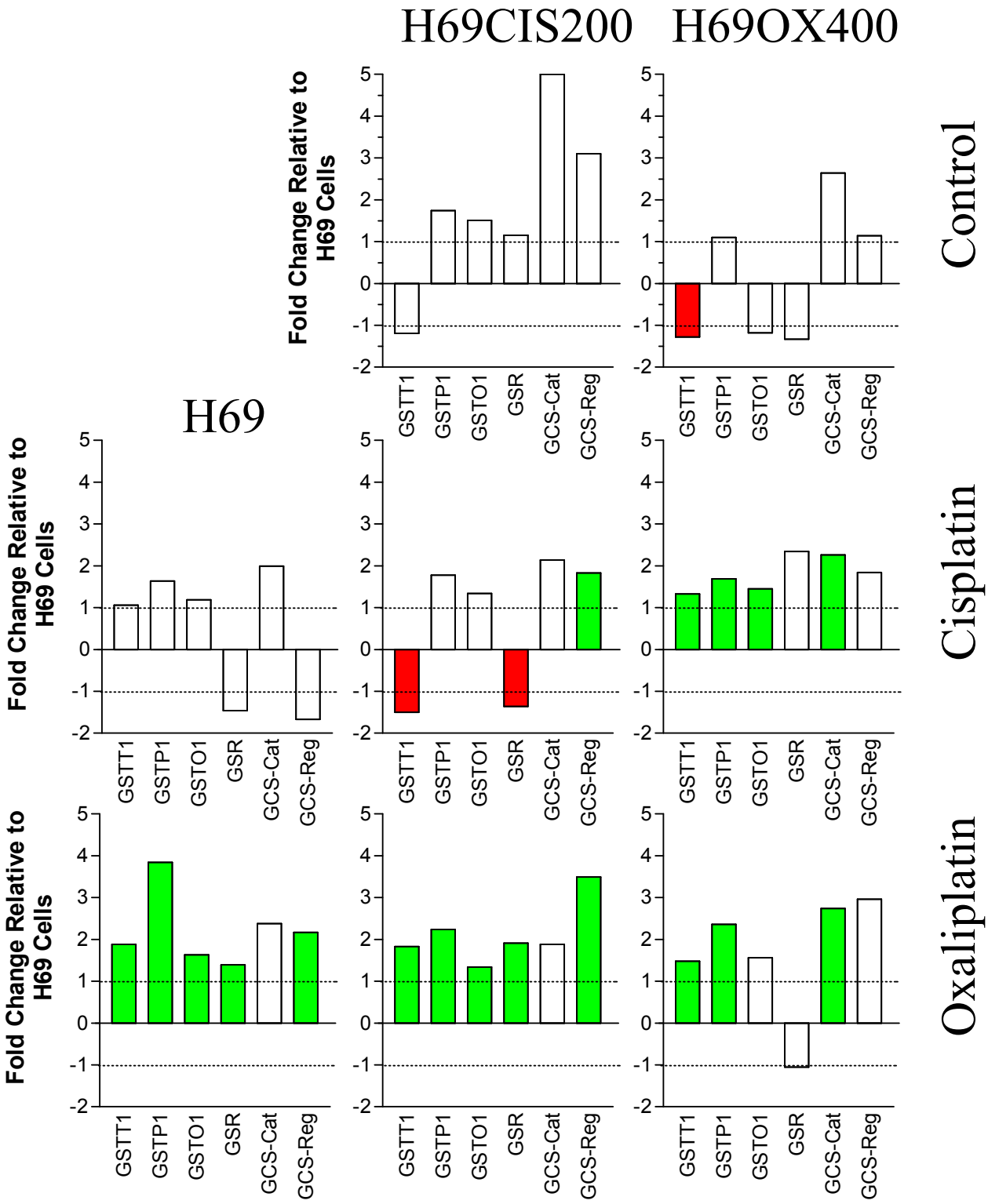

Figure 7.1 mRNA expression data for glutathione related genes. H69, H69CIS200 and H69OX400 cells were grown for four days either in drug-free media, 200 ng/ml cisplatin or 400 ng/ml oxaliplatin. mRNA was extracted, converted to cDNA and assayed by real time PCR as described in section 2.12. Means of duplicate experiments are presented, standard deviations have been omitted for clarity. Significant differences from the H69 control are indicated in green, significant decreases in red. Significant differences were determined using a student's t-test $p < 0.05$. Replotted from Figure 5.4.

H69OX400 cells (1.33-fold). GSTT1 mRNA expression was significantly increased in response to oxaliplatin treatment in all three cell lines H69 (1.88-fold), H69CIS200 (1.83-fold), and H69OX400 (1.48-fold).

7.2.1.2 Glutathione-S-transferase pi 1 (GSTP1)

GSTP1 was identified as being differentially expressed by the Atlas nylon array analysis (Chapter 5). In addition to catalysing the conjugation of electrophiles GSTP1 participates in cellular survival and death signals via interactions with JNK1 and ASK1 (Townsend et al., 2003b). There was a trend for increased GSTP1 mRNA expression in the untreated H69CIS200 cells but not in the untreated H69OX400 cells. GSTP1 mRNA was significantly increased in response to cisplatin treatment in only the H69OX400 cells (1.69-fold). GSTP1 mRNA was significantly increased in response to oxaliplatin treatment in all three cell lines H69 (3.84-fold), H69CIS200 (2.24-fold), and H69OX400 (2.36-fold) (Figure 7.1).

7.2.1.3 Glutathione-S-transferase omega 1 (GSTO1)

GSTO1 was chosen for real-time PCR analysis because of its high level of abundance as determined by the Atlas nylon array analysis. GSTO1 has not been previously associated with platinum drug resistance. There was no significant change or consistent trend in GSTO1 in the untreated resistant cell lines. There was a trend for both cisplatin and oxaliplatin treatment to increase the expression of GSTO1 mRNA. This increase was significant in the in the H69OX400 cells (1.45-fold) in response to cisplatin and the H69 (1.63-fold) and H69CIS200 cells (1.34-fold) in response to oxaliplatin (Figure 7.1).

7.2.2 Glutathione reductase (GSR)

Glutathione reductase (GSR) was identified as being differentially expressed by the Atlas nylon array analysis (Chapter 5). GSR reduces oxidised glutathione utilising NADPH (Rahman et al., 1999) (Figure 1.4). There was no significant change or consistent trend in GSR in the untreated resistant cell lines. GSR mRNA was significantly decreased in expression in response to cisplatin treatment in the

H69CIS200 cells (-1.36-fold). GSR mRNA was significantly increased in response to oxaliplatin treatment in the H69 (1.39-fold) and H69CIS200 cells (1.91-fold) (Figure 7.1).

7.2.3 Gamma glutamyl cysteine synthetase regulatory and catalytic subunits (γGCS-Reg and γGCS-Cat)

Gamma glutamyl cysteine synthetase (γGCS) is the rate limiting enzyme in the synthesis of glutathione (Rahman et al., 1999) (Figure 1.4). The γGCS subunits were chosen for analysis by real-time PCR as this is the enzyme inhibited by BSO treatment. There was a trend for increased mRNA expression of both subunits with the development of resistance and platinum drug treatment. The response to platinum drug treatment was similar in all three cell lines. The mRNA expression of γGCS-Cat was significantly increased in expression in the H69OX400 cell line in response to both cisplatin (2.26-fold) and oxaliplatin (2.74-fold) treatment. The mRNA expression of γGCS-Reg was significantly increased in expression in the H69CIS200 cell line in response to both cisplatin (1.83-fold) and oxaliplatin (3.49-fold) treatment. The mRNA expression of γGCS-Reg was also significantly increased in the H69 parental cells in response to cisplatin treatment (2.17-fold) (Figure 7.1).

7.3 γGCS catalytic subunit protein expression

The protein expression of the γGCS catalytic subunit was analysed by Western blot. The cell lines were examined in their resting state as well as when treated with 200 ng/ml cisplatin or 400 ng/ml oxaliplatin for 4 days. The γGCS-Cat antibody gave multibanding. However, the highest band corresponds to 73 kDa which is the expected molecular weight of the γGCS catalytic subunit (Figure 7.2). When quantitated there was a large decrease in expression in the resistant cell lines compared to the parental cells and a further decrease in expression upon platinum drug treatment. The H69CIS200 cells treated with platinum drugs showed a significant decrease in expression in response to cisplatin (-2.73-fold) and oxaliplatin (-2.79-fold) from their untreated control (indicated by * in Figure 7.2 $p < 0.05$ students t-test). This represents a -6.28-fold and -6.43-fold change respectively from

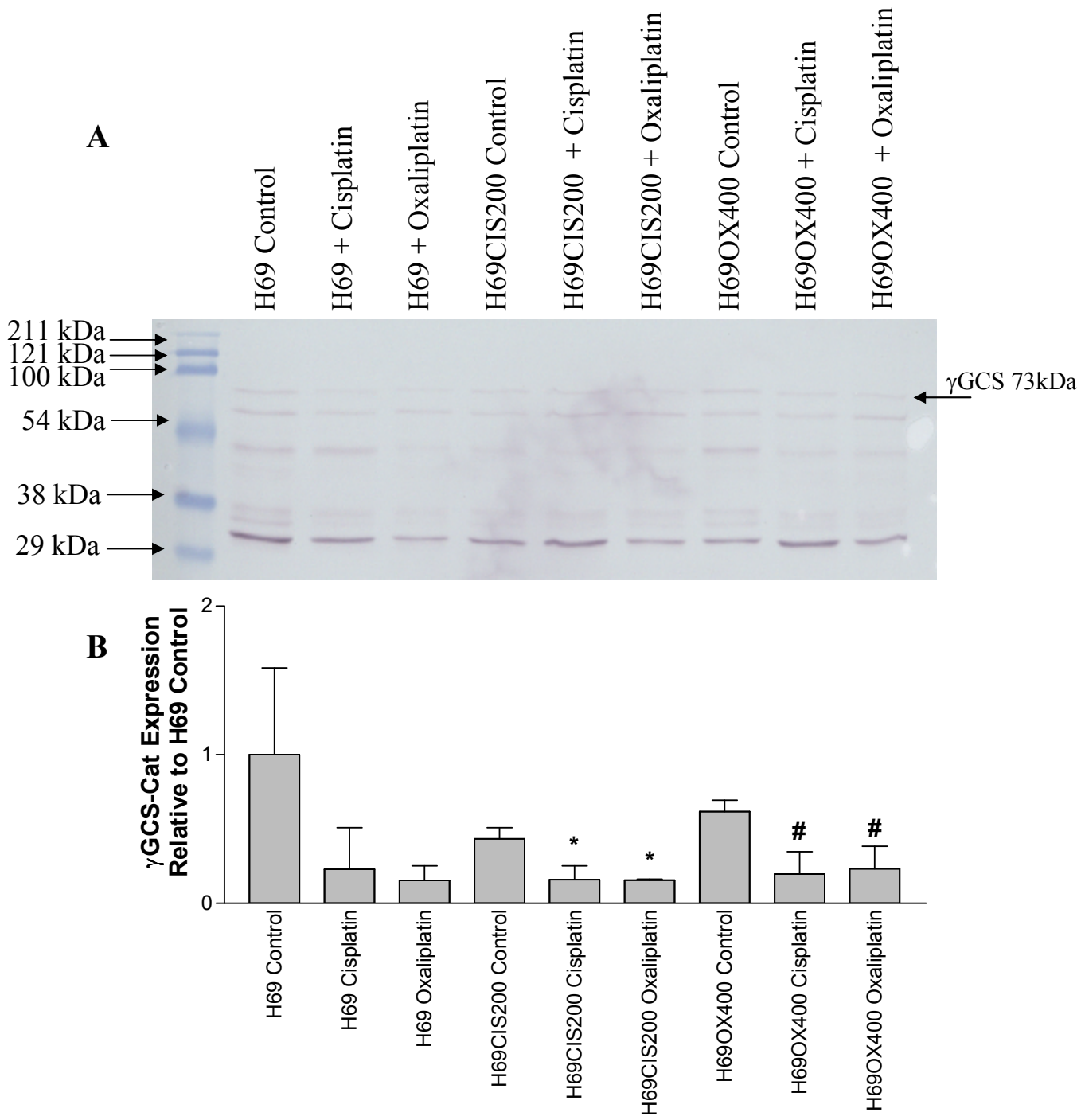

Figure 7.2 γGCS-catalytic subunit protein expression determined by Western blot. A) H69, H69CIS200 and H69OX400 cells were grown for four days either in drug-free media, 200 ng/ml cisplatin or 400 ng/ml oxaliplatin. Protein was extracted and 20 μg subjected to SDS-PAGE and Western blotting as described in section 2.13. γGCS-catalytic subunit was detected with a primary antibody and an alkaline phosphatase labelled secondary antibody as described in section 2.13.4.1. B) Quantitation of the γGCS-catalytic subunit bands was determined by Quantity-one software and adjusted for protein loading by ponceau staining. The mean and standard deviation of two independent experiments are presented. * = significant decrease from H69CIS200 control, # = significant decrease from H69OX400 control using the student's t-test p □0.05.

the untreated H69 cells. Similarly in the H69OX400 cells there was a significant decrease in expression in response to cisplatin (-3.13-fold) and oxaliplatin (-2.64-fold) from their untreated control (indicated by # in Figure 7.2 $p < 0.05$ students t-test). This represents a –5.07-fold and –4.29-fold change respectively from the untreated H69 cells.

mRNA expression of γGCS-Cat increased in the resistant cell lines and in response to drug treatment. However, the protein expression for γGCS-Cat decreased under the same conditions. This illustrates that increases in mRNA do not necessarily lead to increases in protein expression. This may be due to the interaction of different regulatory pathways or this result could be the product of only assaying one timepoint, mRNA expression has increased at 4-days and the protein expression may change later.

The lowest band on the γGCS Western blot is approximately 33 kDa which is the same weight as the γGCS regulatory subunit. The γGCS-Cat antibody is not meant to bind to the γGCS-Reg subunit. However, when the subunits are compared by ClustalW protein alignment (Chenna et al., 2003), there is some homology in the region of the epitope (Figure 7.3A). It is possible that this band is the γGCS-regulatory subunit or a breakdown product of the catalytic subunit. This can't be resolved without further analysis. However, other γGCS antibodies have shown reactivity to both subunits (Godwin et al., 1992). The 33 kDa band showed a trend for decreased expression in the untreated H69CIS200 and H69OX400 cells. Cisplatin treatment did not alter the expression of the 33 kDa band in the parental H69 cells, but tended to increase expression in the resistant cells in response to cisplatin. Oxaliplatin treatment decreased the expression of the 33 kDa band in all cell lines. This decrease was small but significant in the H69OX400 cells (Figure 7.3B).

7.4 Thioredoxin analysis

Thioredoxin is another cellular redox enzyme that plays multiple functions in regulation of cell growth and apoptosis. The cellular concentration of thioredoxin in mammals is low compared to glutathione yet thioredoxin is still an abundant protein.

A

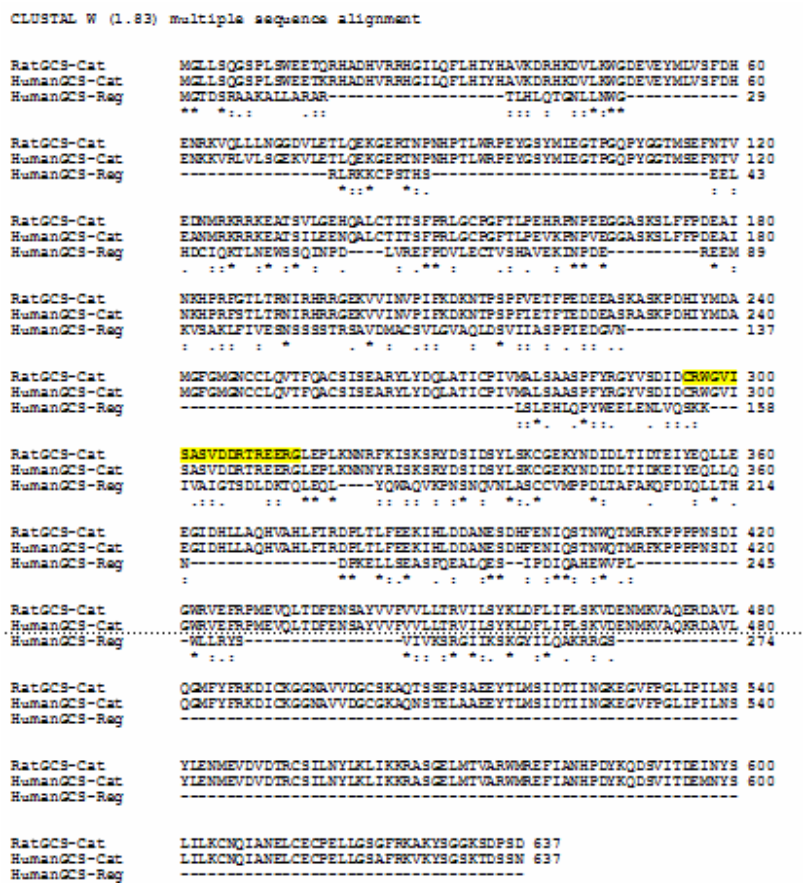

B

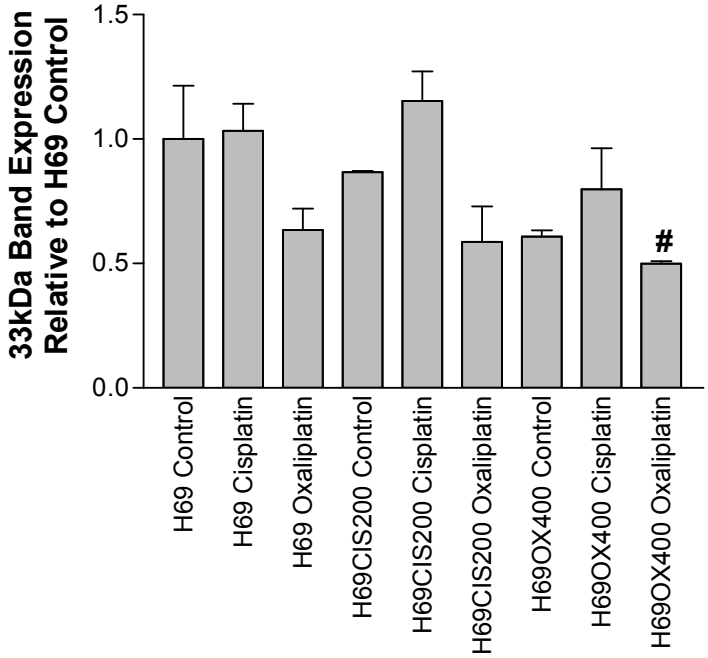

Figure 7.3 Homology between γGCS-Cat and γGCS-Reg proteins. A) Homology between human γGCS-Cat and γGCS-Reg and rat γGCS-Cat by ClustalW analysis, the epitope of the antibody is shown in yellow. B) Quantitative analysis of the 33 kDa band from Figure 7.2A using Quantity-one software, the mean and standard deviation of two independent experiments are presented. # = significant decrease from H69OX400 control using the student's t-test $p < 0.0$□

Increases in thioredoxin in mammalian cells represents an additional cellular defence against stress and potentially a mechanism of drug resistance. Thioredoxin has been shown to be overexpressed in cisplatin-resistant HeLa cells (Nakamura et al., 2000).

7.4.1 Thioredoxin protein expression

The protein expression of thioredoxin was determined by Western blot. The cell lines were examined in their resting state as well as when treated with 200 ng/ml cisplatin or 400 ng/ml oxaliplatin for 4 days (Figure 7.4). The H69CIS200 (-1.75-fold) and H69OX400 cells (-1.66-fold) had significantly less thioredoxin in their resting state than the parental cell line. There was also a significant decrease in thioredoxin expression in response to cisplatin (-1.57-fold) and oxaliplatin (-1.42-fold) treatment in the H69 parental cells. Platinum drug treatment increased the expression of thioredoxin in the H69CIS200 cell line to almost the level of thioredoxin in the parental cells. However, platinum drug treatment induced no change in thioredoxin in the H69OX400 cells, remaining significantly decreased compared to the H69 parental cells.

7.4.2 Thioredoxin immunocytochemistry

The cellular distribution of thioredoxin protein was examined by immunocytochemistry in untreated H69, H69CIS200 and H69OX400 cells. Thioredoxin was distributed throughout the cytoplasm and nucleus but was strongly associated with the nucleolus (Figure 7.5). The nucleolus is a small dense body in the nucleus of eukaryotic cells in which the ribosomal RNA is transcribed and combined with proteins to form the major subunits of ribosomes (Uvarov et al., 1993). The nucleolus is visible in the DAPI images as a small non-staining region in the nucleus. This region corresponds to the intense staining of thioredoxin in the FITC image.

There is no difference in thioredoxin protein distribution between the parental and the resistant cell lines (Figure 7.5). The distribution of thioredoxin was also examined in cells treated with 200 ng/ml cisplatin or 400 ng/ml oxaliplatin for 4 days (Figures 7.6 and 7.7), the same conditions used for the Western blot analysis. Platinum drug treatment caused an increase in cell size in all cell lines, this caused some distortion of

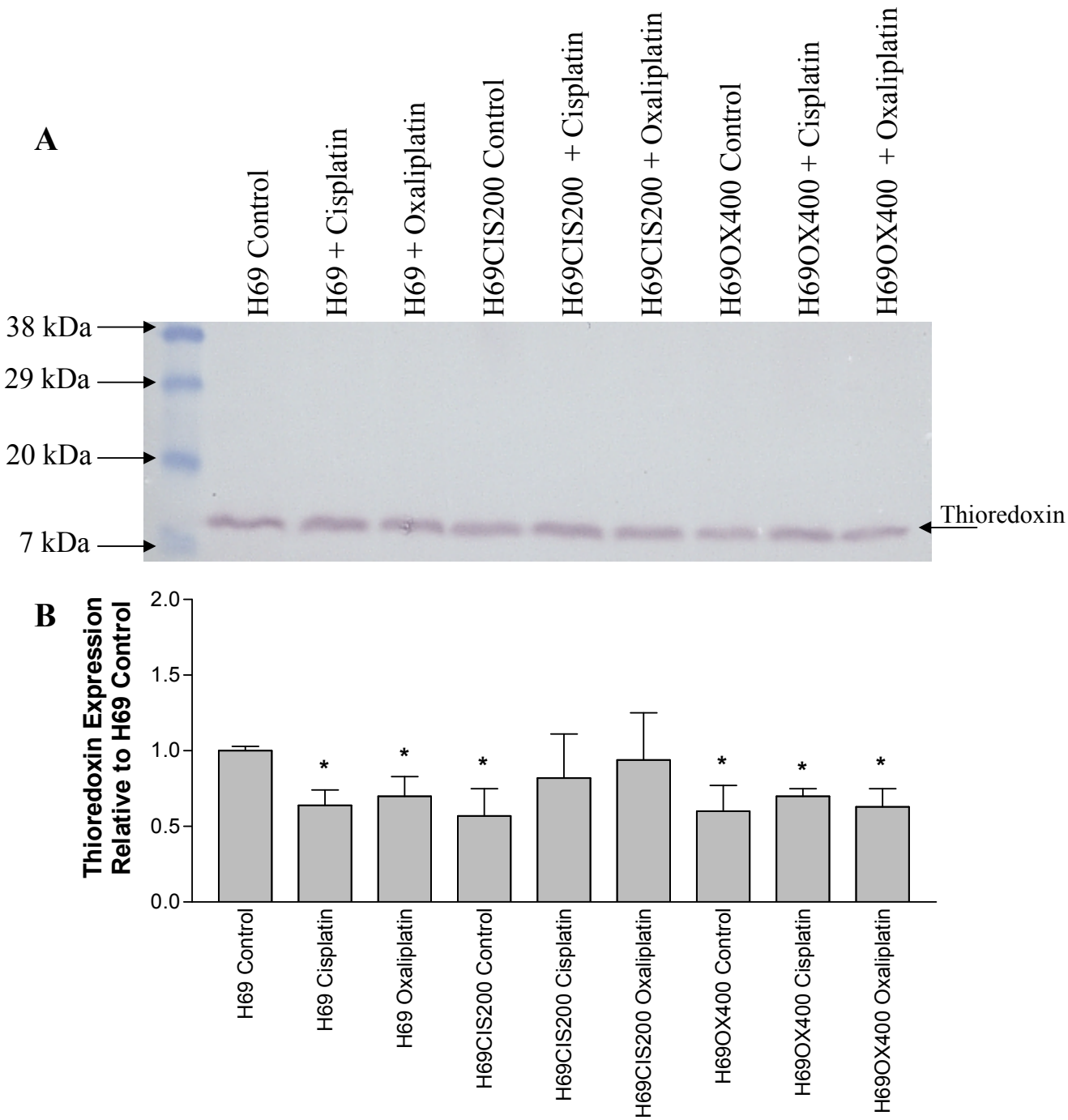

Figure 7.4 Thioredoxin protein expression determined by Western blot. A) H69, H69CIS200 and H69OX400 cells were grown for four days either in drug-free media, 200 ng/ml cisplatin or 400 ng/ml oxaliplatin. Protein was extracted and 20 µg subjected to SDS-PAGE and Western blotting as described in section 2.13. Thioredoxin was detected with a primary antibody and an alkaline phosphatase labelled secondary antibody as described in section 2.13.4.1. B) Quantitation of the thioredoxin bands was determined by Quantity-one software and adjusted for protein loading by ponceau staining. The mean and standard deviation of two independent experiments are presented. * = significant decrease from H69 control using the student's t-test $p < 0.05$.

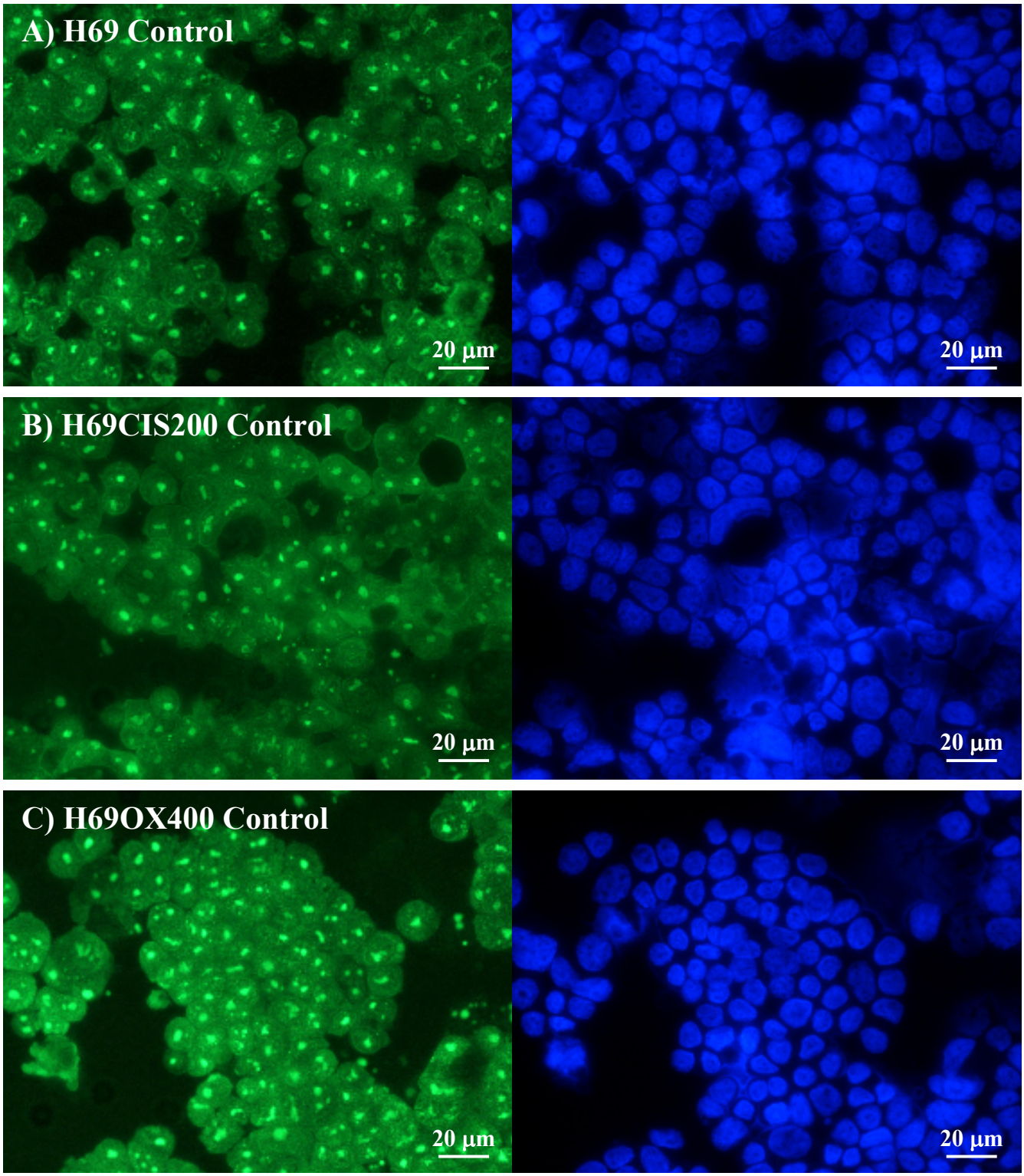

Figure 7.5 Thioredoxin immunocytochemistry control cells. A) H69 B) H69CIS200 and C) H69OX400 cells were grown for 4 days in drug-free culture and prepared as cytospins. Slides were stained with a thioredoxin primary antibody and detected with a FITC labelled secondary antibody shown on the left and counterstained with DAPI shown on the right as described in section 2.14.

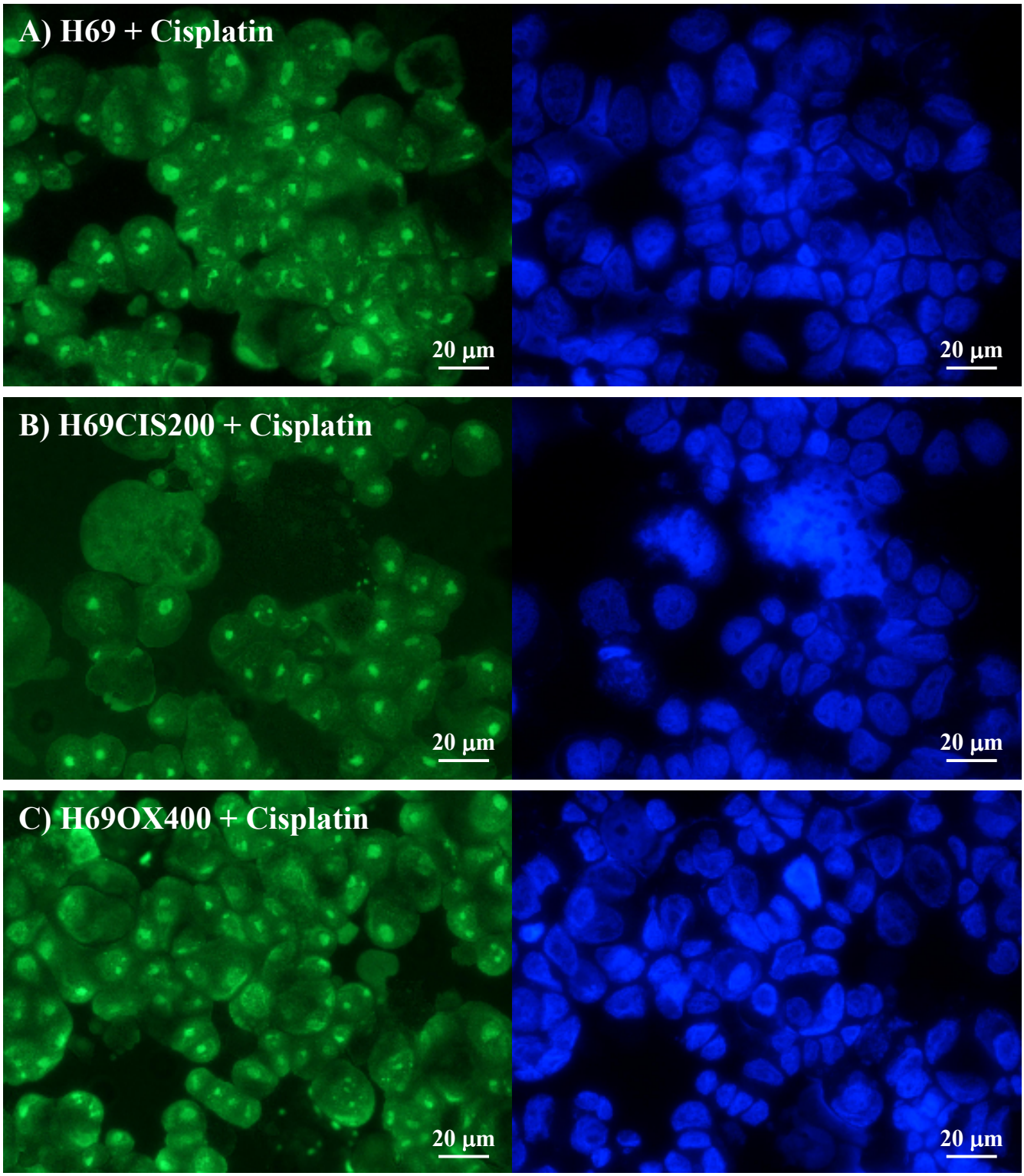

Figure 7.6 Thioredoxin immunocytochemistry cisplatin treated cells. A) H69 B) H69CIS200 and C) H69OX400 cells were grown for 4 days in 200 ng/ml cisplatin and prepared as cytospins. Slides were stained with a thioredoxin primary antibody and detected with a FITC labelled secondary antibody shown on the left and counterstained with DAPI shown on the right as described in section 2.14.

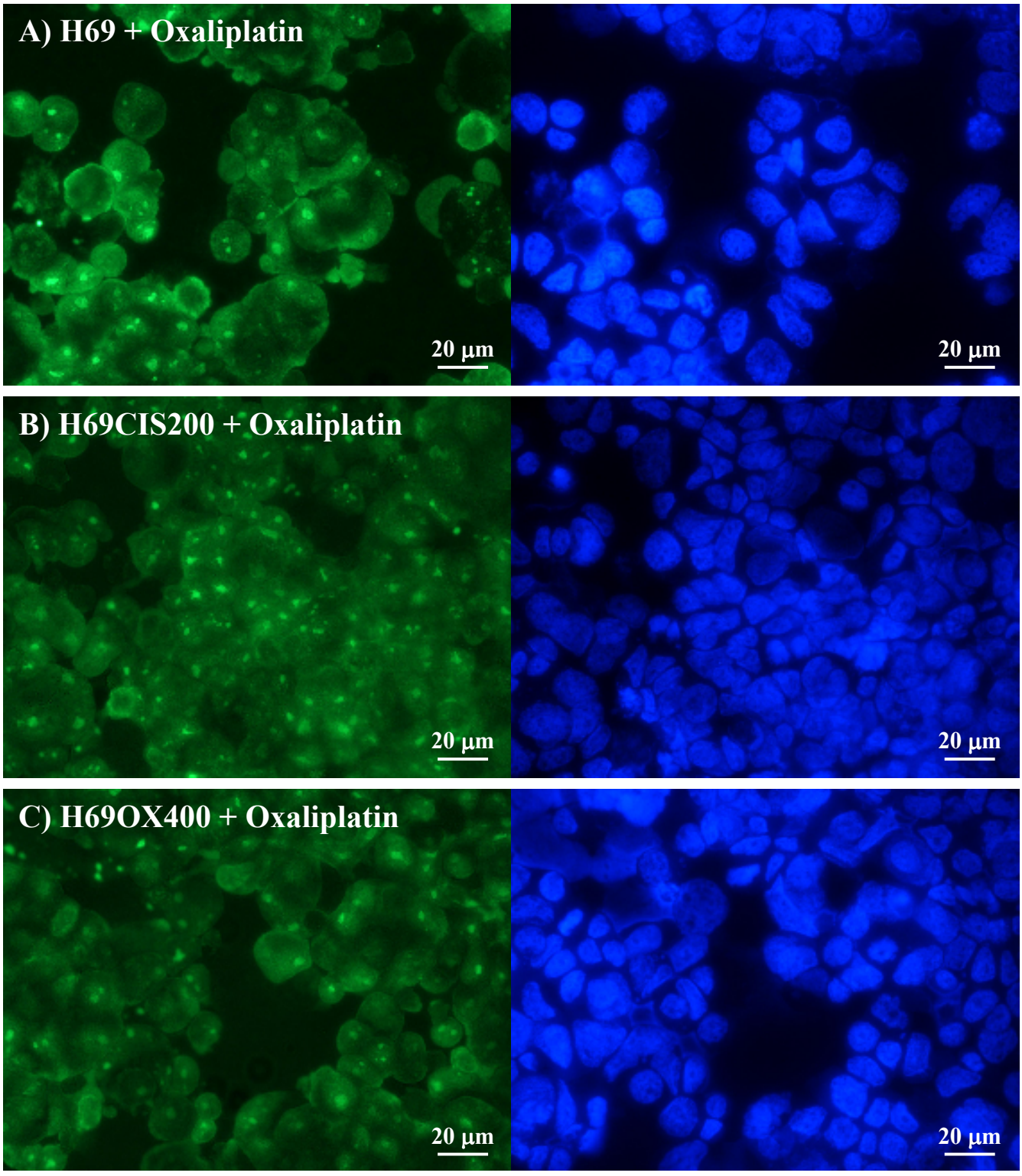

Figure 7.7 Thioredoxin immunocytochemistry oxaliplatin treated cells. A) H69 B) H69CIS200 and C) H69OX400 cells were grown for 4 days in 400 ng/ml oxaliplatin and prepared as cytospins. Slides were stained with a thioredoxin primary antibody and detected with a FITC labelled secondary antibody shown on the left and counterstained with DAPI shown on the right as described in section 2.14.

the nucleus and nucleolus. Thioredoxin remained in the cytoplasm of platinum treated cells and strongly associated with the nucleolus. There was no difference in thioredoxin distribution between the resistant and sensitive cell lines in response to platinum drug treatment.

7.5 Influence of sodium selenite on platinum cytotoxicity

Sodium selenite is used as a source of selenium in culture media. The presence of selenium activates selenoproteins such as thioredoxin reductase. Figure 3.9 showed that the H69CIS200 and H69OX400 cell lines were slightly sensitive to sodium selenite but this change was not significant. The influence of a physiological concentration of selenium (2.5 μM) on platinum resistance was investigated. There was no difference in cisplatin or oxaliplatin cytotoxicity in any of the cell lines in the presence of 2.5 μM selenium (Figure 7.8).

7.6 Discussion

7.6.1 BSO Resistance

Resistance to BSO has been studied in many cell lines developed with acquired resistance to BSO (Table 7.□). The majority of studes report an increase in γGCS-Cat mRNA and protein expression and a decrease in GSTP□mRNA and protein expression. The H69CIS200 cell line, which is resistant to BSO, do not follow this trend. The H69CIS200 cells have a trend towards increased γGCS-Cat mRNA expression in untreated cells and again in response to platinum drug treatment. However, protein expression levels of γGCS-Cat are decreased in the untreated cells, relative to untreated H69 cells, and further decreased in all cell lines on platinum drug treatment. The H69CIS200 cells also show a trend of increased GSTP□ mRNA rather than decreased expression as observed in other BSO resistant cell lines (Yokomizo et al., □995b; Tanaka et al., □998; Tanaka et al., □**99**). The H69OX400 cell line, which is sensitive to BSO, show a very similar pattern to the BSO resistant H69CIS200 cells, with an overall trend for increased mRNA of γGCS-Cat and GSTP□ and decreased γGCS-Cat protein. This suggests that changes in the expression of γGCS-

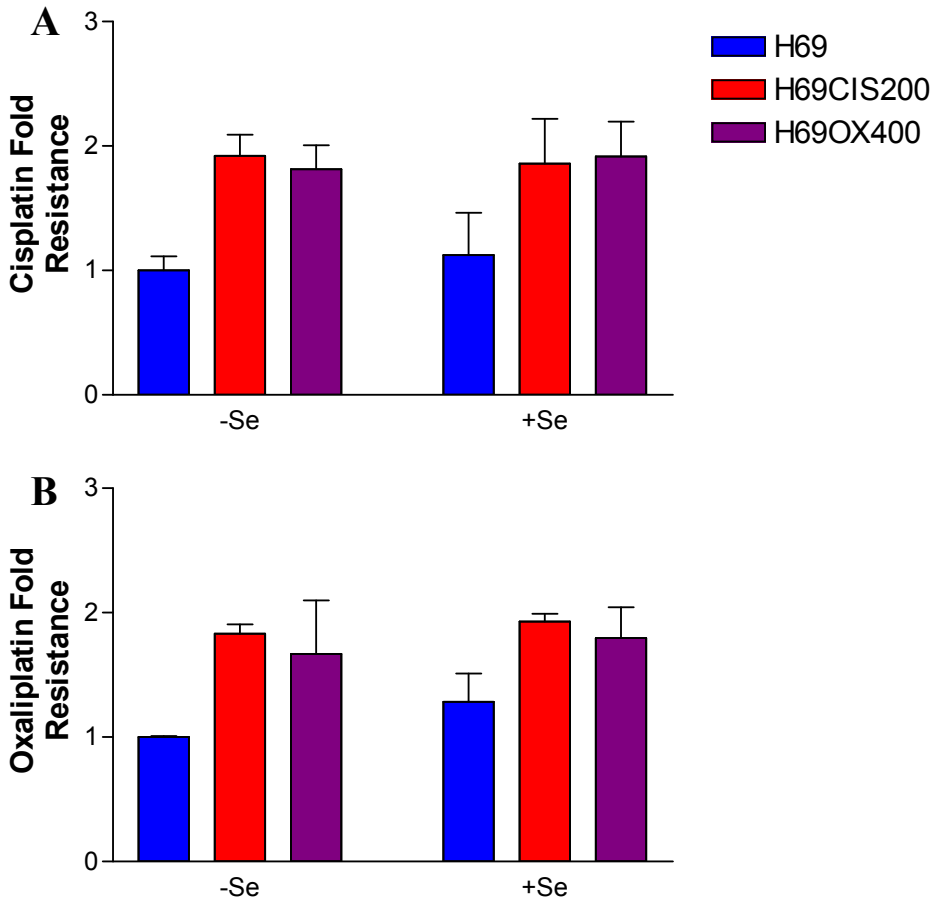

Figure 7.8 Influence of sodium selenite on platinum cytotoxicity. MTT cytotoxicity assays to A) cisplatin and B) oxaliplatin were performed on the H69, H69CIS200 and H69OX400 cell lines in the presence and absence of a physiological concentration of selenium (2.5 μM) as described in section 2.3.

Table 7.1 Mechanisms of acquired BSO resistance.

Cell Line	Cancer	Selecting Agent	Fold BSO Resistance	Fold Cisplatin Resistance	Mechanism	Reference
KB/BSO1	Epidermoid	BSO	10	0.8	↑γGCS mRNA (subunit not specified) ↓GSTP1 mRNA	(Yokomizo et al., 1995b)
KB/BSO2	Epidermoid	BSO	11	0.8	↑γGCS mRNA (subunit not specified) ↓GSTP1 mRNA	(Yokomizo et al., 1995b)
KB/BSO3	Epidermoid	BSO	13	0.7	↑γGCS mRNA (subunit not specified) ↓GSTP1 mRNA	(Yokomizo et al., 1995b)
CC531/CCBR25	Rat Colorectal	BSO	50	nd	↑Bcl-2 protein, same GSH level	(Vahrmeijer et al., 2000)
HLE/BSO1-1	Hepatic	BSO	35	nd	↑GSH, ↓GSTP1 mRNA and protein, ↑γGCS-Cat mRNA and protein	(Tanaka et al., 1998)
HLE/BSO1-2	Hepatic	BSO	40	nd	↑GSH, ↓GSTP1 mRNA and protein, ↑γGCS-Cat mRNA and protein	(Tanaka et al., 1998)
HLE/BSO2-1	Hepatic	BSO	10	nd	↑GSH, ↓GSTP1 mRNA, ↓γGCS-Cat mRNA	(Tanaka et al., 1999)
HLE/BSO2-2	Hepatic	BSO	6	nd	↑GSH, ↓GSTP1 mRNA, ↓γGCS-Cat mRNA	(Tanaka et al., 1999)
M14-R	Melanoma	BSO	10-20	nd	↓GSTM1 protein, ↓GSTP1 mRNA	(Fruehauf et al., 1998)
ZAZ-R	Melanoma	BSO	10-20	nd	↓GSTM1 protein, no change GSTP1 mRNA	(Fruehauf et al., 1998)

BSO – buthionine sulfoximine, γGCS – gamma glutamyl cysteine synthetase, GSH – glutathione, GST – glutathione-S-transferase, nd – not determined.

Cat or GSTP1 are not involved in the mechanism of BSO resistance or sensitivity in these platinum-resistant cell lines.

BSO resistance may arise from different mechanisms in a platinum resistance model compared to resistant cell lines developed by BSO treatment. Few studies have examined BSO cytotoxicity in a model of acquired resistance to another drug. The vast majority of studies use BSO in its traditional fashion, to inhibit glutathione synthesis and to determine if BSO modulates the resistance. Studies which have studied BSO cytotoxicity include, a doxorubicin-resistant SCLC cell line which was cross-resistant to both cisplatin and BSO (Larsson et al., 1991), however the mechanism of resistance to all three compounds was not determined. Another doxorubicin-resistant SCLC cell line, the H69AR cells were sensitive to both cisplatin and BSO (Cole et al., 1990; Campling et al., 1991). However, the H69AR cells had decreased glutathione levels from the parental H69 cells, which explains the increased sensitivity to both cisplatin and BSO.

An increase in the expression of the anti-apoptotic protein Bcl-2 has also been associated with resistance to BSO in rat colorectal cancer cells (Vahrmeijer et al., 2000). These cells had no change in glutathione similar to the H69CIS200 cells. BSO treatment has also been shown to upregulate Bcl-2 expression in leukemia cells (D'Alessio et al., 2004). Increases (Sartorius et al., 2002) and decreases (Henness et al., 2002; Kumar et al., 2004) in the expression of Bcl-2 have been associated with platinum resistance in SCLC cell models.

Changes in the expression of γGCS and GSTP1 do not explain the BSO resistance in the H69CIS200 cells and BSO sensitivity in the H69OX400 cells. BSO resistance in platinum-resistant cell lines may therefore work differently to that of models developed with BSO selection (Table 7.1). Increased expression of Bcl-2 has also been associated with BSO resistance and should be further investigated in the H69CIS200 and H69OX400 cells in the future.

7.6.2 Platinum resistance and the glutathione pathway

There is an increased expression of glutathione related genes in response to oxaliplatin in all cell lines, but only in response to cisplatin in the H69OX400 cell line. This suggests that this pathway is more important in the response to oxaliplatin than cisplatin in these cell models.

Increased expression of γGCS-Cat mRNA and protein have been associated with cisplatin resistance in ovarian and colon carcinoma (Iida et al., 1999). However, the H69CIS200 and H69OX400 cells showed a decrease in γGCS protein and a further significant decrease on platinum drug treatment (Figure 7.2). If the expression of γGCS-Cat protein is drastically inhibited by platinum then this may explain the limited impact of BSO on the cytotoxicity of platinum as there is less to inhibit (Figure 3.11). However, the pattern of inhibition is the same in both resistant cell lines, so this does not explain the resistance of the H69CIS200 and the sensitivity of the H69OX400 cells to BSO.

When treated with cisplatin or oxaliplatin the resistant cell lines increase their glutathione levels to the same extent as the parental cell line (Figure 3.10). This increase in glutathione is unlikely to be mediated by γGCS-Cat as its expression is drastically inhibited by treatment with platinum. The increase in cellular glutathione must therefore be mediated by the glutathione salvage pathway or downstream of the rate limiting enzyme γGCS (Figure 1.4).

γGlutamyl transpeptidase (γGT) controls the synthesis of glutathione by salvage from outside the cell rather than de novo synthesis which is governed by γGCS (Figure 1.4). Increased expression of γGT mRNA was associated with increased glutathione in both cisplatin- (Godwin et al., 1992) and oxaliplatin-resistant ovarian carcinoma cell lines (El-akawi et al., 1996). The expression of γGT should be examined in the H69CIS200 and H69OX400 cells in future studies.

7.6.3 Platinum resistance and the thioredoxin pathway

An increase in the expression of thioredoxin has been associated with cisplatin resistance in HeLa cells (Nakamura et al., 2000). An increase in expression of thioredoxin by transfection has also led to cisplatin resistance in some cell models (Sasada et al., 1996) but not others (Yamada et al., 1997). This suggests that an increase in thioredoxin may lead to cisplatin resistance but is not sufficient to produce resistance in all circumstances. Thioredoxin expression is decreased in response to platinum drug treatment in the H69 parental cell line. Thioredoxin expression is also decreased in both the untreated H69CIS200 and H69OX400 cell lines. Thioredoxin expression is upregulated to the level of the parental cells in response to platinum treatment in the H69CIS200 cells, but not in the H69OX400 cells (Figure 7.4). There is therefore no increase in thioredoxin expression in the resistant cells contributing to the mechanism of platinum resistance.

The cellular distribution of thioredoxin remained unchanged between the sensitive and resistant cell lines and there was no change in response to platinum drug treatment. However, the localisation of thioredoxin in the cell, highly expressed in the nucleolus may give some indication as to its biological function. Thioredoxin has been previously shown to be present in the nucleolus of endometrial stromal cells (Maruyama et al., 1999) but not with as strong staining as observed in Figures 7.5, 7.6 and 7.7. The nucleolus is responsible for the biosynthesis of ribosomes, which control the translation of proteins (Uvarov et al., 1993). Cisplatin treatment has been shown to inhibit the synthesis of ribosomal RNA in HeLa cells (Jordan et al., 1998). Perhaps thioredoxin is partly responsible for maintaining the redox state of the nucleolus ensuring the successful synthesis of ribosomes.

Thioredoxin reductases play a large role in protection against oxidant stress due to their broad substrate specificity. They reduce not only thioredoxin but other proteins as well. The broad substrate specificity of mammalian thioredoxin reductase is due to a second redox-active site, a C-terminal -Cys-SeCys- (where SeCys is selenocysteine), that is not found in glutathione reductase (Mustacich et al., 2000). The availability of selenium is a key factor determining thioredoxin reductase activity both in cell culture and *in vivo*. Exposure of cell cultures to selenite leads to a large

increase in thioredoxin reductase activity highlighting an important trace element deficiency in some culture media (Berggren et al., 1997; Bjorkhem-Bergman et al., 2002). The addition of a physiological concentration of selenium to a platinum cytotoxicity assay showed no effect in all cell lines (Figure 7.8). This suggests that there is no difference in the expression of thioredoxin reductase between the sensitive and resistant cell lines. Unlike glutathione reductase, thioredoxin reductase is efficiently inhibited by treatment with cisplatin or oxaliplatin at similar doses to that used in the platinum cytotoxicity assays (Witte et al., 2005). This suggests that an increased expression of thioredoxin reductase is unlikely to be involved in a mechanism of platinum resistance as it is inhibited by this group of compounds.

Several studies have demonstrated a correlation between the cellular toxicity of cisplatin and the inhibition of the activity of thioredoxin reductase (Arner et al., 2001; Witte et al., 2005). When platinum enters a cell possibly only 1% of the intracellular cisplatin actually reacts with genomic DNA while the major intracellular metabolite is the glutathione-platinum conjugate, accounting for up to 60% of the intracellular platinum content (Arner et al., 2001). Glutaredoxin is a small 12 kDa dithiol protein similar in function to thioredoxin. Thioredoxin reacts to all reactive oxygen species whereas glutaredoxin is reduced by glutathione, which in turn is reduced by NADPH and glutathione reductase (Song et al., 2002). The glutathione-platinum conjugate has been shown to be an inhibitor of both the thioredoxin and glutaredoxin systems, demonstrating an additional level of cisplatin derived inhibition of these central systems for cellular thiol redox control (Arner et al., 2001). Figure 7.9 shows the inhibition of the thioredoxin and glutaredoxin systems by cisplatin and cisplatin-glutathione conjugates. There is a decrease in thioredoxin protein in the H69CIS200 and H69OX400 resistant cell lines and in response to platinum drug treatment in all cell lines. Decreased activity of thioredoxin reductase and the thioredoxin system have been associated with the response to cisplatin, this inhibition may extend to a decrease in thioredoxin protein synthesis in the H69 cells and resistant cell lines.

There is no upregulation of the thioredoxin system contributing to the mechanism of platinum resistance in the H69CIS200 and H69OX400 cells. Rather there is a decrease in thioredoxin expression. However, this result provides further evidence of change in redox related pathways associated with the cellular response to platinum

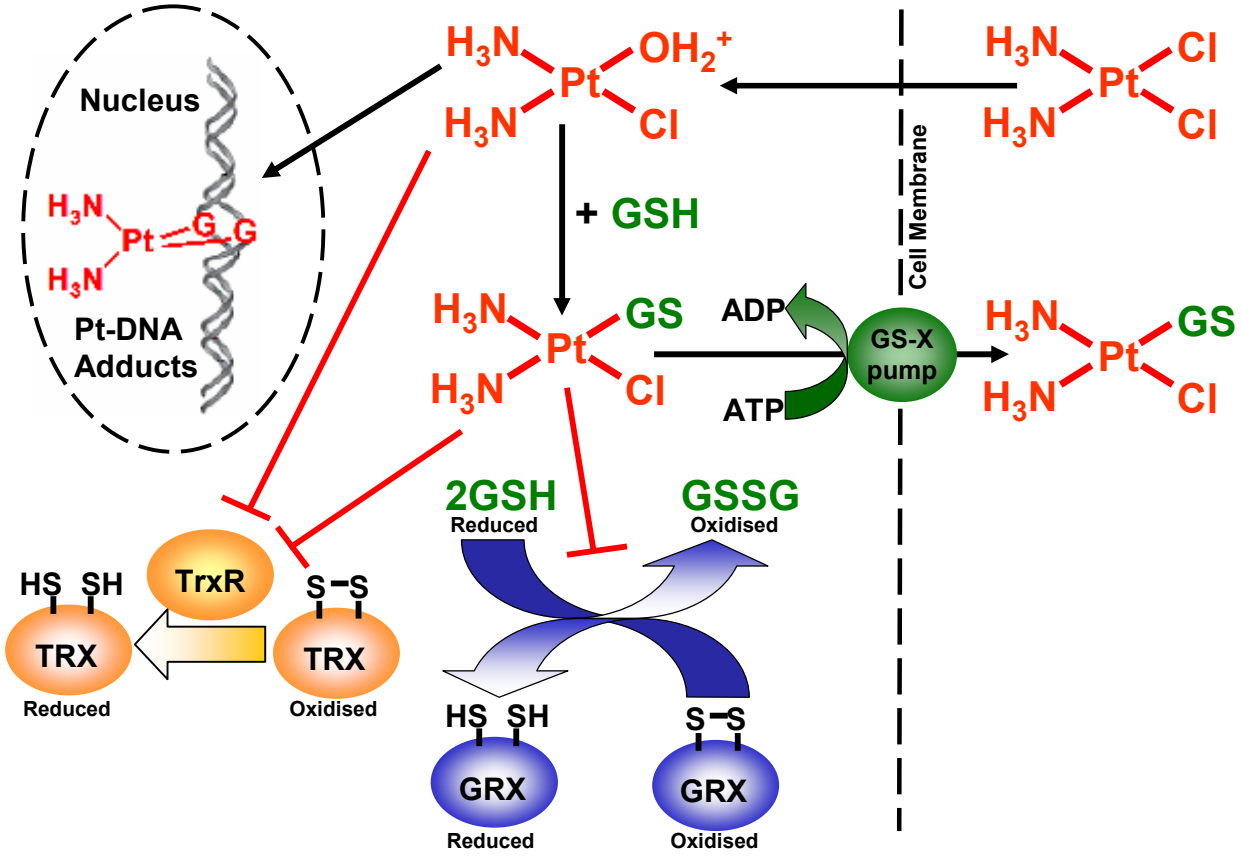

Figure 7.9 Cisplatin metabolism and inhibition of the thiol redox systems. Cisplatin is conjugated to glutathione and effluxed from the cell via the GS-X pump. Cisplatin and cisplatin-glutathione conjugates inhibit the function of both the thioredoxin and glutaredoxin systems. Adapted from Arner et al., 2001.

GSH/GSSG – glutathione, GRX - glutaredoxin, GS-X – glutathione conjugate, TRX – thioredoxin, TrxR – thioredoxin reductase.

drug treatment. Perhaps a change in redox mediated cell signalling may be more important than the redox state of the cell in the resistance of the H69CIS200 and H69OX400 cells.

7.6.4 Redox related signalling and platinum resistance

Apoptosis signal-regulating kinase 1 (ASK1) is part of the MAP kinase signalling pathway and plays an important part in control of activation of the apoptotic pathways. ASK1 is a MAP kinase kinase kinase and is therefore at the top of the MAP kinase signalling cascade. ASK1 is activated in response to various cytotoxic stresses and activates the JNK and p38 and apoptotic pathways (Ichijo et al., 1997; Tobiume et al., 2001). ASK1 is pivotal in the cellular decision making process of life versus death as it responds to the redox state of the cell (Saitoh et al., 1998; Song et al., 2002; Song et al., 2003) and interacts with both the Bcl-2 (Yamamoto et al., 1999) and Fas mediated apoptotic pathways (Cho et al., 2001).

Thioredoxin in its reduced state was found to associate with the N-terminal portion of ASK1 whereas reduced glutaredoxin, associates with the C-terminal portion of ASK1 (Song et al., 2003). Bound thioredoxin or glutaredoxin inhibits ASK1 kinase activity as well as apoptosis. Thioredoxin and glutaredoxin are released from ASK1 in response to increasing levels of reactive oxygen species in the cell triggering the apoptotic pathway. Glutaredoxin oxidises and dissociates from ASK1 in a highly specific manner using reduced glutathione (Song et al., 2002; Song et al., 2003), whereas thioredoxin oxidises and dissociates in response to increased reactive oxygen species (Saitoh et al., 1998; Liu et al., 2002b).

Cisplatin treatment activates multiple signal transduction pathways, which can lead to several cellular responses including cell cycle arrest, DNA repair, survival or apoptosis (Persons et al., 1999). Activation of ASK1 in response to the stress of cisplatin treatment has been demonstrated in several cell lines (Chen et al., 1999; Desbiens et al., 2003). The inhibition of the formation of the reduced state of thioredoxin and glutaredoxin by cisplatin and cisplatin-glutathione conjugates, discussed previously (Figure 7.9), may be a mechanism of activation of ASK1 (Figure 7.10). A decrease in thioredoxin protein expression as in the response to platinum

drug treatment in the parental and resistant cell lines (Figure 7.4) would also lead to an increase in ASK1 activity. This may, in part, mediate the apoptotic response to cisplatin.

Cisplatin activation of ASK1 can be prevented via phosphorylation of ASK1 at Ser-83, resulting in an inhibition of its kinase activity (Yuan et al., 2003). The protein AKT2 is frequently overexpressed in cancer cells and can phosphorylate ASK1 to its inactive state, therefore blocking downstream apoptotic signalling and playing an important role in chemoresistance (Yuan et al., 2003). The activation of the PI3K/Akt/mTOR pathway has been discussed in Chapter 6 and may play a role in the mechanism of platinum resistance in the H69CIS200 and H69OX400 cells. The activation of the PI3K/Akt/mTOR pathway may counteract the apoptotic response mediated by ASK1 (Figure 7.10).

The P and M classes of glutathione-S-transferases play a regulatory role in the MAP kinase pathway via protein interactions with JNK1 and ASK1 (Townsend et al., 2003b). GSTP1 binds to the C-terminus of JNK1 inhibiting its kinase activity (Wang et al., 2001). GSTP1 has also been shown to inhibit apoptosis in ASK1 overexpressing cells (Gilot et al., 2002). GSTM1 binds to the N-terminal of ASK1 and inhibits its kinase activity (Cho et al., 2001; Dorion et al., 2002). GSTM1 dissociates from ASK1 in response to heat shock, not oxidative stress like thioredoxin and glutaredoxin (Dorion et al., 2002). GSTs can therefore serve two distinct roles in the development of platinum drug resistance via direct detoxification as well as acting as an inhibitor of apoptosis via the MAP kinase pathway (Townsend et al., 2003b). The increases in GSTP1 mRNA expression observed in the H69 cells and the resistant cell lines on treatment with platinum (Figure 7.1) may therefore have two roles, conjugation to glutathione and inhibition of the apoptotic pathway.

7.7 Conclusion

The glutathione and thioredoxin systems are not being upregulated to provide an increased redox capacity in the platinum-resistant cell lines. However the decrease in thioredoxin protein expression may be part of the apoptotic signalling response to

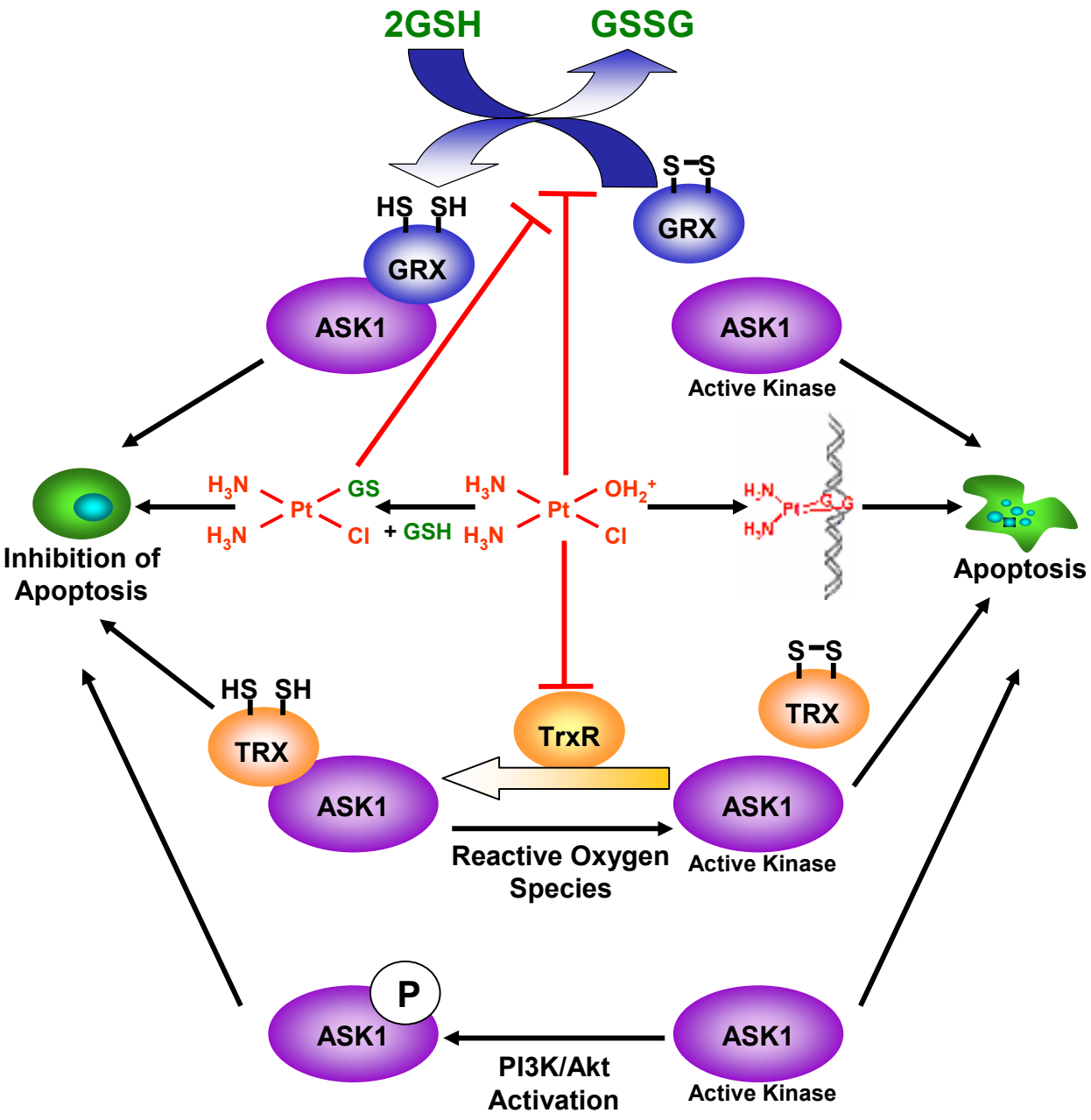

Figure 7.10 Regulation of ASK1 kinase activity by cisplatin. The dissociation of either thioredoxin or glutaredoxin from ASK1 in response to cisplatin, cisplatin generated reactive oxygen species and cisplatin-glutathione conjugates leads to the activation of ASK1 and initiation of apoptotic signalling. The activation of ASK1 can be inhibited by phosphorylation mediated by Akt.

ASK1 – apoptosis signal regulating kinase 1, GSH/GSSG – glutathione, GRX - glutaredoxin, TRX – thioredoxin, TrxR – thioredoxin reductase.

cisplatin treatment. Redox mediated apoptotic signalling may therefore play a role in both the cytotoxic response and resistance to platinum in this model.

The BSO resistance in the H69CIS200 cells is not being mediated by changes in γGCS and GSTP1 expression as in cells with acquired BSO resistance, as the BSO-sensitive H69OX400 cells show the same pattern of mRNA and protein expression for these genes. The involvement of γGT and Bcl-2 should be further examined to help understand the BSO resistance and sensitivity in this platinum-resistant model.

CHAPTER 8.0

DNA REPAIR PATHWAYS, CELL CYCLE CHECKPOINTS AND PLATINUM DRUG RESISTANCE

8.1 Introduction

Many genes associated with DNA repair were found to be differentially expressed by the Atlas nylon array analysis in Chapter 5. Analysis of mRNA expression was performed by real-time PCR. Protein expression was analysed for some genes by Western blot. mRNA and protein samples were isolated from the H69, H69CIS200 and H69OX400 cell lines under the following conditions, untreated controls, cells treated with either 200 ng/ml cisplatin or 400 ng/ml oxaliplatin for 4 days. All mRNA and protein expression levels were analysed in comparison to untreated H69 cells.

8.2 DNA repair

8.2.1 MutY homolog (MutY)

MutY has been linked the long patch base excision DNA repair pathway, and acts as part of the recognition step for a mispaired adenine to a guanine base (Parker et al., 200□). MutY mRNA was significantly decreased in both untreated resistant cell lines H69CIS200 (-2.75-fold) and H69OX400 (-2.18-fold) compared to the untreated H69 cells (Figure 8.1). MutY was also further significantly decreased on cisplatin drug treatment in the H69 parental cells (-□.24-fold) and in the H69CIS200 cells (-□.94-fold). However, MutY was restored to the level of the untreated H69 cells by treating the H69CIS200 cells with cisplatin and the H69OX400 cells with cisplatin or oxaliplatin.

8.2.2 RAD51 Homolog 2 (RAD51B)

Double-strand breaks and interstrand cross links in DNA can be produced by cisplatin or cisplatin induced reactive oxygen species. One mechanism for repairing these breaks and cross links is homologous recombination repair which is in part mediated by RAD51 proteins. Homologous recombination recovers the information lost in DNA damage from a homologous piece of DNA such as the second copy of a chromosome (Figure 1.8A) (Sancar et al., 2004). There was no change in RAD51B in the untreated resistant cell lines (Figure 8.1). There was a trend for increased expression of RAD51B mRNA on cisplatin and oxaliplatin drug treatment in all cell

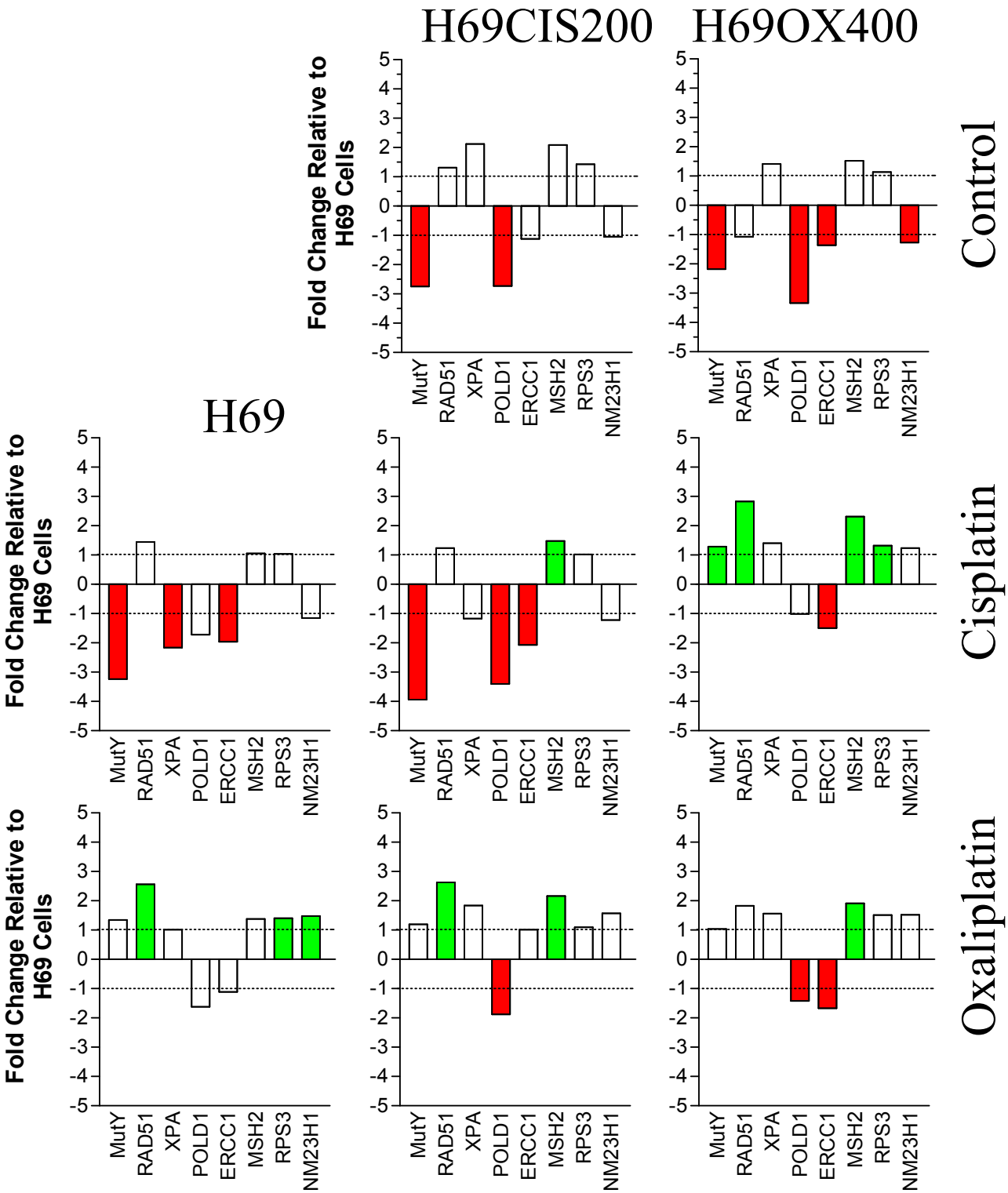

Figure 8.1 mRNA expression data for DNA repair genes. H69, H69CIS200 and H69OX400 cells were grown for four days either in drug-free media, 200 ng/ml cisplatin or 400 ng/ml oxaliplatin. mRNA was extracted, converted to cDNA and assayed by real time PCR as described in section 2.12. Means of duplicate experiments are presented, standard deviations have been omitted for clarity. Significant increases from the H69 control are indicated in green, significant decreases in red. Significant differences were determined using a student's t-test $p < 0.05$. Replotted from Figure 5.4

lines in comparison to untreated H69 cells. RAD51B mRNA expression was significantly increased on cisplatin treatment in the H69OX400 cells (2.83-fold) and on oxaliplatin treatment in the H69 (2.56-fold) and H69CIS200 cells (2.63-fold).

The protein expression of RAD51B was analysed by Western blot (Figure 8.2). There was an overall trend for decreased expression of RAD51B associated with platinum resistance and drug treatment. This decrease was significant in the H69OX400 cells treated with oxaliplatin. This is in contrast to the increases in RAD51B mRNA expression observed in response to platinum drug treatment.

The cellular distribution of RAD51B was analysed by immunocytochemistry. After exposure to DNA damage, RAD51 is concentrated in multiple discrete foci, which are thought to represent nuclear domains for homologous recombination repair (Raderschall et al., 2002). Therefore the morphology of RAD51 can indicate if it is actively repairing DNA. RAD51B foci were examined in the H69, H69CIS200 and H69OX400 cell lines. The same treatment conditions as used for the mRNA and protein analysis were used, untreated controls (Figure 8.3), cisplatin (Figure 8.4) and oxaliplatin (Figure 8.5) treated cells exposed for 4 days.

The number of cells positive for RAD51B foci was counted for 6 fields of view under the microscope, analysing in total around 400 cells per slide. Cells were deemed positive for RAD51B foci if they had greater than 5 foci in their nuclei, this criteria has been used in other RAD51 studies (Russell et al., 2003). Figure 8.6 presents the percentage of cells staining positive for RAD51B foci. The H69 control cells had 30.9% of cells positive for RAD51B foci, which indicates the normal activity of homologous recombination. When the H69 sensitive cell line is treated with platinum drugs the level of RAD51B foci increases to 62.3% with cisplatin and 55% with oxaliplatin treatment. The untreated H69CIS200 cells have 43.2% cells positive for RAD51B foci which is a higher level than the untreated H69 cells indicating a higher rate of homologous recombination in these cells without recent exposure to DNA damaging agents. The H69CIS200 cells treated with cisplatin show an increase in RAD51B foci, 58.9%. The H69CIS200 cells treated with oxaliplatin show a decrease in RAD51B foci, 31.7%, which is similar to the level of foci in the untreated parental cell line. The H69OX400 cells showed lower levels of RAD51B foci under all

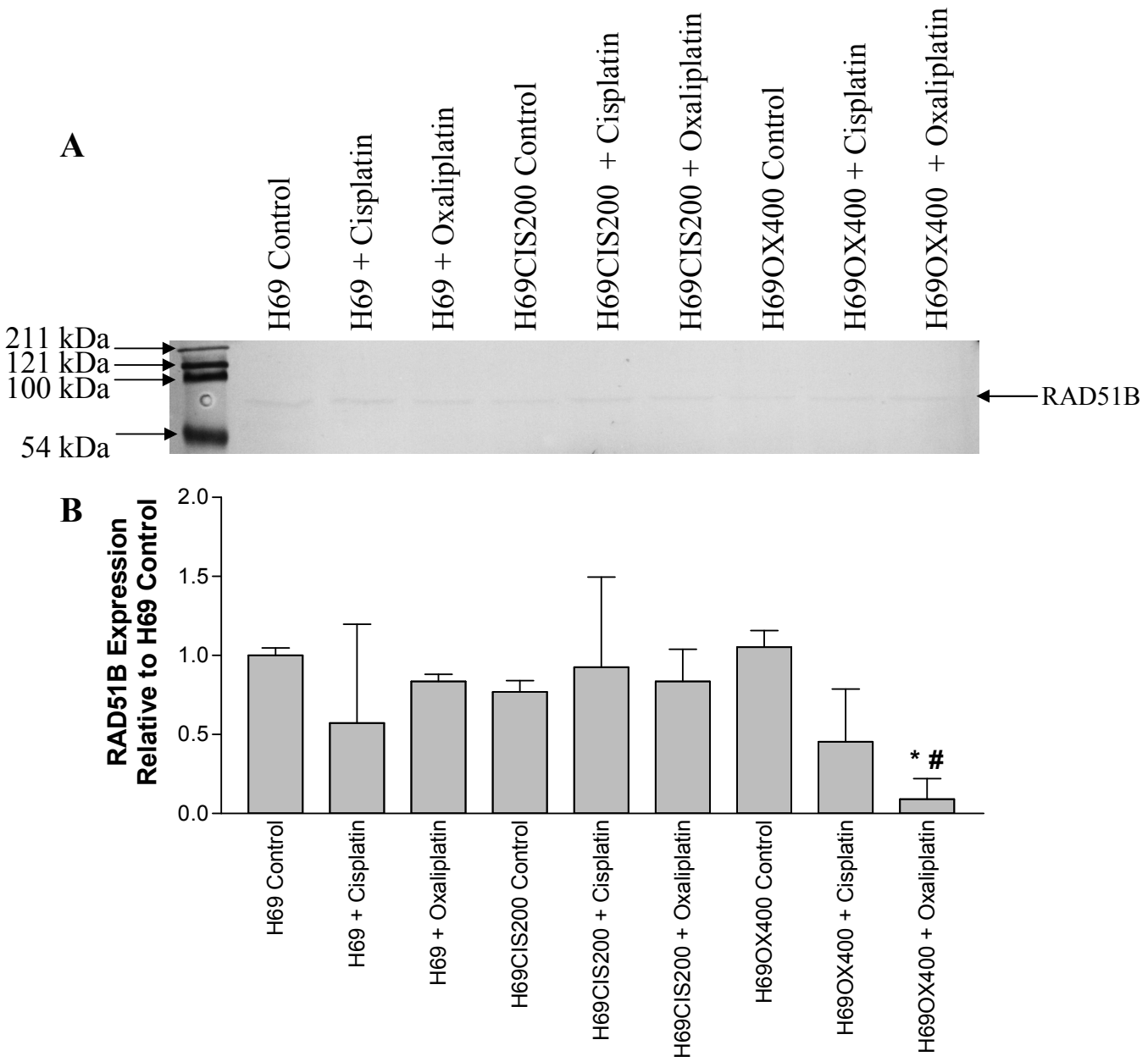

Figure 8.2 RAD51B protein expression determined by Western blot. A) H69, H69CIS200 and H69OX400 cells were grown for four days either in drug-free media, 200 ng□ml cisplatin or 400 ng□ml oxaliplatin. Total protein was extracted and 20 µg subjected to SDS-PAGE and Western blotting as described in section 2.13. RAD51B was detected with a primary antibody and an alkaline phosphatase labelled secondary antibody as described in section 2.13.4.1. B) Quantitation of the RAD51B bands was determined by Quantity-one software and adjusted for protein loading by ponceau staining. The mean and standard deviation of two independent experiments are presented. * - Significant decrease from H69 control, # - significant decrease from H69OX400 control as determined by the student's t-test $p<0.05$.

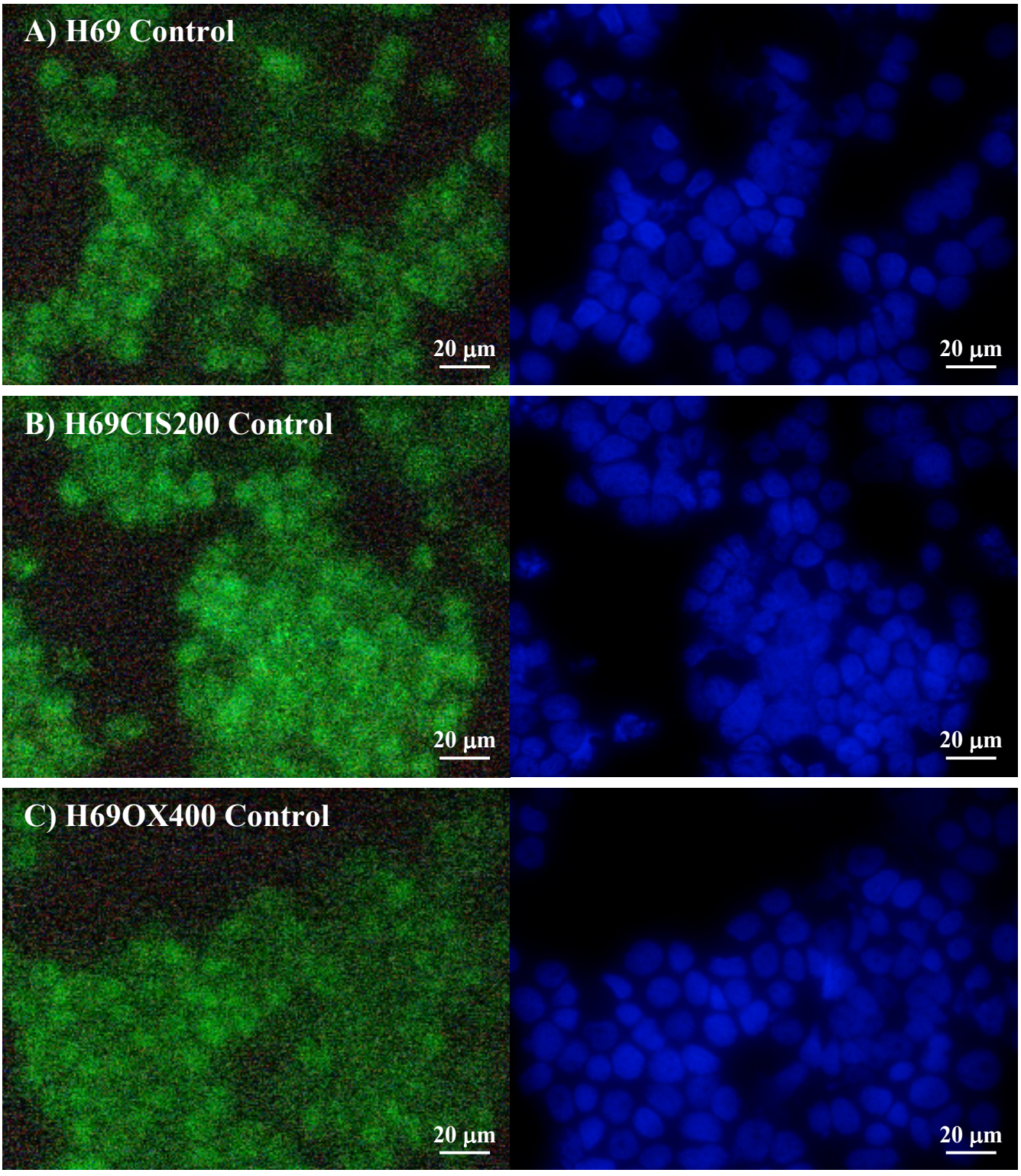

Figure 8.3 RAD51B immunocytochemistry control cells. A) H69 B) H69CIS200 and C) H69OX400 cells were grown for 4 days in drug-free culture and prepared as cytospins. Slides were stained with a RAD51B primary antibody and detected with a FITC labelled secondary antibody shown on the left and counterstained with DAPI shown on the right as described in section 2.14.

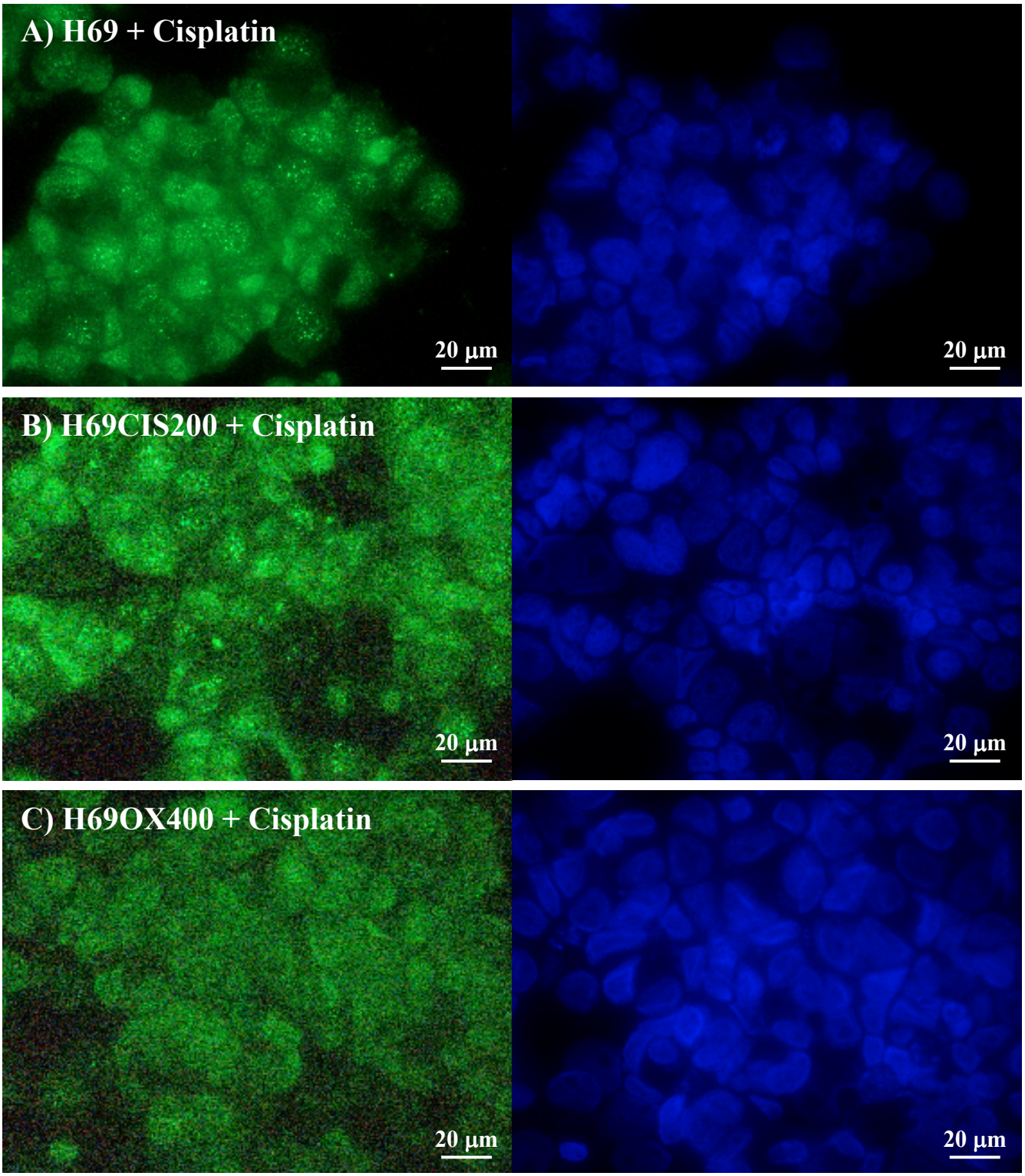

Figure 8.4 RAD51B immunocytochemistry cisplatin treated cells. A) H69 B) H69CIS200 and C) H69OX400 cells were grown for 4 days in 200 ng/ml cisplatin and prepared as cytospins. Slides were stained with a RAD51B primary antibody and detected with a FITC labelled secondary antibody shown on the left and counterstained with DAPI shown on the right as described in section 2.14.

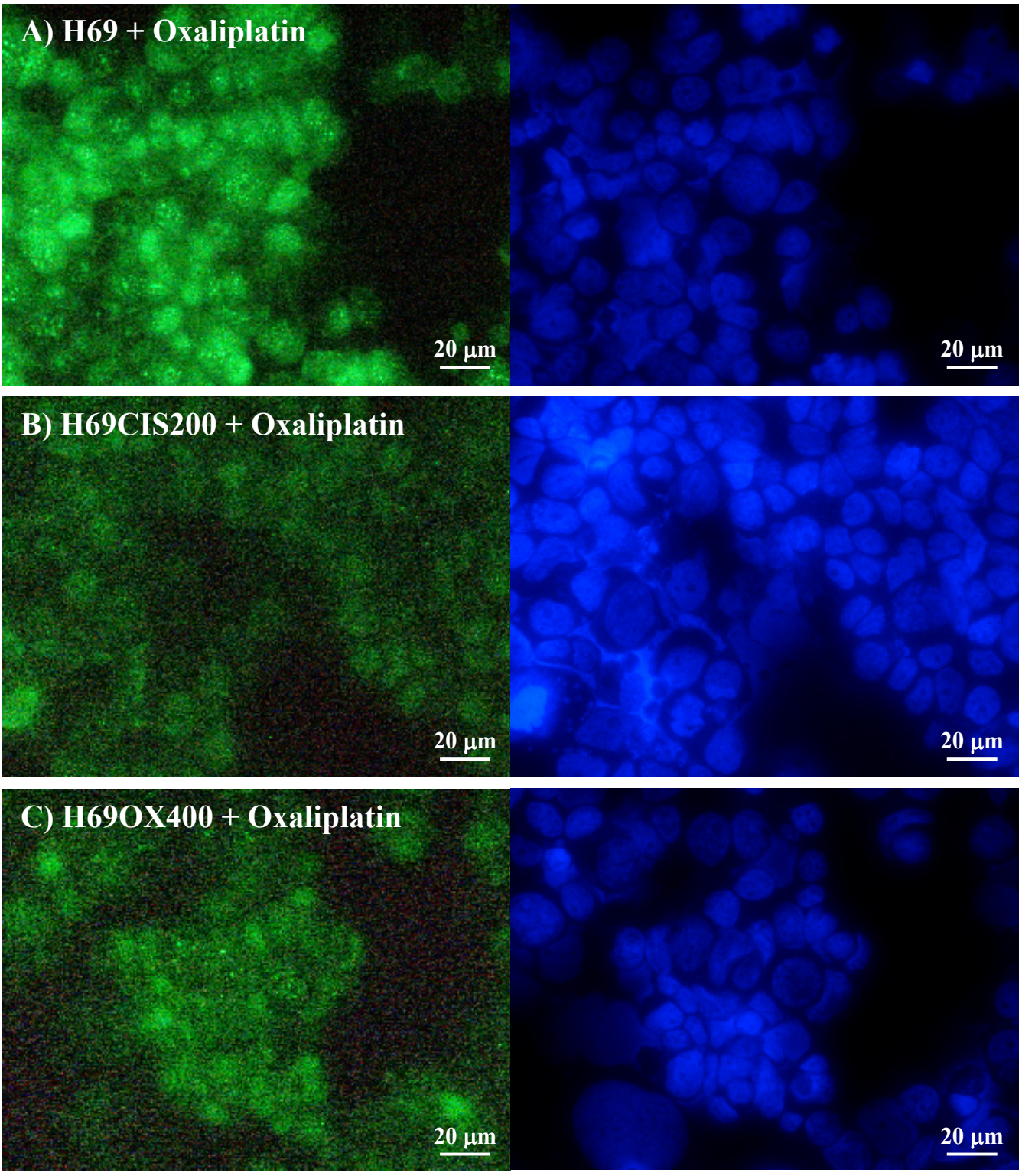

Figure 8.5 RAD51B immunocytochemistry oxaliplatin treated cells. A) H69 B) H69CIS200 and C) H69OX400 cells were grown for 4 days in 400 ng/ml oxaliplatin and prepared as Slides were stained with a RAD51B primary antibody and detected with a FITC labelled secondary antibody shown on the left and counterstained with DAPI shown on the right as described in section 2.14.

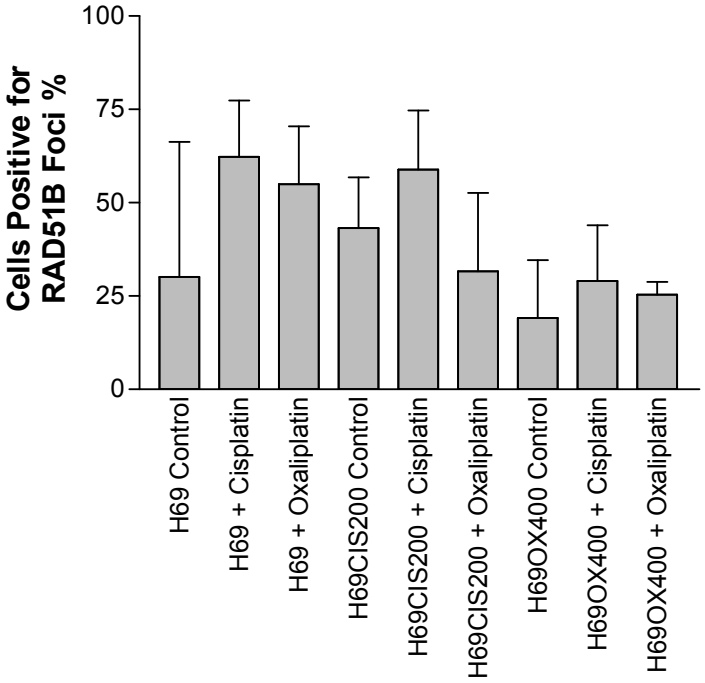

Figure 8.6 Percentage of cells staining positive for RAD51B foci. Cytospun slides were stained with RAD51B and a DAPI counterstain as described in section 2.14. 6 fields of view were photographed for each slide, recording both the FITC stained RAD51B and DAPI stained nuceli. The number of cells in each field was determined by counting the nuclei. The number of cells with RAD51B foci was determined by counting all cells with greater than 5 foci in their nuclei. Greater than 400 cells were analysed per slide. The number of RAD51B foci cells was then compared as a percentage. The mean and standard deviation of the percentage obtained for two independent experiments is presented above.

conditions, control 19.1%, cisplatin treated 29.0% and oxaliplatin treated 25.4%. This suggests both a lower rate of homologous recombination in response to oxaliplatin in the resistant cell lines and a lower level of homologous recombination in the H69OX400 in response to DNA damage. This is consistent with the lower RAD51B protein expression observed in the platinum treated H69OX400 cells (Figure 8.2).

8.2.3 Xeroderma pigmentosum group A complementing protein (XPA)

XPA is involved in nucleotide excision repair the major DNA repair pathway responsible for removing platinum adducts from DNA. XPA helps stabilise the unwound DNA so the damaged piece of DNA can be excised and removed from the strand. (Figure 1.7). There was a trend for increased XPA mRNA expression in the untreated resistant cell lines compared to untreated H69 cells. There was a significant decrease in XPA mRNA expression in H69 cells treated with cisplatin (-2.16-fold), there was no change in H69 cells treated with oxaliplatin (Figure 8.1). There was no significant change or consistent trend in XPA mRNA expression in response to platinum drug treatment in the resistant cell lines.

8.2.4 DNA polymerase delta catalytic subunit (POLD1)

DNA polymerase δ (POLD1) is one of the DNA polymerases that cannot bypass platinum adducts. POLD1 is involved in normal DNA replication and in the last steps of nucleotide excision repair and base excision repair (long patch) (Figures 1.7 and 1.9). POLD1 mRNA expression was decreased in the untreated resistant cell lines and in response to platinum drug treatment (Figure 8.1). POLD1 mRNA was significantly decreased in untreated H69CIS200 (-2.73-fold) and H69OX400 (-3.34-fold) cells. POLD1 was significantly decreased in the H69CIS200 cells treated with cisplatin (-3.40-fold) and oxaliplatin (-1.88-fold). POLD1 was also significantly decreased in the H69OX400 cells treated with oxaliplatin (-1.42-fold).

8.2.5 Excision repair deficiency complementation group 1 (ERCC1)

ERCC1 is also involved in the nucleotide excision repair removal of platinum adducts. It binds to XPF and cuts on the 5' side of the damaged DNA to be excised and replaced (Figure 1.7). There was an overall trend of decreased ERCC1 mRNA expression in the resistant cell lines and in response to platinum drug treatment compared to the untreated H69 cells (Figure 8.1). The mRNA expression of ERCC1 was significantly decreased in all cell lines in response to cisplatin treatment, H69 (-1.96-fold), H69CIS200 (-2.07-fold) and H69OX400 (-1.5-fold). The mRNA expression of ERCC1 was also significantly decreased in untreated H69OX400 cells (-1.36-fold) and in oxaliplatin treated H69OX400 cells (-1.67-fold) compared to the untreated H69 cells.

The protein expression levels of ERCC1 was examined by Western blot (Figure 8.7). There were no significant differences from the H69 control. However, there was a trend for decreased expression of ERCC1 with cisplatin and oxaliplatin treatment in all cells. While this change is consistent with the decreases in ERCC1 mRNA expression, the decrease in protein expression seems to be associated with the formation of a lower molecular weight band. No cleavage product or degradation of ERCC1 has previously been reported in the literature.

8.2.6 MSH2

The mismatch repair protein MSH2 corrects mismatches in replicating DNA (Figure 1.13). The mismatch repair system also plays a role in the cytotoxicity of platinum adducts by triggering an apoptotic response (Figure 1.12). There was a trend for increased MSH2 mRNA expression in the resistant cell lines and in response to platinum drug treatment compared to the untreated H69 cells (Figure 8.1). MSH2 mRNA was significantly increased in response to cisplatin and oxaliplatin treatment in both resistant cell lines. Cisplatin treated H69CIS200 cells showed a 1.48-fold increase and H69OX400 cells a 2.31-fold increase in MSH2 mRNA expression. Oxaliplatin treated H69CIS200 cells showed a 2.16-fold increase and H69OX400 cells a 1.91-fold increase in MSH2 mRNA expression.

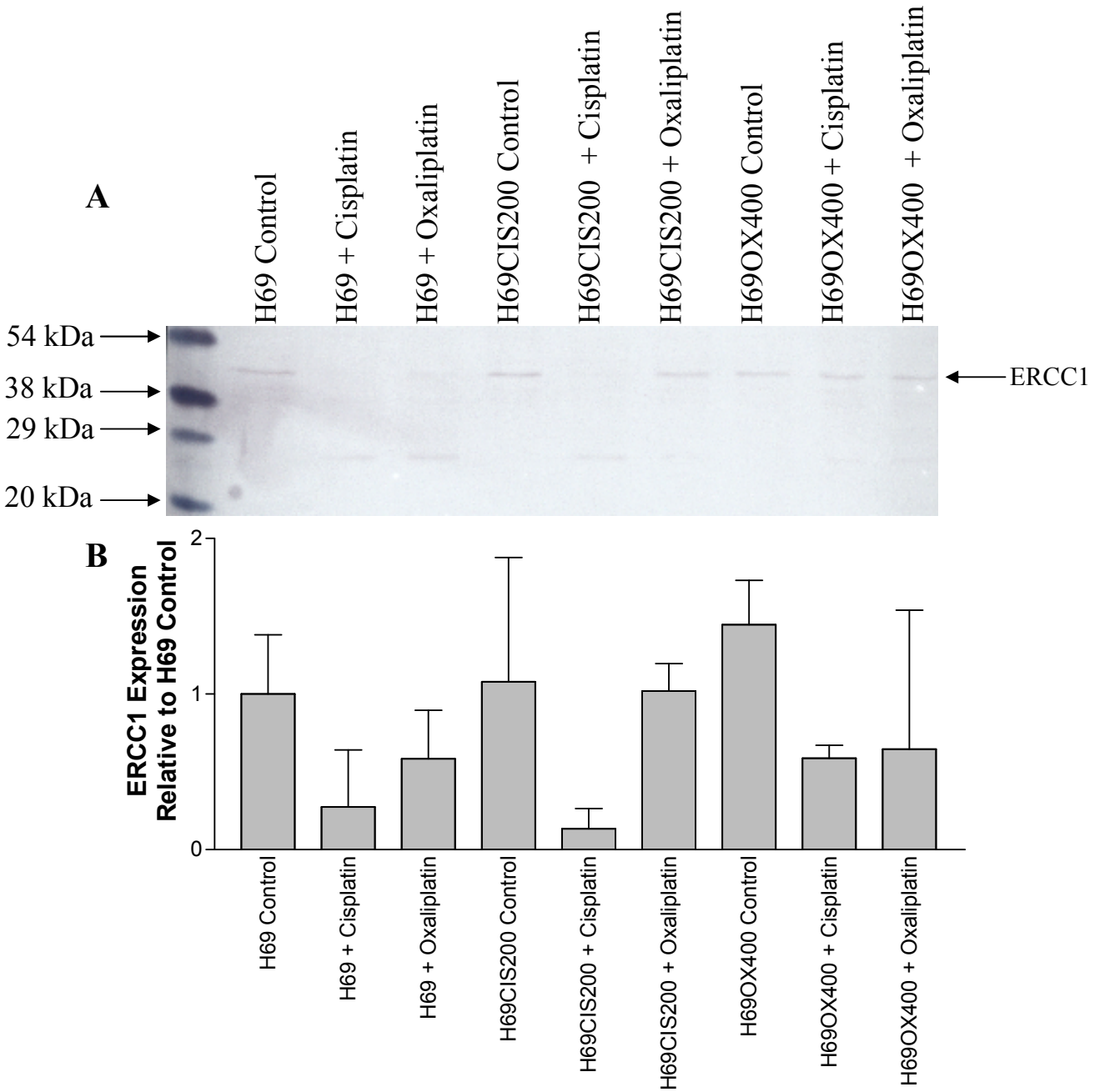

Figure 8.7 ERCC1 protein expression determined by Western blot. A) H69, H69CIS200 and H69OX400 cells were grown for four days either in drug-free media, 200 ng/ml cisplatin or 400 ng/ml oxaliplatin. Total protein was extracted and 20 μg subjected to SDS-PAGE and Western blotting as described in section 2.13. ERCC1 was detected with a primary antibody and an alkaline phosphatase labelled secondary antibody as described in section 2.13.4.1. B) Quantitation of the RAD51B bands was determined by Quantity-one software and adjusted for protein loading by ponceau staining. The mean and standard deviation of two independent experiments are presented.

MSH2 protein expression levels were determined by Western blot (Figure 8.8). MSH2 appeared as a doublet, each band was quantitated separately and as together for total MSH2 expression. There were no significant differences in MSH2 expression, total, upper or lower band. However, the expression of the lower MSH2 band tended to increase on drug treatment with both cisplatin and oxaliplatin in all cell lines. Little has been reported about phosphorylation of MSH2. However, one study has suggested that phosphorylation is required for MSH2 binding to GT mismatches (Pfeiffer et al., 2004). An increase in the lower MSH2 band may indicate a loss of phosphorylation and therefore a loss of activity in response to platinum drug treatment.

8.2.7 RPS3

Apart from RPS3's role in the ribosomal machinery it also functions as a DNA repair endonuclease in base excision repair (Kim et al., 1995; Hegde et al., 2004) and is involved in apoptosis by activating caspase-8 (Jang et al., 2004). These two separate functions use independent functional domains of the protein, suggesting that DNA repair and apoptotic pathways may crosstalk via RPS3 (Jang et al., 2004). RPS3 has not been previously associated with cisplatin resistance. The expression of RPS3 mRNA was significantly increased compared to untreated H69 cells in H69OX400 cells treated with cisplatin (1.32-fold) and H69 cells treated with oxaliplatin (1.40-fold).

8.2.8 NM23-H1 (NDK1)

Nucleoside diphosphate kinases (NDKs), synthesise nucleoside triphosphates from nucleoside diphosphates and ATP. NM23-H1 which is also known as NDK1 has been reported to also have 3' to 5' exonuclease activity suggesting that, in addition to maintenance of the nucleotide pool balance NM23-H1 may have a role in DNA repair (Yoon et al., 2005). There was a trend for decreased expression of NM23-H1 mRNA in the untreated resistant cell lines and in the H69 and H69CIS200 cells in response to cisplatin. There was a trend for increased expression of NM23-H1 mRNA in response to cisplatin treatment in the H69OX400 cells and in all cell lines in response to oxaliplatin treatment. The only significant differences relative to untreated H69 cells

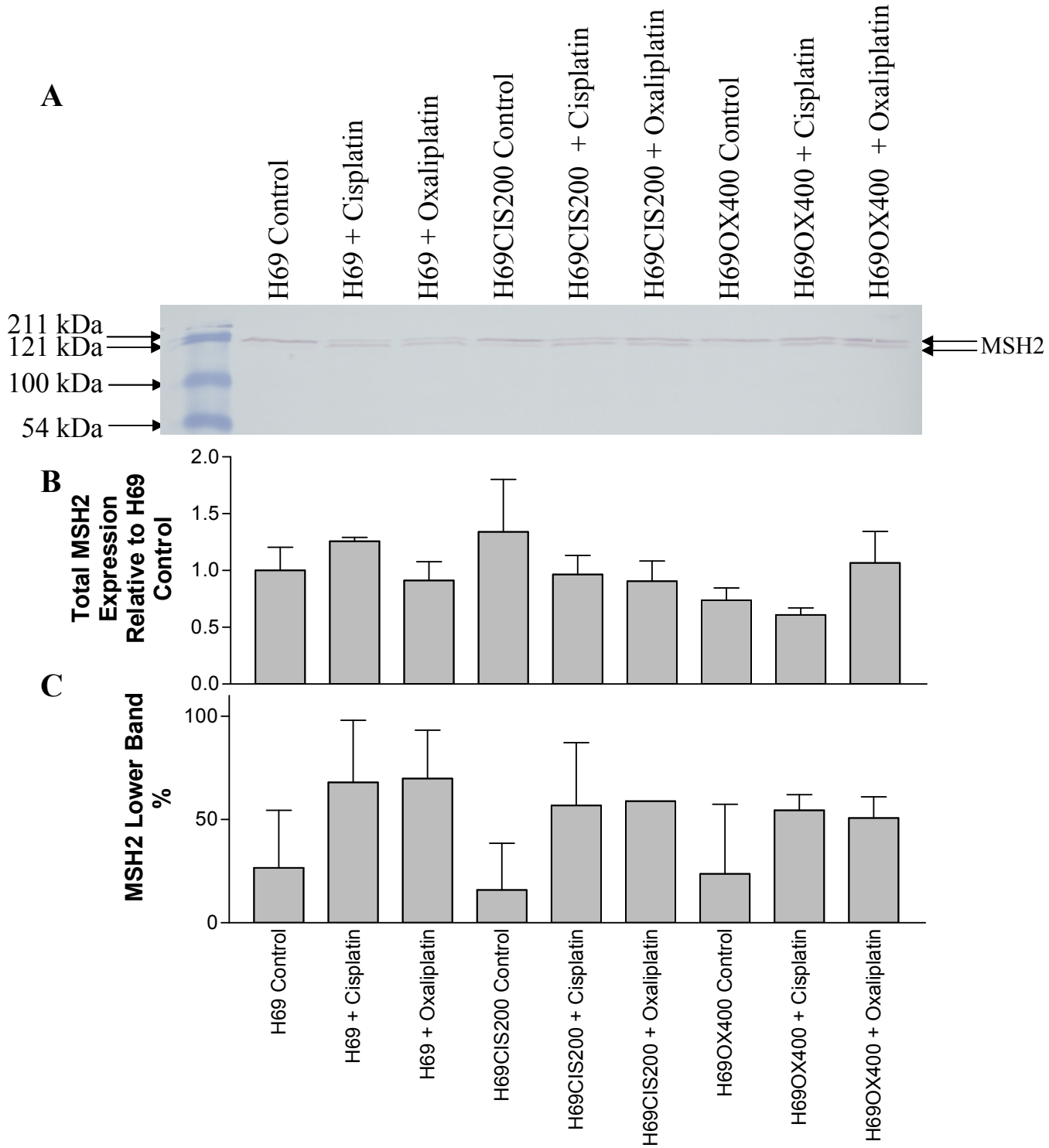

Figure 8.8 MSH2 total protein expression determined by Western blot. A) H69, H69CIS200 and H69OX400 cells were grown for four days either in drug-free media, 200 ng/ml cisplatin or 400 ng/ml oxaliplatin. Total protein was extracted and 20 μg subjected to SDS-PAGE and Western blotting as described in section 2.13. MSH2 was detected with a primary antibody and an alkaline phosphatase labelled secondary antibody as described in section 2.13.4.1. B) Quantitation of the MSH2 doublet and C) The lower MSH2 band percentage was determined by Quantity-one software and adjusted for protein loading by ponceau staining. The mean and standard deviation of two independent experiments are presented.

was a 1.48-fold increase in H69 cells treated with oxaliplatin and a –1.27-fold decrease in untreated H69OX400 cells.

8.3 Determination of radiation resistance

Cells with enhanced DNA repair capacity are often also resistant to radiation. The radiation resistance of the H69, H69CIS200 and H69OX400 cell lines was determined by MTT cytotoxicity assay. The cells exposed at the same cell density as used in the chemotherapy cytotoxicity assays (3.0×10^5 cells/ml) failed to reach an IC_{50} even at high doses of radiation >20 Gy (Figure 8.9A). However, cells exposed at a lower cell density (5.0×10^4 cells/ml) reached an IC_{50} dose (Figure 8.9B). The H69CIS200 cells showed no difference from the parental cell line. However, the H69OX400 cells were significantly 2.68-fold resistant to radiation compared to the parental H69 cells (Figure 8.9C).

8.4 Analysis of genes associated with the cell cycle

The gene for p107 was found to be differentially expressed by the Atlas nylon array analysis (Chapter 5). p107 is a member of the retinoblastoma protein family which controls cell cycle progression from G_1 to S (Kondo et al., 2001). There was no change in the expression of p107 mRNA in untreated H69CIS200 and H69OX400 cells compared to the untreated H69 cells (Figure 8.10). p107 was significantly decreased in response to cisplatin treatment in the H69 (-2.25-fold) and H69CIS200 cells (-1.47-fold). p107 was significantly increased in the H69OX400 cells in rapid activation of the G1/S checkpoint pathway, within 1 hour, incl**u**ding

8.5 Discussion

8.5.1 Nucleotide excision repair

Nucleotide excision repair recognises damaged regions of DNA based on their abnormal structure, then excises and replaces them (Figure 1.7). Nucleotide excision repair is the only mechanism by which bulky DNA adducts, including those generated by platinum drugs, are removed from DNA in human cells (Reardon et al., 1999).

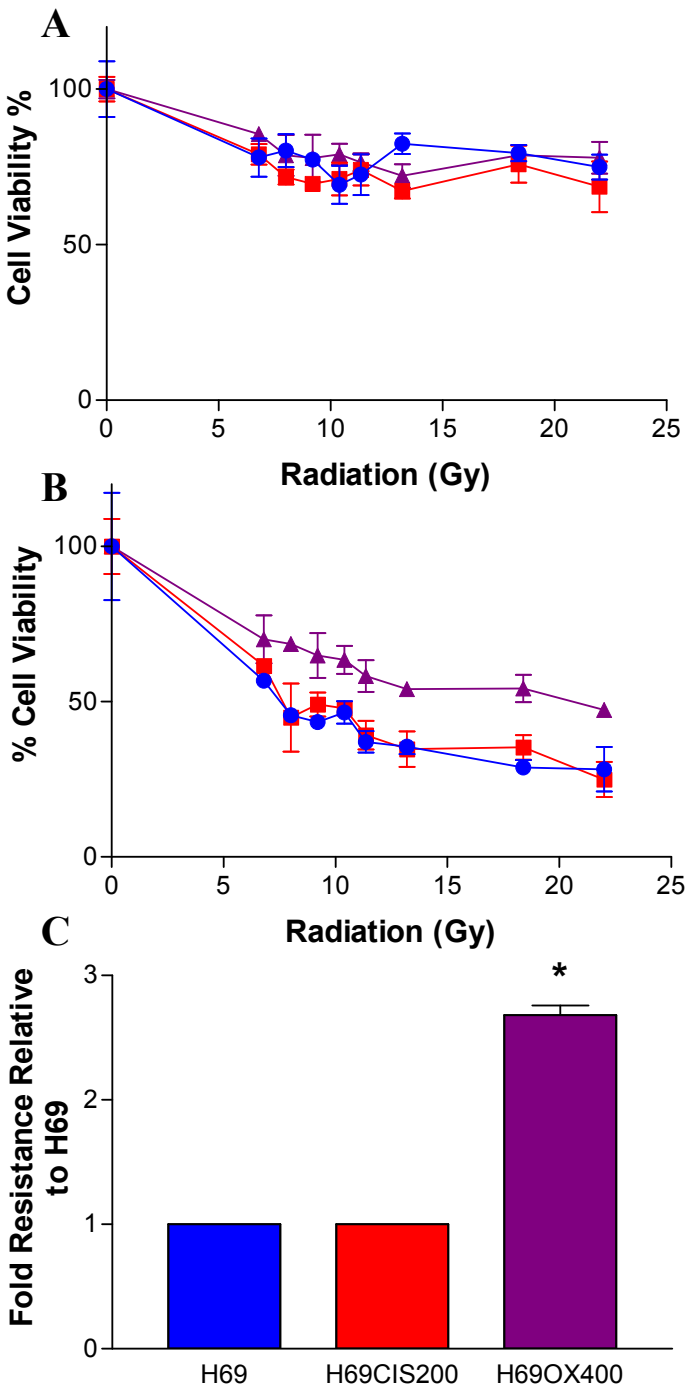

Figure 8.9 Radiation resistance in the H69, H69CIS200 and H69OX400 cells. Resistance of the H69 (●), H69CIS200 (■) and H69OX400 (▲) sublines to radiation was determined using a 5 day MTT cytotoxicity assay as described in section 2.3. A) Cells were at a density of 3 x 10^5/ml B) Cells were at a density of 5 x 10^4/ml. C)The mean fold resistance and standard deviation relative to the H69 cells for the radiation cytotoxicity at 5 x 10^4/ml for at least two independent experiments is shown. Significant differences from the H69 cells as determined by a student's t-test $p<0.05$ is represented by a *****.

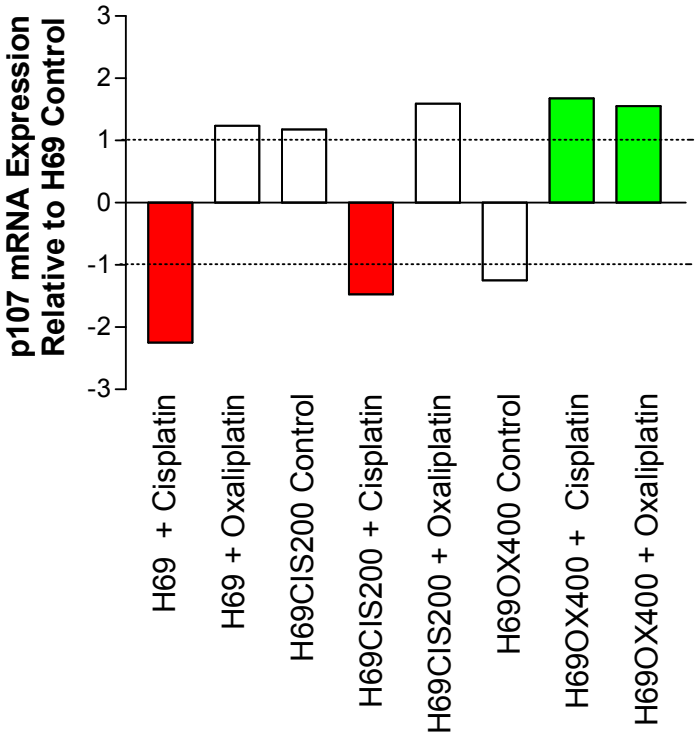

Figure 8.10 mRNA expression of p107. H69, H69CIS200 and H69OX400 cells were grown for four days either in drug-free media, 200 ng/ml cisplatin or 400 ng/ml oxaliplatin. mRNA was extracted, converted to cDNA and assayed by real-time PCR for p107 as described in section 2.12. Means of duplicate experiments are presented, standard deviations have been omitted for clarity. Significant differences from the H69 control are indicated in green, significant decreases in red. Significant differences were determined using a student's t-test $p < 0.05$.

Cisplatin and oxaliplatin DNA adducts are removed to a similar extent by nucleotide excision repair due to its broad substrate range (Reardon et al., 1999). Increased expression of genes and protein products of the nucleotide excision repair pathway have been associated with cisplatin-resistant ovarian carcinoma cells (Ferry et al., 2000; Hector et al., 2001; Selvakumaran et al., 2003), epidermoid carcinoma cells (Mukai et al., 2002) and in platinum-resistant ovarian tumours (Dabholkar et al., 1994).

In contrast, in the H69CIS200 and H69OX400 cells have significant decreases in the expression of genes associated with nucleotide excision repair, ERCC1, XPA and POLD1 (Figure 8.1). The sensitive and resistant cell lines also have decreased ERCC1 protein expression in response to cisplatin and oxaliplatin treatment (Figure 8.7). An increase in nucleotide excision repair is therefore not responsible for the platinum resistance in this cell model.

Decreases in the expression of nucleotide excision repair genes is usually associated with sensitivity to cisplatin, not cisplatin resistance such as in testicular carcinomas which are very sensitive to cisplatin therapy (Koberle et al., 1999). Decreases in the nucleotide excision repair pathway may however, play a role in the regrowth resistance phenotype of the H69CIS200 and H69OX400 resistant cell lines.

8.5.2 Homologous recombination repair

Cross links due to platinum adducts are thought to be repaired by a combination of nucleotide excision repair and homologous recombination repair. Double-strand breaks can be repaired by homologous recombination repair which depends on the RAD51 family of proteins (Figure 1.8). MCF-7 breast cancer cells deficient in homologous recombination repair become hypersensitive to cisplatin (Xu et al., 2005).

RAD51 activity is strictly regulated by a number of RAD51 cofactors including five RAD51 paralogs, RAD51B, RAD51C, RAD51D, XRCC2 and XRCC3. These proteins interact as two independent complexes composed of either RAD51B/C/D/XRCC2 or RAD51C/XRCC3 (Yonetani et al., 2005). A double

deletion of genes involving both complexes had an additive effect on the sensitivity to cisplatin in chicken B lymphocyte cells. The double deletion of genes in the same complex, on the other hand, did not further increase the sensitivity to cisplatin (Yonetani et al., 2005). Chicken B lymphocyte cells which have had RAD51B individually knocked out are also more sensitive to cisplatin (Takata et al., 2000).

There was a trend for increased expression of RAD51B mRNA in response to treatment with both cisplatin and oxaliplatin drug treatment (Figure 8.1). However, there was no consequent increase in RAD51B protein expression (Figure 8.2). There was a significant decrease in RAD51B protein in H69OX400 cells treated with oxaliplatin. A decrease in RAD51B protein would suggest a sensitivity to platinum rather than resistance as observed. Only RAD51B has been examined for mRNA and protein expression so this does not rule out other homologous recombination proteins contributing to the platinum resistance in the H69CIS200 and H69OX400 cells. However, the mRNA of RAD51B was the only homologous recombination protein determined to be differentially expressed by the Atlas nylon array which also screened for RAD51, RAD51C, RAD51D, XRCC2 and BRCA1. XRCC3 was however not screened by the Atlas nylon array.

The analysis of RAD51B foci showed no increase in foci formation in the resistant cell lines in response to drug than in the parental cell line (Figure 8.6). The H69OX400 cells showed lower levels of foci formation in response to cisplatin and oxaliplatin than the parental cell line. The H69CIS200 cells showed an increase in foci formation in response to cisplatin treatment but not to oxaliplatin treatment. Suggesting that homologous recombination repair is more active in response to cisplatin treatment than oxaliplatin treatment in this cell model. There have been no previous studies examining RAD51 in response to oxaliplatin treatment. The platinum resistance in the H69CIS200 and H69OX400 cells is not mediated by an increase in homologous recombination repair due to increased protein expression or activity of RAD51B. Rather a decrease in activity of the homologous recombination pathway is associated with oxaliplatin treatment in this cell model. This is the reverse of what has been previously associated with platinum resistance and may play a role in the regrowth resistance of the H69CIS200 and H69OX400 cell lines.

8.5.3 Mismatch repair

The binding of the mismatch repair complex to damaged DNA can result in either successful mismatch repair (Figure 1.13) or it can trigger an apoptotic response through the inhibition of anti-apoptotic Bcl-2 (Figure 1.12). The binding of the mismatch repair complex to Pt–DNA adducts appears to increase the cytotoxicity of the adducts, either by activating apoptosis or by causing "futile cycling" during translesion synthesis past Pt–DNA adducts (Chaney et al., 2005). Therefore the downregulation of mismatch repair has been associated with cisplatin resistance as this leads to a decrease in adduct cytotoxicity (Aebi et al., 1997; Francia et al., 2005).

The mRNA expression of MSH2 was significantly increased in response to both cisplatin and oxaliplatin treatment in the H69CIS200 and H69OX400 cell lines (Figure 8.1). However, there were no significant changes in MSH2 protein expression levels in the resistant cell lines or on treatment with platinum drugs (Figure 8.8). The platinum resistance in the H69CIS200 and H69OX400 cells is therefore not associated with a loss of mismatch repair in contrast to many previous studies into platinum resistance.

Platinum drug treatment increased the ratio of the lower MSH2 band in all cell lines (Figure 8.8C). This may be a shift from phosphorylated MSH2 to non-phosphorylated MSH2. One study has suggested that phosphorylation is required for MSH2 binding to GT mismatches (Pfeiffer et al., 2004). An increase in the lower MSH2 band may indicate a loss of phosphorylation and therefore a loss of activity of MSH2 in response to platinum drug treatment. However, this loss of activity is not part of the mechanism of platinum resistance as the sensitive and resistant cell lines respond in the same manner. Cells deficient in mismatch repair also usually have large decreases in the expression of MSH2.

The activity of oxaliplatin in cisplatin-resistant cell lines is thought to be due to repair or damage recognition processes that discriminate between cisplatin and oxaliplatin

adducts. A loss of mismatch repair increases resistance to cisplatin adducts, but has no effect on oxaliplatin adducts (Chaney et al., 2005). The H69CIS200 cisplatin-resistant cells are also cross-resistant to oxaliplatin. If the resistance was mediated by a loss of mismatch repair this cross resistance to oxaliplatin may not have occurred.

8.5.4 Base excision repair

In base excision repair the damaged base is removed by a DNA glycosylase to generate an abasic site in the DNA-strand. MutY functions as a DNA glycosylase (Fourrier et al., 2003) creating abasic sites in the place of 8-oxoG lesions in DNA which are then detected by APE1 initiating long patch repair (Figure 1.11). Interestingly, MutY's ability to bind to the damaged base is dependent on the mismatch repair MSH2/MSH6 protein complex (Parker et al., 2003). Therefore MutY mediated base excision repair may cooperate with mismatch repair in repairing 8-oxoG lesions (Gu et al., 2002). Changes in the expression of MutY has not been previously associated with cisplatin resistance.

There was a significant decrease in MutY mRNA expression in the untreated H69CIS200 and H69OX400 cell lines compared with the untreated H69 cells (Figure 8.1). This significant decrease was also present in the H69 and H69CIS200 cells treated with cisplatin. However, the level of MutY mRNA expression was restored to that of the parental cell line in the H69CIS200 cells treated with oxaliplatin and the H69OX400 cells treated with both cisplatin and oxaliplatin. This suggests a differential response between acute cisplatin and oxaliplatin treatment in the resistant cell lines. As the expression of MutY is significantly decreased in the untreated cell lines and on cisplatin treatment it is unlikely that MutY mediated base excision repair is contributing to the platinum-resistant phenotype of the cell lines.

RPS3 functions as a DNA repair endonuclease in base excision repair (Kim et al., 1995; Hegde et al., 2004) and is involved in apoptosis activating caspase-8 (Jang et al., 2004). The expression of RPS3 mRNA was significantly increased compared to untreated H69 cells in H69OX400 cells treated with cisplatin (1.32-fold) and H69 cells treated with oxaliplatin (1.40-fold). This increase in gene expression may

increase base excision repair or could be part of the apoptotic response to drug treatment.

8.5.5 NM23-H1 (NDK1)

The NM23 family of genes were initially documented as suppressors of the invasive phenotype in some cancer types and are also involved in the control of normal development and differentiation. Reduced expression of NM23-H1 has been associated with the aggressive progression of cancer (Lombardi et al., 2000). Nucleoside diphosphate kinases (NDKs), synthesise nucleoside triphosphates from nucleoside diphosphates and ATP. NM23-H1 which is also known as NDK1 has been reported to also have 3' to 5' exonuclease activity. When HeLa cells were treated with cisplatin, NM23-H1 translocated from the cytoplasm to the nucleus. This suggests that, in addition to maintenance of the nucleotide pool balance NM23-H1 may have a role in DNA repair (Yoon et al., 2005).

Increased expression of NM23-H1 by transfection has been associated with sensitivity to cisplatin in breast carcinoma, ovarian carcinoma and murine melanoma cell lines (Ferguson et al., 1996). Decreased expression of NM23-H1 has also been associated with resistance to cisplatin in oesophageal squamous cell carcinoma cells (Iizuka et al., 1999). This is thought to be mediated by a decrease in DNA damage that may be mediated by changes in drug accumulation (Iizuka et al., 2000). However this inverse relationship between cisplatin resistance and expression of NM23-H1 is not the case in all studies; an increased expression of NM23-H1 was associated with poor survival in patients with epithelial ovarian carcinoma receiving platinum-based therapy (Srivatsa et al., 1996).

There was a trend for decreased expression of NM23-H1 mRNA in the untreated resistant cell lines and in the H69 and H69CIS200 cells in response to cisplatin which correlates with previous cisplatin resistance studies (Iizuka et al., 1999). There was a trend for increased expression of NM23-H1 mRNA in response to cisplatin treatment in the H69OX400 cells and in all cell lines in response to oxaliplatin treatment. This suggests that cisplatin and oxaliplatin have differing effects on the expression of NM23-HI. The role of NM23-H1 in oxaliplatin resistance is unknown.

8.5.6 Cell cycle checkpoints

The H69CIS200 and H69OX400 cells when treated with platinum slow their growth but do not enter a lengthy cell cycle arrest like the parental H69 cells (Figure 3.5). This suggests that changes in cell cycle are associated with the regrowth resistance phenotype of the resistant cell lines. The responses of a cell to DNA damage include the repair of damaged DNA and apoptosis which eliminates highly damaged or deregulated cells. DNA damage can also activate a DNA damage checkpoint which arrests the cell cycle to allow for repair and prevention of the transmission of damaged chromosomes.

DNA damage checkpoints are biochemical pathways that delay or arrest cell cycle progression in response to DNA damage (Sancar et al., 2004). In an normal cell cycle, the transition points G_1/S and G_2/M, as well as S-phase progression, are tightly controlled, and that the same proteins involved in regulating the orderly progression through the cell cycle are also involved in the checkpoint responses (Sancar et al., 2004).

Rapamycin blocks mTORs activation downstream signalling elements, which results in cell cycle arrest in the G_1 phase of the cell cycle (Mita et al., 2003). Rapamycin reverses platinum resistance in the H69CIS200 and H69OX400 cells suggesting that the ability to proliferate through the G_1/S checkpoint is part of the platinum resistance mechanism (Figure 6.18).

The G_1/S checkpoint prevents cells from entering the S phase in the presence of DNA damage by inhibiting the initiation of replication (Figure 8.11). If there is DNA damage, however, entry into S phase is prevented by the activation of two signal transduction pathways, one to initiate and one to maintain the G_1/S arrest. The rapid G_1/S arrest is followed by a p53 mediated maintenance of G_1/S arrest. p53 activates its target genes, including $p21^{WAF\text{-}1/Cip1}$(p21), which maintains the G_1/S arrest. p21 binds to the Cdk4-CyclinD complex and prevents it from phosphorylating pRb. The phosphorylation of Rb results in its release of the E2F transcription factor, which is the signal for the transcription of S-phase genes (Sancar et al., 2004).

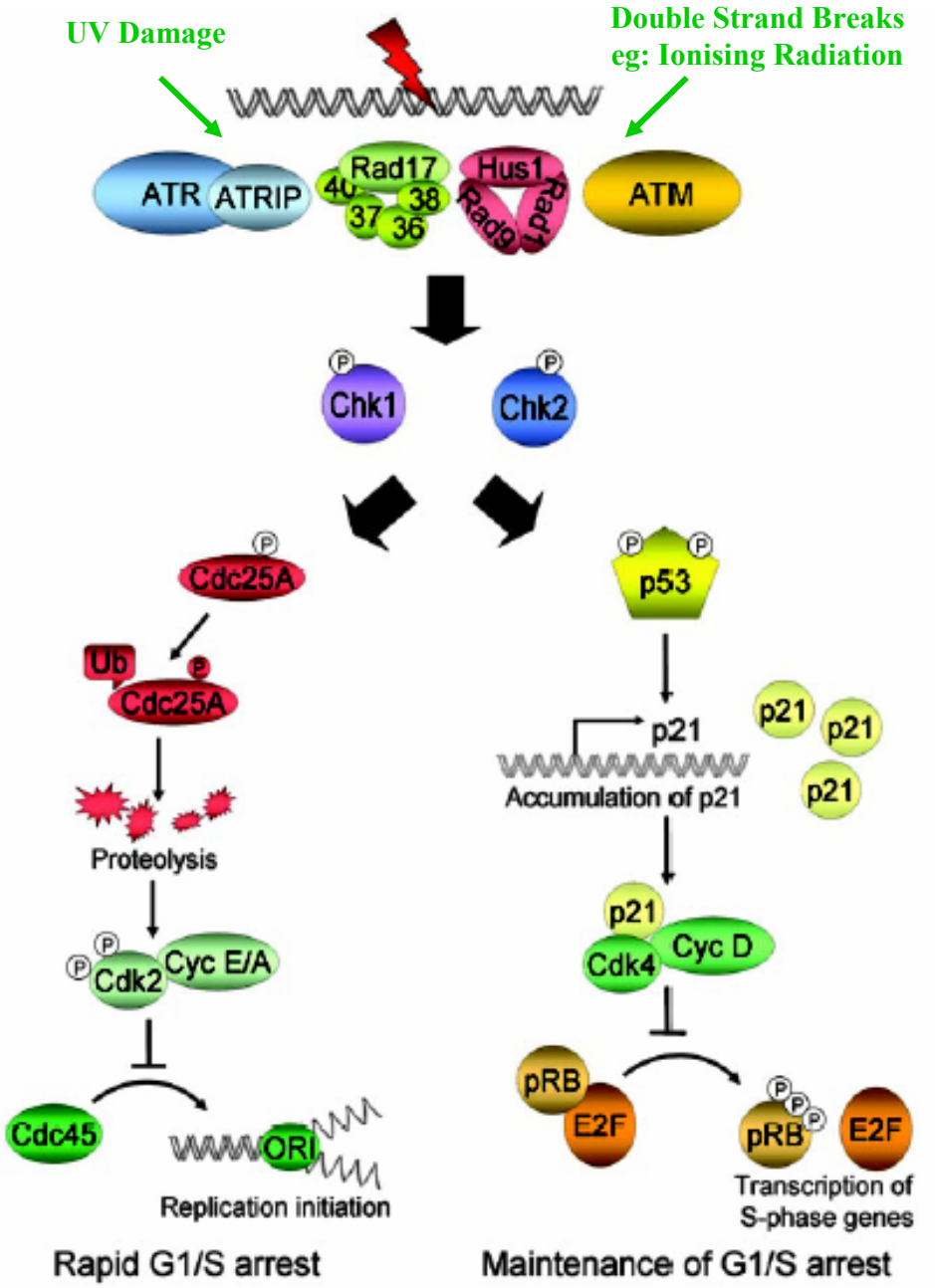

Figure 8.11 The G_1/S cell cycle checkpoint. Adapted from Sancar et al., 2004.

Resistance to cisplatin in IGROV1 cells was associated with the ability of the treated cells to progress through the cell cycle beyond the G_1/S checkpoint (Poulain et al., 1998). The IGROV1 cells had an increased propensity to proliferate after cytotoxic treatment, in other words regrowth resistance similar to the H69CIS200 and H69OX400 cells. Cells are maximally sensitive to cisplatin in the G_1 phase of the cell cycle, just prior to DNA synthesis (Donaldson et al., 1994). Perhaps regrowth resistance is the ability of cells to recover and progress beyond the cell cycle checkpoints despite DNA damage induced checkpoint signalling.

8.5.7 DNA repair pathways and the G_1/S checkpoint

The H69CIS200 and H69OX400 cells have a downregulation of nucleotide excision repair, base excision repair and homologous recombination repair of platinum adducts. All of these changes suggest a associated with sensitivity to platinum rather than resistance. This suggests that the DNA repair genes are being differentially expressed for other reasons rather than to increase DNA repair. One potential effect of change in expression of DNA repair genes is a change in activation of the cell cycle checkpoint pathways.

The platinum drug treated samples can be divided into two groups based on their cell cycle and growth status at the time the mRNA and protein samples were collected. At the time point of 4 days in drug the cells were either experiencing a maintenance of the G_1/S arrest or a rapid recovery from this G_1/S arrest (Figure 8.11). From the cell cycle and growth analysis in Chapter 3 (Figures 3.5 and 3.6), it is known that at the end of the 4 day drug treatment that H69 cells treated with either cisplatin or oxaliplatin are entering a lengthy growth arrest. Likewise the H69CIS200 cells treated with cisplatin are also in growth arrest even though they will recover over a week before the treated H69 cells. Therefore at this time point these cell lines are experiencing a maintenance of G_1/S arrest. The H69OX400 cells treated with oxaliplatin grow rapidly out of drug treatment (Figure 3.5) and are therefore experiencing a G_1/S arrest recovery. Three week growth curves for the treatment the cisplatin-resistant cell line with oxaliplatin and the oxaliplatin-resistant cell line with cisplatin was not performed in the initial stages of the project due to the large number of samples already being analysed. However from the real-time PCR analysis of these

samples it is clear that the pattern of gene expression for these samples is similar to that of the H69OX400 cells treated with oxaliplatin (Chapter 5), suggesting that this is due to the samples being in a similar state of growth and recovery from the G_1/S arrest.

ERCC1 deficient hepatocytes and ovarian carcinoma cells arrest in the G_2 phase of the cell cycle in association with an increased expression of cyclin dependent kinase inhibitor p21 (Melton et al., 1998 Nunez et al., 2000). The accumulation of p21 has been associated with the maintenance of a G_1/S checkpoint arrest (Figure 8.11). The decrease in ERCC1 expression is greatest in the samples experiencing a maintenance of the G_1/S cell cycle arrest (Figure 8.12). Perhaps the decreased expression of ERCC1 is increasing the levels of p21 and maintaining the protective cell cycle arrest associated with the regrowth resistance phenotype. The expression of ERCC1 is higher in the samples experiencing a rapid recovery from G_1/S arrest suggesting that these samples are not accumulating as much p21. The molecular differences between the samples maintaining G_1/S arrest and those progressing to the S phase is presented in Figure 8.13.

After exposure to DNA damage, RAD51 is concentrated in multiple discrete foci, which are thought to represent nuclear domains for homologous recombination (Raderschall et al., 2002). Downregulation of the cyclin dependent kinase inhibitor p21 inhibits the formation of RAD51 foci suggesting a functional link between RAD51 protein and p21-mediated cell cycle regulation (Raderschall et al., 2002). The levels of RAD51B foci formation in those samples recovering from G_1/S arrest was much lower than those samples in a G_1/S arrest maintenance phase (Figure 8.12). This suggests that the cell lines which recover from growth arrest fastest have sacrificed some of their DNA repair ability for the ability to rapidly proliferate which may be mediated by changes in the expression of p21 (Figure 8.13).

The expression of MutY has been shown to be altered at different phases of the cell cycle, reaching maximum levels in S phase compared to early G_1. MutY has also been shown to associate at DNA replication foci (Boldogh et al., 2001). This cell cycle dependent expression and localisation of MutY at sites of DNA replication suggest a role in post replication DNA base excision repair (Boldogh et al., 2001). The

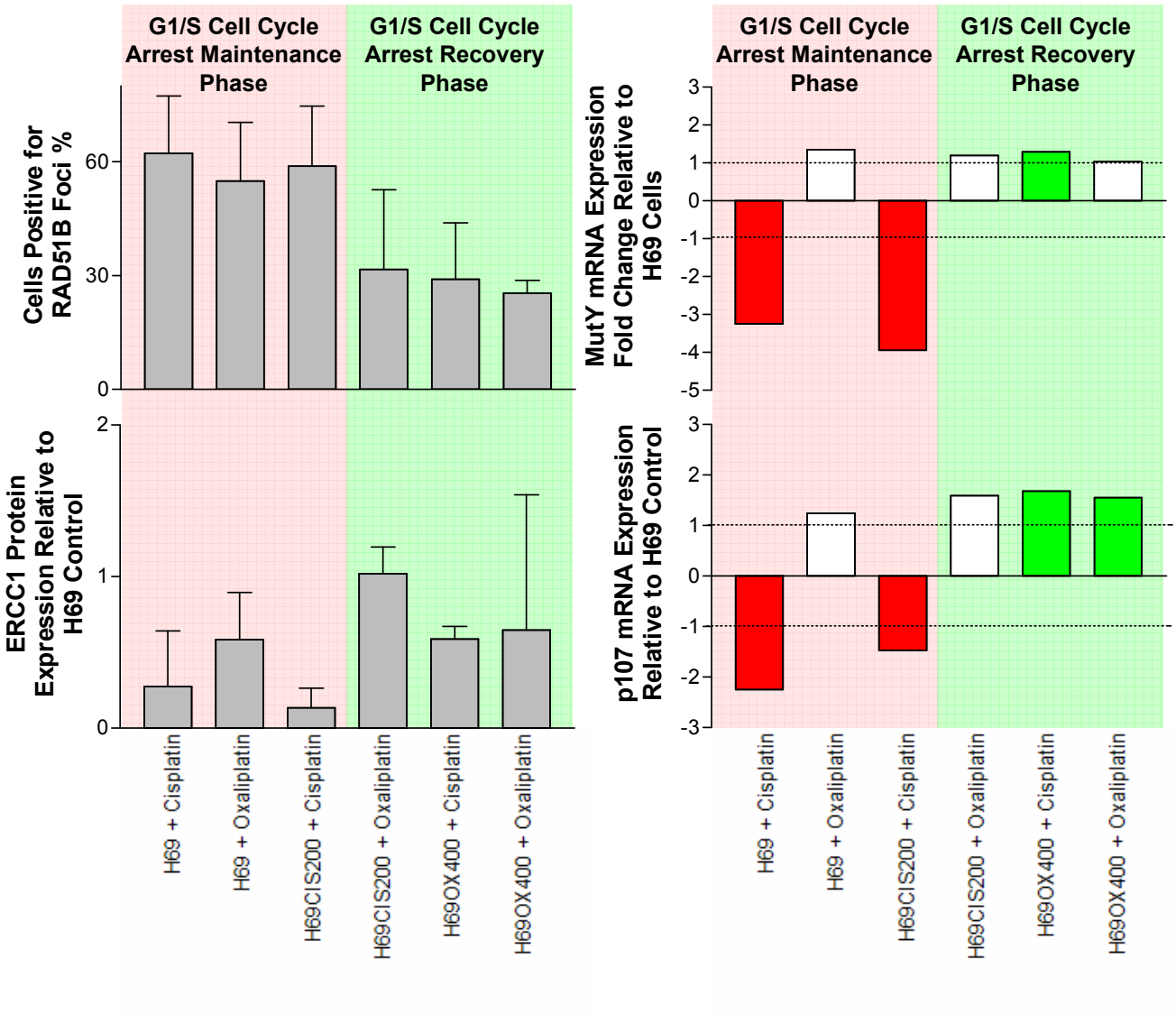

Figure 8.12 Differential expression of genes and proteins reflecting the phase of the cell cycle. Data from previous figures have been combined and the samples categorised by cell cycle phase. RAD51 foci (Figure 8.6), ERCC1 protein (Figure 8.7), MutY mRNA (Figure 8.1) and p107 mRNA (Figure 8.10).

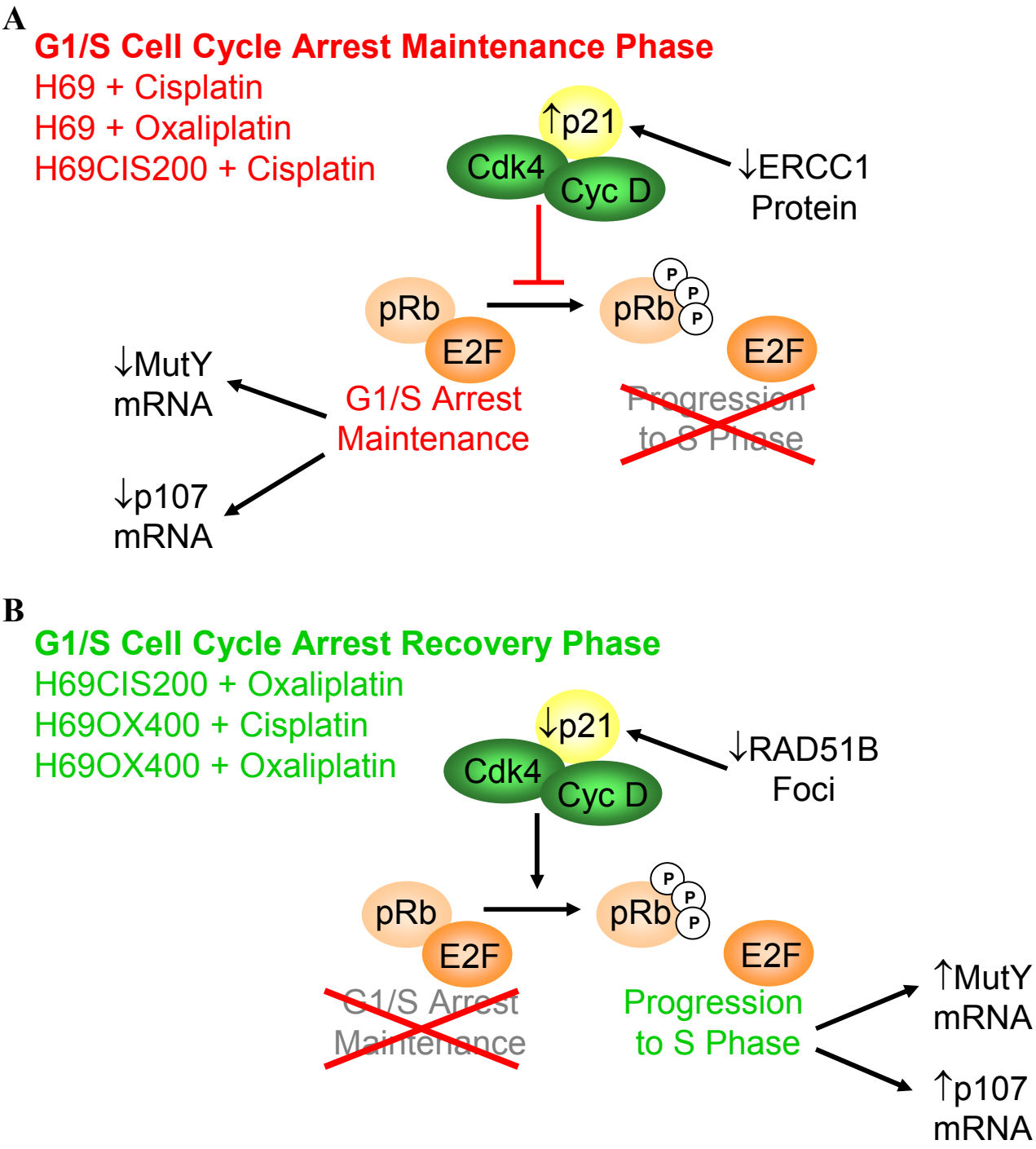

Figure 8.13 Model of G_1/S maintenance phase versus progression to S phase. A) Samples in the G_1/S cell cycle maintenance phase show decreased expression of ERCC1 protein which may increase the levels of p21 signalling the maintenance of the arrest. This results in a decrease in mRNA expression of both MutY and p107. B) Samples in the G1/S cell cycle recovery phase show decreased amounts of RAD51B foci which may decrease the levels of p21 signalling progression to S phase. This results in an increase in the mRNA expression of both MutY and p107.

untreated H69CIS200 and H69OX400 cell lines show a significant decrease from the untreated H69 cells (Figure 8.1). As the untreated cells are reaching confluence at the end of a 4 day incubation and the resistant cell lines grow slightly faster than the parental cell line (Figure 3.3C). This decrease in MutY mRNA expression may reflect a greater degree of confluence with less cells entering the S phase of the cell cycle. The H69 and H69CIS200 cells treated with cisplatin have a significant decrease in MutY mRNA expression (Figure 8.12), this reflects the maintenance of cell cycle arrest of these samples at this time point. The H69OX400 cell line treated with cisplatin shows a small but significant increase in MutY expression (Figure 8.12) suggesting an increase in MutY mediated post replication base excision repair. The differential expression of MutY is therefore likely to reflect the phase of the cell cycle of the samples at the end of a 4 day drug treatment (Figure 8.13).

8.5.8 Cell cycle genes and the G_1/S checkpoint

The cell cycle gene p107 was found to be differentially expressed in the Atlas nylon array analysis (Chapter 5). The passage through the G_1/S checkpoint is controlled by the retinoblastoma protein family which consists of pRB, p107 and p130 (Kondo et al., 2001). The pRB family proteins act as negative growth regulators and interact with the E2F family of transcriptional factors preventing cell cycle progression from G_1 to S (Kondo et al., 2001) (Figure 8.11). p107 expression levels increase as the cell cycle progresses, relatively low levels are expressed in G_0 and mid G_1, then in late G_1 the levels start to increase and continue to increase through the synthesis phase and G_2/M (Grana et al., 1998). Changes in p107 throughout the cell cycle are thought to be mediated by changes in mRNA expression.

p107 mRNA expression is decreased in H69 and H69CIS200 cells treated with cisplatin which are maintaining a G_1/S growth arrest (Figure 8.12). p107 mRNA is increased in H69CIS200 treated with oxaliplatin and H69OX400 cells treated with cisplatin and oxaliplatin which are coming out of a G_1/S growth arrest. The expression of p107 mRNA therefore correlates with the phase of the cell cycle of the samples assayed (Figure 8.13).

8.5.9 Cross resistance, DNA repair and the G_1/S checkpoint

The cross resistance to other chemotherapeutics in the H69CIS200 and H69OX400 cell lines was examined in Chapter 3. Some of these chemotherapeutics damage DNA as part of their mechanism of cytotoxicity. However, the kind of DNA damage caused and the way this DNA damage is signalled is different to that of platinum chemotherapeutics. The pattern of cross resistance observed in the resistant cell lines can be explained by the activity of DNA repair pathways and alterations in the G_1/S checkpoint.

8.5.9.1 Topoisomerase inhibitors

Topoisomerases participate in DNA replication, transcription, repair, recombination, and chromosome segregation. They transiently cleave DNA strands to relax supercoiled DNA by forming a covalent bond with DNA. This is followed by religation of the cleaved DNA and dissociation of the topoisomerase. Topoisomerase inhibitors interfere with topoisomerase activity by reversibly stabilising the covalent complex formed between the enzymes and the cleaved DNA, usually referred to as a cleavage complex (Meyers et al., 2004).

Resistance to topoisomerase inhibitors can arise due to changes in expression, activity or mutations in topoisomerases (Xu et al., 2002). Increased DNA repair of the topoisomerase cleavage complex can also lead to resistance as summarised for topoisomerase I in Figure 8.14 (Pommier et al., 2003). Homologous repair, non-homologous end joining, nucleotide excision repair and base excision repair pathways have all been associated with repairing DNA damage induced by the topoisomerase I cleavage complex. Topoisomerase II cleaves both strands of DNA, its stabilisation by topoisomerase II inhibitors causes double-strand breaks (Peters et al., 1990). Repair pathways of homologous repair and non-homologous end joining are important in repairing the double-strand breaks induced by the topoisomerase II cleavage complex. The H69CIS200 and H69OX400 cells are not cross-resistant to the topoisomerase I inhibitor irinotecan or topoisomerase II inhibitors etoposide, epirubicin and daunorubicin (Figure 3.9). This correlates with the lack of increased activity of DNA

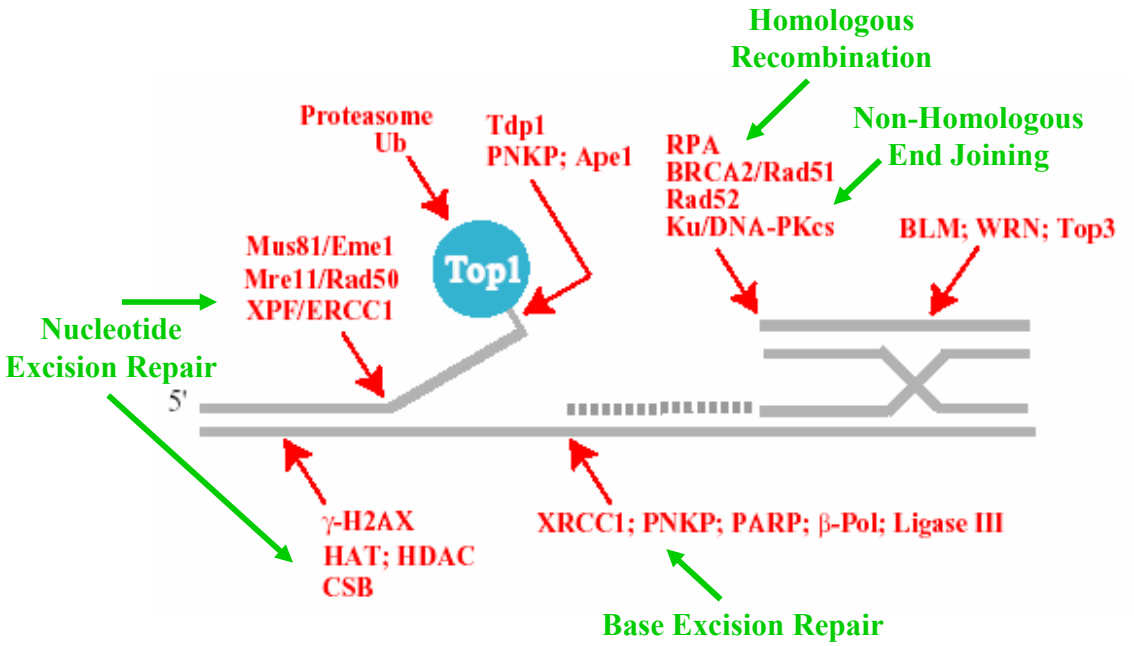

Figure 8.14 DNA repair pathways involved in the repair of the topoisomerase I cleavage complex. Genes involved in repairing the damage caused by the TopoI cleavage complex are shown in red, DNA repair pathways in green. Homologous repair, non-homologous end joining, nucleotide excision repair and base excision repair pathways have all been associated with repairing DNA damage induced by the TopoI cleavage complex. Adapted from Pommier et al., 2003.

repair pathways responsible for repair of the topoisomerase cleavage complex. The lack of cross resistance to topoisomerase inhibitors also indicates no changes in expression, activity or mutations in topoisomerase I and II.

There have been many reports of cross resistance between cisplatin and topoisomerase inhibitors in the literature. However, the cell lines which exhibit this pattern of cross resistance usually have resistance mechanisms which would confer resistance to topoisomerase inhibitors other than DNA repair. Changes in the expression of TopoI (Bergman et al., 2000), TopoII (Bergman et al., 2000; Henness et al., 2002; Locke et al., 2003) and MRP1 (Henness et al., 2002; Locke et al., 2003) confer resistance to topoisomerase inhibitors in cell lines that are also resistant to cisplatin and therefore changes in DNA repair are not often examined.

Loss of mismatch repair has been associated with resistance to topoisomerase inhibitors etoposide and epirubicin (Aebi et al., 1997; Fedier et al., 2001). There is no loss of mismatch repair associated with platinum resistance in the H69CIS200 and H69OX400 cells (Figure 8.8). This correlates with a lack of cross resistance to etoposide and epirubicin.

8.5.9.2 Radiation

Radiation produces a wide spectrum of DNA lesions, including the formation of modified nucleotides, abasic sites, DNA-protein crosslinks, DNA single- and double-strand breaks. The most lethal damage is considered to be double-strand break formation. DNA mismatches might arise directly from radiation treatment, or as a result of later error prone repair processes (Meyers et al., 2004).

The H69, H69CIS200 and H69OX400 cells were examined for their sensitivity to radiation. The cell lines failed reach an IC_{50} in response to doses of radiation higher than 20 Gy (Figure 8.9A). The cell lines would always reach at least an IC_{90} dose of drug in any cytotoxicity assay to a chemotherapeutic. Radiation assays are performed with a single burst of radiation at the start of the 5 day assay, whereas chemotherapy assays have the drug present for the whole assay. It was theorised that the cells may have been surviving the radiation based on cell to cell interactions that would have

been drastically inhibited by exposure to chemotherapy. Such as the activity of the PI3K/Akt pathway which has been related to the ability for H69 cells to adhere (Tsurutani et al., 2005), which has also been associated with the mechanism of platinum resistance and taxane sensitivity of the resistant cell lines in Chapter 6.

When the cell density of the cytotoxicity assay was dropped from 3 x 10^5 cells/ml to 5 x 10^4 cells/ml an IC_{50} response to radiation was achieved (Figure 8.9B). Under these conditions the H69OX400 cells were significantly 2.68-fold resistant to radiation compared to the parental H69 cells, whereas the H69CIS200 cells were not (Figure 8.9C). The H69OX400 cell line can survive and proliferate in response to the double-strand breaks induced by radiation but not topoisomerase inhibitors. As no mechanisms of repair for double-strand breaks are upregulated in the H69OX400 cells, the difference may be due to how the double-strand break DNA damage is signalled in response to radiation versus topoisomerase inhibitors.

The H69CIS200 cells are not resistant to radiation in a 5 day MTT cytotoxicity assay whereas the H69OX400 cells are 2.68-fold resistant. This difference may be due to the speed of recovery from a G_1/S arrest. The H69OX400 cells recover from oxaliplatin induced growth arrest faster than the H69CIS200 cells recover from a cisplatin induced growth arrest (Figure 3.5). The H69CIS200 cells take an extra week to achieve a cell division compared to the H69OX400 cells which rapidly proliferate out of drug treatment. If this same speed of recovery applies to the growth arrest from radiation, then the H69CIS200 cells are likely to be more viable than the parental H69 cells but this difference is not detectable over a 5 day cytotoxicity assay.

Cross resistance between cisplatin and radiation has been reported in many cell lines. Most studies have associated both cisplatin and radiation resistance with increased cellular glutathione (Oshita et al., 1992) or alterations in glutathione metabolism (Henness et al., 2002). There is no increase in glutathione in either the H69CIS200 and H69OX400 cell lines, but there is a difference in their glutathione metabolism indicated by resistance and sensitivity to BSO respectively (Figure 3.9). This difference may contribute to the resistance of the H69OX400 cells to radiation.

8.5.9.3 G_1/S checkpoint and cross resistance

The rapid activation of the G_1/S checkpoint is governed by the proteolysis of Cdc25A (Figure 8.11). Different groups of chemotherapeutics interact with the G_1/S checkpoint in a differential manner. Exposure of human osteosarcoma cells to topoisomerase inhibitors camptothecin, etoposide, and adriamycin resulted in rapid activation of the G_1/S checkpoint pathway, within 1 hour, including degradation of the Cdc25A phosphatase (Agner et al., 2005). Interestingly, cisplatin also induced proteolysis of Cdc25A, however this response was 8-12 hours after drug treatment. In contrast, taxol failed to activate the G_1/S checkpoint even after a prolonged treatment (Agner et al., 2005).

This differential response of G_1/S checkpoint activation may explain the pattern of cross resistance observed in the H69CIS200 and H69OX400 cell lines. Cisplatin induced a slow activation of the checkpoint which required ATM and activated Chk2 (Figure 8.11). Interestingly, G_1/S checkpoint activation in response to radiation also requires ATM and activates Chk2 (Agner et al., 2005) which may explain the cross resistance between platinum and radiation in the H69OX400 cells. Topoisomerase inhibitors cause similar DNA double-strand breaks as induced by cisplatin or radiation and are therefore repaired by the same DNA damage pathways. However, topoisomerase inhibitors do not signal G_1/S checkpoint activation with ATM (Agner et al., 2005). The resistant cell lines may therefore only be cross-resistant to DNA damaging agents which activate the G_1/S checkpoint in a ATM mediated manner as cisplatin damage is detected.

Taxol fails to activate the G_1/S checkpoint, even after lengthy exposures to the drug (Agner et al., 2005). Taxol binds to and inhibits tubulin mediating its cytotoxicity in the G_2/M phase of the cell cycle. This corresponds to a lack of cross resistance to taxol in the H69CIS200 and H69OX400 cells.

8.5.10 DNA repair pathways and chromosomal stability

There is a struggle within a cell to balance the need for perfect DNA repair and proliferation. Part of the development of resistance while upregulating the DNA repair

pathways can also be the ignoring of DNA adducts, increasing the tolerance for DNA damage and allowing cell division. This can increase the number of chromosomal rearrangements. As discussed in Chapter 4 the chromosomal changes due to exposure to cisplatin and oxaliplatin may be in places of inherent vulnerability in the H69 cells and some changes were associated with the resistant phenotype. The number of chromosomal aberrations was surprising in the H69CIS200 and H69OX400 cells considering the low doses of chemotherapeutic used in development of the cell lines. The decreased activity of DNA repair pathways may have contributed to these chromosomal changes.

ERCC1 plays a role in chromosome instability. ERCC1 knockout cells are extremely sensitive to DNA damage from radiation resulting in an increase in chromosomal fragment formation (Griffin et al., 2005). ERCC1 deficient mouse embryos, primary fibroblast cultures and immortalised cell lines have all been shown to have a higher level of genome instability than wild-type controls. The loss of ERCC1 leads to increased levels of unrepaired lesions and double-strand breaks causing increased mutation frequency and genomic instability (Melton et al., 1998; Sargent et al., 2000). The H69CIS200 and H69OX400 resistant cell lines have consistently lower levels of ERCC1 mRNA levels than that of the parent cell line and ERCC1 protein expression decreases in response to cisplatin and oxaliplatin treatment. These changes may have played a part in the chromosomal rearrangements described in Chapter 4. The resistant cell lines were also shown to have increased genome instability compared to the parental cell line in a 3 month drug-free culture (Figure 4.18).

The RAD51 proteins are involved in the homologous recombination pathway which repairs double-strand breaks in DNA. There was a significant decrease in RAD51B protein in H69OX400 cells treated with oxaliplatin (Figure 8.2). There was also a decrease in the formation of RAD51B foci in the H69OX400 cells in response to drug treatment compared to the H69 and H69CIS200 cells (Figure 8.6). RAD51B double knockout cells show increased levels of spontaneous chromosomal aberrations which may be caused by defective homologous recombination repair of replication associated double-strand breaks (Takata et al., 2000). The H69OX400 cells showed a more chromosomal aberrations than the H69CIS200 cells (Figure 4.8). The decreased

expression and activity of RAD51B may in part explain the increase in chromosomal breakage in the H69OX400 cells through an inhibition of the homologous recombination pathway.

8.6 Conclusion

The platinum resistance in the H69CIS200 and H69OX400 cell lines is not mediated by an increase in nucleotide excision repair, base excision repair or homologous recombination repair or a decrease in mismatch repair as in other platinum-resistant cell lines. The H69CIS200 and H69OX400 cells appear to have exchanged some of their DNA repair capacity for increased regrowth resistance mediated by changes in G_1/S checkpoint signalling. The differential expression of genes and proteins in these cell lines is largely mediated by the stage in the cell cycle at which the sample was taken. Changes in the expression of ERCC1 and RAD51B potentially contribute to the ability of p21 to regulate the G_1/S checkpoint. The different stage of the cell cycle in the respective samples leads to the differential expression of both MutY and p107 mRNA.

The cross resistance pattern of the resistant cell lines can in part be explained by the manner in which DNA damage is signalled. Cross resistance does not occur to topoisomerase poisons in this model as the DNA damage at the G_1/S checkpoint is signalled by a differing group of proteins to that of cisplatin and radiation. The decrease in DNA repair pathways may have also contributed to the chromosomal aberrations in these resistant cell models.

CHAPTER 9.0

CONCLUSIONS AND FUTURE DIRECTIONS

9.1 Conclusions

Patients with SCLC have an average life expectancy of around one year from diagnosis and platinum-based combination chemotherapy is the only therapeutic option currently available for the treatment of this disease. SCLC patients initially respond well to platinum-based therapy but then relapse with resistant disease. Previous cell models of cisplatin-resistant SCLC have, in general, produced higher levels of resistance than is clinically relevant and most have the common platinum resistance mechanisms of increased cellular glutathione and decreased platinum accumulation (Table 1.4).

The H69CIS200 and H69OX400 cell lines are novel cellular models of low-level, platinum-resistant SCLC. These cell lines do not have the common platinum resistance mechanisms of increased levels of cellular glutathione or decreased accumulation. Rather these cell lines have a unique cell cycle based mechanism of resistance which has been characterised as 'regrowth resistance'. Regrowth resistance allows cells to survive platinum treatment by entering a lengthy growth arrest. With repeated treatments of platinum this growth arrest period reduces until the cell line can rapidly proliferate immediately post drug treatment (Figure 3.□). Regrowth resistance may be the kind of resistance emerging in the rapid relapse of SCLC patients.

Oxaliplatin has been widely regarded to have activity in cisplatin-resistant cancer. However, this evidence comes from highly drug resistant models. At high levels of resistance to either cisplatin or oxaliplatin the other compound does show increased activity, but this is still at levels well above that of clinical platinum resistance (Figure 1.2). At lower levels of resistance, such as that observed in the H69CIS200 and H69OX400 cells, true cross resistance between cisplatin and oxaliplatin is observed. Clinical studies into the use of oxaliplatin as a single agent suggest decreased activity in patients classed as cisplatin-resistant by Markman's criteria. The resistance to oxaliplatin was developed more easily than resistance to cisplatin in the H69 SCLC cells. Dose escalation also produced more surviving sublines in response to oxaliplatin than cisplatin treatment. This suggests that oxaliplatin may be less effective than cisplatin in the treatment of SCLC.

The chromosomes of the H69 parental cells and the H69CIS200 and H69OX400 resistant cell lines were analysed by both Affymetrix 10K SNP array and cytogenetics. The H69 parental cells are near tetraploid cells harbouring a large c-myc amplification (Figure 4.3), which may have contributed to the cancerous phenotype of the original tumour. The resistant cell lines showed many chromosomal aberrations (Figure 4.8) considering the low-level of platinum chemotherapeutics used in the development of the cell lines. The decreased activity of several DNA repair pathways (Chapter 8), particularly in the H69OX400 cells which had more chromosomal change may account for the extent of chromosome damage. Several chromosomal changes were found in both the H69CIS200 and H69OX400 cells suggesting an involvement in the platinum-resistant phenotype. Chromosomal aberrations have been studied extensively in cisplatin-resistant cell lines but never successfully linked to the resistant phenotype (Figure 4.1). By analysing the sensitive revertant cell lines H69CIS200-S and H69OX400-S it was found that the changes in common between the resistant cell lines were not associated with the resistant phenotype (Figure 4.17) and may be a result of inherent vulnerabilities in the parent H69 cells.

The H69CIS200 and H69OX400 cells have become more sensitive to taxanes, another class of chemotherapeutic drug, in association with their development of platinum resistance. This relationship between platinum resistance and taxane sensitivity occurs in many models of acquired drug resistance (Figure 6.1) and has been reported in both animal models and clinical studies. However, little is known about the molecular mechanism of this phenomena. The molecular target of taxanes, tubulin, was studied extensively in the resistant cell lines for changes in expression (Figure 6.3), polymerisation (Figure 6.4) and morphology (Figures 6.6 – 6.11). No change which could explain the large degree of hypersensitivity to taxol in the H69CIS200 and H69OX400 cells was found. The Atlas nylon array analysis revealed changes in genes associated with the PI3K/Akt/mTOR signalling pathway and the G1/S cell cycle checkpoint. Cisplatin and taxol have both been associated with the mTOR signalling pathway (Figure 6.16). mTORs downstream effects include control of growth and proliferation factors as well as influence over the cell cycle at the G1/S checkpoint. Treatment with mTOR's inhibitor rapamycin reversed both platinum resistance and taxane sensitivity in the resistant cell lines (Figure 6.18). mTOR was found to be

phosphorylated and therefore active in the resistant cell lines, however platinum drug treatment decreased mTOR expression in all cell lines. Changes in the mTOR pathway could therefore be involved in the molecular mechanism for the regrowth resistance phenotype and taxane sensitivity observed in the platinum-resistant cell lines. Changes in the mTOR signalling pathway could possibly explain the wider phenomena of the inverse relationship between cisplatin and taxol resistance.

The levels of cellular glutathione were shown to increase in response to the stress of platinum drug treatment in all cell lines (Figure 3.10). However, the resistant cell lines did not increase their levels of glutathione to a greater extent than the sensitive cells, suggesting that an increase in the level of glutathione is not a mechanism of resistance in the platinum-resistant cell lines. Several glutathione related genes were found to be differentially expressed in the Atlas nylon array analysis. These changes seem to be associated with the stress response to platinum drug treatment rather than the mechanism of platinum resistance as changes occurred in all cell lines. Decreases in the redox protein thioredoxin (Figure 7.4) may indicate the activation of apoptosis signal regulating kinase 1 as part of the cytotoxic response to platinum treatment. Activation of the PI3K/Akt/mTOR pathway may compensate for this apoptotic signal in the resistant cell lines (Figure 7.10).

The H69CIS200 cell line has become resistant to BSO, an inhibitor of glutathione synthesis. In contrast the H69OX400 cell line has become sensitive to BSO. This is an unusual response for cell lines with no changes in the amount of cellular glutathione. The resistant cell lines show no increase in γGCS (Figure 7.2) or decreases in GSTP1 (Figure 7.1) which have been previously associated with acquired BSO resistance (Table 7.1). The resistant cell lines both show the reverse pattern of decreased γGCS and increased GSTP1, suggesting that the BSO resistance and sensitivity are governed by different factors as both cell lines show the same pattern of expression for these genes.

Changes in DNA repair pathways in the H69CIS200 and H69OX400 cells show the opposite pattern from what one would predict from previous models of cisplatin resistance. The resistant cell lines have lower levels of nucleotide excision repair

genes and proteins (Figures 8.1 and 8.7), the only mechanism capable of removing platinum adducts from the DNA strand. The resistant cells also have lower levels of homologous recombination repair proteins and activity (Figures 8.2 and 8.6), the mechanism responsible for the repair of double-strand breaks caused by platinum interstrand adducts. The resistant cells also have no decrease in mismatch repair (Figure 8.8), which would reduce the cytotoxicity of platinum adducts.

Some of these changes in DNA repair may have been sacrificed in favour of expedient recovery from the G_1/S cell cycle checkpoint. ERCC1 protein expression and the formation of RAD□1 foci shows a differential response depending on the cell cycle stage of the sample being analysed (Figure 8.12). Samples in the G_1/S cell cycle maintenance phase after a 4 day platinum drug treatment (H69 cells treated with cisplatin or oxaliplatin and H69CIS200 cells treated with cisplatin) show decreased expression of ERCC1 protein which may increase the levels of p21 signalling the maintenance of the arrest. This results in a decrease in mRNA expression of both MutY and p107. Samples in the G_1/S cell cycle recovery phase after a 4 day platinum drug treatment (H69CIS200 cells treated with oxaliplatin and H69OX400 cells treated with cisplatin or oxaliplatin) show decreased amounts of RAD□1B foci which may decrease the levels of p21 signalling progression to S phase. This results in an increase in the mRNA expression of both MutY and p107 (Figure 8.13).

The mechanism of regrowth resistance in the platinum-resistant H69CIS200 and H69OX400 cells is a combination of activation of PI3K/Akt/mTOR signalling and alterations in control of the G_1/S cell cycle checkpoint as summarised in Figure 9.1. However, more work remains to determine which factors in these pathways are governing this novel mechanism of platinum resistance.

9.2 Future Directions

Further investigation of the PI3K/Akt/mTOR pathway in the H69CIS200 and H69OX400 cell lines is required to fully understand the mechanism of platinum resistance in these cell lines. Changes in the mTOR pathway also contribute to the mechanism of hypersensitivity to taxol. If the inverse relationship between cisplatin and taxol resistance can be further understood this would lead to improved cancer

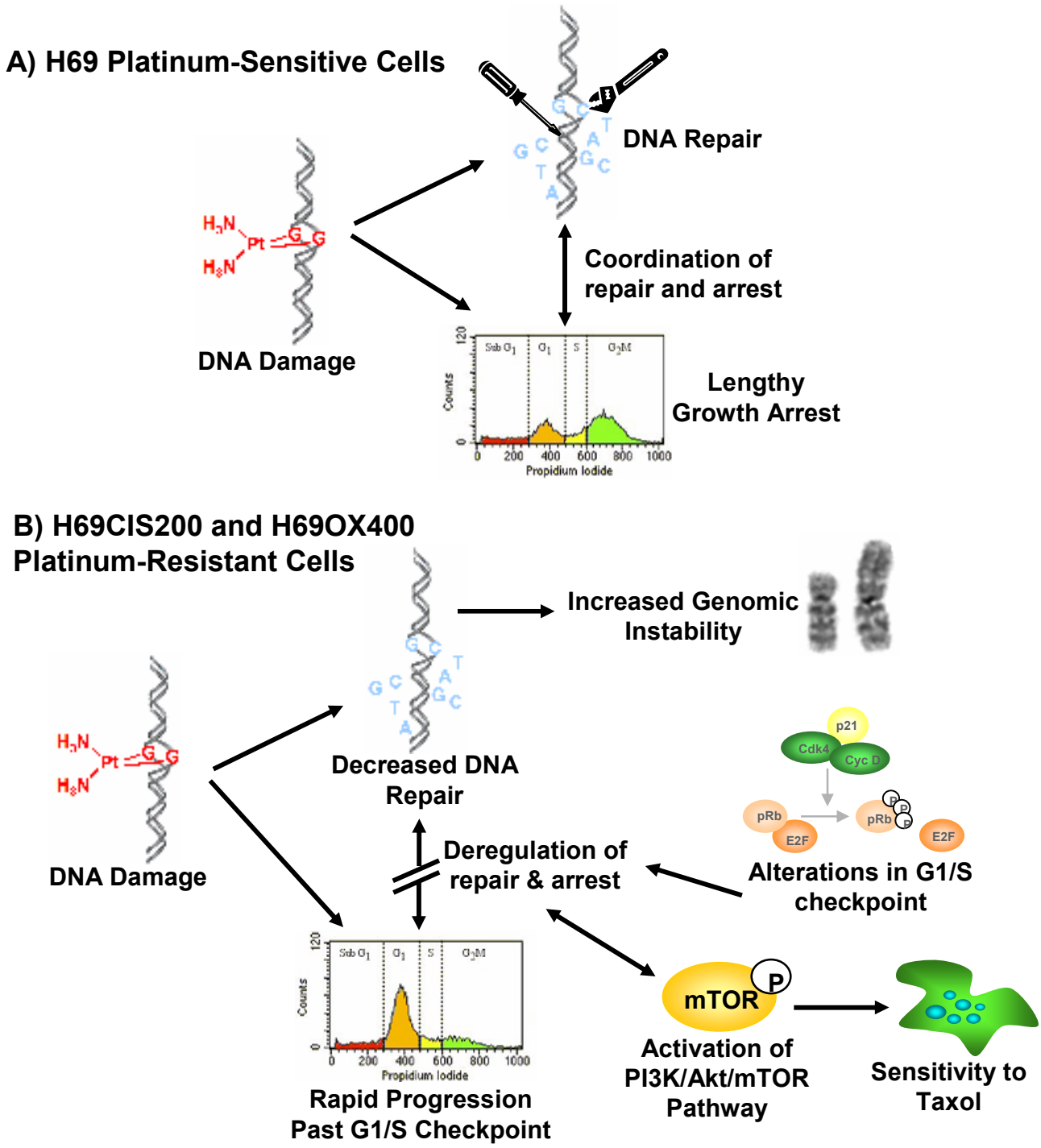

Figure 9.1 Summary of the mechanism of resistance. A) The H69 sensitive cells respond to platinum induced DNA damage with coordinated DNA repair and a lengthy growth arrest. B) The H69CIS200 and H69OX400 cells respond to platinum induced DNA damage with a deregulation of DNA repair and arrest. This leads to a rapid progression past the G_1/S checkpoint which may be mediated by changes in DNA repair, the G_1/S checkpoint itself and activation of the PI3K/Akt/mTOR pathway. The activation of the mTOR pathway may be responsible for the sensitivity to taxol in the resistant cell lines.

therapy. So far only the expression of mTOR in response to platinum treatment has been examined in the H69CIS200 and H69OX400 cell lines. The expression of mTOR in response to taxol treatment and in combination with rapamycin also needs to be examined.

The cell cycle response of the H69CIS200 and H69OX400 cell lines to treatment with cisplatin and oxaliplatin has already been studied (Figure 3.6). However, the cell cycle response to taxanes and influence of rapamycin has not been examined. If rapamycin reverses the protective cell cycle response to platinum this will confirm that mTOR signalling is required for the platinum resistance in these cell lines. The downstream signalling activity from mTOR also needs to be examined to determine if there is a differential response to treatment with platinums and taxanes.

The anti-apoptotic protein Bcl-2 has been associated with mTOR signalling in response to taxol treatment (Figure 6.16). Increased expression of Bcl-2 has also been implicated in resistance to BSO in cell lines with no change in cellular glutathione (Vahrmeijer et al., 2000). If the H69CIS200 cells had increased levels of Bcl-2 this would explain both their resistance to BSO and sensitivity to taxol. The H69OX400 cells also show sensitivity to taxol like the H69CIS200 cells but are sensitive to BSO treatment. An increased expression of Bcl-2 in the H69OX400 cells would therefore not explain the pattern of cross resistance observed. The protein expression of Bcl-2 should be examined in the H69CIS200 and H69OX400 cell lines in response to platinum, taxol, rapamycin and BSO treatment in order understand the role of this protein in the pattern of cross resistance observed.

The H69OX400 cells are also resistant to *vinca* alkaloids, suggesting that changes in microtubule associated proteins such as MAP4 may play a role in the taxane sensitivity and *vinca* alkaloid resistance in this cell line. mRNA analysis of MAP4 shows increased expression of MAP4 in the resistant cell lines and in response to platinum drug treatment. However, MAP4 protein expression has not been examined. The protein expression of MAP4 should be examined in the H69CIS200 and H69OX400 cell lines in response to platinum, taxol and *vinca* alkaloid treatment in ociated with cisplatinole of this protein in the pattern of cross resistance observed.

The expression of p21 needs to be examined to confirm if changes in the activity of DNA repair proteins ERCC1 and RAD51B have influenced the expression of p21 and consequently the maintenance or progression from G_1/S cell cycle arrest. If there are no changes in the expression of p21 then other proteins involved in the G_1/S checkpoint need to be examined to determine the mechanism of platinum resistance. DNA damage signalling protein ATM plays a role in the detection of platinum damage and may play a role in the resistance mechanism. The expression of p53 also plays a significant role in cell cycle control. The H69 cells are known to have mutant p53 but changes in expression associated with resistance has not been examined in this cell model.

The analysis of mTOR, Bcl-2, MAP4, p21, p53, PI3K/Akt/mTOR and G1/S checkpoint pathways will further characterise the novel mechanisms of resistance in the H69CIS200 and H69OX400 cells. A greater understanding of the mechanism of platinum resistance and taxane sensitivity in these clinically relevant models of SCLC will lead to improved use of both platinums and taxanes in the clinical treatment of cancer.

CHAPTER 10.0

REFERENCES

10.1 References

Abal M, Andreu JM, Barasoain I. 2003. Taxanes: microtubule and centrosome targets, and cell cycle dependent mechanisms of action. *Current Cancer Drug Targets.* **3**:193–203.

Aebi S, Fink D, Gordon R, Kim HK, Zheng H, Fink JL, Howell SB. 1997. Resistance to cytotoxic drugs in DNA mismatch repair-deficient cells. *Clinical Cancer Research* **3**:1763–1767.

Agner J, Falck J, Lukas J, Bartek J. 2005. Differential impact of diverse anticancer chemotherapeutics on the Cdc25A-degradation checkpoint pathway. *Experimental Cell Research* **302**:162–169.

Altomare DA, Wang HQ, Skele KL, De Rienzo A, Klein-Szanto AJ, Godwin AK, Testa JR. 2004. AKT and mTOR phosphorylation is frequently detected in ovarian cancer and can be targeted to disrupt ovarian tumor cell growth. *Oncogene* **23**:5853–5857.

Altschul SF, Madden TL, Schaffer AA, Zhang J, Zhang Z, Miller W, Lipman DJ. 1997. Gapped BLAST and PSI-BLAST: a new generation of protein database search programs. *Nucleic Acids Research* **25**:3389–3402.

Amati B, Alevizopoulos K, Vlach J. 1998. Myc and the cell cycle. *Frontiers in Bioscience.* **3**:d250–d268.

Aoki K, Ogawa T, Ito Y, Nakashima S. 2004. Cisplatin activates survival signals in UM-SCC-23 squamous cell carcinoma and these signal pathways are amplified in cisplatin-resistant squamous cell carcinoma. *Oncology Reports.* **11**:375–379.

Ark-Otte J, Samelis G, Rubio G, Lopez Saez JB, Pinedo HM, Giaccone G. 1998. Effects of tubulin-inhibiting agents in human lung and breast cancer cell lines with different multidrug resistance phenotypes. *Oncology Reports.* **5**:249–255.

Arner ES, Nakamura H, Sasada T, Yodoi J, Holmgren A, Spyrou G. 2001. Analysis of the inhibition of mammalian thioredoxin, thioredoxin reductase, and glutaredoxin

by cis-diamminedichloroplatinum (II) and its major metabolite, the glutathione-platinum complex. *Free Radical Biology & Medicine* **31**:1170-1178.

Ashman JN, Brigham J, Cowen ME, Bahia H, Greenman J, Lind M, Cawkwell L. 2002. Chromosomal alterations in small cell lung cancer revealed by multicolour fluorescence in situ hybridization. *International Journal of Cancer* **102**:230-236.

Asnaghi L, Calastretti A, Bevilacqua A, D'Agnano I, Gatti G, Canti G, Delia D, Capaccioli S, Nicolin A. 2004a. Bcl-2 phosphorylation and apoptosis activated by damaged microtubules require mTOR and are regulated by Akt. *Oncogene* **23**:5781-5791.

Asnaghi L, Bruno P, Priulla M, Nicolin A. 2004b. mTOR: a protein kinase switching between life and death. *Pharmacological Research* **50**:545-549.

Azios NG and Dharmawardhane SF. 2005. Resveratrol and estradiol exert disparate effects on cell migration, cell surface actin structures, and focal adhesion assembly in MDA-MB-231 human breast cancer cells. *Neoplasia (New York)* **7**:128-140.

Bassett E, Vaisman A, Havener JM, Masutani C, Hanaoka F, Chaney SG. 2003. Efficiency of extension of mismatched primer termini across from cisplatin and oxaliplatin adducts by human DNA polymerases beta and eta in vitro. *Biochemistry* **42**:14197-14206.

Beale PJ, Rogers P, Boxall F, Sharp SY, Kelland LR. 2000. BCL-2 family protein expression and platinum drug resistance in ovarian carcinoma. *British Journal of Cancer* **82**:436-440.

Behrens BC, Hamilton TC, Masuda H, Grotzinger KR, Whang-Peng J, Louie KG, Knutsen T, McKoy WM, Young RC, Ozols RF. 1987. Characterization of a cis-diamminedichloroplatinum(II)-resistant human ovarian cancer cell line and its use in evaluation of platinum analogues. *Cancer Research* **47**:414-418.

Bell DR, Trent JM, Willard HF, Riordan JR, Ling V. 1987. Chromosomal location of human P-glycoprotein gene sequences. *Cancer Genetics & Cytogenetics* **25**:141-148.

Belvedere G, Imperatori L, Damia G, Tagliabue G, Meijer C, de Vries EG, D'Incalci M. 1996. In vitro and in vivo characterisation of low-resistant mouse reticulosarcoma (M5076-sublines obtained after pulse and continuous exposure to cisplatin. *European Journal of Cancer* **32A**:2011-2018.

Belyanskaya LL, Hopkins-Donaldson S, Kurtz S, Simoes-Wust AP, Yousefi S, Simon HU, Stahel R, Zangemeister-Wittke U. 2005. Cisplatin activates Akt in small cell lung cancer cells and attenuates apoptosis by survivin upregulation. *International Journal of Cancer* **117**:755-763.

Berggren M, Gallegos A, Gasdaska J, Powis G. 1997. Cellular thioredoxin reductase activity is regulated by selenium. *Anticancer Research* **17**:3377-3380.

Bergman AM, Giaccone G, van Moorsel CJ, Mauritz R, Noordhuis P, Pinedo HM, Peters GJ. 2000. Cross-resistance in the 2',2'-difluorodeoxycytidine (gemcitabine)-resistant human ovarian cancer cell line AG6000 to standard and investigational drugs. *European Journal of Cancer* **36**:1974-1983.

Bernstein C, Bernstein H, Payne CM, Garewal H. 2002. DNA repair/pro-apoptotic dual-role proteins in five major DNA repair pathways: fail-safe protection against carcinogenesis. *Mutation Research* **511**:145-178.

Berrieman HK, Lind MJ, Cawkwell L. 2004. Do beta-tubulin mutations have a role in resistance to chemotherapy? *Lancet Oncology* **5**:158-164.

Bhatia M, Kirkland JB, Meckling-Gill KA. 1996. Overexpression of poly(ADP-ribose)-polymerase promotes cell cycle arrest and inhibits neutrophilic differentiation of NB4 acute promyelocytic leukemia cells. *Cell Growth & Differentiation* **7**:91-100.

Bjorkhem-Bergman L, Jonsson K, Eriksson LC, Olsson JM, Lehmann S, Paul C, Bjornstedt M. 2002. Drug-resistant human lung cancer cells are more sensitive to selenium cytotoxicity. Effects on thioredoxin reductase and glutathione reductase. *Biochemical.Pharmacology* **63**:1875-1884.

Boldogh I, Milligan D, Lee MS, Bassett H, Lloyd RS, McCullough AK. 2001. hMYH cell cycle-dependent expression, subcellular localization and association with

replication foci: evidence suggesting replication-coupled repair of adenine:8-oxoguanine mispairs. *Nucleic Acids Research* **29**:2802-2809.

Bompard G, Puech C, Prebois C, Vignon F, Freiss G. 2002. Protein-tyrosine phosphatase PTPL1/FAP-1 triggers apoptosis in human breast cancer cells. *Journal of Biological Chemistry* **277**:47861-47869.

Borst P, Evers R, Kool M, Wijnholds J. 2000. A family of drug transporters: the multidrug resistance-associated proteins. *Journal of the National Cancer Institute.* **92**:1295-1302.

Brogger A. 1977. Non-random localization of chromosome damage in human cells and targets for clastogenic action. *Chromosomes Today* **6**:297-306.

Brooks SC, III, Sturgill R, Choi J, Yen A. 1997. An RXR-selective analog attenuates the RAR alpha-selective analog-induced differentiation and non-G1-restricted growth arrest of NB4 cells. *Experimental Cell Research* **234**:259-269.

Burns BS, Edin ML, Lester GE, Tuttle HG, Wall ME, Wani MC, Bos GD. 2001. Selective drug resistant human osteosarcoma cell lines. *Clinical Orthopaedics & Related Research* 259-267.

Busund LT, Richardsen E, Busund R, Ukkonen T, Bjornsen T, Busch C, Stalsberg H. 2005. Significant expression of IGFBP2 in breast cancer compared with benign lesions. *Journal of Clinical Pathology* **58**:361-366.

Calastretti A, Bevilacqua A, Ceriani C, Vigano S, Zancai P, Capaccioli S, Nicolin A. 2001. Damaged microtubules can inactivate BCL-2 by means of the mTOR kinase. *Oncogene* **20**:6172-6180.

Calvert P, Yao KS, Hamilton TC, O'Dwyer PJ. 1998. Clinical studies of reversal of drug resistance based on glutathione. *Chemico-Biological Interactions.* **111-112**:213-224.

Campling BG, Pym J, Baker HM, Cole SP, Lam YM. 1991. Chemosensitivity testing of small cell lung cancer using the MTT assay. *British Journal of Cancer* **63**:75-83.

Carloni V, Mazzocca A, Ravichandran KS. 2004. Tetraspanin CD81 is linked to ERK/MAPKinase signaling by Shc in liver tumor cells. *Oncogene* **23**:1566–1574.

Cassinelli G, Supino R, Perego P, Polizzi D, Lanzi C, Pratesi G, Zunino F. 2001. A role for loss of p53 function in sensitivity of ovarian carcinoma cells to taxanes. *International Journal of Cancer* **92**:738–747.

Celli A, Que FG, Gores GJ, LaRusso NF. 1998. Glutathione depletion is associated with decreased Bcl-2 expression and increased apoptosis in cholangiocytes. *American Journal of Physiology.* **275**:G749–G757.

Chan MW, Chiang CD, Song EJ, Yang VC. 1998. Effects of cytoskeletal inhibitors on the accumulation of vincristine in a resistant human lung cancer cell line with high level of polymerized tubulin. *Cancer Biochemistry Biophysics.* **16**:347–363.

Chaney SG, Campbell SL, Bassett E, Wu Y. 2005. Recognition and processing of cisplatin- and oxaliplatin-DNA adducts. *Critical Reviews in Oncology-Hematology.* **53**:3–11.

Chaney SG, Campbell SL, Temple B, Bassett E, Wu Y, Faldu M. 2004. Protein interactions with platinum-DNA adducts: from structure to function. *Journal of Inorganic Biochemistry* **98**:1551–1559.

Chen GK, Lacayo NJ, Duran GE, Wang Y, Bangs CD, Rea S, Kovacs M, Cherry AM, Brown JM, Sikic BI. 2002a. Preferential expression of a mutant allele of the amplified MDR1 (ABCB1)-gene in drug-resistant variants of a human sarcoma. *Genes, Chromosomes & Cancer* **34**:372–383.

Chen CR, Kang Y, Siegel PM, Massague J. 2002b. E2F4/5 and p107 as Smad cofactors linking the TGFbeta receptor to c-myc repression. *Cell* **110**:19–32.

Chen Z, Seimiya H, Naito M, Mashima T, Kizaki A, Dan S, Imaizumi M, Ichijo H, Miyazono K, Tsuruo T. 1999. ASK1 mediates apoptotic cell death induced by genotoxic stress. *Oncogene* **18**:173–180.

Chenna R, Sugawara H, Koike T, Lopez R, Gibson TJ, Higgins DG, Thompson JD. 2003. Multiple sequence alignment with the Clustal series of programs. *Nucleic Acids Research* **31**:3497–3500.

Cho SG, Lee YH, Park HS, Ryoo K, Kang KW, Park J, Eom SJ, Kim MJ, Chang TS, Choi SY, Shim J, Kim Y, Dong MS, Lee MJ, Kim SG, Ichijo H, Choi EJ. 2001. Glutathione S-transferase mu modulates the stress-activated signals by suppressing apoptosis signal-regulating kinase 1. *Journal of Biological Chemistry* **276**:12749–12755.

Chollet P, Bensmaine MA, Brienza S, Deloche C, Cure H, Caillet H, Cvitkovic E. 1996. Single agent activity of oxaliplatin in heavily pretreated advanced epithelial ovarian cancer. *Annals of Oncology* **7**:1065–1070.

Christen RD, Jekunen AP, Jones JA, Thiebaut F, Shalinsky DR, Howell SB. 1993. In vitro modulation of cisplatin accumulation in human ovarian carcinoma cells by pharmacologic alteration of microtubules. *Journal of Clinical Investigation.* **92**:431–440.

Christodoulou C and Skarlos DV. 2005. Treatment of small cell lung cancer. *Seminars in Respiratory & Critical Care Medicine* **26**:333–341.

Chung YM, Park S, Park JK, Kim Y, Kang Y, Yoo YD. 2000. Establishment and characterization of 5-fluorouracil-resistant gastric cancer cells. *Cancer Letters* **159**:95–101.

Cole SP, Bhardwaj G, Gerlach JH, Mackie JE, Grant CE, Almquist KC, Stewart AJ, Kurz EU, Duncan AM, Deeley RG. 1992. Overexpression of a transporter gene in a multidrug-resistant human lung cancer cell line. *Science* **258**:1650–1654.

Cole SP, Downes HF, Mirski SE, Clements DJ. 1990. Alterations in glutathione and glutathione-related enzymes in a multidrug-resistant small cell lung cancer cell line. *Molecular Pharmacology* **37**:192–197.

Creagh EM, Sheehan D, Cotter TG. 2000. Heat shock proteins—modulators of apoptosis in tumour cells. *Leukemia* **14**:1161–1173.

Cullen KJ, Newkirk KA, Schumaker LM, Aldosari N, Rone JD, Haddad BR. 2003. Glutathione S-transferase pi amplification is associated with cisplatin resistance in head and neck squamous cell carcinoma cell lines and primary tumors. *Cancer Research* **63**:8097-8102.

Culy CR, Clemett D, Wiseman LR. 2000. Oxaliplatin. A review of its pharmacological properties and clinical efficacy in metastatic colorectal cancer and its potential in other malignancies. *Drugs* **60**:895-924.

D'Alessio M, Cerella C, Amici C, Pesce C, Coppola S, Fanelli C, De Nicola M, Cristofanon S, Clavarino G, Bergamaschi A, Magrini A, Gualandi G, Ghibelli L. 2004. Glutathione depletion up-regulates Bcl-2 in BSO-resistant cells. *FASEB Journal* **18**:1609-1611.

Dabholkar M, Vionnet J, Bostick-Bruton F, Yu JJ, Reed E. 1994. Messenger RNA levels of XPAC and ERCC1 in ovarian cancer tissue correlate with response to platinum-based chemotherapy. *Journal of Clinical Investigation.* **94**:703-708.

Damia G, Filiberti L, Vikhanskaya F, Carrassa L, Taya Y, D'Incalci M, Broggini M. 2001. Cisplatinum and taxol induce different patterns of p53 phosphorylation. *Neoplasia (New York)* **3**:10-16.

Dasso M. 2002. The Ran GTPase: Theme and Variations. *Current Biology* **12**:R502-R508.

Davey RA, Locke VL, Henness S, Harvie RM, Davey MW. 2004. Cellular models of drug- and radiation-resistant small cell lung cancer. *Anticancer Research* **24**:465-471.

Davies SP, Reddy H, Caivano M, Cohen P. 2000. Specificity and mechanism of action of some commonly used protein kinase inhibitors. *Biochemical Journal* **351**:95-105.

Dempke W, Voigt W, Grothey A, Hill BT, Schmoll HJ. 2000. Cisplatin resistance and oncogenes - a review. *Anti-Cancer Drugs* **11**:225-236.

Desbiens KM, Deschesnes RG, Labrie MM, Desfosses Y, Lambert H, Landry J, Bellmann K. 2003. c-Myc potentiates the mitochondrial pathway of apoptosis by

acting upstream of apoptosis signal-regulating kinase 1 (Ask1) in the p38 signalling cascade. *Biochemical Journal* **372**:631-641.

Dieras V, Bougnoux P, Petit T, Chollet P, Beuzeboc P, Borel C, Husseini F, Goupil A, Kerbrat P, Misset JL, Bensmaine MA, Tabah-Fisch I, Pouillart P. 2002. Multicentre phase II study of oxaliplatin as a single agent in cisplatin/carboplatin +/- taxane-pretreated ovarian cancer patients. *Annals of Oncology* **13**:258-266.

Donaldson KL, Goolsby GL, Wahl AF. 1994. Cytotoxicity of the anticancer agents cisplatin and taxol during cell proliferation and the cell cycle. *International Journal of Cancer* **57**:847-855.

Dorion S, Lambert H, Landry J. 2002. Activation of the p38 signaling pathway by heat shock involves the dissociation of glutathione S-transferase Mu from Ask1. *Journal of Biological Chemistry* **277**:30792-30797.

Dunn TA, Schmoll HJ, Grunwald V, Bokemeyer C, Casper J. 1997. Comparative cytotoxicity of oxaliplatin and cisplatin in non-seminomatous germ cell cancer cell lines. *Investigational New Drugs* **15**:109-114.

El-akawi Z, Abu-hadid M, Perez R, Glavy J, Zdanowicz J, Creaven PJ, Pendyala L. 1996. Altered glutathione metabolism in oxaliplatin resistant ovarian carcinoma cells. *Cancer Letters.* **105**:5-14.

Fedier A, Schwarz VA, Walt H, Carpini RD, Haller U, Fink D. 2001. Resistance to topoisomerase poisons due to loss of DNA mismatch repair. *International Journal of Cancer* **93**:571-576.

Ferguson AW, Flatow U, MacDonald NJ, Larminat F, Bohr VA, Steeg PS. 1996. Increased sensitivity to cisplatin by nm23-transfected tumor cell lines. *Cancer Research* **56**:2931-2935.

Ferry KV, Hamilton TC, Johnson SW. 2000. Increased nucleotide excision repair in cisplatin-resistant ovarian cancer cells: role of ERCC1-XPF. *Biochemical Pharmacology* **60**:1305-1313.

Fojo T, Farrell N, Ortuzar W, Tanimura H, Weinstein J, Myers TG. 2005. Identification of non-cross-resistant platinum compounds with novel cytotoxicity profiles using the NCI anticancer drug screen and clustered image map visualizations. *Critical Reviews in Oncology-Hematology*. **53**:25-34.

Fougere-Deschatrette C, Schimke RT, Weil D, Weiss MC. 1984. A study of chromosomal changes associated with amplified dihydrofolate reductase genes in rat hepatoma cells and their dedifferentiated variants. *Journal of Cell Biology* **99**:497-502.

Foulstone E, Prince S, Zaccheo O, Burns JL, Harper J, Jacobs C, Church D, Hassan AB. 2005. Insulin-like growth factor ligands, receptors, and binding proteins in cancer. *Journal of Pathology* **205**:145-153.

Fourrier L, Brooks P, Malinge JM. 2003. Binding discrimination of MutS to a set of lesions and compound lesions (base damage and mismatch-reveals its potential role as a cisplatin-damaged DNA sensing protein. *Journal of Biological Chemistry* **278**:21267-21275.

Francia G, Green SK, Bocci G, Man S, Emmenegger U, Ebos JML, Weinerman A, Shaked Y, Kerbel RS. 2005. Down-regulation of DNA mismatch repair proteins in human and murine tumor spheroids: implications for multicellular resistance to alkylating agents. *Molecular Cancer Therapeutics* **4**:1484-1494.

Fruehauf JP, Zonis S, al Bassam M, Kyshtoobayeva A, Dasgupta C, Milovanovic T, Parker RJ, Buzaid AC. 1998. Melanin content and downregulation of glutathione S-transferase contribute to the action of L-buthionine-S-sulfoximine on human melanoma. *Chemico-Biological Interactions*. **111-112**:277-305.

Fukuda M, Ohe Y, Kanzawa F, Oka M, Hara K, Saijo N. 1995. Evaluation of novel platinum complexes, inhibitors of topoisomerase I and II in non-small cell lung cancer (NSCLC-sublines resistant to cisplatin. *Anticancer Research* **15**:393-398.

Furuta T, Ueda T, Aune G, Sarasin A, Kraemer KH, Pommier Y. 2002. Transcription-coupled nucleotide excision repair as a determinant of cisplatin sensitivity of human cells. *Cancer Research* **62**:4899-4902.

Galanis E, Buckner JC, Maurer MJ, Kreisberg JI, Ballman K, Boni J, Peralba JM, Jenkins RB, Dakhil SR, Morton RF, Jaeckle KA, Scheithauer BW, Dancey J, Hidalgo M, Walsh DJ, North Central Cancer Treatment Group. 2005. Phase II trial of temsirolimus (CCI-779) in recurrent glioblastoma multiforme: a North Central Cancer Treatment Group Study. *Journal of Clinical Oncology* **23**:5294-5304.

Ghobrial IM, Witzig TE, Adjei AA. 2005. Targeting apoptosis pathways in cancer therapy. *CA: a Cancer Journal for Clinicians.* **55**:178-194.

Giannakakou P, Sackett DL, Kang YK, Zhan Z, Buters JT, Fojo T, Poruchynsky MS. 1997. Paclitaxel-resistant human ovarian cancer cells have mutant beta-tubulins that exhibit impaired paclitaxel-driven polymerization. *Journal of Biological Chemistry* **272**:17118-17125.

Gibbons GR, Kaufmann WK, Chaney SG. 1991. Role of DNA replication in carrier-ligand-specific resistance to platinum compounds in L1210 cells. *Carcinogenesis* **12**:2253-2257.

Gilot D, Loyer P, Corlu A, Glaise D, Lagadic-Gossmann D, Atfi A, Morel F, Ichijo H, Guguen-Guillouzo C. 2002. Liver protection from apoptosis requires both blockage of initiator caspase activities and inhibition of ASK1/JNK pathway via glutathione S-transferase regulation. *Journal of Biological Chemistry* **277**:49220-49229.

Godwin AK, Meister A, O'Dwyer PJ, Huang CS, Hamilton TC, Anderson ME. 1992. High resistance to cisplatin in human ovarian cancer cell lines is associated with marked increase of glutathione synthesis. *Proceedings of the National Academy of Sciences of the United States of America.* **89**:3070-3074.

Gourdier I, Del Rio M, Crabbe L, Candeil L, Copois V, Ychou M, Auffray C, Martineau P, Mechti N, Pommier Y, Pau B. 2002. Drug specific resistance to oxaliplatin is associated with apoptosis defect in a cellular model of colon carcinoma. *FEBS Letters* **529**:232-236.

Grana X, Garriga J, Mayol X. 1998. Role of the retinoblastoma protein family, pRB, p107 and p130 in the negative control of cell growth. *Oncogene* **17**:3365-3383.

Griffin C, Waard H, Deans B, Thacker J. 2005. The involvement of key DNA repair pathways in the formation of chromosome rearrangements in embryonic stem cells. *DNA Repair* **4**:1019–1027.

Gu Y, Parker A, Wilson TM, Bai H, Chang DY, Lu AL. 2002. Human MutY Homolog, a DNA Glycosylase Involved in Base Excision Repair, Physically and Functionally Interacts with Mismatch Repair Proteins Human MutS Homolog 2/Human MutS Homolog 6. *Journal of Biological Chemistry* **277**:11135–11142.

Guertin DA and Sabatini DM. 2005. An expanding role for mTOR in cancer. *Trends in Molecular Medicine* **11**:353–361.

Hande KR. 1998. Clinical applications of anticancer drugs targeted to topoisomerase II. *Biochimica et Biophysica Acta* **1400**:173–184.

Hector S, Bolanowska-Higdon W, Zdanowicz J, Hitt S, Pendyala L. 2001. In vitro studies on the mechanisms of oxaliplatin resistance. *Cancer Chemotherapy & Pharmacology* **48**:398–406.

Hegde V, Wang M, Deutsch WA. 2004. Human ribosomal protein S3 interacts with DNA base excision repair proteins hAPE/Ref-1 and hOGG1. *Biochemistry* **43**:14211–14217.

Henness S, Davey MW, Harvie RM, Davey RA. 2002. Fractionated irradiation of H69 small-cell lung cancer cells causes stable radiation and drug resistance with increased MRP1, MRP2, and topoisomerase IIalpha expression. *International Journal of Radiation Oncology, Biology, Physics.* **54**:895–902.

Heuser M, Kopun M, Rittgen W, Granzow C. 2005. Cytotoxicity determination without photochemical artifacts. *Cancer Letters* **223**:57–66.

Hipfner DR, Deeley RG, Cole SP. 1999. Structural, mechanistic and clinical aspects of MRP1. *Biochimica et Biophysica Acta* **1461**:359–376.

Hong WS, Saijo N, Sasaki Y, Minato K, Nakano H, Nakagawa K, Fujiwara Y, Nomura K, Twentyman PR. 1988. Establishment and characterization of cisplatin-

resistant sublines of human lung cancer cell lines. *International Journal of Cancer* **41**:462–467.

Horns RC, Jr., Dower WJ, Schimke RT. 1984. Gene amplification in a leukemic patient treated with methotrexate. *Journal of Clinical Oncology* **2**:2–7.

Hospers GA, Mulder NH, de Jong B, de Ley L, Uges DR, Fichtinger-Schepman AM, Scheper RJ, de Vries EG. 1988. Characterization of a human small cell lung carcinoma cell line with acquired resistance to cis-diamminedichloroplatinum(II) in vitro. *Cancer Research* **48**:6803–6807.

Huang C, Zhou C, Zhao M. 2000. [The effect of antisense hsp90 beta on the malignant phenotype and sensitivity of HeLa cells to chemotherapeutic drugs]. [Chinese]. *Chung-Hua Chung Liu Tsa Chih [Chinese Journal of Oncology]* **22**:14–16.

Huberman JA. Nucleotide Excision Repair. [Online]. 2005. Website updated 31.10.05, Material downloaded 30.1.06. Available from *http://saturn.roswellpark.org/huberman/DNA_Repair/ner.html*

Ibrahim A, Hirschfeld S, Cohen MH, Griebel DJ, Williams GA, Pazdur R. 2004. FDA drug approval summaries: oxaliplatin. *Oncologist.* **9**:8–12.

Ichijo H, Nishida E, Irie K, ten Dijke P, Saitoh M, Moriguchi T, Takagi M, Matsumoto K, Miyazono K, Gotoh Y. 1997. Induction of apoptosis by ASK1, a mammalian MAPKKK that activates SAPK/JNK and p38 signaling pathways. *Science* **275**:90–94.

Iida T, Mori E, Mori K, Goto S, Urata Y, Oka M, Kohno S, Kondo T. 1999. Co-expression of gamma-glutamylcysteine synthetase sub-units in response to cisplatin and doxorubicin in human cancer cells. *International Journal of Cancer* **82**:405–411.

Iizuka N, Hirose K, Noma T, Hazama S, Tangoku A, Hayashi H, Abe T, Yamamoto K, Oka M. 1999. The nm23-H1 gene as a predictor of sensitivity to chemotherapeutic agents in oesophageal squamous cell carcinoma. *British Journal of Cancer* **81**:469-475.

Iizuka N, Miyamoto K, Tangoku A, Hayashi H, Hazama S, Yoshino S, Yoshimura K, Hirose K, Yoshida H, Oka M. 2000. Downregulation of intracellular nm23-H1 prevents cisplatin-induced DNA damage in oesophageal cancer cells: possible association with Na(+), K(+)-ATPase. *British Journal of Cancer* **83**:1209-1215.

Ikubo S, Takigawa N, Ueoka H, Kiura K, Tabata M, Shibayama T, Chikamori M, Aoe K, Matsushita A, Harada M. 1999. In vitro evaluation of antimicrotubule agents in human small-cell lung cancer cell lines. *Anticancer Research* **19**:3985-3988.

Ireland CM, Pittman SM, Jones SL, Harnett PR. 1994. Establishment of an in vitro model for cisplatin resistance in human neuroblastoma cell lines. *Anticancer Research* **14**:2397-2403.

Ivanov VN, Lopez BP, Maulit G, Sato TA, Sassoon D, Ronai Z. 2003. FAP-1 association with Fas (Apo-1) inhibits Fas expression on the cell surface. *Molecular & Cellular Biology* **23**:3623-3635.

Jain N, Lam YM, Pym J, Campling BG. 1996. Mechanisms of resistance of human small cell lung cancer lines selected in VP-16 and cisplatin. *Cancer* **77**:1797-1808.

James KW. 2002. BLAT -The BLAST-Like Alignment Tool. *Genome Research* **12**:656-664.

Jang CY, Lee JY, Kim J. 2004. RpS3, a DNA repair endonuclease and ribosomal protein, is involved in apoptosis. *FEBS Letters* **560**:81-85.

Jansen BA, Brouwer J, Reedijk J. 2002. Glutathione induces cellular resistance against cationic dinuclear platinum anticancer drugs. *Journal of Inorganic Biochemistry* **89**:197-202.

Jekunen AP, Christen RD, Shalinsky DR, Howell SB. 1994. Synergistic interaction between cisplatin and taxol in human ovarian carcinoma cells in vitro. *British Journal of Cancer* **69**:299-306.

Jensen PB, Holm B, Sorensen M, Christensen IJ, Sehested M. 1997. In vitro cross-resistance and collateral sensitivity in seven resistant small-cell lung cancer cell lines:

preclinical identification of suitable drug partners to taxotere, taxol, topotecan and gemcitabin. *British Journal of Cancer* **75**:869–877.

Johnson SW, Shen D, Pastan I, Gottesman MM, Hamilton TC. 1996. Cross-resistance, cisplatin accumulation, and platinum-DNA adduct formation and removal in cisplatin-sensitive and -resistant human hepatoma cell lines. *Experimental Cell Research* **226**:133–139.

Jordan P and Carmo-Fonseca M. 1998. Cisplatin inhibits synthesis of ribosomal RNA in vivo. *Nucleic Acids Research* **26**:2831–2836.

Jung Y and Lippard SJ. 2003. Multiple states of stalled T7 RNA polymerase at DNA lesions generated by platinum anticancer agents. *Journal of Biological Chemistry* **278**:52084–52092.

Kartalou M and Essigmann JM. 2001. Mechanisms of resistance to cisplatin. *Mutation Research* **478**:23–43.

Kashani-Sabet M, Lu Y, Leong L, Haedicke K, Scanlon KJ. 1990. Differential oncogene amplification in tumor cells from a patient treated with cisplatin and 5-fluorouracil. *European Journal of Cancer* **26**:383–390.

Katano K, Kondo A, Safaei R, Holzer A, Samimi G, Mishima M, Kuo YM, Rochdi M, Howell SB. 2002. Acquisition of resistance to cisplatin is accompanied by changes in the cellular pharmacology of copper. *Cancer Research* **62**:6559–6565.

Kavallaris M, Tait AS, Walsh BJ, He L, Horwitz SB, Norris MD, Haber M. 2001. Multiple Microtubule Alterations Are Associated with Vinca Alkaloid Resistance in Human Leukemia Cells. *Cancer Research* **61**:5803–5809.

Kawai H, Kiura K, Tabata M, Yoshino T, Takata I, Hiraki A, Chikamori K, Ueoka H, Tanimoto M, Harada M. 2002. Characterization of non-small-cell lung cancer cell lines established before and after chemotherapy. *Lung Cancer* **35**:305–314.

Kelland LR, Mistry P, Abel G, Freidlos F, Loh SY, Roberts JJ, Harrap KR. 1992a. Establishment and characterization of an in vitro model of acquired resistance to

cisplatin in a human testicular nonseminomatous germ cell line. *Cancer Research* **52**:1710–1716.

Kelland LR and Abel G. 1992b. Comparative in vitro cytotoxicity of taxol and Taxotere against cisplatin-sensitive and -resistant human ovarian carcinoma cell lines. *Cancer Chemotherapy & Pharmacology* **30**:444–450.

Kern MA, Helmbach H, Artuc M, Karmann D, Jurgovsky K, Schadendorf D. 1997. Human melanoma cell lines selected in vitro displaying various levels of drug resistance against cisplatin, fotemustine, vindesine or etoposide: modulation of proto-oncogene expression. *Anticancer Research* **17**:4359–4370.

Kim J, Chubatsu LS, Admon A, Stahl J, Fellous R, Linn S. 1995. Implication of mammalian ribosomal protein S3 in the processing of DNA damage. *Journal of Biological Chemistry* **270**:13620–13629.

Koberle B, Masters JR, Hartley JA, Wood RD. 1999. Defective repair of cisplatin-induced DNA damage caused by reduced XPA protein in testicular germ cell tumours. *Current Biology* **9**:273–276.

Kollmannsberger C, Beyer J, Liersch R, Schoeffski P, Metzner B, Hartmann JT, Rick O, Stengele K, Hohloch K, Spott C, Kanz L, Bokemeyer C. 2004. Combination chemotherapy with gemcitabine plus oxaliplatin in patients with intensively pretreated or refractory germ cell cancer: a study of the German Testicular Cancer Study Group. *Journal of Clinical Oncology* **22**:108–114.

Kollmannsberger C, Mayer F, Kuczyk M, Kanz L, Bokemeyer C. 2001. Treatment of patients with metastatic germ cell tumors relapsing after high-dose chemotherapy. *World Journal of Urology* **19**:120–125.

Kollmannsberger C, Rick O, Derigs HG, Schleucher N, Schoffski P, Beyer J, Schoch R, Sayer HG, Gerl A, Kuczyk M, Spott C, Kanz L, Bokemeyer C. 2002. Activity of oxaliplatin in patients with relapsed or cisplatin-refractory germ cell cancer: a study of the German Testicular Cancer Study Group. *Journal of Clinical Oncology* **20**:2031–2037.

Kondo T, Higashi H, Nishizawa H, Ishikawa S, Ashizawa S, Yamada M, Makita Z, Koike T, Hatakeyama M. 2001. Involvement of pRB-related p107 protein in the inhibition of S phase progression in response to genotoxic stress. *Journal of Biological Chemistry* **276**:17559-17567.

Kotoh S, Naito S, Yokomizo A, Kohno K, Kuwano M, Kumazawa J. 1997. Enhanced expression of gamma-glutamylcysteine synthetase and glutathione S-transferase genes in cisplatin-resistant bladder cancer cells with multidrug resistance phenotype. *Journal of Urology* **157**:1054-1058.

Kotoh S, Naito S, Yokomizo A, Kumazawa J, Asakuno K, Kohno K, Kuwano M. 1994. Increased expression of DNA topoisomerase I gene and collateral sensitivity to camptothecin in human cisplatin-resistant bladder cancer cells. *Cancer Research* **54**:3248-3252.

Krummrei U, Baulieu EE, Chambraud B. 2003. The FKBP-associated protein FAP48 is an antiproliferative molecule and a player in T cell activation that increases IL2 synthesis. *Proceedings of the National Academy of Sciences of the United States of America.* **100**:2444-2449.

Kudoh K, Takano M, Koshikawa T, Hirai M, Yoshida S, Mano Y, Yamamoto K, Ishii K, Kita T, Kikuchi Y, Nagata I, Miwa M, Uchida K. 1999. Gains of 1q21-q22 and 13q12-q14 are potential indicators for resistance to cisplatin-based chemotherapy in ovarian cancer patients. *Clinical Cancer Research* **5**:2526-2531.

Kumar BS, Huang J, Persaud S, Basu A. 2004. Down-regulation of Bcl-2 is associated with cisplatin resistance in human small cell lung cancer H69 cells. *Molecular Cancer Therapeutics* **3**:327-334.

Kuppen PJ, Schuitemaker H, 't Veer LJ, de Bruijn EA, van Oosterom AT, Schrier PI. 1988. cis-diamminedichloroplatinum(II)-resistant sublines derived from two human ovarian tumor cell lines. *Cancer Research* **48**:3355-3359.

Kuroda H, Sugimoto T, Ueda K, Tsuchida S, Horii Y, Inazawa J, Sato K, Sawada T. 1991. Different drug sensitivity in two neuroblastoma cell lines established from the

same patient before and after chemotherapy. *International Journal of Cancer* **47**:732–737.

Kwok C, Zeisig BB, Dong S, So CWE. 2006. Forced homo-oligomerization of RARα leads to transformation of primary hematopoietic cells. *Cancer Cell* **9**:95–108.

Laemmli UK. 1970. Cleavage of structural proteins during the assembly of the head of bacteriophage T4. *Nature* **227**:680–685.

Lai SL, Hwang J, Perng RP, Whang-Peng J. 1995. Modulation of cisplatin resistance in acquired-resistant nonsmall cell lung cancer cells. *Oncology Research* **7**:31–38.

Lan L, Hayashi T, Rabeya RM, Nakajima S, Kanno S, Takao M, Matsunaga T, Yoshino M, Ichikawa M, Riele H, Tsuchiya S, Tanaka K, Yasui A. 2004. Functional and physical interactions between ERCC1 and MSH2 complexes for resistance to cis-diamminedichloroplatinum(II)-in mammalian cells. *DNA Repair* **3**:135–143.

Lanzi C, Perego P, Supino R, Romanelli S, Pensa T, Carenini N, Viano I, Colangelo D, Leone R, Apostoli P, Cassinelli G, Gambetta RA, Zunino F. 1998. Decreased drug accumulation and increased tolerance to DNA damage in tumor cells with a low level of cisplatin resistance. *Biochemical Pharmacology* **55**:1247–1254.

Larsson R, Bergh J, Nygren P. 1991. Combination of cyclosporin A and buthionine sulfoximine (BSO)-as a pharmacological strategy for circumvention of multidrug resistance in small cell lung cancer cell lines selected for resistance to doxorubicin. *Anticancer Research* **11**:455–459.

Lebwohl D and Canetta R. 1998. Clinical development of platinum complexes in cancer therapy: an historical perspective and an update. *European Journal of Cancer* **34**:1522–1534.

Lee S, Choi EJ, Jin C, Kim DH. 2005. Activation of PI3K/Akt pathway by PTEN reduction and PIK3CA mRNA amplification contributes to cisplatin resistance in an ovarian cancer cell line. *Gynecologic Oncology* **97**:26–34.

Lehmann S, Paul C, Torma H. 2001. Retinoid Receptor Expression and Its Correlation to Retinoid Sensitivity in Non-M3 Acute Myeloid Leukemia Blast Cells. *Clinical Cancer Research* **7**:367-373.

Lenz G, Hacker UT, Kern W, Schalhorn A, Hiddemann W. 2003. Adverse reactions to oxaliplatin: a retrospective study of 25 patients treated in one institution. *Anti-Cancer Drugs* **14**:731-733.

Levine AJ, Feng Z, Mak TW, You H, Jin S. 2006. Coordination and communication between the p53 and IGF-1-AKT-TOR signal transduction pathways. *Genes & Development* **20**:267-275.

Lewandowicz GM, Britt P, Elgie AW, Williamson CJ, Coley HM, Hall AG, Sargent JM. 2002. Cellular glutathione content, in vitro chemoresponse, and the effect of BSO modulation in samples derived from patients with advanced ovarian cancer. *Gynecologic Oncology* **85**:298-304.

Leyland-Jones B, Kelland LR, Harrap KR, Hiorns LR. 1999. Genomic imbalances associated with acquired resistance to platinum analogues. *American Journal of Pathology* **155**:77-84.

Li L, Luan Y, Wang G, Tang B, Li D, Zhang W, Li X, Zhao J, Ding H, Reed E, Li QQ. 2004. Development and characterization of five cell models for chemoresistance studies of human ovarian carcinoma. *International Journal of Molecular Medicine* **14**:257-264.

Liang Y, Meleady P, Cleary I, McDonnell S, Connolly L, Clynes M. 2001. Selection with melphalan or paclitaxel (Taxol-yields variants with different patterns of multidrug resistance, integrin expression and in vitro invasiveness. *European Journal of Cancer* **37**:1041-1052.

Ling YH, Donato NJ, Perez-Soler R. 2001. Sensitivity to topoisomerase I inhibitors and cisplatin is associated with epidermal growth factor receptor expression in human cervical squamous carcinoma ME180 sublines. *Cancer Chemotherapy & Pharmacology* **47**:473-480.

Liu J, Kraut E, Bender J, Brooks R, Balcerzak S, Grever M, Stanley H, D'Ambrosio S, Gibson D'Ambrosio R, Chan KK. 2002a. Pharmacokinetics of oxaliplatin (NSC 266046) alone and in combination with paclitaxel in cancer patients. *Cancer Chemotherapy & Pharmacology* **49**:367–374.

Liu Y and Min W. 2002b. Thioredoxin promotes ASK1 ubiquitination and degradation to inhibit ASK1-mediated apoptosis in a redox activity-independent manner. *Circulation Research* **90**:1259–1266.

Locke V. 2001. Drug Resistance in Small Cell Lung Cancer. 2001. PhD Thesis University of Technology, Sydney.

Locke V, Davey R, Davey M. 2001. Paclitaxel sensitization of multidrug-resistant cells to chemotherapy is independent of the cell cycle. *Cytometry* **43**:170–174.

Locke VL, Davey RA, Davey MW. 2003. Modulation of drug and radiation resistance in small cell lung cancer cells by paclitaxel. *Anti-Cancer Drugs* **14**:523–531.

Lombardi D, Lacombe ML, Paggi MG. 2000. nm23: unraveling its biological function in cell differentiation. *Journal of Cellular Physiology*. **182**:144–149.

Lord RV, Brabender J, Gandara D, Alberola V, Camps C, Domine M, Cardenal F, Sanchez JM, Gumerlock PH, Taron M, Sanchez JJ, Danenberg KD, Danenberg PV, Rosell R. 2002. Low ERCC1 expression correlates with prolonged survival after cisplatin plus gemcitabine chemotherapy in non-small cell lung cancer. *Clinical Cancer Research* **8**:2286–2291.

Ma J, Murphy M, O'Dwyer PJ, Berman E, Reed K, Gallo JM. 2002. Biochemical changes associated with a multidrug-resistant phenotype of a human glioma cell line with temozolomide-acquired resistance. *Biochemical Pharmacology* **63**:1219–1228.

Mamenta EL, Poma EE, Kaufmann WK, Delmastro DA, Grady HL, Chaney SG. 1994. Enhanced replicative bypass of platinum-DNA adducts in cisplatin-resistant human ovarian carcinoma cell lines. *Cancer Research* **54**:3500–3505.

Mansouri A, Zhang Q, Ridgway LD, Tian L, Claret FX. 2003. Cisplatin resistance in an ovarian carcinoma is associated with a defect in programmed cell death control through XIAP regulation. *Oncology Research* **13**:399–404.

Margolin K, Longmate J, Baratta T, Synold T, Christensen S, Weber J, Gajewski T, Quirt I, Doroshow JH. 2005. CCI-779 in metastatic melanoma: a phase II trial of the California Cancer Consortium. *Cancer* **104**:1045–1048.

Markman M and Hoskins W. 1992. Responses to salvage chemotherapy in ovarian cancer: a critical need for precise definitions of the treated population. *Journal of Clinical Oncology* **10**:513–514.

Marks DC, Belov L, Davey MW, Davey RA, Kidman AD. 1992. The MTT cell viability assay for cytotoxicity testing in multidrug-resistant human leukemic cells. *Leukemia Research* **16**:1165–1173.

Marquez N, Chappell SC, Sansom OJ, Clarke AR, Teesdale-Spittle P, Errington RJ, Smith PJ. 2004. Microtubule stress modifies intra-nuclear location of Msh2 in mouse embryonic fibroblasts. *Cell Cycle* **3**:662–671.

Martello LA, Verdier-Pinard P, Shen HJ, He L, Torres K, Orr GA, Horwitz SB. 2003. Elevated levels of microtubule destabilizing factors in a Taxol-resistant/dependent A549 cell line with an alpha-tubulin mutation. *Cancer Research* **63**:1207–1213.

Maruyama T, Sachi Y, Furuke K, Kitaoka Y, Kanzaki H, Yoshimura Y, Yodoi J. 1999. Induction of thioredoxin, a redox-active protein, by ovarian steroid hormones during growth and differentiation of endometrial stromal cells in vitro. *Endocrinology* **140**:365–372.

Masuda A and Takahashi T. 2002. Chromosome instability in human lung cancers: possible underlying mechanisms and potential consequences in the pathogenesis. *Oncogene* **21**:6884–6897.

Materna V, Liedert B, Thomale J, Lage H. 2005. Protection of platinum-DNA adduct formation and reversal of cisplatin resistance by anti-MRP2 hammerhead ribozymes in human cancer cells. *International Journal of Cancer* **115**:393–402.

Matsuzaki H, Loi H, Dong S, Tsai YY, Fang J, Law J, Di X, Liu WM, Yang G, Liu G, Huang J, Kennedy GC, Ryder TB, Marcus GA, Walsh PS, Shriver MD, Puck JM, Jones KW, Mei R. 2004. Parallel genotyping of over 10,000 SNPs using a one-primer assay on a high-density oligonucleotide array. *Genome Research* **14**:414-425.

Mattaj IW and Englmeier L. 1998. Nucleocytoplasmic transport: the soluble phase. *Annual Review of Biochemistry* **67**:265-306.

McCann L. Characterisation of Cisplatin Resistance in a Model Leukaemia Cell Line. 2003. Honours Thesis. University of Technology, Sydney.

Melton DW, Ketchen AM, Nunez F, Bonatti-Abbondandolo S, Abbondandolo A, Squires S, Johnson RT. 1998. Cells from ERCC1-deficient mice show increased genome instability and a reduced frequency of S-phase-dependent illegitimate chromosome exchange but a normal frequency of homologous recombination. *Journal of Cell Science* **111**:395-404.

Meyers M, Hwang A, Wagner MW, Boothman DA. 2004. Role of DNA mismatch repair in apoptotic responses to therapeutic agents. *Environmental & Molecular Mutagenesis* **44**:249-264.

Meyne J, Lockhart LH, Arrighi FE. 1979. Nonrandom distribution of chromosomal aberrations induced by three chemicals. *Mutation Research* **63**:201-209.

Miller CA, III and Costa M. 1989. Analysis of proteins cross-linked to DNA after treatment of cells with formaldehyde, chromate, and cis-diamminedichloroplatinum(II). *Molecular Toxicology* **2**:11-26.

Mishima M, Samimi G, Kondo A, Lin X, Howell SB. 2002. The cellular pharmacology of oxaliplatin resistance. *European Journal of Cancer* **38**:1405-1412.

Mita MM, Mita A, Rowinsky EK. 2003. The molecular target of rapamycin (mTOR) as a therapeutic target against cancer. *Cancer Biology & Therapy*. **2**:S169-S177.

Miyajima A, Nakashima J, Yoshioka K, Tachibana M, Tazaki H, Murai M. 1997. Role of reactive oxygen species in cis-dichlorodiammineplatinum-induced cytotoxicity on bladder cancer cells. *British Journal of Cancer* **76**:206-210.

Moore W, Zhang C, Clarke PR. 2002. Targeting of RCC1 to chromosomes is required for proper mitotic spindle assembly in human cells. *Current Biology* **12**:1442–1447.

Moritaka T, Kiura K, Ueoka H, Tabata M, Segawa Y, Shibayama T, Takigawa N, Ohnoshi T, Harada M. 1998. Cisplatin-resistant human small cell lung cancer cell line shows collateral sensitivity to vinca alkaloids. *Anticancer Research* **18**:927–933.

Mukai M, Kanzaki A, Chen ZS, Miyashita H, Sumizawa T, Furukawa T, Haraguchi M, Takebayashi Y, Takamatsu H, Akiyama S. 2002. Enhanced nucleotide excision repair in cisplatin resistant human KB carcinoma cells. *Oncology Reports.* **9**:839–844.

Mullan PB, Quinn JE, Gilmore PM, McWilliams S, Andrews H, Gervin C, McCabe N, McKenna S, White P, Song YH, Maheswaran S, Liu E, Haber DA, Johnston PG, Harkin DP. 2001. BRCA1 and GADD45 mediated G2/M cell cycle arrest in response to antimicrotubule agents. *Oncogene* **20**:6123–6131.

Mustacich D and Powis G. 2000. Thioredoxin reductase. *Biochemical Journal* **346 Pt 1**:1–8.

Nakamura H, Bai J, Nishinaka Y, Ueda S, Sasada T, Ohshio G, Imamura M, Takabayashi A, Yamaoka Y, Yodoi J. 2000. Expression of thioredoxin and glutaredoxin, redox-regulating proteins, in pancreatic cancer. *Cancer Detection.& Prevention.* **24**:53–60.

Nakayama K, Kanzaki A, Ogawa K, Miyazaki K, Neamati N, Takebayashi Y. 2002. Copper-transporting P-type adenosine triphosphatase (ATP7B) as a cisplatin based chemoresistance marker in ovarian carcinoma: comparative analysis with expression of MDR1, MRP1, MRP2, LRP and BCRP. *International Journal of Cancer* **101**:488–495.

Nomura T, Yamasaki M, Nomura Y, Mimata H. 2005. Expression of the inhibitors of apoptosis proteins in cisplatin-resistant prostate cancer cells. *Oncology Reports.* **14**:993–997.

Nunez F, Chipchase MD, Clarke AR, Melton DW. 2000. Nucleotide excision repair gene (ERCC1)-deficiency causes G2 arrest in hepatocytes and a reduction in liver binucleation: the role of p53 and p21. *FASEB J.* **14**:1073–1082.

Ogawa J, Iwazaki M, Inoue H, Koide S, Shohtsu A. 1993. Immunohistochemical study of glutathione-related enzymes and proliferative antigens in lung cancer. Relation to cisplatin sensitivity. *Cancer* **71**:2204-2209.

Ohta S, Nishio K, Kubo S, Nishio M, Ohmori T, Takahashi T, Saijo N. 1993. Characterisation of a vindesine-resistant human small-cell lung cancer cell line. *British Journal of Cancer* **68**:74-79.

Ohta S, Nishio K, Kubota N, Ohmori T, Funayama Y, Ohira T, Nakajima H, Adachi M, Saijo N. 1994. Characterization of a taxol-resistant human small-cell lung cancer cell line. *Japanese Journal of Cancer Research* **85**:290-297.

Orr GA, Verdier-Pinard P, McDaid H, Horwitz SB. 2003. Mechanisms of Taxol resistance related to microtubules. *Oncogene* **22**:7280-7295.

Oshita F, Fujiwara Y, Saijo N. 1992. Radiation sensitivities in various anticancer-drug-resistant human lung cancer cell lines and mechanism of radiation cross-resistance in a cisplatin-resistant cell line. *Journal of Cancer Research & Clinical Oncology* **119**:28-34.

Paces J, Zika R, Paces V, Pavlicek A, Clay O, Bernardi G. 2004. Representing GC variation along eukaryotic chromosomes. *Gene* **333**:135-141.

Parekh H and Simpkins H. 1996. Cross-resistance and collateral sensitivity to natural product drugs in cisplatin-sensitive and -resistant rat lymphoma and human ovarian carcinoma cells. *Cancer Chemotherapy & Pharmacology* **37**:457-462.

Parekh H, Wiesen K, Simpkins H. 1997. Acquisition of taxol resistance via P-glycoprotein- and non-P-glycoprotein-mediated mechanisms in human ovarian carcinoma cells. *Biochemical Pharmacology* **53**:461-470.

Parker AR and Eshleman JR. 2003. Human MutY: gene structure, protein functions and interactions, and role in carcinogenesis. *Cellular & Molecular Life Sciences* **60**:2064-2083.

Pectasides D, Pectasides M, Farmakis D, Aravantinos G, Nikolaou M, Koumpou M, Gaglia A, Kostopoulou V, Mylonakis N, Skarlos D. 2004a. Gemcitabine and

oxaliplatin (GEMOX) in patients with cisplatin-refractory germ cell tumors: a phase II study. *Annals of Oncology* **15**:493–497.

Pectasides D, Pectasides M, Farmakis D, Aravantinos G, Nikolaou M, Koumpou M, Gaglia A, Kostopoulou V, Mylonakis N, Economopoulos T, Raptis SA. 2004b. Oxaliplatin and irinotecan plus granulocyte-colony stimulating factor as third-line treatment in relapsed or cisplatin-refractory germ-cell tumor patients: a phase II study. *European Urology* **46**:216–221.

Perego P, Romanelli S, Carenini N, Magnani I, Leone R, Bonetti A, Paolicchi A, Zunino F. 1998. Ovarian cancer cisplatin-resistant cell lines: multiple changes including collateral sensitivity to Taxol. *Annals of Oncology* **9**:423–430.

Persons DL, Yazlovitskaya EM, Cui W, Pelling JC. 1999. Cisplatin-induced activation of mitogen-activated protein kinases in ovarian carcinoma cells: inhibition of extracellular signal-regulated kinase activity increases sensitivity to cisplatin. *Clinical Cancer Research* **5**:1007–1014.

Peters GB, Dale BM, Sage RE, Ford JH. 1990. Novel translocations in acute nonlymphocytic leukemia. Two cases involving chromosome 21, band q22. *Cancer Genetics & Cytogenetics* **44**:99–105.

Pfeiffer P, Goedecke W, Kuhfittig-Kulle S, Obe G. 2004. Pathways of DNA double-strand break repair and their impact on the prevention and formation of chromosomal aberrations. *Cytogenetic & Genome Research* **104**:7–13.

Pommier Y, Redon C, Rao VA, Seiler JA, Sordet O, Takemura H, Antony S, Meng L, Liao Z, Kohlhagen G, Zhang H, Kohn KW. 2003. Repair of and checkpoint response to topoisomerase I-mediated DNA damage. *Mutation Research* **532**:173–203.

Por SB, Cooley MA, Breit SN, Penny R, French PW. 1991. Antibodies to tubulin and actin bind to the surface of a human monocytic cell line, U937. *Journal of Histochemistry & Cytochemistry*. **39**:981–985.

Poulain L, Lincet H, Duigou F, Deslandes E, Sichel F, Gauduchon P, Staedel C. 1998. Acquisition of chemoresistance in a human ovarian carcinoma cell is linked to a defect in cell cycle control. *International Journal of Cancer* **78**:454–463.

Prat AG and Cantiello HF. 1996. Nuclear ion channel activity is regulated by actin filaments. *American Journal of Physiology.* **270**:C1532–C1543.

Preisler HD. 1995. Multidrug resistance is more than MDR1 activity. *Leukemia Research* **19**:429–431.

Preisler HD and Gopal V. 1994. Regrowth resistance in leukemia and lymphoma: the need for a new system to classify treatment failure and for new approaches to treatment. *Leukemia Research* **18**:149–160.

Pu YS, Chen J, Huang CY, Guan JY, Lu SH, Hour TC. 2001. Cross-resistance and combined cytotoxic effects of paclitaxel and cisplatin in bladder cancer cells. *Journal of Urology* **165**:2082–2085.

Pu YS, Tsai TC, Cheng AL, Tsai CY, Tseng NF, Su IJ, Hsieh CY, Lai MK. 1996. Expression of MDR-1 gene in transitional cell carcinoma and its correlation with chemotherapy response. *Journal of Urology* **156**:271–275.

Raaphorst GP, Cybulski SE, Sobol R, Ng CE. 2001. The response of human breast tumour cell lines with altered polymerase beta levels to cisplatin and radiation. *Anticancer Research* **21**:2079–2083.

Raderschall E, Bazarov A, Cao J, Lurz R, Smith A, Mann W, Ropers HH, Sedivy JM, Golub EI, Fritz E, Haaf T. 2002. Formation of higher-order nuclear Rad51 structures is functionally linked to p21 expression and protection from DNA damage-induced apoptosis. *Journal of Cell Science* **115**:153–164.

Rahman Q, Abidi P, Afaq F, Schiffmann D, Mossman BT, Kamp DW, Athar M. 1999. Glutathione redox system in oxidative lung injury. *Critical Reviews in Toxicology* **29**:543–568.

Rao PH, Houldsworth J, Palanisamy N, Murty VV, Reuter VE, Motzer RJ, Bosl GJ, Chaganti RS. 1998. Chromosomal amplification is associated with cisplatin resistance of human male germ cell tumors. *Cancer Research* **58**:4260–4263.

Reardon JT, Vaisman A, Chaney SG, Sancar A. 1999. Efficient nucleotide excision repair of cisplatin, oxaliplatin, and Bis-aceto-ammine-dichloro-cyclohexylamine-

platinum(IV (JM216 platinum intrastrand DNA diadducts. *Cancer Research* **59**:3968 3971.

Reilly PA, Heerema NA, Sledge GW, Jr., Palmer CG. 1993. Unusual distribution of chromosome 12 in a testicular germ cell tumor cell line (833K and its cisplatin resistant derivative (64CP9. *Cancer Genetics & Cytogenetics.* **68**:114 121.

Rennicke A, Voigt W, Mueller T, Fruehauf A, Schmoll HJ, Beyer C, Dempke W. 2005. Resistance mechanisms following cisplatin and oxaliplatin treatment of the human teratocarcinoma cell line 2102EP. *Anticancer Research* **25**:1147 1155.

Rixe O, Ortuzar W, Alvarez M, Parker R, Reed E, Paull K, Fojo T. 1996. Oxaliplatin, tetraplatin, cisplatin, and carboplatin: spectrum of activity in drug resistant cell lines and in the cell lines of the National Cancer Institute's Anticancer Drug Screen panel. *Biochemical Pharmacology* **52**:1855 1865.

Rosell R and Felip E. 2001. Predicting response to paclitaxel/carboplatin based therapy in non small cell lung cancer. *Seminars in Oncology* **28**:37 44.

Rosell R, Taron M, Barnadas A, Scagliotti G, Sarries C, Roig B. 2003. Nucleotide excision repair pathways involved in Cisplatin resistance in non small cell lung cancer. *Cancer Control* **10**:297 305.

Rossi A, Maione P, Colantuoni G, Guerriero C, Gridelli C. 2004. The role of new targeted therapies in small cell lung cancer. *Critical Reviews in Oncology Hematology.* **51** :45 53.

Rozen S and Skaletsky H. 2000. Primer3 on the WWW for general users and for biologist programmers. *Methods in Molecular Biology* **132**:365 386.

Ruggero D and Pandolfi PP. 2003. Does the ribosome translate cancer? *Nature Reviews.* **Cancer. 3**:179 192.

Russell JS, Brady K, Burgan WE, Cerra MA, Oswald KA, Camphausen K, Tofilon PJ. 2003. Gleevec mediated inhibition of Rad51 expression and enhancement of tumor cell radiosensitivity. *Cancer Research* **63**:7377 7383.

Safaei R and Howell SB. 2005. Copper transporters regulate the cellular pharmacology and sensitivity to Pt drugs. *Critical Reviews in Oncology Hematology*. **53**:13 23.

Safaei R, Katano K, Samimi G, Naerdemann W, Stevenson JL, Rochdi M, Howell SB. 2004. Cross resistance to cisplatin in cells with acquired resistance to copper. *Cancer Chemotherapy & Pharmacology* **53**:239 246.

Saitoh M, Nishitoh H, Fujii M, Takeda K, Tobiume K, Sawada Y, Kawabata M, Miyazono K, Ichijo H. 1998. Mammalian thioredoxin is a direct inhibitor of apoptosis signal regulating kinase (ASK 1. *EMBO Journal* **17**:2596 2606.

Sakamoto M, Kondo A, Kawasaki K, Goto T, Sakamoto H, Miyake K, Koyamatsu Y, Akiya T, Iwabuchi H, Muroya T, Ochiai K, Tanaka T, Kikuchi Y, Tenjin Y. 2001. Analysis of gene expression profiles associated with cisplatin resistance in human ovarian cancer cell lines and tissues using cDNA microarray. *Human Cell* **14**:305 315.

Sancar A, Lindsey Boltz LA, Unsal Kacmaz K, Linn S. 2004. Molecular mechanisms of mammalian DNA repair and the DNA damage checkpoints. *Annual Review of Biochemistry* **73**:39 85.

Sandler AB. 2003. Chemotherapy for small cell lung cancer. *Seminars in Oncology* **30**:9 25.

Santoro MG. 2000. Heat shock factors and the control of the stress response. *Biochemical Pharmacology* **59**:55 63.

Sargent RG, Meservy JL, Perkins BD, Kilburn AE, Intody Z, Adair GM, Nairn RS, Wilson JH. 2000. Role of the nucleotide excision repair gene ERCC1 in formation of recombination dependent rearrangements in mammalian cells. *Nucleic Acids Research* **28**:3771 3778.

Sartorius UA and Krammer PH. 2002. Upregulation of Bcl 2 is involved in the mediation of chemotherapy resistance in human small cell lung cancer cell lines. *International Journal of Cancer* **97**:584 592.

Sasada T, Iwata S, Sato N, Kitaoka Y, Hirota K, Nakamura K, Nishiyama A, Taniguchi Y, Takabayashi A, Yodoi J. 1996. Redox control of resistance to cis diamminedichloroplatinum (II (CDDP : protective effect of human thioredoxin against CDDP induced cytotoxicity. *Journal of Clinical Investigation.* **97**:2268 2276.

Savaraj N, Wu C, Wangpaichitr M, Kuo MT, Lampidis T, Robles C, Furst AJ, Feun L. 2003. Overexpression of mutated MRP4 in cisplatin resistant small cell lung cancer cell line: collateral sensitivity to azidothymidine. *International Journal of Oncology* **23**:173 179.

Sawada S, Mese H, Sasaki A, Yoshioka N, Matsumura T. 2003. Combination chemotherapy of paclitaxel and cisplatin induces apoptosis with Bcl 2 phosphorylation in a cisplatin resistant human epidermoid carcinoma cell line. *Cancer Chemotherapy & Pharmacology* **51**:505 511.

Scanlon KJ, Kashani Sabet M, Sowers LC. 1989. Overexpression of DNA replication and repair enzymes in cisplatin resistant human colon carcinoma HCT8 cells and circumvention by azidothymidine. *Cancer Communications.* **1**:269 275.

Schondorf T, Becker M, Gohring UJ, Wappenschmidt B, Kolhagen H, Kurbacher CM. 2001. Interaction of cisplatin, paclitaxel and adriamycin with the tumor suppressor PTEN. *Anti Cancer Drugs* **12**:797 800.

Selvakumaran M, Pisarcik DA, Bao R, Yeung AT, Hamilton TC. 2003. Enhanced cisplatin cytotoxicity by disturbing the nucleotide excision repair pathway in ovarian cancer cell lines. *Cancer Research* **63**:1311 1316.

Sharp SY, O'Neill CF, Rogers P, Boxall FE, Kelland LR. 2002. Retention of activity by the new generation platinum agent AMD0473 in four human tumour cell lines possessing acquired resistance to oxaliplatin. *European Journal of Cancer* **38**:2309 2315.

Shen DW, Liang XJ, Gawinowicz MA, Gottesman MM. 2004. Identification of cytoskeletal [14C]carboplatin binding proteins reveals reduced expression and disorganization of actin and filamin in cisplatin resistant cell lines. *Molecular Pharmacology* **66**:789 793.

Slovak ML, Ho JP, Bhardwaj G, Kurz EU, Deeley RG, Cole SP. 1993. Localization of a novel multidrug resistance-associated gene in the HT1080/DR4 and H69AR human tumor cell lines. *Cancer Research* **53**:3221-3225.

Smith V, Raynaud F, Workman P, Kelland LR. 2001. Characterization of a human colorectal carcinoma cell line with acquired resistance to flavopiridol. *Molecular Pharmacology* **60**:885-893.

Sockalingam R, Filippich L, Charles B, Murdoch B. 2002. Cisplatin-induced ototoxicity and pharmacokinetics: preliminary findings in a dog model. *Annals of Otology, Rhinology & Laryngology*. **111**:745-750.

Song JJ and Lee YJ. 2003. Differential role of glutaredoxin and thioredoxin in metabolic oxidative stress-induced activation of apoptosis signal-regulating kinase 1. *Biochemical Journal* **373**:845-853.

Song JJ, Rhee JG, Suntharalingam M, Walsh SA, Spitz DR, Lee YJ. 2002. Role of glutaredoxin in metabolic oxidative stress. Glutaredoxin as a sensor of oxidative stress mediated by H2O2. *Journal of Biological Chemistry* **277**:46566-46575.

Soulie P, Bensmaine A, Garrino C, Chollet P, Brain E, Fereres M, Jasmin C, Musset M, Misset JL, Cvitkovic E. 1997. Oxaliplatin/cisplatin (L-OHP/CDDP) combination in heavily pretreated ovarian cancer. *European Journal of Cancer* **33**:1400-1406.

Srivatsa PJ, Cliby WA, Keeney GL, Dodson MK, Suman VJ, Roche PC, Podratz KC. 1996. Elevated nm23 protein expression is correlated with diminished progression-free survival in patients with epithelial ovarian carcinoma. *Gynecologic Oncology* **60**:363-372.

Stevens EV, Raffeld M, Espina V, Kristensen GB, Trope' CG, Kohn EC, Davidson B. 2005. Expression of xeroderma pigmentosum A protein predicts improved outcome in metastatic ovarian carcinoma. *Cancer* **103**:2313-2319.

Stojic L, Brun R, Jiricny J. 2004. Mismatch repair and DNA damage signalling. *DNA Repair* **3**:1091-1101.

Su GM, Davey MW, Davey RA. 1998. Induction of broad drug resistance in small cell lung cancer cells and its reversal by paclitaxel. *International Journal of Cancer* **76**:702–708.

Suzukake K, Petro BJ, Vistica DT. 1982. Reduction in glutathione content of L-PAM resistant L1210 cells confers drug sensitivity. *Biochemcal Pharmacology* **31**:121–124.

Takano M, Kudo K, Goto T, Yamamoto K, Kita T, Kikuchi Y. 2001. Analyses by comparative genomic hybridization of genes relating with cisplatin-resistance in ovarian cancer. *Human Cell* **14**:267–271.

Takata M, Sasaki MS, Sonoda E, Fukushima T, Morrison C, Albala JS, Swagemakers SM, Kanaar R, Thompson LH, Takeda S. 2000. The Rad51 paralog Rad51B promotes homologous recombinational repair. *Molecular & Cellular Biology* **20**:6476–6482.

Takata M, Sasaki MS, Tachiiri S, Fukushima T, Sonoda E, Schild D, Thompson LH, Takeda S. 2001. Chromosome instability and defective recombinational repair in knockout mutants of the five Rad51 paralogs. *Molecular & Cellular Biology* **21**:2858–2866.

Tanaka T, Uchiumi T, Kohno K, Tomonari A, Nishio K, Saijo N, Kondo T, Kuwano M. 1998. Glutathione homeostasis in human hepatic cells: overexpression of gamma-glutamylcysteine synthetase gene in cell lines resistant to buthionine sulfoximine, an inhibitor of glutathione synthesis. *Biochemical & Biophysical.Research Communications.* **246**:398–403.

Tanaka T, Uchiumi T, Nomoto M, Kohno K, Kondo T, Nishio K, Saijo N, Kuwano M. 1999. Cellular balance of glutathione levels through the expression of gamma-glutamylcysteine synthetase and glutathione thiol transferase genes in human hepatic cells resistant to a glutathione poison. *Biochimica et Biophysica Acta* **1427**:367–377.

Tashiro T, Kawada Y, Sakurai Y, Kidani Y. 1989. Antitumor activity of a new platinum complex, oxalato (trans-l-1,2-diaminocyclohexane-platinum (II): new experimental data. *Biomedicine & Pharmacotherapy* **43**:251–260.

Teicher BA, Holden SA, Herman TS, Sotomayor EA, Khandekar V, Rosbe KW, Brann TW, Korbut TT, Frei E, III. 1991. Characteristics of five human tumor cell lines and sublines resistant to cis-diamminedichloroplatinum(II). *International Journal of Cancer* **47**:252-260.

Tew KD and Ronai Z. 1999. GST function in drug and stress response. *Drug Resistance Updates* **2**:143-147.

Tisman G, MacDonald D, Shindell N, Reece E, Patel P, Honda N, Nishimora EK, Garris J, Shannahan W, Chisti N, McCarthy J, Nasser MS, Sargent D, Plant A. 2004. Oxaliplatin toxicity masquerading as recurrent colon cancer. *Journal of Clinical Oncology* **22**:3202-3204.

Tobiume K, Matsuzawa A, Takahashi T, Nishitoh H, Morita K, Takeda K, Minowa O, Miyazono K, Noda T, Ichijo H. 2001. ASK1 is required for sustained activations of JNK/p38 MAP kinases and apoptosis. *EMBO Reports*. **2**:222-228.

Tonini R, Grohovaz F, Laporta CA, Mazzanti M. 1999. Gating mechanism of the nuclear pore complex channel in isolated neonatal and adult mouse liver nuclei. *FASEB Journal* **13**:1395-1403.

Toshimitsu H, Hashimoto K, Tangoku A, Iizuka N, Yamamoto K, Kawauchi S, Oga A, Furuya T, Oka M, Sasaki K. 2004. Molecular signature linked to acquired resistance to cisplatin in esophageal cancer cells. *Cancer Letters* **211**:69-78.

Townsend DM, Tew KD, Tapiero H. 2003a. The importance of glutathione in human disease. *Biomedicine & Pharmacotherapy* **57**:145-155.

Townsend DM and Tew KD. 2003b. The role of glutathione-S-transferase in anti-cancer drug resistance. *Oncogene* **22**:7369-7375.

Tracy E, Roder D, Bishop J, Chen S, Chen W. 2005. Cancer in NSW Incidence and Mortality 2003. NSW Central Cancer Registry. Cancer Insitute NSW.

Tsurutani J, West KA, Sayyah J, Gills JJ, Dennis PA. 2005. Inhibition of the phosphatidylinositol 3-kinase/Akt/mammalian target of rapamycin pathway but not the MEK/ERK pathway attenuates laminin-mediated small cell lung cancer cellular

survival and resistance to imatinib mesylate or chemotherapy. *Cancer Research* **65**:8423–8432.

Twentyman PR, Wright KA, Mistry P, Kelland LR, Murrer BA. 1992. Sensitivity to novel platinum compounds of panels of human lung cancer cell lines with acquired and inherent resistance to cisplatin. *Cancer Research* **52**:5674–5680.

Twentyman PR, Wright KA, Rhodes T. 1991. Radiation response of human lung cancer cells with inherent and acquired resistance to cisplatin. *International Journal of Radiation Oncology, Biology, Physics.* **20**:217–220.

Uechi T, Tanaka T, Kenmochi N. 2001. A complete map of the human ribosomal protein genes: assignment of 80 genes to the cytogenetic map and implications for human disorders. *Genomics* **72**:223–230.

Uvarov E.B. and Isaacs A. 1993. The Penguin Dictionary of Science. Seventh Edition. Penguin Books. Nucleolus; p302.

Vahrmeijer AL, Hoetelmans RW, Mulder GJ, Schutrups J, van Vlierberghe RL, van de Velde CJ, van Dierendonck JH. 2000. Development of resistance to glutathione depletion–induced cell death in CC531 colon carcinoma cells: association with increased expression of bcl-2. *Biochemical Pharmacology* **59**:1557–1562.

Vaisman A and Chaney SG. 2000. The efficiency and fidelity of translesion synthesis past cisplatin and oxaliplatin GpG adducts by human DNA polymerase beta. *Journal of Biological Chemistry* **275**:13017–13025.

VanderWeele DJ, Zhou R, Rudin CM. 2004. Akt up-regulation increases resistance to microtubule-directed chemotherapeutic agents through mammalian target of rapamycin. *Molecular Cancer Therapeutics* **3**:1605–1613.

Vara JAF, Casado E, de Castro J, Cejas P, Belda-Iniesta C, Gonzalez-Baron M. 2004. PI3K/Akt signalling pathway and cancer. *Cancer Treatment Reviews* **30**:193–204.

Varma RR, Hector SM, Clark K, Greco WR, Hawthorn L, Pendyala L. 2005. Gene expression profiling of a clonal isolate of oxaliplatin-resistant ovarian carcinoma cell line A2780/C10. *Oncology Reports.* **14**:925–932.

Verrills NM and Kavallaris M. 2005. Improving the targeting of tubulin-binding agents: lessons from drug resistance studies. *Current Pharmaceutical Design.* **11**:1719-1733.

Wachters FM, Wong LS, Timens W, Kampinga HH, Groen HJ. 2005. ERCC1, hRad51, and BRCA1 protein expression in relation to tumour response and survival of stage III/IV NSCLC patients treated with chemotherapy. *Lung Cancer* **50**:211-219.

Waddell TK and Shepherd FA. 2004. Should aggressive surgery ever be part of the management of small cell lung cancer? *Thoracic Surgery Clinics.* **14**:271-281.

Walker MC, Povey S, Parrington JM, Riddle PN, Knuechel R, Masters JR. 1990. Development and characterization of cisplatin-resistant human testicular and bladder tumour cell lines. *European Journal of Cancer* **26**:742-747.

Walkley CR, Purton LE, Snelling HJ, Yuan YD, Nakajima H, Chambon P, Chandraratna RA, McArthur GA. 2004. Identification of the molecular requirements for an RAR alpha-mediated cell cycle arrest during granulocytic differentiation. *Blood* **103**:1286-1295.

Wang D and Lippard SJ. 2005a. Cellular processing of platinum anticancer drugs. *Nature Reviews.* **Drug Discovery. 4**:307-320.

Wang T, Arifoglu P, Ronai Z, Tew KD. 2001. Glutathione S-transferase P1-1 (GSTP1-1) inhibits c-Jun N-terminal kinase (JNK1) signaling through interaction with the C terminus. *Journal of Biological Chemistry* **276**:20999-21003.

Wang Z, Xie Y, Wang H. 2005b. Changes in Survivin Messenger RNA level during Chemotherapy Treatment in Ovarian Cancer Cells. *Cancer Biology & Therapy.* **4**:716-719.

Wasenius VM, Jekunen A, Monni O, Joensuu H, Aebi S, Howell SB, Knuutila S. 1997. Comparative genomic hybridization analysis of chromosomal changes occurring during development of acquired resistance to cisplatin in human ovarian carcinoma cells. *Genes, Chromosomes & Cancer* **18**:286-291.

Whang-Peng J, Bunn PA, Jr., Kao-Shan CS, Lee EC, Carney DN, Gazdar A, Minna JD. 1982. A nonrandom chromosomal abnormality, del 3p(14-23), in human small cell lung cancer (SCLC). *Cancer Genetics & Cytogenetics* **6**:119-134.

Whiteside MA, Chen DT, Desmond RA, Abdulkadir SA, Johanning GL. 2004. A novel time-course cDNA microarray analysis method identifies genes associated with the development of cisplatin resistance. *Oncogene* **23**:744-752.

Wilson C, Yang J, Strefford JC, Summersgill B, Young BD, Shipley J, Oliver T, Lu YJ. 2005. Overexpression of genes on 16q associated with cisplatin resistance of testicular germ cell tumor cell lines. *Genes, Chromosomes.& Cancer* **43**:211-216.

Witte AB, Anestal K, Jerremalm E, Ehrsson H, Arner ES. 2005. Inhibition of thioredoxin reductase but not of glutathione reductase by the major classes of alkylating and platinum-containing anticancer compounds. *Free Radical Biology & Medicine* **39**:696-703.

Wittig R, Nessling M, Will RD, Mollenhauer J, Salowsky R, Munstermann E, Schick M, Helmbach H, Gschwendt B, Korn B, Kioschis P, Lichter P, Schadendorf D, Poustka A. 2002. Candidate genes for cross-resistance against DNA-damaging drugs. *Cancer Research* **62**:6698-6705.

Wong KK, Tsang YTM, Shen J, Cheng RS, Chang YM, Man TK, Lau CC. 2004. Allelic imbalance analysis by high-density single-nucleotide polymorphic allele (SNP)-array with whole genome amplified DNA. *Nucleic Acids Research* **32**:e69-76.

Woynarowski JM, Chapman WG, Napier C, Herzig MC, Juniewicz P. 1998. Sequence- and region-specificity of oxaliplatin adducts in naked and cellular DNA. *Molecular Pharmacology* **54**:770-777.

Woynarowski JM, Faivre S, Herzig MC, Arnett B, Chapman WG, Trevino AV, Raymond E, Chaney SG, Vaisman A, Varchenko M, Juniewicz PE. 2000. Oxaliplatin-induced damage of cellular DNA. *Molecular Pharmacology* **58**:920-927.

Wozniak K and Blasiak J. 2002. Recognition and repair of DNA-cisplatin adducts. *Acta Biochimica Polonica* **49**:583-596.

Wu C, Wangpaichitr M, Feun L, Kuo MT, Robles C, Lampidis T, Savaraj N. 2005. Overcoming cisplatin resistance by mTOR inhibitor in lung cancer. *Molecular Cancer* **1**:25–34

Xu Y and Villalona-Calero MA. 2002. Irinotecan: mechanisms of tumor resistance and novel strategies for modulating its activity. *Annals of Oncology* **13**:1841–1851.

Xu ZY, Loignon M, Han FY, Panasci L, Aloyz R. 2005. Xrcc3 induces cisplatin resistance by stimulation of Rad51-related recombinational repair, S-phase checkpoint activation, and reduced apoptosis. *Journal of Pharmacology & Experimental Therapeutics* **314**:495–505.

Yamada M, Tomida A, Yoshikawa H, Taketani Y, Tsuruo T. 1996. Increased expression of thioredoxin/adult T-cell leukemia-derived factor in cisplatin-resistant human cancer cell lines. *Clinical Cancer Research* **2**:427–432.

Yamada M, Tomida A, Yoshikawa H, Taketani Y, Tsuruo T. 1997. Overexpression of thioredoxin does not confer resistance to cisplatin in transfected human ovarian and colon cancer cell lines. *Cancer Chemotherapy & Pharmacology* **40**:31–37.

Yamamoto K, Ichijo H, Korsmeyer SJ. 1999. BCL-2 is phosphorylated and inactivated by an ASK1/Jun N-terminal protein kinase pathway normally activated at G(2)/M. *Molecular & Cellular Biology*. **19**:8469–8478.

Yamamoto K, Kikuchi Y, Kudoh K, Nagata I. 2000a. Modulation of cisplatin sensitivity by taxol in cisplatin-sensitive and -resistant human ovarian carcinoma cell lines. *Journal of Cancer Research & Clinical.Oncology* **126**:168–172.

Yamamoto K, Kikuchi Y, Kudoh K, Hirata J, Kita T, Nagata I. 2000b. Treatment with paclitaxel alone rather than combination with paclitaxel and cisplatin may be selective for cisplatin-resistant ovarian carcinoma. *Japanese Journal of Clinical Oncology* **30**:446–449.

Yasui K, Mihara S, Zhao C, Okamoto H, Saito-Ohara F, Tomida A, Funato T, Yokomizo A, Naito S, Imoto I, Tsuruo T, Inazawa J. 2004. Alteration in copy numbers of genes as a mechanism for acquired drug resistance. *Cancer Research* **64**:1403–1410.

Yasuno T, Matsumura T, Shikata T, Inazawa J, Sakabe T, Tsuchida S, Takahata T, Miyairi S, Naganuma A, Sawada T. 1999. Establishment and characterization of a cisplatin‐resistant human neuroblastoma cell line. *Anticancer Research* **19**:4049‐4057.

Yokomizo A, Ono M, Nanri H, Makino Y, Ohga T, Wada M, Okamoto T, Yodoi J, Kuwano M, Kohno K. 1995a. Cellular levels of thioredoxin associated with drug sensitivity to cisplatin, mitomycin C, doxorubicin, and etoposide. *Cancer Research* **55**:4293‐4296.

Yokomizo A, Kohno K, Wada M, Ono M, Morrow CS, Cowan KH, Kuwano M. 1995b. Markedly decreased expression of glutathione S‐transferase pi gene in human cancer cell lines resistant to buthionine sulfoximine, an inhibitor of cellular glutathione synthesis. *Journal of Biological Chemistry* **270**:19451‐19457.

Yokomizo A, Tindall DJ, Drabkin H, Gemmill R, Franklin W, Yang P, Sugio K, Smith DI, Liu W. 1998. PTEN/MMAC1 mutations identified in small cell, but not in non‐small cell lung cancers. *Oncogene* **17**:475‐479.

Yonetani Y, Hochegger H, Sonoda E, Shinya S, Yoshikawa H, Takeda S, Yamazoe M. 2005. Differential and collaborative actions of Rad51 paralog proteins in cellular response to DNA damage. *Nucleic Acids Research* **33**:4544‐4552.

Yoon JH, Singh P, Lee DH, Qiu J, Cai S, O'Connor TR, Chen Y, Shen B, Pfeifer GP. 2005. Characterization of the 3' → 5' exonuclease activity found in human nucleoside diphosphate kinase 1 (NDK1) and several of its homologues. *Biochemistry* **44**:15774‐15786.

Youn CK, Kim MH, Cho HJ, Kim HB, Chang IY, Chung MH, You HJ. 2004. Oncogenic H‐Ras Up‐Regulates Expression of ERCC1 to Protect Cells from Platinum‐Based Anticancer Agents. *Cancer Research* **64** :4849‐4857.

Yuan ZQ, Feldman RI, Sussman GE, Coppola D, Nicosia SV, Cheng JQ. 2003. AKT2 inhibition of cisplatin‐induced JNK/p38 and Bax activation by phosphorylation of ASK1: implication of AKT2 in chemoresistance. *Journal of Biological Chemistry* **278**:23432‐23440.

Zeng HH, Xu ZH, Wang K. 1997. FT-Raman studies on the transformation of G-actin to F-actin, the binding of cisplatin and transplatin to F-actin and the effects of the conformation of F-actin. *International Journal of Biological Macromolecules* **20**:107-113.

Zhai X, Beckmann H, Jantzen HM, Essigmann JM. 1998. Cisplatin-DNA adducts inhibit ribosomal RNA synthesis by hijacking the transcription factor human upstream binding factor. *Biochemistry* **37** :16307-16315.

Zhang CC, Yang JM, White E, Murphy M, Levine A, Hait WN. 1998. The role of MAP4 expression in the sensitivity to paclitaxel and resistance to vinca alkaloids in p53 mutant cells. *Oncogene* **16** :1617-1624.

Zhang L and Hanigan MH. 2003. Role of cysteine S-conjugate beta-lyase in the metabolism of cisplatin. *Journal of Pharmacology & Experimental Therapeutics* **306**:988-994.

Zhao X, Li C, Paez JG, Chin K, Janne PA, Chen TH, Girard L, Minna J, Christiani D, Leo C, Gray JW, Sellers WR, Meyerson M. 2004. An integrated view of copy number and allelic alterations in the cancer genome using single nucleotide polymorphism arrays. *Cancer Research* **64**:3060-3071.

Zhou C, Huang P, Liu J. 2005. The carboxyl-terminal of BRCA1 is required for subnuclear assembly of RAD51 after treatment with cisplatin but not ionizing radiation in human breast and ovarian cancer cells. *Biochemical & Biophysical Research Communications.* **336**:952-960.